UNIWERSYTET ŚLĄSKI W KATOWICACH

WYDZIAŁ NAUK PRZYRODNICZYCH

INSTYTUT NAUK O ZIEMI

ALEKSANDRA KATARZYNA OSIKA

Historia zlodowacenia południowego Spitsbergenu w holocenie

History of glaciation of southern Spitsbergen in the Holocene

Praca doktorska

Promotor: prof. dr hab. Jacek Jania

Promotor pomocniczy: dr Joanna E. Szafraniec

SOSNOWIEC 2025

SPIS TREŚCI

PODZIĘKOWANIA

Powstanie tej pracy oraz towarzyszące jej przedsięwzięcia w ciągu ostatnich sześciu lat nie byłyby możliwe bez pomocy wielu życzliwych osób, z którymi mam przyjemność i przywilej współpracować, a których liczba rosła z biegiem kolejnych lat realizacji projektu doktorskiego.

Dziękuję Promotorowi, prof. dr. hab. Jackowi Jani, za wprowadzenie w arktyczny świat, zaszczepienie fascynacji glacjologią, nieodzowną pomoc, wsparcie i życzliwość w każdym czasie. Dziękuję za motywację do dalszego rozwoju naukowego i poszukiwania odpowiedzi na najbardziej aktualne pytania, jak również odważnego stawiania pytań, które nie zostały wypowiedziane lub pozostają mało popularne.

Dziękuję Promotorowi Pomocniczemu, dr Joannie Szafraniec, za nieodzowną pomoc, życzliwość, wsparcie i opiekę merytoryczną oraz inspirację do poszukiwań nowych problemów badawczych do rozwiązania. Dziękuję za możliwość udziału w pracach terenowych na Islandii, które pozwoliły mi poznać tę (sub)polarną część Północy, do której na pewno wrócę niejeden raz.

Dziękuję Członkom Zespołu Kriosfera i Geoinformacja za wspólny czas, wszystkie porady, uwagi oraz wszelką życzliwość i pomoc. Uczestnikom Wypraw Uniwersytetu Śląskiego na Spitsbergen w latach 2020–2025 za pomoc w pracach terenowych oraz załodze Polskiej Stacji Polarnej Hornsund za serdeczną gościnność.

Dziękuję Współautorom artykułów za wkład w różnej formie oraz Redaktorom i Recenzentom, prof. Andrew Fowler, dr. Haroldowi Lovell i anonimowym za szczegółowe recenzje, komentarze i konstruktywne uwagi, które pozwoliły dopracować artykuły.

Dziękuję Austriackiej Bibliotece Narodowej i Norweskiemu Instytutowi Polarnemu za udostępnienie fotografii archiwalnych lodowców z 1872 i 1918 r. Dr. Dariuszowi Ignatiukowi i dr. Heikki'emu Lihavainen za przyjęcie na staż w SIOS-KC w 2020 r. w ramach programu PROM. Prof. Jonowi Ove Hagenowi za wsparcie w realizacji Arctic Field Grant, życzliwość, inspirację i zainteresowanie postępami w przygotowaniu pracy doktorskiej i dalszymi planami podczas spotkań w różnych okolicznościach. Prof. Andreasowi Vieli za przyjęcie i opiekę merytoryczną podczas stażu na Uniwersytecie w Zurychu z programu Bekker NAWA. Dr. Wesley'owi Farnsworth i dr. Ívarowi Benediktsson za przyjęcie i opiekę merytoryczną podczas stażu Erasmus+ na Uniwersytecie Islandzkim. Unnur Björk Lárusdóttir za serdeczną gościnność w Reykjaviku. Prof. Andersowi Schomackerowi za zaproszenie na staż absolwencki Erasmus+ na Uniwersytecie w Trømso. Dr. Janowi Kavanowi za cenne komentarze oraz zaproszenie do współpracy w badaniach Lodowca Pencka na Svalbardzie. Inicjatorom inwentaryzacji lodowców uchodzących do jezior na potrzeby GLIMS/RGI, w szczególności dr. Williamowi Kochtitzky'emu, za możliwość pracy przy tym przedsięwzięciu. Rodzinie za wyrozumiałość i wsparcie.

FINANSOWANIE

Badania przedstawione w niniejszej pracy były finansowane ze środków:

- NCN PRELUDIUM, 2021/41/N/ST10/02070: Rekonstrukcja zasięgu lodowców i środowiska południowego Svalbardu podczas Optimum Klimatycznego Holocenu jako wzorca konsekwencji współczesnego ocieplenia klimatu,
- The Research Council of Norway, Arctic Field Grant 2020, 31066: Detection of Holocene frontal moraines underneath glaciers,
- Centrum Studiów Polarnych, Uniwersytet Śląski w Katowicach – Krajowy Naukowy Ośrodek Wiodący w zakresie nauk o Ziemi (2014–2018), 03/KNOW2/2014,
- Środków statutowych Intytutu Nauk o Ziemi Uniwersytetu Śląskiego w Katowicach.
- Środków Department of Geography, University of Zurich

Staż w SIOS-KC (sierpień 2020 r.) został zrealizowany ze środków projektu PROM – Międzynarodowa wymiana stypendialna doktorantów i kadry akademickiej, współfinansowanego ze środków Europejskiego Funduszu Społecznego w ramach Programu Operacyjnego Wiedza Edukacja Rozwój, projekt pozakonkursowy pt. „Międzynarodowa wymiana stypendialna doktorantów i kadry akademickiej”, realizowanego w ramach Działania określonego we wniosku o dofinansowanie projektu nr POWR.03.03.00-00-PN13/18.

Staż w Uniwersytecie w Zurychu (październik – grudzień 2022 r.) został dofinansowany ze środków projektu Bekker NAWA, BPN/BEK/2021/1/00412, *Od przeszłego klimatu do dalszego scenariusza cofania się lodowców na Svalbardzie - ujęcie modelowe*.

Staż w Uniwersytecie Islandzkim (maj-czerwiec 2025 r.) został dofinansowany ze środków programu Erasmus+ w ramach wyjazdów studentów i doktorantów Uniwersytetu Śląskiego w Katowicach.

Lista artykułów składających się na rozprawę doktorską

1. Osika A., Jania J., Szafraniec J.E., 2022: Holocene ice-free strait followed by dynamic Neoglacial fluctuations: Hornsund, Svalbard. The Holocene, 32(7), 664–679. https://doi.org/10.1177/09596836221088232 (**Załącznik 1**) – 140 pkt; IF: 1,8

2. Osika A., Jania J., 2024: Geomorphological and historical records of the surge-type behaviour of Hansbreen (Svalbard). Annals of Glaciology, 65, e31. https://doi.org/10.1017/aog.2024.32 (**Załącznik 6**) – 100 pkt. MNiSW; IF: 2,1

3. Osika A., Jania J., Piotrowska N., Tikhomirov D., Szafraniec J.E., Devendra D., Christl M., Egli M., Vieli A., 2025: Holocene glacial history of southern Spitsbergen. Złożono do *Quaternary Science Reviews* dnia 22.09.2025 r. (**Załącznik 7**)

STRESZCZENIE

Konsekwencją współczesnego ocieplenia klimatu jest recesja lodowców różnych regionów świata, w tym Svalbardu, który od 1979 r. ocieplał się siedem razy szybciej, niż średnia globalna. Szczególnie wrażliwe na ocieplenie klimatu są nisko położone lodowce południowego Spitsbergenu, które wykazują jedne z najbardziej negatywnych wartości bilansu masy na Svalbardzie. Znajomość fluktuacji lodowców w przeszłości, w szczególności w okresach cieplejszego klimatu i recesji lodowców, jest istotna dla zrozumienia możliwych skutków współczesnego ocieplenia Arktyki. Mimo rozwoju badań paleogeograficznych Svalbardu, większość opracowań dotyczy centralnej i północnej części Spitsbergenu. Ewolucja lodowców południowej części archipelagu w okresie poprzedzającym regularny monitoring w oparciu o badania terenowe i dane teledetekcyjne pozostaje stosunkowo słabo rozpoznana. Celem niniejszej pracy była rekonstrukcja zmian zasięgu wybranych lodowców południowego Spitsbergenu w holocenie, w tym (1) wyznaczenie okresów awansów i recesji lodowców na podstawie wyników datowania ^{14}C i ^{10}Be, (2) identyfikacja znaczenia szarż lodowców na podstawie dowodów geomorfologicznych i materiałów historycznych oraz (3) wskazanie głównych czynników warunkujących zmiany zasięgu wybranych lodowców w holocenie. Obszar szczegółowych badań obejmował lodowce Hornbreen, Hansbreen, Vestre Torellbreen i Werenskioldbreen oraz ich przedpola. Wykorzystałam także obserwacje porównawcze, dane literaturowe oraz historyczne dane kartograficzne i fotograficzne dla innych lodowców badanego regionu.

Wyniki kartowania geomorfologicznego przedpoli lodowców przeprowadzonego w oparciu o dane teledetekcyjne wysokiej rozdzielczości i badania terenowe wykazały obecność charakterystycznych form rzeźby terenu dla lodowców szarżujących, jak grzbiety z wyciśnięcia szczelin dennych (crevasse-squeeze ridges, CSRs), ozy harmonijkowe (concertina eskers), lineacje lodowcowe (streamlined glacial lineations) oraz moreny czołowe spiętrzone. Podczas badań pobrałam próbki muszli małży morskich, tundry subfosylnej i drewna dryftowego. Wykorzystałam także cztery próbki muszli małży i żebra wieloryba z osadów lodowcowych z zasobów Instytutu Nauk o Ziemi. 63 nowe daty radiowęglowe zestawiłam z opublikowanymi wcześniej datami z przedpoli badanych lodowców (25 próbek). Wyniki datowania radiowęglowego pozwoliły na wskazanie okresów recesji lodowców i kolonizacji nowych fiordów przez małże i lądowych części przedpoli przez roślinność tundrową. Oprócz próbek materiału organicznego do datowania ^{14}C, podczas badań terenowych pozyskałam łącznie 11 próbek głazów z moreny i trimline lodowca Hansbreen do datowania metodą izotopu kosmogenicznego ^{10}Be. Wyniki datowania ^{10}Be wykazały anomalnie „postarzone" wartości nie odzwierciedlające rzeczywistego wieku moren, co przypisałam obecności nuklidów odziedziczonych z wczesnego i środkowego holocenu. Mapy historyczne z XVII–XX w. dostarczyły danych jakościowych na temat zmian zasięgu lodowców uchodzących do morza, których przejawem były zmiany długości poszczególnych odgałęzień Hornsundu. Fotografie archiwalne z 1872, 1899– 1901, 1917–1918 i 1936 r. pozwoliły mi zidentyfikować dowodów szarż lodowców, jak zafałdowania i zapętlenia moren środkowych oraz zafalowania foliacji, zestromienie czół w formie nabrzmiałych lobów, silne i chaotyczne uszczelinienie powierzchni sięgające często górnej części lodowca oraz widoczne strefy ścinania na granicy lodowca szarżującego z lodowcami dopływowymi w fazie uspokojenia.

Na podstawie nowych wyników datowania, opublikowanych dat ^{14}C i ^{10}Be, materiałów historycznych oraz opublikowanych danych paleoklimatycznych wyróżniłam następujące okresy zmian zasięgu wybranych lodowców południowego Spitsbergenu: (1) deglacjację, (2) recesję lodowców we wczesnym i środkowym holocenie, (3) rozwój lodowców w pierwszej połowie późnego holocenu, (4) awanse lodowców ok. 2,2–1,5 cal ka BP, (5) recesję lodowców ok. 1,5–1,0 cal ka BP, (6) awanse lodowców od ok. 0,7 cal ka BP oraz (7) Małą Epokę Lodową (MEL). Wyniki datowania radiowęglowego muszli z moreny czołowej lodowca Werenskioldbreen wskazały na jego recesję przed 12,5 cal ka BP, która utrzymywała się do okresu wyniesienia terasy morskiej po 10,0 cal ka BP. Najstarsze próbki muszli pobrane z przedpoli pozostałych lodowców (Hansbreen: 11,3 cal ka BP, Hornbreen: 10,9 cal ka BP, Vestre Torellbreen: 10,5 cal ka BP) wykazały ich recesję w podobnym okresie. Nowe i pozyskane z literatury daty radiowęglowe dowiodły recesji lodowców we wczesnym i środkowym holocenie, kiedy klimat Svalbardu był cieplejszy, niż współcześnie. Daty radiowęglowe dostarczyły również przesłanek ograniczonego zasięgu lodowców (w porównaniu z maksimum MEL) w pierwszej połowie późnego holocenu i recesji ok. 1,6–0,7 cal ka BP, co mogło być związane ze wzrostem temperatury powietrza i wody morskiej w obszarze badań. Zidentyfikowane maksymalne zasięgi lodowców z późnego holocenu były efektem szarż poprzedzonych długotrwałym gromadzeniem masy w strefie rezerwuarowej w warunkach chłodniejszego klimatu oraz prawdopodobnym wzrostem śnieżnych opadów atmosferycznych w okresie narastania fazy ocieplenia. Czynnikiem wyzwalającym mogła być zwiększona dostawa wód roztopowych do podłoża lodowców w okresach cieplejszych. Konsekwencją synchronicznych szarż lodowców było zamknięcie cieśniny Hornsund i rozwój pomostu lodowego łączącego Torell Land i Sørkapp Land.

Szczególną uwagę poświęciłam systemowi glacjalnemu Hornbreen-Hambergbreen, którego dynamika decyduje o funkcjonowaniu Hornsundu jako fiordu lub cieśniny między Morzem Grenlandzkim i Morzem Barentsa. Fluktuacje lodowców odtworzyłam na podstawie nowych i opublikowanych dat ^{14}C oraz opublikowanych dat ^{10}Be głazów morenowych z przedpola lodowca Hornbreen. Recesja lodowców we wczesnym holocenie doprowadziła do otwarcia cieśniny ok. 10,9 cal ka BP lub wcześniej. Awans lodowców i zamknięcie cieśniny nastąpiły ok. 3,9 cal ka BP lub później, ok. 2,1 cal ka BP lub dopiero 1,9 ± 0,3 ka (Philipps i in., 2017). Ponowne otwarcie cieśniny mogło nastąpić ok. 1,3 cal ka BP do kolejnego awansu lodowców ok. 0,7 ± 0,2 ka (Birkenmajer, Olsson, 1997; Philipps i in., 2017).

Fluktuacje lodowców obszaru badań przebiegały synchronicznie z pozostałą częścią Svalbardu i podobnie jak w innych regionach, odzwierciedlały zmiany temperatury powietrza i wody morskiej. Nisko położone strefy akumulacyjne sprzyjały szybkiej recesji lodowców w okresach ocieplenia i jednocześnie ograniczały tempo ich odbudowy w okresach chłodniejszych. Wyniki wskazują na kluczową rolę szarż lodowców w ewolucji pokrywy lodowej regionu, które m.in. kilkakrotnie doprowadziły do utworzenia pomostu lodowego łączącego Torell Land i Sørkapp Land.

Słowa kluczowe: lodowce, Svalbard, szarże lodowców, fluktuacje lodowców, geomorfologia glacjalna, datowanie radiowęglowe, optimum klimatyczne holocenu, neoglacjał, średniowieczny okres ciepły, mała epoka lodowa

SUMMARY

Climate warming is leading to glacier recession in different parts of the world, including Svalbard. Since 1979, Svalbard has warmed seven times faster than the global average. Low-elevated glaciers in southern Spitsbergen are particularly sensitive to ongoing warming as they have one of the most negative mass balances in Svalbard. Knowledge of the past glacial fluctuations, in particular in the warmer phases with glacier retreat, is crucial for understanding the possible consequences of contemporary warming in the Arctic. Despite recent advances in the paleogeography of Svalbard, most studies address the central and northern part of Spitsbergen. Knowledge of glacier evolution in the southern part of the archipelago before the regular monitoring based on field measurements and remote sensing data remains limited. This work aimed to reconstruct the fluctuations of selected glaciers in southern Spitsbergen in the Holocene, including (1) identification of the phases of glacier advances and recession based on ^{14}C and ^{10}Be dating, (2) identification of the role of glacier surges based on geomorphological and historical data, and (3) identification of the main factors of the fluctuations of selected glaciers in the Holocene. Detailed studies included four glaciers and their forefields: Hornbreen, Hansbreen, Vestre Torellbreen and Werenskioldbreen. In addition, I used comparative observations, literature data, and historical cartographic and photographic data for other glaciers of the investigated region.

Geomorphological mapping of the glacier forefields based on high-resolution remote sensing data and field investigation revealed characteristic landforms of surging glaciers, including crevasse-squeeze ridges (CSRs), concertina eskers and thrust-block moraines. During field work, I collected samples of marine mollusc shells, subfossil vegetation and driftwood. I also used four samples of mollusc shells and a sample of a whalebone from glacial sediments in the resources of the Institute of Earth Sciences. Sixty-three new radiocarbon dates were compiled with twenty-five previously published ^{14}C dates from the glacier forefields. The ages indicate the periods of glacier recession, which allowed the colonization of new fjords and ice-free terrestrial areas by marine molluscs and tundra. I also collected 11 samples of boulders from the moraine and trimline of Hansbreen for ^{10}Be dating. The ^{10}Be ages were anomalously old due to nuclide inheritance from the previous exposure in the Early and Middle Holocene. Therefore, they have not revealed the age of moraine abandonment. Historical maps from the 1600s to 1900s provided qualitative data on the fluctuations of tidewater glaciers indicated by changes in the extent of particular branches of Hornsund. Archival photographs from 1872, 1899–1901, 1917–1918 and 1936 had documented characteristic features in glaciers' surface morphology, which provided evidence for glacier surges: folded and looped moraines and deformed ice structures, a steepened and bulging terminus, heavy and extensive surface crevassing reaching high up the glacier, shear margins on the glacier surface between surging flow units and tributary glaciers in the quiescent phase.

Compilation of new and published ^{14}C and ^{10}Be ages together with geomorphological, historical and published paleoclimatic data allowed me to identify the following phases of glacier changes in southern Spitsbergen: (1) deglaciation, (2) glacier recession in the Early and Middle

Holocene, (3) glacier re-growth in the first half of the Late Holocene, (4) glacier advances in c. 2.2–1.5 cal ka BP, (5) glacier recession c. 1.5–1.0 cal ka BP, (6) glacier advances after c. 0.7 cal ka BP and (7) Little Ice Age (LIA). The ^{14}C ages of marine mollusc shells from the terminal moraine of Werenskioldbreen indicated glacier recession by 12.5 cal ka BP until the emergence of a raised marine terrace sometime after 10.0 cal ka BP. The oldest shell samples from the forefields of other glaciers also demonstrated glacier retreat in this period (Hansbreen: 11.3 ka cal BP; Hornbreen: 10.9 cal ka BP; Vestre Torellbreen: 10.5 cal ka BP). New and published radiocarbon dates indicated glacier retreat in the Early and Middle Holocene, when the climate of Svalbard was warmer than present. The ^{14}C ages also evidenced reduced glacier extent (compared to the LIA maximum) in the first half of the Late Holocene, as well as glacier recession in c. 1.6–0.7 cal ka BP, which may have been related to the increase in air temperature and sea surface temperature in Hornsund. The maximum Late Holocene glacier extent identified in this work corresponded to glacier surges, preceded by long-lasting mass accumulation in the reservoir area due to the climate cooling and increase in snow precipitation at the beginning of the warmer phase. Glacier surges may have occurred in response to increased water content at the glacier beds in the warmer phases. Synchronous glacier surges blocked the Hornsund strait and developed an ice bridge linking Torell Land and Sørkapp Land.

I paid particular attention to the Hornbreen-Hambergbreen glacier system as its dynamics decide whether Hornsund has been a fjord or a strait between the Greenland Sea and the Barents Sea. I reconstructed the fluctuations of this glacier system using new and published ^{14}C ages and published ^{10}Be ages of moraine boulders from the Hornbreen forefield. Glacier recession in the Early Holocene led to the opening of the strait c. 10.9 cal ka BP or earlier. Glacier advances blocked the strait c. 3.9 cal ka BP or later, 2.1 cal ka BP or even 1.9 ± 0,3 ka (Philipps et al., 2017). Subsequent re-opening of the strait may have occurred c. 1.3 cal ka BP until the next glacier advance c. 0.7 ± 0.2 ka (Birkenmajer, Olsson, 1997; Philipps et al., 2017).

Fluctuations of glaciers in the study area were synchronous with the rest of Svalbard. Similar to other parts of the archipelago, they reflected changes in the air and seawater temperatures. Low-elevated accumulation areas facilitated rapid glacier recession in the warmer periods and hindered their regrowth in the colder phases of the Holocene. Glacier surges played a key role in the glacial evolution of this region as they allowed for the build-up of the ice bridge between Torell Land and Sørkapp Land.

Keywords: glaciers, Svalbard, glacier surges, glacier fluctuations, glacial geomorphology, radiocarbon dating, Holocene Climatic Optimum, neoglacial, Medieval Warm Period, Little Ice Age

WPROWADZENIE

Konsekwencją postępującego obecnie ocieplenia klimatu jest recesja lodowców obserwowana w różnych regionach świata, w szczególności w ciągu ostatnich 15 lat (Zemp i in., 2019, 2025). Od 1979 r. Arktyka ocieplała się niemal cztery, a Svalbard siedem razy szybciej, niż średnia globalna (Nordli i in., 2020; Rantanen i in., 2022). Zjawisko to określane jest jako „arktyczne wzmocnienie" (*Arctic amplification*) w konsekwencji zaniku lodu morskiego, zmiany albedo i dodatniego sprzężenia zwrotnego prowadzącego do dalszego ocieplania się klimatu Arktyki (Previdi i in., 2021). Około 2010 r. lodowce stanowiły 57% powierzchni lądowej Svalbardu, norweskiego archipelagu arktycznego (Nuth i in., 2013). Ich recesja obserwowana jest od maksimum Małej Epoki Lodowej na przełomie XIX i XX w. i gwałtownie postępuje od lat 90. XX w. (Nuth i in., 2007; Martín-Moreno i in., 2017). W latach 2000-2019 regionalny bilans masy lodowców Svalbardu wynosił -8 ± 6 Gt r^{-1} (Schuler i in., 2020), a ich całkowite stopnienie wiązałoby się ze wzrostem średniego globalnego poziomu morza o 1.7 ± 0.5 cm (Farinotti i in., 2019). Tempo recesji jest większe w przypadku lodowców uchodzących do morza, które dodatkowo tracą masę przez ablację frontalną (np. Błaszczyk i in., 2013). Wraz z ociepleniem klimatu Arktyki następuje wzrost liczby lodowców, które w przeszłości uchodziły do morza, ale obecnie kończą się na lądzie i nie posiadają kontaktu z sąsiednim akwenem (Kochtitzky, Copland, 2022). Fluktuacje lodowców Svalbardu odzwierciedlają zmiany średnich wartości temperatury powietrza i wody morskiej (powierzchniowej i w głębszych warstwach), zmiany sumy opadów, warunków topograficznych (głębokości wody akwenu, do którego uchodzą), jak również szarże (Luckman i in., 2015; Holmes i in., 2019; Błaszczyk i in., 2023). Szarża to nagły wzrost prędkości powierzchniowej lodowca 10–1000 razy niż zazwyczaj, związany z niestabilnym przepływem lodu z obszaru rezerwuarowego do odbierającego (Meier, Post, 1969; Raymond, 1987; Jania, 1997). Zjawisku szarży zazwyczaj towarzyszy rozległy awans lodowców. Przykładowo, w latach 2008–2013 svalbardzki lodowiec Nathorstbreen awansował 15 km, zwiększając zasięg powierzchniowy o 20% i stając się lodowcem uchodzącym do morza (Sund i in., 2014). Svalbard jest jednym z klastrów przestrzennych lodowców szarżujących na świecie definiowanych warunkami klimatycznymi (*optimal climatic envelope*) oraz geometrią lodowców (Sevestre, Ben, 2015). Większość lodowców szarżujących Arktyki i obszarów wysokogórskich Azji występuje w obszarach o średniej rocznej temperaturze powietrza od –10 °C do 0 °C i rocznej sumie opadów 200–2000 mm (Sevestre, Benn, 2015; Benn, 2021). Lodowce szarżujące zazwyczaj charakteryzują się większą powierzchnią i długością oraz mniejszym nachyleniem, niż lodowce nieszarżujące w tym samym obszarze (Sevestre, Benn, 2015). Czynnikiem sprzyjającym występowaniu szarż jest również obecność osadów drobnoziarnistych w podłożu lodowca (Jiskoot i in., 2000). Lodowce szarżujące charakteryzują się stosunkowo długą fazą uspokojenia, która na Svalbardzie wynosi od kilkudziesięciu do ponad 150, a nawet 500 lat, oraz krótką fazą aktywną przyspieszonego ruchu, która na Svalbardzie zazwyczaj nie przekracza 10 lat (Dowdeswell i in., 1991). Ze względu na ocieplenie klimatu Svalbardu, w przyszłości należy spodziewać się dalszych szarż lodowców politermalnych z uwagi na zwiększoną dostawę wody roztopowej do podłoża, jak również zanik małych lodowców zimnych, które mogły szarżować w przeszłości w warunkach politermalnych (Lovell i in., 2015; Hanssen-Bauer i in., 2019; Mannerfelt i in., 2024).

Znajomość fluktuacji lodowców w przeszłości jest istotna dla określenia możliwych skutków współczesnego ocieplenia klimatu (Lyså i in., 2022) oraz przewidywania dalszej deglacjacji. Zmiany zasięgu lodowców w holocenie przebiegały podobnie w różnych regionach Arktyki, a różnice dotyczyły ram czasowych poszczególnych faz ocieplenia i ochłodzenia (Larocca, Axford, 2022). Optimum klimatyczne holocenu (Holocene Climatic Optimum) było okresem znaczącego ocieplenia we wczesnym holocenie, kiedy średnia temperatura powietrza wielu obszarów Arktyki, w tym Svalbardu, była wyższa od współczesnej (m.in. Kaufman i in., 2004). W tym czasie mniejsze lodowce Svalbardu zanikły, a wiele lodowców współcześnie uchodzących do morza kończyło się na lądzie (Røthe i in., 2018; Farnsworth i in., 2020). Prawdopodobną przyczyną ocieplenia był wzrost natężenia promieniowania słonecznego związany z cyklami Milankovicia, którego efekt został wzmocniony przez redukcję lodu morskiego i jej konsekwencje (m.in. zmniejszenie albedo powierzchni), a w przypadku Svalbardu również zwiększony napływ ciepłej wody atlantyckiej transportowanej przez Prąd Zachodniospitsbergeński (Ślubowska-Woldengen i in., 2007; Jakobsson i in., 2010; Werner i in., 2013; Park i in., 2019). Spadek natężenia promieniowania słonecznego, ochłodzenie klimatu i rozwój lodowców nastąpiły w neoglacjale od ok. 4,0 cal ka BP (Philipps i in., 2017; Allaart i in., 2021). W późnym holocenie występowały również krótsze okresy ocieplenia i recesji lodowców, jak Średniowieczny Okres Ciepły (Medieval Warm Period) około 1,2–0,7 cal ka BP (Dzierżek i in., 1990; Divine i in., 2011).

W porównaniu z centralną i północną częścią Svalbardu, fluktuacje lodowców południowej części archipelagu w holocenie były słabo rozpoznane (Farnsworth i in., 2020). Wyniki dotychczasowych badań sugerują, że zmiany zasięgu lodowców południowego Spitsbergenu prawdopodobnie przebiegały synchronicznie z pozostałymi obszarami Svalbardu. Opracowania te dostarczyły dowodów recesji lodowców we wczesnym holocenie i Średniowiecznym Okresie Ciepłym, jak również awansów w późnym holocenie, przed i podczas Małej Epoki Lodowej (MEL; Baranowski, Karlén, 1976; Lindner i in., 1984, 1986, 1987; Dzierżek i in., 1990; Lindner, Marks, 1993; Birkenmajer, Olsson, 1997, 1998; Philipps i in., 2017). Niemniej, wyniki datowania niektórych awansów były przedmiotem dyskusji i wymagają weryfikacji, a daty radiowęglowe kalibracji w oparciu o aktualne krzywe kalibracyjne (Baranowski, 1977; Birkenmajer, Olsson, 1997).

Badania współczesnych fluktuacji lodowców południowego Spitsbergenu uchodzących do morza jako główne czynniki warunkujące tempo ich recesji wskazują wzrost temperatury powietrza oraz temperatury wody morskiej (Błaszczyk i in., 2021, 2023). Czynniki te zapewne odgrywały główną rolę w recesji lodowców w cieplejszych okresach holocenu, jak optimum klimatyczne holocenu i Średniowieczny Okres Ciepły. Wydaje się, że ze względu na lokalizację w stosunku do napływu cieplejszych mas powietrza oraz ciepłego Prądu Zachodniospitsbergeńskiego oraz topografię lodowców, lodowce południowego Spitsbergenu współcześnie wykazują większą podatność na zmiany w bilansie masy w porównaniu z pozostałą częścią archipelagu, co pozwala przypuszczać o podobnej wrażliwości na ocieplenie klimatu w przeszłości (Schmidt i in., 2023; van Pelt, Frank, 2025). Szczególną rolę odgrywa topografia lodowców uchodzących do morza: nisko położone pola akumulacyjne i rozległe przegłębienia zlodzonych dolin poniżej poziomu morza, którą będą sprzyjały szybszej recesji po wycofaniu się czół lodowców na głębszą wodę (Grabiec i in., 2012). Przegłębienia dna lodowców poniżej poziomu morza pozwalają przypuszczać, że w przeszłości zasięg poszczególnych odnóg fiordu Hornsund był znacznie większy, niż współcześnie, a Hornsund mógł być cieśniną łączącą Morze Grenlandzkie z Morzem Barentsa (Grabiec i in., 2018). Grabiec i inni (2018) oraz Saferna i inni (2023) szacują, że otwarcie cieśniny Hornsund wskutek recesji lodowców uchodzących do morza nastąpi między 2053–2065 r.

Obserwacje współczesnych szarż lodowców uchodzących do Hornsundu skłaniają do postawienia pytania o występowanie szarż w przeszłości oraz możliwą synchroniczność okresów szarż lodowców w różnych obszarach Svalbardu z uwagi na wspólne czynniki wyzwalające, jak zwiększona dostawa wody do podłoża lodowca w cieplejszym klimacie (Jania, 1988; Błaszczyk i in., 2023). Zapis geomorfologiczny oraz mapy i fotografie historyczne wykazały, że szarże występowały w różnych obszarach Svalbardu również we wcześniejszych okresach holocenu (np. Farnsworth et al., 2016; Flink et al., 2018; Lovell et al., 2018; Aradóttir i in., 2019; Zagórski et al., 2023). Obecność charakterystycznych form rzeźby terenu dla lodowców szarżujących, takich jak grzbiety z wyciśnięcia szczelin dennych (*crevasse-squeeze ridges; CSRs*) lub wielkoskalowe lineacje glacjalne (*mega-scale glacial lineations; MSGLs*) dowodziłaby występowaniu szarż lodowców południowego Spitsbergenu w przeszłości (Evans, Rea, 1999; Ottesen i in., 2008; Farnsworth i in., 2016). Tym samym szarże lodowców tego obszaru odgrywałyby istotną rolę w zmianach ich zasięgu w holocenie. Farnsworth i inni (2016) korzystając ze zdjęć lotniczych wysokiej rozdzielczości zidentyfikowali grzbiety z wyciśnięcia szczelin dennych na przedpolach niektórych lodowców południowego Spitsbergenu, również tych, których szarżujący charakter był przedmiotem licznych dyskusji (np. Jania, Głowacki, 1996; Ćwiąkała i in., 2018). Weryfikacja w terenie pozwoli na identyfikację lodowców, które szarżowały przed okresem regularnych obserwacji glacjologicznych, kwestionując klasyfikację niektórych lodowców jako nieszarżujące w globalnej inwentaryzacji Randolph Glacier Inventory (RGI; Maussion i in., 2023; RGI 7.0 Consortium, 2023).

W niniejszej pracy stosuję nazwy geograficzne norweskie, zgodnie z opracowaniem *The Place Names of Svalbard* (Jaklin, 2003). Korzystałam również z zaktualizowanego zestawienia dostępnego w cyfrowej bazie danych Norweskiego Instytutu Polarnego (https://data.npolar.no/placename).

CEL BADAŃ

Głównym celem pracy doktorskiej była rekonstrukcja zmian zlodowacenia, w tym zmian zasięgu wybranych lodowców południowego Spitsbergenu w holocenie w kontekście roli szarż lodowcowych w ewolucji pokrywy lodowej wyspy. Nie analizowano szczegółowo fluktuacji lodowców od drugiej połowy lat 1970-tych, które stanowiły przedmiot licznych badań glacjologicznych z wykorzystaniem danych teledetekcyjnych (np. Błaszczyk i in., 2013, 2023; Ziaja i Ostafin, 2015; Saferna i in., 2023; Pawłowski i Ostafin, 2024), ale wykorzystano te wyniki dla zrozumienia procesu szarży i zmian ich zasięgu. Cele szczegółowe pracy doktorskiej obejmowały:

1) Ustalenie okresów awansów i recesji lodowców południowego Spitsbergenu na podstawie wyników datowania ^{14}C i ^{10}Be;

2) Identyfikację szarż wybranych lodowców sprzed okresu obserwacji satelitarnych (od II poł. lat 1970-tych) na podstawie dowodów geomorfologicznych i materiałów historycznych;

3) Wskazanie głównych czynników warunkujących zmiany zasięgu lodowców południowego Spitsbergenu w holocenie, ze szczególnym uwzględnieniem znaczenia szarż lodowców, jako procesu przyspieszającego deglacjację.

OBSZAR BADAŃ

Svalbard to archipelag wysp na Oceanie Arktycznym, rozciągający się między 74° a 81° N oraz 10° a 35° E. Do największych wysp należą: Spitsbergen, Nordaustlandet, Edgeøya, Barentsøya, Kvitøya, Prins Karl Forland, Kongsøya oraz Bjørnøya (Ryc. 1 a, b). Klimat Svalbardu kształtowany jest przez ujemny bilans radiacyjny, napływające z północy zimne masy powietrza arktycznego i cieplejsze, wilgotniejsze masy powietrza z południa, oraz ciepły Prąd Zachodniospitsbergeński i zimny Prąd Wschodniospitsbergeński (Walczowski, Piechura, 2011; Gjelten i in., 2016; Przybylak i in., 2016). Charakterystyczną cechą Svalbardu jest gradient klimatyczny między cieplejszym zachodnim Spitsbergenem a chłodniejszą wschodnią częścią archipelagu.

Obszar badań leży w południowej części Spitsbergenu i obejmuje wybrane lodowce w otoczeniu Hornsundu i w jego sąsiedztwie (Ryc. 1). Hornsund to najdalej położony na południe fiord Spitsbergenu o długości około 35 km i powierzchni 320 km^2, pomiędzy ziemiami Wedel Jarslberg Land i Torell Land na północy a Sørkapp Land na południu (Promińska i in., 2018). Lodowce pokrywają 67% powierzchni basenu glacjalnego Hornsundu (około 1200 km^2) i zdecydowaną większość stanowią lodowce uchodzące do morza, które reprezentują 97% zlodzonego obszaru (Błaszczyk i in., 2013). Większość lodowców wykazuje przebieg południkowy w nawiązaniu do głównych nasunięć i uskoków (Jania, 1988; Birkenmajer, 1990). Podobnie równoleżnikowy przebieg fiordu Hornsund nawiązuje do orientacji uskoków (Bednarek i in., 1993). Skały budujące obszar badań obejmują od metamorficznych i węglanowych skał prekambryjskich w zachodniej, przez paleozoiczne i triasowe skały węglanowe, piaskowce, zlepieńce i łupki w centralnej części Hornsundu po kredowe i paleoceńskie łupki, mułowce i piaskowce we wschodniej części fiordu (Birkenmajer, 1990; Harland, 1997). W latach 1979–2018 średnia roczna temperatura powietrza monitorowana w okolicy Polskiej Stacji Polarnej Hornsund (77°00’ N, 15°33’ E) wynosiła –3.7°C i wzrastała o 1,14°C na dekadę (Wawrzyniak, Osuch, 2020). Średnia roczna suma opadów w tym okresie wynosiła 478 mm i wzrastała o 61,6 mm na dekadę.

Obszar moich szczegółowych badań terenowych obejmował lodowce Hornbreen, Hansbreen, Vestre Torellbreen i Werenskioldbreen oraz ich przedpola. Hornbreen i Hansbreen uchodzą do Hornsundu, a Vestre Torellbreen kończy się częściowo na lądzie, a częściowo w zatoce Isfjellbukta. Werenskioldbreen w całości zakończony jest na lądzie. Charakterystykę lodowców przedstawiłam w artykułach składających się na niniejszą pracę doktorską (Osika i in., 2022; Osika, Jania, 2024; Osika i in., 2025a). Szerszy obszar objęto rekonesansowymi obserwacjami porównawczymi, a zwłaszcza analizie danych literaturowych oraz historycznych danych kartograficznych i fotograficznych.

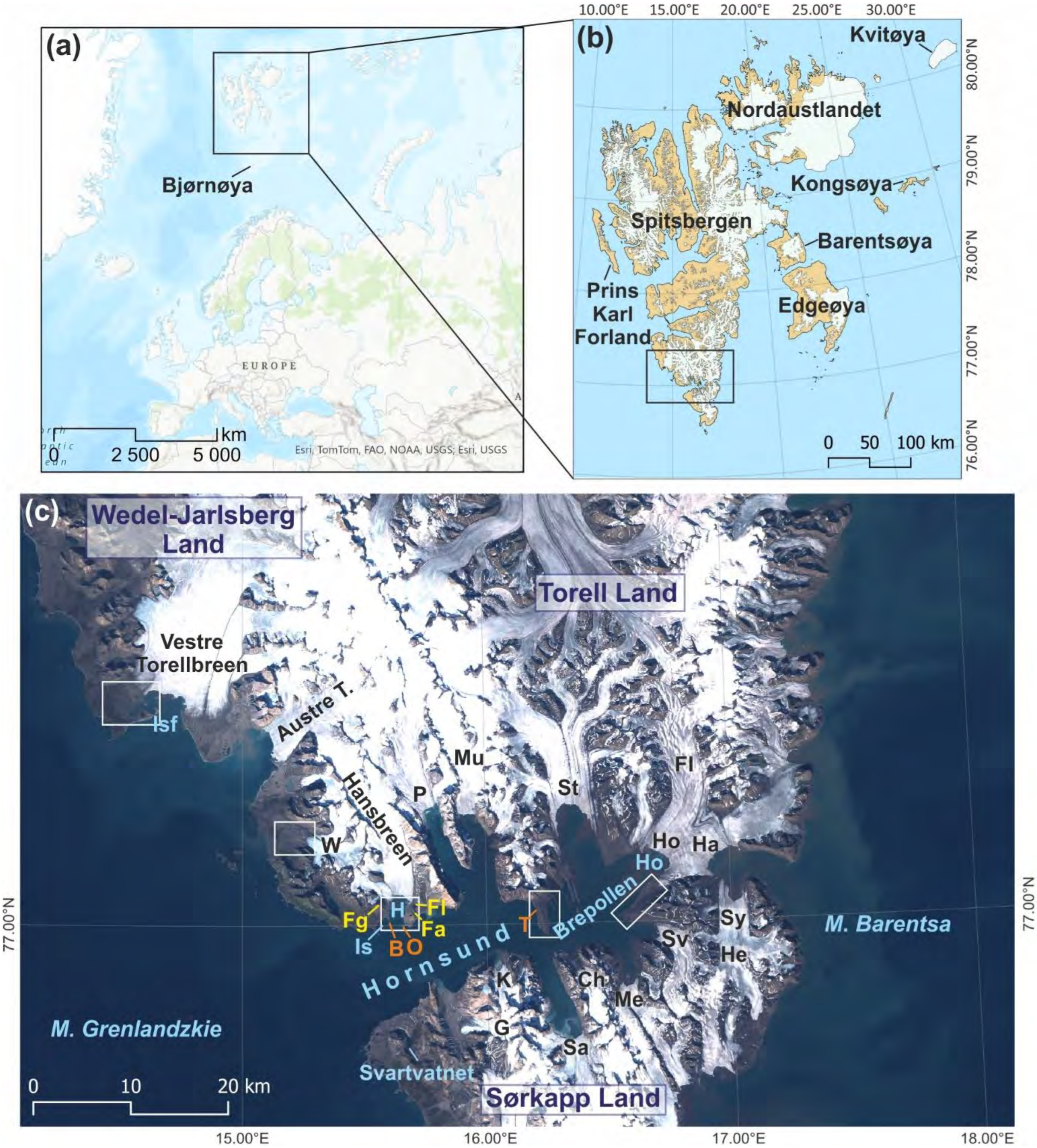

Ryc. 1. Obszar badań. **(a)** Lokalizacja Svalbardu; w tle: ESRI World Topographic Map oraz ESRI World Hillshade. **(b)** Obszar badań w południowym Spitsbergenie; dane wektorowe za © Norwegian Polar Institute (2014). **(c)** Obszar badan terenowych i poboru materiału do datowania ^{14}C i ^{10}Be (białe prostokąty). Lodowce (czarny tekst): Austre T. – Austre Torellbreen, Ch – Chomjakovbreen, Fl – Flatbreen, G – Gåsbreen, Ha – Hambergbreen, He – Hedgehogfonna, Ho – Hornbreen, K – Körberbreen, Me – Mendeleevbreen, Mu – Mühlbacherbreen, P – Paierlbreen, Sa – Samarinbreen, Sv – Svalisbreen, Sy – Sykorabreen, W – Werenskioldbreen. Zatoki (niebieski tekst): H – Hansbukta, Ho – Hornbukta, Is – Isbjørnhamna, Isf – Isfjellbukta. Półwyspy (pomarańczowy tekst): B – Baranowskiodden, O – Oseanograftnagen, T – Treskelen. Szczyty górskie i przełęcze (żółty tekst): Fa – Fannytoppen, Fg – Fugleberget, Fl – Flatpasset. W tle: zobrazowanie satelitarne Sentinel-2A z 08.08.2024 (https://browser.dataspace.copernicus.eu/).

Źródło: Osika i in. (2025a), zmienione

METODY

Podstawowym źródłem danych do opracowania niniejszej pracy były badania terenowe, które zrealizowałam podczas około 3-tygodniowych wypraw Uniwersytetu Śląskiego w sierpniu 2020, 2021, 2022 oraz 2024 r. Dodatkowe obserwacje przeprowadziłam podczas kilkudniowego pobytu w Hornsundzie na początku września 2023 r. Celem badań terenowych było kartowanie geomorfologiczne przedpoli lodowców oraz pobór materiału do datowania ^{14}C i ^{10}Be. Rekonstrukcję zmian zasięgu wybranych lodowców przeprowadziłam z wykorzystaniem różnego rodzaju danych i metod badawczych.

1. Studia literatury na temat paleogeografii Arktyki, Svalbardu i obszaru badań dostarczyły informacji na temat głównych okresów fluktuacji lodowców i warunków klimatycznych w holocenie (np. Divine i in., 2011; Luoto i in., 2018; Devendra i in., 2023; Jang i in., 2025) oraz danych geochronologicznych. Nowe wyniki i opublikowane daty ^{14}C i ^{10}Be były podstawą wyznaczenia okresów awansu i recesji lodowców południowego Spitsbergenu w holocenie (Osika i in., 2022, 2025a). Opracowania geomorfologiczne przedpoli lodowców (np. Ćwiąkała i in., 2018) oraz zestawienia lodowców szarżujących lub takich, które mogły szarżować w przeszłości (Farnsworth i in., 2016; RGI 7.0 Consortium, 2023) były punktem wyjścia analiz geomorfologicznych i identyfikacji szarż lodowców w przeszłości.

2. Kartowanie geomorfologiczne przedpoli lodowców przeprowadziłam na podstawie danych teledetekcyjnych wysokiej rozdzielczości oraz badań terenowych. Głównym celem kartowania była identyfikacja form rzeźby terenu charakterystycznych dla lodowców szarżujących, jak grzbiety z wyciśnięcia szczelin dennych (*crevasse-squeeze ridges*), ozy harmonijkowe (*concertina eskers*) lub wielkoskalowe lineacje glacjalne i podwodne systemy moren końcowych ze spływami osadów, które świadczyłyby o występowaniu szarż w przeszłości (Ryc. 2 i 3; Evans, Rea, 1999; Ottesen, Dowdeswell, 2006). Mapy i szkice opracowałam w programie QGIS w układzie współrzędnych WGS84/UTM33N. Jako źródła danych wykorzystałam:

(1) ortofotomapy przedpoli lodowców Hansbreen i Werenskioldbreen (rozdzielczość ok. 8 i 9 cm) oraz cyfrowe modele wysokości (rozdzielczość ok. 17 cm) ze zdjęć lotniczych pozyskanych podczas kampanii SIOS w czerwcu 2020 r., opracowane i opublikowane przez Błaszczyk i in. (2022),

(2) zobrazowania ESRI World Imagery (ESRI, 2025) o rozdzielczości 1,2 m, stosowane w opracowaniach geomorfologicznych (np. Reinthaler, Paul, 2023; McCerery i in., 2024),

(3) ortofotomapy o rozdzielczości 40 cm opracowane ze zdjęć lotniczych z 2010 i 2011 r., opublikowane jako wirtualny serwer mapowy WMTS przez Norweski Instytut Polarny (https://geodata.npolar.no),

(4) cyfrowy model wysokości ArcticDEM o rozdzielczości 2 m (Porter i in., 2023),

(5) cyfrowe modele dna morskiego na przedpolu lodowca Hansbreen udostępnione przez Norweską Służbę Hydrograficzną oraz z danych batymetrycznych opracowanych i opublikowanych przez Błaszczyk i in. (2021).

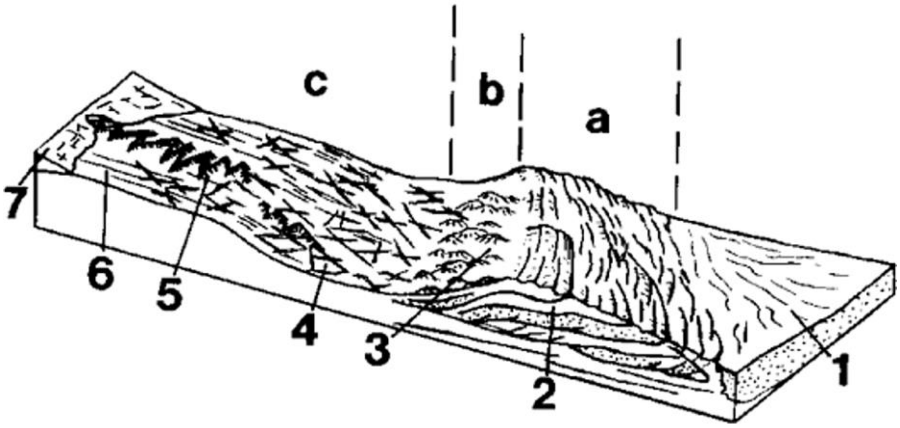

Ryc. 2. Zespół form rzeźby terenu charakterystycznych dla lodowców szarżujących (lądowa część przedpola): a) strefa zewnętrzna z proglacjalnie nasuniętymi osadami sprzed okresu wystąpienia fazy aktywnej szarży; b) strefa słabo rozwiniętej moreny pagórkowatej; c) strefa moreny żłobkowanej (*fluted moraine*), grzbietów z wyciśnięcia szczelin dennych (*crevasse-squeeze ridges*) i ozów harmonijkowych (*concertina eskers*); 1) proglacjalny stożek napływowy (*proglacial outwash fan*); 2) glacitektoniczna morena końcowa (*thrust-block moraine*); 3) morena pagórkowata (*hummocky moraine*); 5) oz harmonijkowy (*concertina esker*); 6) grzbiet moreny żłobkowanej (*fluting*); 7) lodowiec.

Źródło: Evans, Rea, 1999.

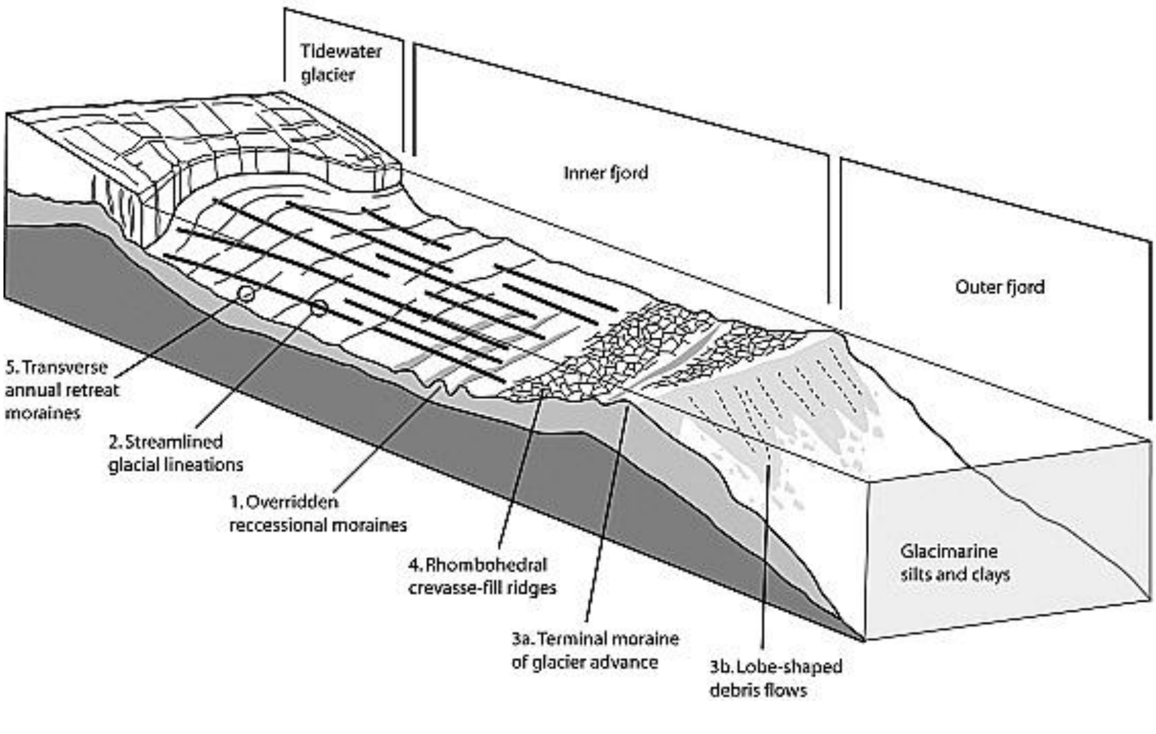

Ryc. 3. Zespół form rzeźby terenu charakterystycznych dla lodowców szarżujących uchodzących do morza (podwodna część przedpola): 1) moreny recesyjne przekroczone; 2) lineacje glacjalne; 3a) morena końcowa; 3b) loby spływów osadów na dystalnej stronie moreny końcowej; 4) grzbiety wypełnienia szczelin dennych o układzie romboedrycznym; 5) morenki roczne z awansów w okresie zimowym.

Źródło: Ottesen, Dowdeswell, 2006.

3. Analiza archiwalnych map i fotografii w celu analizy zmian zasięgu lodowców i rozpoznania szarż w przeszłości na podstawie charakterystycznych cech powierzchni lodowców (Tab. 1, Ryc. 4). Fotografie pozyskałam z Cyfrowego Archiwum Obrazów Biblioteki Narodowej Austrii (https://onb.digital/), cyfrowego archiwum fotografii Norweskiego Instytutu Polarnego (https://bildearkiv.npolar.no/fotoweb/), cyfrowego Archiwum Nikolaia Aleksandrovicha Morozova w Rosyjskiej Akademii Nauk (https://www.ras.ru/namorozovarchive/about.aspx) oraz archiwum obrazów lotniczych TopoSvalbard (https://toposvalbard.npolar.no/). Podobnie jak w opracowaniach na temat szarż lodowców w różnych częściach Arktyki (Jania, 1988; Lefauconnier, Hagen, 1991; Copland i in., 2003; Grant i in., 2009; Sund i in., 2009), jako najważniejsze kryteria identyfikacji szarż przyjęłam:

1) nagły, znaczący awans lodowca,

2) zafałdowania i zapętlenia moren środkowych oraz zafalowania foliacji,

3) stromość czoła, które przyjmuje formę nabrzmiałego lobu,

4) silne i chaotyczne uszczelinienie powierzchni, często sięgające górnej części lodowca.

5) widoczne strefy ścinania na granicy lodowca szarżującego z lodowcami dopływowymi w fazie uspokojenia.

4. Datowania ^{14}C materiału organicznego pozyskanego z osadów lodowcowych (muszli małży morskich, gleb kopalnych, drewna dryftowego i kości wieloryba). Materiał pozyskałam podczas prac terenowych w latach 2020–2022. Część muszli oraz żebro wieloryba pozyskano wcześniej (2019 i 1985 r.). Wybrane próbki materiału przekazałam do datowania radiowęglowego techniką AMS w Gliwickim i Poznańskim Laboratorium Radiowęglowym. Nowe (63) i opublikowane wcześniej daty (25) skalibrowałam w programie OxCal 4.4 stosując krzywe kalibracyjne Marine20 i IntCal20 (Heaton i in, 2020; Reimer i in., 2020) oraz korektę o pozorny wiek wody morskiej związany z efektem rezerwuarowym (Pieńkowski i in., 2022). Wyniki datowania przedstawiałam w artykułach Osika i in. (2022, 2025a) oraz w zestawie danych w repozytorium Zenodo (łącznie 88 dat, Osika i in., 2025b).

5. Datowania próbek skał z moreny Lodowca Hansa metodą izotopu kosmogenicznego ^{10}Be. Podczas badań terenowych w 2022 r. pozyskałam 3 próbki głazów z bocznej części moreny czołowej na przełęczy Flatpasset (ok. 160 m n.p.m.) oraz jeden głaz z trimline na stoku Fannytoppen. W 2021 i 2022 r. pozyskałam 7 próbek z moreny czołowej u podnóża Fannytoppen. Wstępną preparatykę próbek przeprowadziłam podczas stażu na Uniwersytecie w Zurychu w 2022 r. (kruszenie, przesiewanie, ługowanie wodą królewską, płukanie). Pozostałą część preparatyki chemicznej przeprowadził dr Dmitry Tikhomirov (Uniwersytet w Zurychu). Pomiary techniką AMS przeprowadzono na ETH. Wyniki przedstawiłam w artykule Osika i in. (2025a).

Rok	Rodzaj danych	Źródło
1613	Mapa	Narrative of a voyage to Spitzbergen in the year 1613 (Fotherby, 1613)
1625	Mapa	Mapa “Greneland” [Spitsbergen] w “Purchas His Pilgrimes” (Purchas, 1625)
1634	Mapa	Kaart van Spitsbergen door M.H. Middelhoven (Middelhoven, 1634)
1663	Mapa	Paskaert van Spitsbergen, met alle zijn zeekusten zoo veel tot noch toe bekent is (Doncker, 1663)
1714	Mapa	Nieuwe afteekening van Het Eyland Spits-Bergen opgegeven door de Commandeurs Giles en Outger Rep, en in't Ligt gebrat en uytgegeven (van Keulen, 1714)
1758	Mapa	Carte du Spits-Berg (Bellin, 1758)
1820	Mapa	A chart of Spitzbergen or East Greenland, comprising an original survey of the west coast (Scoresby, 1820)
1861–1864	Mapa	Karta ofver Spetsbergen: hufvudsakligast enligt iakttagelser under de svneska expeditionera aren 1861 och 1864 af N. Duner och A.E. Nordenskiold (Dunér and Nordenskiöld, 1865)
1872	Mapa	Die Arktische Expedition des Grafen Hans Wiltschek nach Spitzbergen & Nowaja Semlja Juni - Sept. 1872, 1:200 000 (Peterman, 1874)
1872	Fotografie	The Austro-Hungarian North Pole expedition (https://onb.digital/)
1897	Mapa	Ekspedycje Sir Martina Conway’a na Spitsbergen (Conway, 1898; https://data.npolar.no/map/archive/)
1899	Mapa	Plan öfver det svebsk-ryska gradmätningsnätet på Spetsbergen efter nyaste sammanstäld Maj 1900, 1:1 000 000 (de Geer, 1923)
1899–1901	Mapa	Océan Glacial arctique. Spitzberg. Région des travaux de l’expédition de l’Académies de sciences de Russie pour la mesure d’un arc de méridien en 1899–1901, 1:200 000 (Wassiliew, 1925)
1899–1901	Fotografie	The Swedish-Russian Arc-of-Meridian Expedition in 1899–1901 (https://www.ras.ru/)
1917–1918	Lądowe zdjęcia fotogrametryczne	Norweskie ekspedycje na Svalbard (https://bildearkiv.npolar.no/fotoweb/)
1918	Mapa	Mapa morska z lat 1917–1921 1917–1921, Hornsund to Dunderbay, 1:100 000 (Norwegian Polar Institute, 1921)
1918	Mapa	Mapa morska nr 504 z 1934 r., Frå Sørkapp til Bellsund, 1:200 000 (Hoel, 1938)
1936	Lotnicze zdjęcia fotogrametryczne (skośne) oraz ortofotomapa	Wyprawa norweska w 1936; Geyman et al., 2022 (dostępne na https://toposvalbard.npolar.no/)
1960	Mapa	Mapa morska nr 504 z 1984 r., Frå Sørkapp til Bellsund, 1:200 000 (Norwegian Polar Institute, 1984)

Tab. 1. Źródła danych historycznych wykorzystane do rekonstrukcji zmian zasięgu i identyfikacji szarż lodowców południowego Spitsbergenu. Za: Osika i in., 2025a (zmienione).

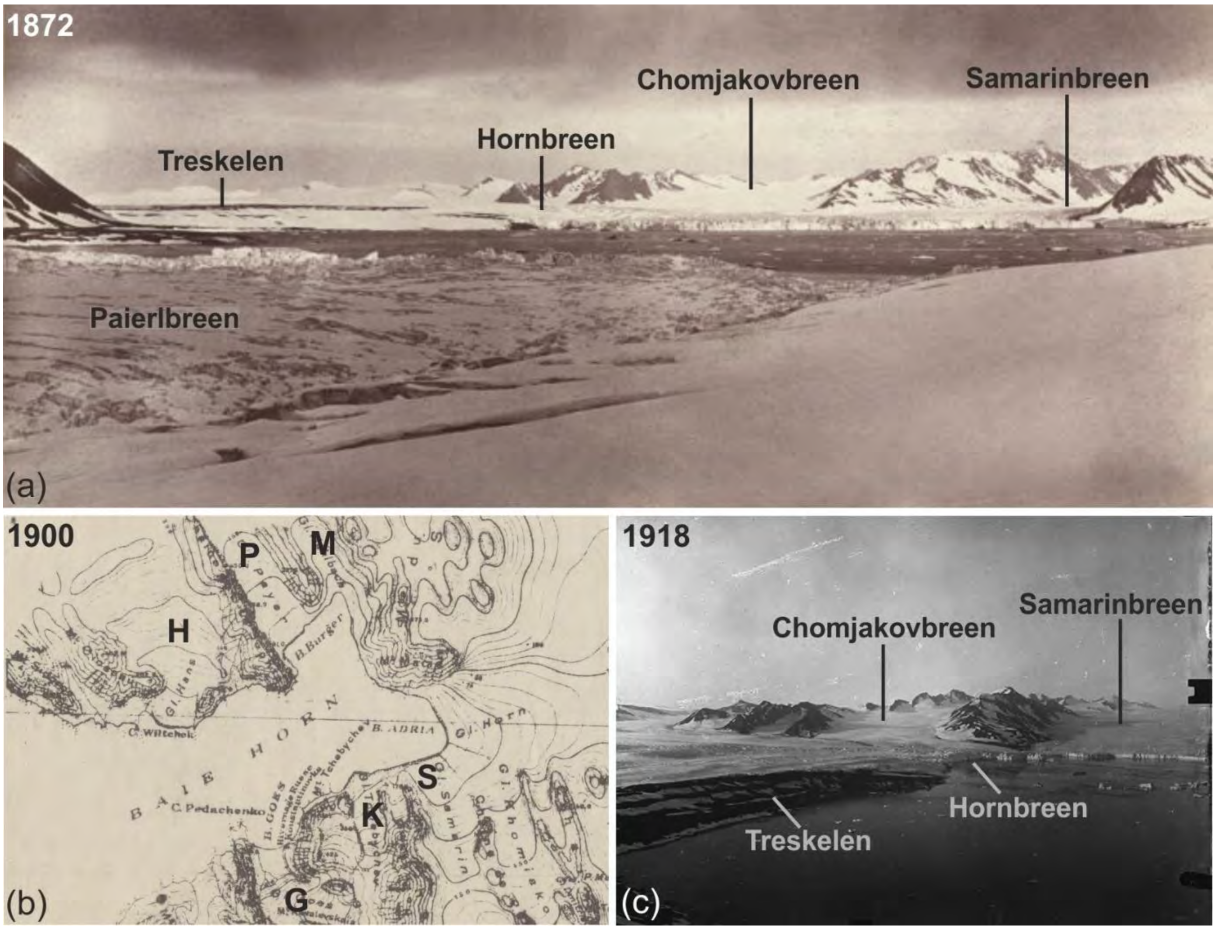

Ryc. 4. Przykłady danych historycznych na temat zasięgu lodowców Hornsundu. **(a)** Paierlbreen, Hornbreen, Chomjakovbreen i Samarinbreen na fotografii z wyprawy austro-węgierskiej w 1872 r. **(b)** Lodowce Hornsundu na mapie z wyprawy rosyjsko-szwedzkiej w latach 1899–1901 (Wassiliew, 1925). **(c)** Hornbreen, Chomjakovbreen i Samarinbreen na zdjęciu fotogrametrycznym z wyprawy norweskiej w 1918 r. Lodowce: G – Gåsbreen, H – Hansbreen, K – Körberbreen, M – Mühlbacherbreen, P – Paierlbreen, S – Samarinbreen.

Źródło: (a) Austrian National Library, Vienna, Signature: Pk 650, 19 (modified). (b) Wassiliew, 1925; https://data.npolar.no/map/archive. (c) © Adolf Hoel, Norsk Polarinstitutt (Numer zdjęcia: NBR9201_05204, zmienione).

WYNIKI

Datowania ^{14}C materiału z osadów lodowcowych

Obecność materiału organicznego (muszli małży morskich, kości wieloryba) w osadach moreny dennej i czołowej świadczy o przemieszczeniu i inkorporacji osadów morskich do systemu glacjalnego podczas awansu lodowców. Podobnie gleby kopalne i roślinność tundrowa znajdująca się poniżej warstwy gliny świadczą o recesji lodowców w cieplejszym klimacie i następującym po nim awansie lub awansach. Tym samym datowanie radiowęglowe materiału organicznego pozwala na odtworzenie zmian zasięgu lodowców w przeszłości.

Wyniki datowania radiowęglowego (63 próbki) i opublikowane wcześniej daty (25 dat) przedstawiałam w pracach Osika i in. (2022, 2025a) oraz w zestawie danych w repozytorium Zenodo (Osika i in., 2025b). Zdecydowaną większość stanowią próbki muszli z osadów moreny dennej i czołowej (70 dat, w tym 54 nowe; Ryc. 5 i 6).

Najwięcej próbek pozyskałam z przedpola lodowca Hansbreen (łącznie 35 dat, w tym 31 nowych). Oprócz 1 daty żebra wieloryba (nowej) i 9 dat tundry subfosylnej (w tym 5 nowych), pozostałe daty pochodzą z próbek muszli z osadów moreny dennej, czołowej i pagórkowatej. Dwie próbki muszli pobrałam z warstwy gliny pokrywającej góry lodowe odcielone z dolnej części klifu lodowca Hansbreen. Wszystkie daty z przedpola lodowca Hornbreen (29, w tym 18 nowych) pochodzą z próbek muszli z moreny dennej i pagórkowatej. Z przedpola Werenskioldbreen pozyskałam 4 nowe daty muszli z moreny dennej i czołowej, obok 10 opublikowanych wcześniej (po 5 dat muszli i tundry kopalnej). Z przedpola Vestre Torellbreen pozyskałam 10 nowych dat (7 dat muszli i 3 daty drewna dryftowego).

Spośród 70 próbek muszli z obszaru badań, 46 pochodzi z wczesnego holocenu, 7 ze środkowego, a 12 z późnego. Pozostałe próbki muszli są starsze, niż 11,7 cal ka BP i wszystkie pochodzą z przedpola Werenskioldbreen. Najstarsze próbki muszli z przedpoli pozostałych lodowców wydatowano na ok. 11,3 cal ka BP (Hansbreen, muszla z góry lodowej odcielonej z dolnej części klifu lodowca), 10,9 cal ka BP (Hornbreen, muszla z południowej części płw. Treskelen) i 10,5 cal ka BP (Vestre Torellbreen, muszla z moreny końcowej z MEL). Najmłodsze próbki muszli z przedpola lodowca Hansbreen zostały wydatowane na ok. 1,6 i 2,8 cal ka BP i pochodzą z moreny pagórkowatej u podnóża Fannytoppen i moreny dennej na płw. Baranowskiodden. 3 próbki muszli z przedpola lodowca Hornbreen są młodsze, niż 1950 r. Oprócz nich, najmłodsze próbki muszli pochodzą z płw. Treskelen i zostały wydatowane na ok. 1,3 cal ka BP (Birkenmajer, Olsson, 1997); 2,1 oraz 2,6 cal ka BP. Podobnie wiek jednej próbki muszli z przedpola Vestre Torellbreen wykracza poza krzywą kalibracyjną Marine20 (Heaton i in., 2020) i jest prawdopodobnie młodszy, niż 1950 r. Oprócz niej, najmłodsze próbki wydatowano na ok. 0,7 i 2,1 cal ka BP. Najmłodsza próbka muszli z przedpola Werenskioldbreen została wydatowana na ok. 10,0 cal ka BP (Traczyk, 2008). Charakterystyczną cechą datowanych muszli występowanie obok siebie próbek o skrajnie odmiennym wieku (od wczesnego po późny holocen), co wskazuje na silne wymieszanie materiału. Podobnie nie stwierdziłam prawidłowości między wiekiem muszli a wysokością nad poziomem morza lub odległością od czoła lodowca w okresie badań.

Materiał organiczny wytapiający się na powierzchni lodowca Hansbreen został wydatowany na środkowy holocen (Karczewski, Rachlewicz, 1999). Dla porównania, próbki drewna dryftowego z przedpola Vestre Torellbreen (nowe) oraz tundry subfosylnej i gleb kopalnych z przedpoli lodowców Hansbreen i Werenskioldbreen (nowe i opublikowane; Baranowski, Karlén, 1976; Pękala, 1989; Kasprzak i in., 2020) pochodzą z późnego holocenu. Wiek górnej warstwy tundry subfosylnej w obrębie moreny dennej lodowca Werenskioldbreen (c. 0,7 cal ka BP; Baranowski, Karlén, 1976) jest podobny do wieku tundry subfosylnej w niewielkiej progracjalnej morenie spiętrzonej (*push moraine*; ok. 0,6 i 0,7 cal ka BP; Kasprzak i in., 2020) oraz wieku listków torfowców w nowych próbkach pozyskanych spod warstwy gliny w południowej części przedpola Lodowca Hansa (ok. 0,6 cal ka BP). Próbki drewna dryftowego z grzbietów morenowych Vestre Torellbreen pozyskane podczas badań terenowych wydatowano na ok. 0,7; 0,6 i 0,2 cal ka BP.

Datowania ^{10}Be z moreny lodowca Hansbreen

Wyniki datowania głazów z moreny czołowej lodowca Hansbreen obejmują okres od $0{,}07^{+0{,}11}_{-0{,}07}$ ka do 10,07 ± 0,56 ka. Wyniki datowania głazu z trimline wskazują wiek 0,2 ± 0,04 ka. Większość dat nie przekracza 1,2 ka, z wyjątkiem jednej próbki z wczesnego holocenu (10,07 ± 0,56 ka) i trzech ze środkowego (6,75 ± 0,36 ka; 4,68 ± 0,27 ka oraz 4,65 ± 0,27 ka). Zarówno na przełęczy Flatpasset jak i u podnóża Fannytoppen nie stwierdziłam prawidłowości przestrzennych wieku próbek. W pierwszym obszarze daty ^{10}Be obejmują okres od 0,45 ± 0,04 ka do 10,07 ± 0,56 ka. U podnóża Fannytoppen, daty ^{10}Be obejmują okres od $0{,}07^{+0{,}11}_{-0{,}07}$ ka do 4,68 ± 0,27 ka (zewnętrzny grzbiet morenowy) oraz od 1,08 ± 0,07 ka do 6,75 ± 0,36 ka (wewnętrzny grzbiet, Ryc. 7).

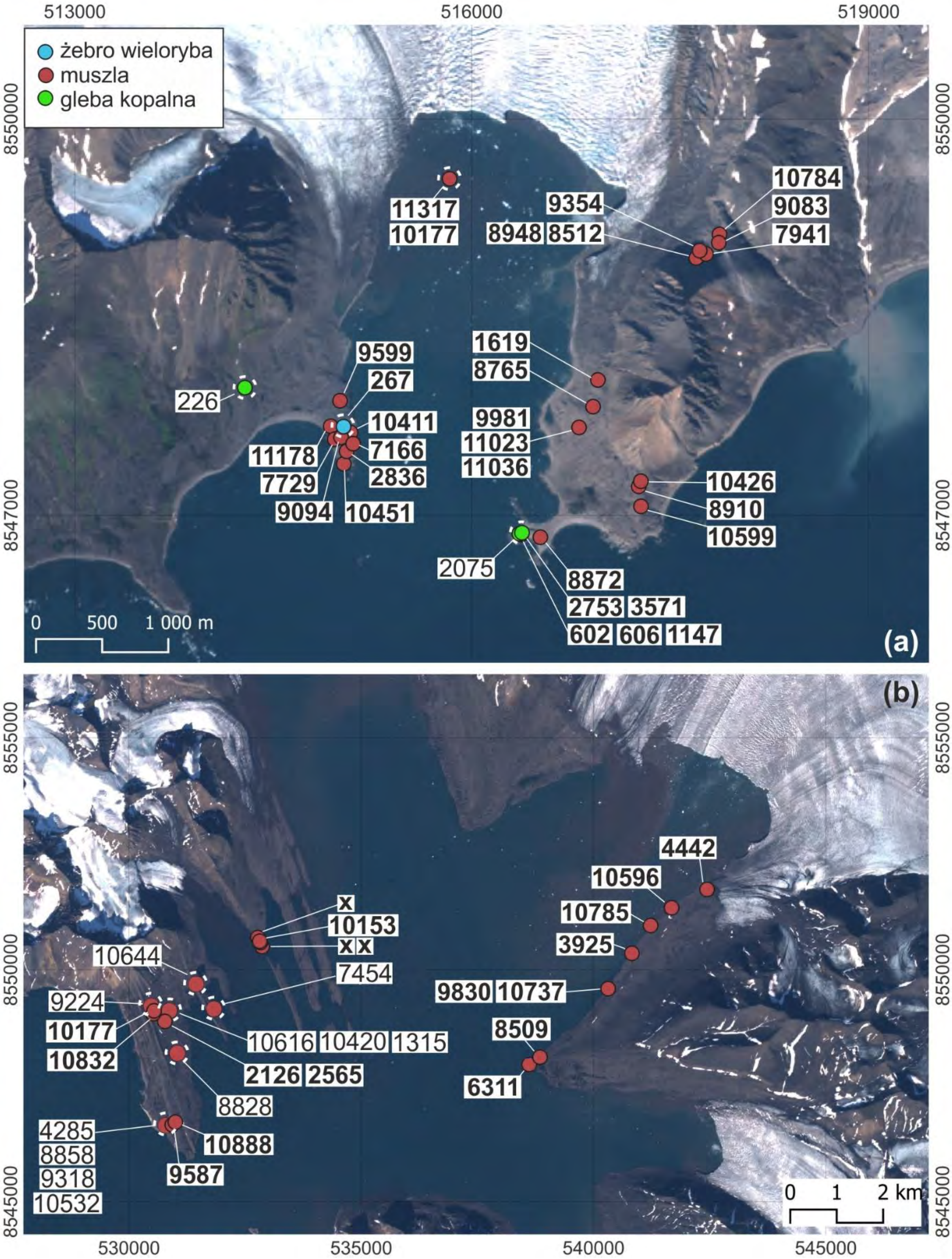

Ryc. 5. Nowe (pogrubione etykiety) i opublikowane wcześniej wyniki datowania radiowęglowego (mediana wieku kalendarzowego, cal BP) z przedpoli lodowców **(a)** Hansbreen i **(b)** Hornbreen. „x" oznaczyłam muszle młodsze, niż 1950 r., których wieku nie kalibrowałam. Linią przerywaną oznaczyłam próbki o przybliżonej lokalizacji. Współrzędne w metrach w układzie WGS 84 UTM 33N. W tle: zobrazowanie satelitarne Sentinel-2A z 08.08.2024 (https://browser.dataspace.copernicus.eu/).

Za: Osika i in., 2025 a, b (zmienione).

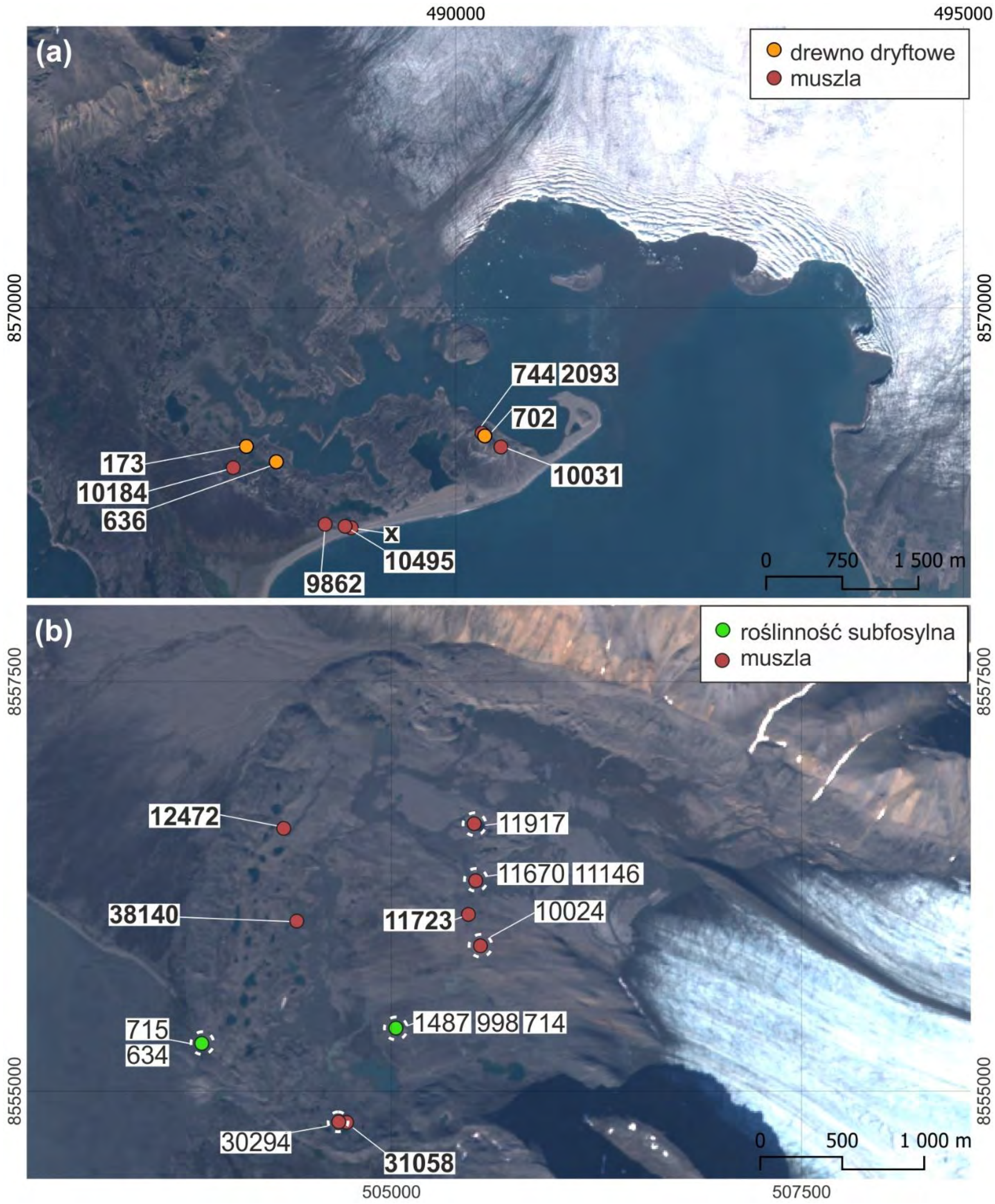

Ryc. 6. Nowe (pogrubione etykiety) i opublikowane wcześniej wyniki datowania radiowęglowego (mediana wieku kalendarzowego, cal BP) z przedpoli lodowców **(a)** Vestre Torellbreen i **(b)** Werenskioldbreen. „x" oznaczyłam muszlę, której wiek kalibrowany przekracza zakres krzywej kalibracyjnej dla organizmów morskich i prawdopodobnie jest młodszy, niż 1950 r. Linią przerywaną oznaczyłam próbki o przybliżonej lokalizacji. Współrzędne w metrach w układzie WGS 84 UTM 33N. W tle: zobrazowanie satelitarne Sentinel-2A z 08.08.2024 (https://browser.dataspace.copernicus.eu/).

Za: Osika i in., 2025 a, b (zmienione).

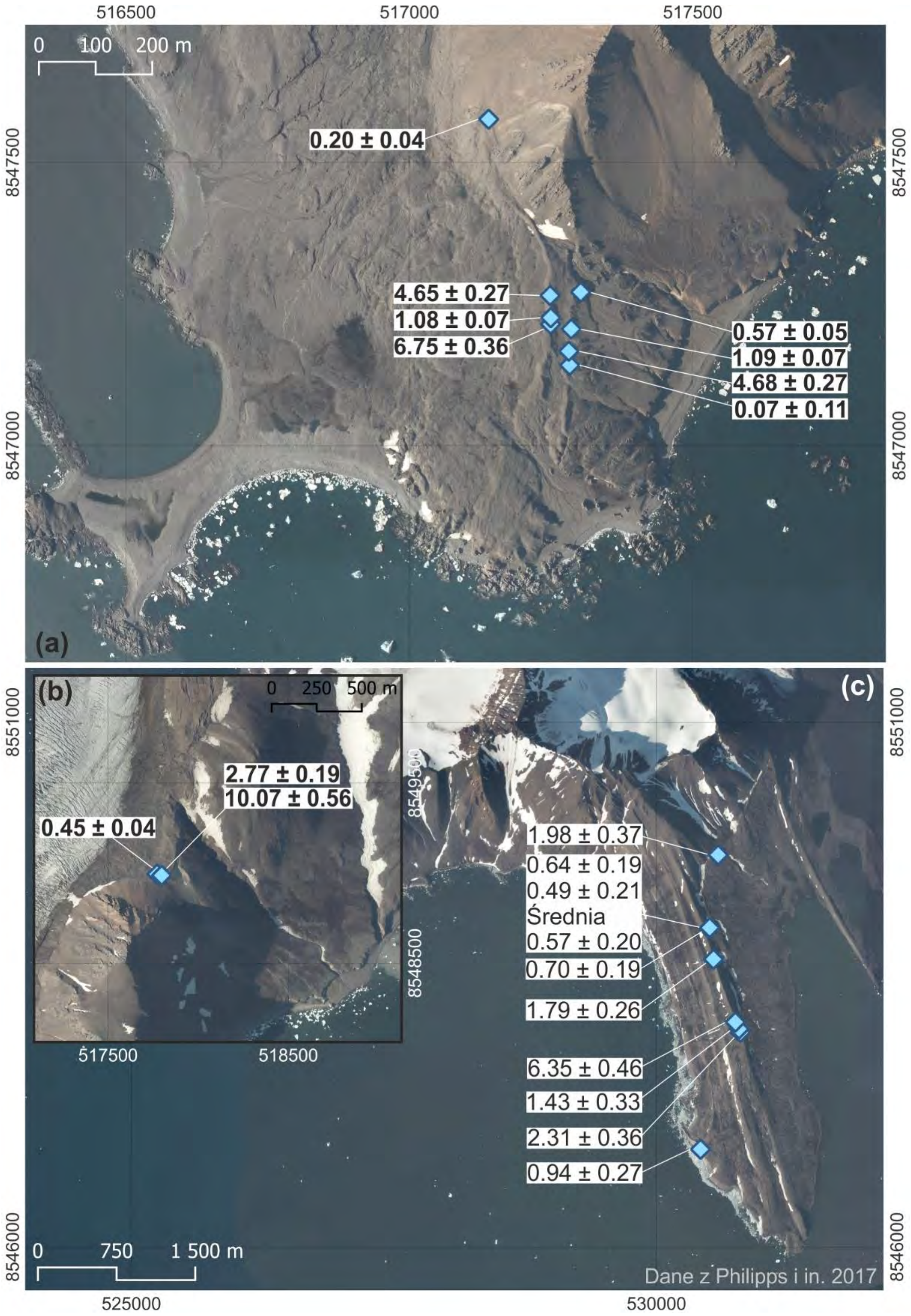

Ryc. 7. Nowe i opublikowane wyniki datowania głazów z moren lodowców w Hornsundzie. **(a, b)** Wyniki datowania ^{10}Be głazów z moreny lodowca Hansbreen. **(c)** Opublikowane daty ^{10}Be głazów z moreny lodowca Hornbreen (Philipps i in., 2017). Współrzędne w metrach w układzie WGS 84 UTM 33N. W tle: TopoSvalbard, © Norwegian Polar Institute (https://toposvalbard.npolar.no/).

Źródło: Osika i in., 2025a (zmienione).

Zapis szarż wybranych lodowców południowego Spitsbergenu w rzeźbie terenu

Wyniki kartowania geomorfologicznego wykazały obecność różnorodnych form rzeźby terenu, w tym grzbietów z wyciśnięcia szczelin dennych (*crevasse-squeeze ridges, CSRs*), uważanych za formy charakterystyczne dla lodowców szarżujących (Tab. 2; Evans, Rea, 1999; Ottesen, Dowdeswell, 2006; Farnsworth i in., 2016; Ben-Yehoshua i in., 2023). Szczególną uwagę zwraca boczna część moreny czołowej Lodowca Hansa na przełęczy Flatpasset (ok. 160 m n.p.m.), która wskazuje próbę przekroczenia masywu górskiego przez awansujący lodowiec. W rzeźbie dna Hansbukty występują lineacje lodowcowe (*streamlined glacial lineations*) oraz formy z wyciśnięcia szczelin dennych i/lub morenki roczne z awansów w okresie zimowym. W obrębie Hansbukty i Isbjørnhamny zidentyfikowałam moreny czołowe ze spływami osadów po stronie dystalnej, które sugerują co najmniej dwie szarże lodowca Hansbreen w przeszłości. Na przedpolach lodowców Werenskioldbreen i Vestre Torellbreen występują ozy harmonijkowe (*concertina eskers*), które również są uważane za formy rzeźby diagnostyczne dla lodowców szarżujących (Evans, Rea, 1999). W środowisku lądowym, formy szczelinowe z wyciśnięcia (*CSRs*) zachowały się w obszarach ograniczonej działalności wód roztopowych, w szczególności na drumlinach i mutonach pokrytych warstwą moreny dennej. Ich identyfikację nierzadko utrudnia zaawansowany stopień zatarcia form, które przyjmują postać kopców zbudowanych z gliny (30–50 cm wysokości) lub pasów osadów (kilka – kilkanaście cm wysokości), których układ nawiązuje do sieci przecinających się grzbietów. Kontrast ten jest szczególnie widoczny na przedpolu lodowca Hansbreen, gdzie grzbiety z wyciśnięcia szczelin dennych przyjmują formę od wyraźnych, przecinających się grzbietów (do 50 cm wysokości) w północno-zachodniej części przedpola, po pojedyncze kopce i pasy osadów w południowo-wschodniej części. Na przedpolu lodowca Werenskioldbreen, formy te występują w południowo-wschodniej części przedpola, w strefie drumlinów skalnych pokrytych warstwą moreny dennej i przyjmują postać niskich grzbietów (do 20 cm wysokości) zbudowanych z gliny. Na przedpolach lodowców Hornbreen i Vestre Torellbreen, grzbiety z wyciśnięcia szczelin dennych są wyraźnie rozwinięte, wyższe (powyżej 1 m) i przyjmują postać kopców oraz przecinających się grzbietów. Opis geomorfologiczny przedpoli lodowców przedstawiłam w artykułach składających się na niniejszą pracę doktorską, w szczególności Osika i Jania (2024).

Lodowiec	Formy rzeźby terenu							
	Grzbiety z wyciśnięcia szczelin dennych (*CSRs*)	Morena żłobkowana (*fluted moraine*)	Drumliny	Ozy harmonijkowe (*concertina eskers*)	Morena pagórkowata	Morena końcowa z jądrem lodowym	Proglacjalna morena czołowa, spiętrzona (thrust block moraine / push moraine)	Rozległe sandry
Hansbreen	+	+	+		+	+		
Hornbreen	+	+			+	+		
Werenskiold-breen	+	+	+	+	+	+	+	+
Vestre Torellbreen	+	+	+	+	+	+	+	+

Tab. 2. Wybrane formy rzeźby terenu lądowej części przedpoli lodowców Hansbreen, Hornbreen, Werenskioldbreen i Vestre Torellbreen.

Zapis szarż wybranych lodowców w materiałach historycznych

Wyniki analiz historycznych map i fotografii przedstawiałam w pracach Osika, Jania (2024) oraz Osika i in. (2025a). Mapy z XVII i XVIII w. mają charakter szkiców przedstawiających uproszczony zarys linii brzegowej Hornsundu (Tab. 1). Niemniej, poszczególne odnogi fiordu wydają się bardziej rozległe, niż w XIX w., co sugeruje mniejszy zasięg lodowców uchodzących do morza w porównaniu z maksimum Małej Epoki Lodowej (MEL). Na mapie z wyprawy szwedzkiej w latach 1861–1864 (Dunér, Nordenskiöld, 1865) zasięg lodowców uchodzących do Hornsundu wydaje się większy, niż w opracowaniach kartograficznych z XVIII w. Dokładność map nie pozwala na dokładniejszą analizę zmian zasięgu lodowców.

Zdecydowanie więcej danych na temat stanu lodowców dostarczają fotografie, w szczególności z wyprawy austro-węgierskiej w 1872 r. i norweskiej w 1918 r. Fotografie z 1872 r. udokumentowały większość lodowców uchodzących do Hornsundu i ujawniły przesłanki trwającej szarży lodowca Hansbreen. W 1872 r. zasięg lodowca był mniejszy, niż lokalizacja moreny końcowej z okresu MEL, a powierzchnia lodowca silnie i chaotycznie uszczeliniona, z widocznym nabrzmieniem w dolnej części lodowca i stromym czołem w formie lobu. Podobnie silnie, chaotycznie uszczeliniona powierzchnia lodowca Paierlbreen i zasięg nawiązujący do lokalizacji moreny czołowej z MEL sugeruje szarżę krótko przed wykonaniem fotografii. W tym czasie Hornbreen spoczywał na płw. Treskelen i przekroczył jego południową część. Zdjęcia fotogrametryczne z wyprawy norweskiej w 1918 r. dostarczają przesłanek fazy uspokojenia lodowca Hansbreen, którego zasięg nawiązywał do lądowej i podmorskiej części moreny końcowej z MEL, a powierzchnia była pokryta siecią wąskich, przecinających się szczelin, obejmujących znaczną część głównego strumienia lodowca. W porównaniu z 1872 r., czoło lodowca Hornbreen wycofało się w południowej części, a Chomjakovbreen i Mühlbacherbreen awansowały. W 1918 r. Werenskioldbreen wykazywał przejawy fazy uspokojenia po szarży, której dowodem była zapętlona morena środkowa. Zdjęcia lotnicze skośne z 1936 r. wykazały rozległą recesję lodowców Hornsundu w porównaniu z 1918 r.

DYSKUSJA

Interpretacja i ograniczenia poszczególnych metod

Kartowanie geomorfologiczne przedpoli lodowców było oparte o dane teledetekcyjne wysokiej rozdzielczości, które pozwoliły na rozpoznanie nawet mniejszych form, jak grzbiety z wyciśnięcia szczelin dennych, poszczególne grzbiety (*flutes*) moreny żłobkowanej oraz kemy. Wyniki kartowania weryfikowałam podczas badań terenowych. Mimo bardzo wysokiej rozdzielczości ortofotomapy, która była podstawą kartowania przedpola lodowca Werenskioldbreen (ok. 9 cm), liczba grzbietów z wyciśnięcia szczelin dennych może być niedoszacowana z uwagi na niewielkie rozmiary form. W południowo-wschodniej części jego przedpola w sierpniu 2024 r. zidentyfikowałam grzbiety o szerokości i wysokości ok. 20 cm, które nie były widoczne na ortofotomapie. Przykład ten wskazuje konieczność badań terenowych w rozpoznaniu form uważanych za diagnostyczne dla szarż lodowców, których rozwój i morfometria ściśle zależą od rodzaju i ilości dostępnego materiału i które szybko ulegają degradacji wskutek działalności wód roztopowych i procesów peryglacjalnych (Farnsworth i in., 2016; Ben-Yehoshua i in., 2023).

Pozyskane muszle małży morskich i żebro wieloryba redeponowane w osadach lodowcowych, jak również gleby kopalne pokryte warstwą gliny, stanowią zapis okresów recesji lodowca w cieplejszych okresach holocenu i następujących po nich awansów. Bardzo duże zróżnicowanie wieku muszli małży morskich w osadach moren dennych i czołowych wskazuje na wymieszanie osadów podczas awansu. Biorąc pod uwagę wymagania środowiskowe datowanych gatunków, wyniki datowania wskazują okresy recesji lodowców uchodzących do morza, która pozwoliła na kolonizację fiordów. Małże *Mya truncata*, *Hiatella arctica*, *Chlamys islandica* czy *Astarte borealis* wykazują wrażliwość na wysoką koncentrację zawieszonych osadów nieorganicznych, typową dla przedpoli lodowców uchodzących do morza. Współcześnie występują w centralnej lub zewnętrznej części fiordów arktycznych, gdzie stężenie materiału jest mniejsze (Włodarska-Kowalczuk i in., 1998; Różycki, 1992; Włodarska-Kowalczuk, 2007; Aswathy et al., 2023). W przypadku odpowiednio dużej liczby próbek, brak małży w poszczególnych okresach może sugerować awans lodowców uchodzących do morza (Osika i in., 2022). Podobnie minimalny wiek awansu lodowców może być interpretowany na podstawie wieku subfosylnych gleb lub tundry kopalnej przykrytej warstwą diamiktonu (Baranowski and Karlén, 1976; Kaprzak i in., 2020).

Datowanie próbek głazów metodą izotopu kosmogenicznego ^{10}Be jest powszechnie stosowane do określenia wieku depozycji moren (Balco, 2011). Wyniki datowania próbek z moreny czołowej lodowca Hansbreen są silnie zróżnicowane zarówno między poszczególnymi stanowiskami poboru głazów, jak również w obrębie poszczególnych grzbietów morenowych. Rozproszone daty ^{10}Be, w szczególności z wczesnego i środkowego holocenu, nie są poparte wynikami datowania radiowęglowego materiału z przedpola lodowca Hansbreen, wynikami datowania ^{10}Be głazów z moreny lodowca Hornbreen (Philipps i in., 2017), ani zmianami zawartości detrytusu glacjalnego z dryfujących gór lodowych (*ice-rafted debris; IRD*) w osadach na przedpolu Hornsundu (Devendra i in., 2023). Z tego względu uważam, że otrzymane daty ^{10}Be nie odzwierciedlają rzeczywistego wieku moren z uwagi na wysoką zawartość nuklidów odziedziczonych z wczesnego i środkowego holocenu. W tym okresie lodowce Arktyki, w tym Svalbardu, uległy recesji wskutek ocieplenia klimatu i osiągnęły minimalne zasięgi w holocenie lub zanikły (Farnsworth i in., 2020; Larocca, Axford, 2022). Problem „postarzonych" dat wystąpił podczas datowania moreny grenlandzkiego lodowca Gletscherlukket, pochodzącej z MEL (Larsen i in., 2021). Otrzymane daty ^{10}Be obejmowały okres od 10.2 to 1.6 ka, co autorzy przypisali obecności nuklidów odziedziczonych z wczesnego i środkowego holocenu. W Hornsundzie, Philipps i in. (2017), analizując zmiany zasięgu Lodowca Horna, pominęli najstarszą datę ^{10}Be głazów morenowych z płw. Treskelen (6,35 ± 0,46 ka) jako odstającą od pozostałych dat, które w większości obejmowały drugą połowę późnego holocenu. Z uwagi na odziedziczenie nuklidów, wyniki datowania ^{10}Be głazów morenowych z przedpola lodowca Hansbreen nie zostały uwzględnione w analizie zmian zasięgu lodowców Hornsundu w holocenie.

Spośród analizowanych materiałów historycznych, najwięcej danych na temat stanu lodowców dostarczyły fotografie z wyprawy austro-węgierskiej w 1872, naziemne zdjęcia fotogrametryczne z wyprawy norweskiej w 1918 r. i zdjęcia lotnicze skośne z 1936 r. Bardzo wysoka jakość zdjęć pozwoliła na rozpoznanie charakterystycznych cech powierzchni lodowców wskazujących fazę aktywną szarży (m.in. gęsta sieć głębokich szczelin o chaotycznym przebiegu obejmujących znaczną część powierzchni lodowca, wypukłe czoło lodowca), wczesną fazę uspokojenia (rozległy zasięg lodowca nawiązujący do rozpoznanych moren końcowych, gęsta sieć zaciśniętych szczelin) lub zaawansowaną recesję lodowców (wklęsły przebieg czoła). Ograniczenia w rozpoznaniu przesłanek szarż dotyczą liczby fotografii dokumentujących poszczególne lodowce oraz odległości, z której wykonano zdjęcia. Przykładowo, fotografie lodowca Hansbreen z 1872 r. udokumentowały strefę czołową, ale nie objęły wyższych partii lodowca. Zdjęcia fotogrametryczne z 1918 r. wykonane z Fannytoppen pozwoliły ocenić stan znacznej części głównego strumienia i zidentyfikować zaciśnięte, przecinające się szczeliny sięgające wysoko w górę lodowca (Osika, Jania, 2024). Zdjęcia fotogrametryczne strefy czołowej niektórych lodowców (np. Vestre Torellbreen z 1918 r.) są silnie prześwietlone, co utrudniło i/lub uniemożliwiło ich interpretację. Ze względu na ograniczoną dokładność, mapy historyczne (Tab. 1) dostarczyły danych jakościowych na temat fluktuacji lodowców (większy/mniejszy zasięg). W przypadku lodowców uchodzących do morza, awans lub recesja były odzwierciedlone zmianą linii brzegowej Hornsundu.

Fluktuacje lodowców południowego Spitsbergenu w holocenie

Na podstawie wyników datowania radiowęglowego, opublikowanych dat radiowęglowych i ^{10}Be z Hornsundu, materiałów historycznych oraz opublikowanych danych paleoklimatycznych (mi.in. Divine i in., 2011; Luoto i in., 2018; Devendra i in., 2023) wyróżniłam następujące okresy fluktuacji lodowców południowego Spitsbergenu:

1. Deglacjację na przełomie plejstocenu i holocenu,
2. Recesję lodowców we wczesnym i środkowym holocenie,
3. Rozwój lodowców w pierwszej połowie późnego holocenu (zasięgi lodowców mniejsze, niż maksymalne z Małej Epoki Lodowej),
4. Awanse lodowców ok. 2,2–1,5 cal ka BP,
5. Recesję lodowców ok. 1,5–1,0 cal ka BP,
6. Awanse lodowców od ok. 0,7 cal ka BP,
7. Małą Epokę Lodową, w której maksymalne zasięgi lodowców były bezpośrednim efektem szarż.

Szczegółowy opis poszczególnych faz znajduje się w artykule Osika i in. (2025a).

Podczas ostatniego zlodowacenia, Hornsund stanowił drogę odpływu jednego ze strumieni lodowych lądolodu Svalbardu i Morza Barentsa (Ottesen i in., 2007). Datowanie wieku ekspozycji powierzchni skalnych izotopami ^{10}Be, ^{26}Al oraz *in situ* ^{14}C dostarczyło przesłanek deglacjacji południowo-zachodniego Spitsbergenu między 18 a 16 ka oraz deglacjacji centralnej i wewnętrznej części Hornsundu przed 13,3 ± 0,6 i 13,0 ± 0,7 ka (Young i in., 2018). Nowe wyniki datowania radiowęglowego muszli z moreny czołowej Werenskioldbreen wskazują na recesję lodowca przed 12,5 cal ka BP. Nowe i opublikowane wcześniej daty muszli z przedpola lodowca i z osadów wytapiających się na jego powierzchni (Birkenmajer, Olsson, 1998) wykazały, że recesja lodowca występowała do okresu wyniesienia terasy morskiej po 10,0 cal ka BP (najmłodsza data muszli). Podobnie jak w innych regionach Svalbardu, recesja lodowców w obszarze badań utrzymywała się we wczesnym i środkowym holocenie ze względu na zwiększone nasłonecznie w okresie letnim i wzrost średnich wartości temperatury powietrza, jak również wzrost temperatury wody morskiej przez zwiększony napływ ciepłej wody atlantyckiej niesionej przez Prąd Zachodniospitsbergeński (Telesiński i in., 2018; Farnsworth i in., 2020; Devendra i in., 2023). Zapisem recesji lodowców są liczne muszle małży z ich przedpoli datowane na wczesny i środkowy holocen oraz niskie wartości detrytusu glacjalnego z dryfujących gór lodowych (*ice-rafted debris; IRD*) w osadach na przedpolu Hornsundu (Ryc. 8; Devendra i in., 2023). Podczas badań nie uzyskałam dowodów awansów lodowców we wczesnym holocenie, które stwierdzono w innych obszarach Svalbardu (np. Kłysz i in., 1988; Farnsworth i in., 2017, 2018, 2024). Lindner i in. (1986) oraz Lindner i Marks (1993) wyróżnili okres awansu lodowców około 8 ka BP (stadiał Grönfjorden), jednak nasze badania nie dostarczyły przesłanek awansu lodowców w tym okresie. Rozbieżności mogą wynikać z ograniczonej liczby datowanych próbek muszli małży z moreny lodowca Hornbreen na płw. Treskelen, jakimi dysponowali Marks i Pękala (1986).

Autorzy zinterpretowali wyniki datowania radiowęglowego (około 8 ka BP) jako przybliżony wiek awansu lodowca Hornbreen i prawdopodobnie pozostałych lodowców Hornsundu. Interpretacja ta była powtarzana w późniejszych pracach (Lindner i in., 1986; Lindner, Marks, 1993). Tarasov i in. (1992) oraz Birkenmajer i Olsson (1997) opublikowali więcej dat muszli z pływ. Treskelen, które objęły zarówno wczesny, środkowy, jak i późny holocen. Na tej podstawie Birkenmajer i Olsson (1997) wykluczyli awans lodowca po pływ. Treskelen we wczesnym holocenie. Podczas badań stwierdziłam podobne zróżnicowanie dat muszli małży z tego obszaru, co wskazuje na silne wymieszanie materiału (Osika i in., 2022, 2025 a, b). Warunki klimatyczne wczesnego holocenu nie zapewniały pozytywnego bilansu masy lodowców i możliwe awanse w tym okresie najpewniej miałyby charakter szarż (Farnsworth i in., 2020). Farnsworth i in. (2024) stwierdzili awanse niektórych lodowców wyprowadzających z czapy lodowej Åsgardfonna na przełomie plejstocenu i holocenu, które wiązali z odprężeniem glacjoizostatycznym i podniesieniem obszaru powyżej wysokości linii równowagi bilansowej (*eguilibrium line altitute; ELA*). Analiza relatywnych krzywych zmian poziomu morza wskazuje mniejsze podniesienie regionu Hornsundu w porównaniu w północno-wschodnim Spitsbergenem (Farnsworth i in., 2020). Ze względu na mniejsze podniesie obszaru, odprężenie glacjoizostatyczne miało ograniczony wpływ na rozwój lodowców południowego Spitsbergenu, a nisko położone pola akumulacyjne dodatkowo utrudniały nagromadzenie masy i odbudowę lodowców. Przypuszczalnie, zasięgi lodowców południowego Spitsbergenu były mniejsze z uwagi na ograniczenia topograficzne, a późniejsze awanse zatarły ślady wcześniejszej dynamiki.

Spadek średnich wartości temperatury powietrza oraz ograniczony napływ ciepłej wody atlantyckiej w późnym holocenie pozwoliły na zmniejszenie ablacji powierzchniowej i frontalnej oraz odbudowę lodowców (np. Forwick i in., 2010; Skirbekk i in., 2010; Telesiński i in., 2018; Allaart i in., 2021; Devendra i in., 2023). Mimo rozwoju lodowców uchodzących do Hornsundu przed ok. 4,0 cal ka BP (Jang i in., 2025), wyniki datowania muszli małży i gleb kopalnych wskazują, że ich zasięgi były znacznie mniejsze, niż podczas maksimum Małej Epoki Lodowej. Małże wrażliwe na wysoką koncentrację zawieszonego materiału nieorganicznego występowały w obrębie maksymalnych zasięgów lodowców z MEL ok. 2,8 cal ka BP (Hansbreen), 2,5 i 2,1 cal ka BP (Hornbreen – pływ. Treskelen) oraz 2,1 cal ka BP (Vestre Torellbreen). Podobnie pływ. Oseanograftangen na przedpolu lodowca Hansbreen był wolny od lodu w pierwszej połowie późnego holocenu, jak wskazują daty gleby kopalnej przykrytej warstwą gliny (ok. 3,6; 2,8 i 2,1 cal ka BP; Pękala, 1989; Osika i in., 2025b). Uważam, że ograniczony zasięg lodowców uchodzących do morza w pierwszej połowie późnego holocenu mógł być związany ze zwiększonym napływem ciepłej wody atlantyckiej i wzrostem temperatury wody, który stwierdzono na przedpolu Hornsundu ok. 2,2–1,8 cal ka BP (Devendra i in., 2023), jak również w Isfjorden (Brice i in., 2023) czy wschodnim Svalbardzie (Pawłowska i in., 2020). Rekonstrukcje paleoklimatyczne na podstawie danych z jeziora Svartvatnet w Hornsundzie dodatkowo wskazały wzrost średniej rocznej i lipcowej temperatury powietrza, który ograniczałby tempo rozwoju lodowców w tym okresie (Ryc. 8; Luoto i in., 2018).

Awanse lodowców południowego Spitsbergenu występowały ok. 2,2–1,5 cal ka BP. Na podstawie wyników datowania ^{10}Be, Hornbreen zwiększył swój zasięg po płw. Treskelen ok. 1,9 ± 0,3 ka (Ryc. 7c; Philipps i in., 2017) i awans ten mógłby nawiązywać do wysokich wartości detrytusu glacjalnego z dryfujących gór lodowych (*IRD*) w osadach na przedpolu Hornsundu i centralnej części fiordu ok. 2,2 cal ka BP (Devendra i in., 2023; Jang i in., 2025). Co istotne, awans ten wystąpił w okresie wzrostu średniej rocznej temperatury powietrza i temperatury wody ok. 2,2–1,9 cal ka BP (Ryc. 8; Luoto i in., 2018; Devendra i in., 2023), co mogłoby sugerować szarżę zamiast awansu związanego wyłącznie z ochłodzeniem klimatu. Spośród lodowców kończących się na lądzie, wyniki datowania radiowęglowego tundry kopalnej pomiędzy dwiema warstwami gliny sugerują awans lodowca Werenskioldbreen przed 1,5 cal ka BP (Baranowski, Karlén, 1976), a wyniki datowania ^{10}Be moren lodowca Scottbreen sugerują jego awans ok. 1,7 ± 0,1 ka (Philipps i in., 2017).

Recesja lodowców wystąpiła podczas Średniowiecznego Okresu Ciepłego między 1,5–0,7 cal ka BP (Miller i in., 2010; Divine i in., 2011). Nowe i opublikowane wyniki datowania muszli małży wskazują recesję lodowca Hansbreen ok. 1,6 cal ka BP, Hornbreen ok. 1,3 cal ka BP (Birkenmajer, Olsson, 1997) oraz Vestre Torellbreen ok. 0,7 cal ka BP. Podobnie wyniki datowania listków torfowców i gleby kopalnej wskazują, że płw. Oseanograftangen był wolny od lodu do 0,6 cal ka BP lub dłużej. Spośród lodowców lądowych, recesję stwierdzono m.in. w przypadku lodowców Werenskioldbreen (1,5–0,7 cal ka BP; Baranowski, Karlén, 1976), Renardbreen (1,1–0,6 cal ka BP; Dzierżek i in., 1990) oraz Longyearbreen (1,9–1,1 cal ka BP; Humlum i in., 2005). Podobnie jak we wcześniejszych okresach ocieplenia, recesja lodowców nastąpiła w odpowiedzi na wzrost temperatury powietrza (średniej rocznej i w okresie letnim) oraz wzrost temperatury wody morskiej. Devendra i in. (2023) stwierdzili zwiększony napływ ciepłej wody atlantyckiej i wzrost temperatury wody u wejścia do Hornsundu ok. 1,5–1,0 cal ka BP, podobnie jak Isfjorden (2,0–1,2 cal ka BP; Brice i in., 2023), wschodnim Svalbardzie (ok. 1,7 cal ka BP; Pawłowska i in., 2020) i zachodniej części Morza Barentsa (Sarnthein i in., 2003). W Hornsundzie, Luoto i in. (2018) odtwarzając warunki paleoklimatyczne z danych z jeziora Svartvatnet stwierdzili wzrost średniej rocznej i lipcowej temperatury powietrza ok. 1,5 cal ka BP (Ryc. 8). Mimo ocieplenia klimatu, Jang i in. (2025) wskazali na możliwe awanse lodowców uchodzących do Hornsundu ok. 940 i 1380 r. na podstawie zawartości izotopów Nd w osadach morskich. Uważam, że awanse te miały charakter szarż z uwagi na warunki klimatyczne oraz jedynie krótkotrwały wzrost zawartości detrytusu glacjalnego z dryfujących gór lodowych (*IRD*) w osadach morskich z Hornsundu (Majewski i in., 2009). Podobne „piki" zawartości IRD towarzyszyły dobrze rozpoznanym szarżom lodowców uchodzących do morza, jak Paulabreen ok. 1300 r. (Hald i in., 2001).

Dane paleoklimatyczne z rdzenia lodowego z Lomonosovfonna sugerują, że do końca XIII w. temperatury w okresie zimowym (grudzień – luty) były zbliżone do wartości w latach 30. i 90. XX w., a w latach 1130 – 1300 nastąpiło wyjątkowo intensywne topnienie w okresie letnim, porównywalne do lat 90. XX w. (Ryc. 8; Grinsted i in., 2006; Divine i in., 2011). Pomimo ocieplenia, Hornbreen ponownie awansował po płw. Treskelen ok. 0.7 ± 0.2 ka (Philipps i in., 2017), podobnie jak Werenskioldbreen po 0,7 cal ka BP (Baranowski and Karlén, 1976; Kasprzak et al., 2020). Wiek listków torfowców wskazuje możliwy awans lodowca Hansbreen po 0,6 cal ka BP, który mógłby nawiązywać do nagłego wzrostu IRD i izotopów Nd w Hornsundzie ok. 0,57 cal ka BP (Jang i in., 2025). W tym okresie wystąpiły dobrze rozpoznane szarże lodowców uchodzących do morza, jak Paulabreen ok. 1300 r. (Hald i in., 2001) i Nathorstbreen ok. 1160 r. (Lovell i in., 2018). Z uwagi na warunki klimatyczne, sprzyjające zwiększonej dostawy wód roztopowych do podłoża lodowców, pojawia się pytanie o charakter awansu lodowców obszaru badań. Joe i in. (2022) powiązali rozbudowaną morenę czołową lodowca Hambergbreen z szarżą lub szarżami ok. 0,7 cal ka BP. Z uwagi na redepozycję materiału podczas Małej Epoki Lodowej, podczas badań terenowych nie stwierdziłam stratyfikacji glin na płw. Treskelen wskazującej na kilka awansów w późnym holocenie, podobnie jak w poprzednich opracowaniach tego obszaru (Marks, 1983; Philipps i in., 2017). Niemniej, Hornbreen jest lodowcem szarżującym, co sugeruje możliwość tego typu awansów w przeszłości (Grabiec i in., 2018). Werenskioldbreen nie rozwinął rozbudowanej, proglacjalnej moreny typu *thrust block moraine* charakterystycznej dla lodowców szarżujących (Lovell, Boston, 2017), ale posiada niewielką morenę czołową spiętrzoną (*push moraine*) w formie pojedynczego grzbietu o wysokości ok. 4 m, z warstwą tundry subfosylnej datowanej na ok. 0,7 i 0,6 cal ka BP (Kasprzak i in., 2020). Niemniej, moreny typu *thrust block moraine* mogły ulec degradacji podczas sztormów i wskutek działalności wód roztopowych, jak również mogła się nie rozwinąć z uwagi na uwarunkowania topograficzne (Szupryczyński, 1963; Lønne, 2016). Zatem brak tego typu moreny nie wyklucza szarży lodowca Werenskioldbreen w tym okresie. Zdaniem Baranowskiego (1968, 1977) morena czołowa z jądrem lodowym jest efektem awansu poprzedzającego Małą Epokę Lodową i została przemodelowana podczas maksimum MEL. Awans ten najprawdopodobniej był szarżą (Baranowski, 1977; Jania, 1988).

Początek Małej Epoki Lodowej nie jest jednoznaczny w danych paleoklimatycznych z rdzenia lodowego z Lomonosovfonna, jednak pierwsze wyraźniejsze oznaki ochłodzenia widoczne są na początku XVII w. (Isaksson et al., 2003; Kekonen et al., 2005; Grinsted et al., 2006). Maksimum ochłodzenia wystąpiło około 1850 r. (Divine i in., 2011). Mapy historyczne (Tab. 1) wskazują, że w XVII i XVIII zasięg lodowców uchodzących do morza był najpewniej mniejszy, niż w XIX w. Nieco inny przebieg fluktuacji lodowców podczas MEL przedstawili Jang i in. (2025), wyróżniając okres ograniczonego zasięgu lodowców na początku MEL, awanse lodowców między 1580 a 1620 r., fazę recesji lodowców oraz drugi okres awansu lodowców około 1900 r. Ostatnie szarże lodowców udokumentowano na fotografiach z 1872 i 1918 r., na których można rozpoznać przejawy trwającej fazy aktywnej lub fazy uspokojenia po przebytej szarży. Przebieg szarż poszczególnych lodowców Hornsundu przedstawiłam w pracach Osika i Jania (2024) oraz Osika i in. (2025a). Co istotne, maksymalne zasięgi lodowców z MEL były tożsame z maksymalnymi zasięgami szarż pod koniec MEL, co wykazałam m.in. w przypadku lodowca Hansbreen (Osika, Jania, 2024). Fotografie z 1872 r. wskazują również trwającą fazę aktywną lub wczesną fazę uspokojenia lodowca Paierlbreen, którego chaotycznie uszczeliniona powierzchnia kontrastowała z sąsiednim lodowcem Mühlbacherbreen w fazie uspokojenia. Oprócz Hornsundu, szarże pod koniec MEL były powszechne na Svalbardzie, a wśród lodowców szarżujących pod koniec XIX w. były m.in. Kongsbreen, Kongsvegen-Kronebreen w 1869 r. (Liestøl, 1988), Nathorstbreen ok. 1870 r. (Liestøl, 1977), Von Postbreen w 1870 r. (Liestøl, 1993), a nawet mniejsze lodowce lądowe w centralnej części Spitsbergenu (Mannerfelt i in., 2024). Zapis geomorfologiczny i dane historyczne wykazały, że maksymalne zasięgi lodowców pod koniec MEL często były bezpośrednio związane z szarżami, podobnie jak w Hornsundzie (Liestøl, 1969; Lefauconnier, Hagen, 1991; Lovell i in., 2018; Dowdeswell i in., 2020; Zagórski i in., 2023; Mannerfelt i in., 2024). Odpowiedzi wymaga pytanie o rolę warunków klimatycznych w synchronicznym występowaniu szarż w różnych obszarach Svalbardu. Szarże lodowców lądowych, współcześnie zimnych, mogły być związane z rozwojem struktury politermalnej wraz z nagromadzeniem masy w warunkach ochłodzenia klimatu (Sevestre i in., 2015). Szarże większych, politermalnych lodowców lądowych i lodowców uchodzących do morza mogły być związane z zwiększoną dostawą wody do podłoża. Dane z rdzenia z Lomonosovfonna wskazują, że lata 60. i 70. XIX w. oraz 1890–1910 był cieplejsze, niż 50. i 80. XIX w. (Divine et al., 2011). Szarże mogły wystąpić w latach cieplejszych, poprzedzonych nagromadzeniem masy w chłodniejszych, wcześniejszych dekadach. Niemniej, odpowiedzi wymaga pytanie o sumę opadów podczas MEL i ich rolę w rozwoju lodowców w tym okresie (np. Nesje i in., 2008).

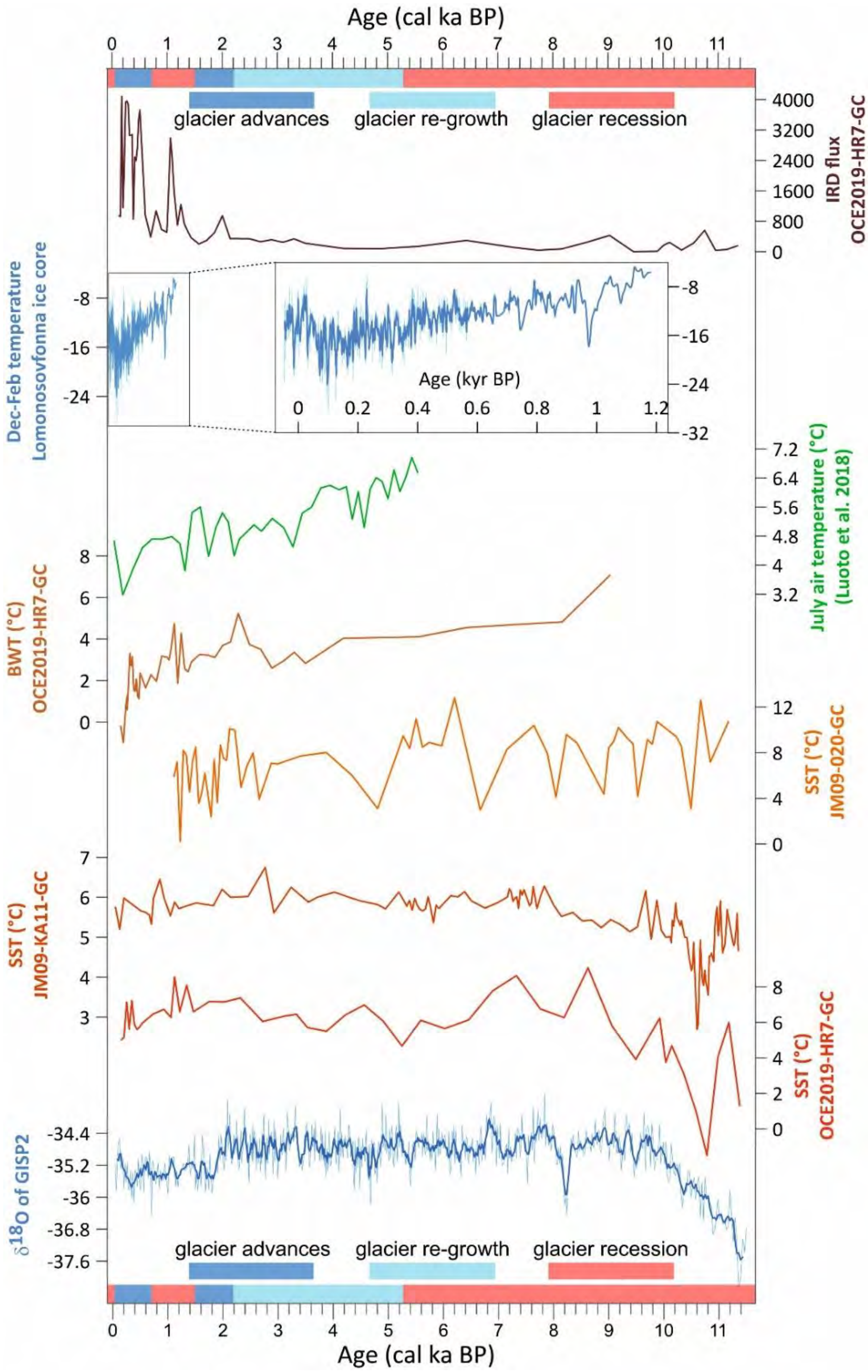

Ryc. 8. Zestawienie danych proxy z holocenu. Od góry: zmiany zawartości detrytusu glacjalnego z dryfujących gór lodowych (ice-rafted debris; IRD) w osadach morskich SW Svalbardu (rdzeń OCE2019-HR7-GC; Devendra i in., 2023); rekonstrukcja temperatury powierzchniowej (*surface air temperature,* SAT) w miesiącach grudzień-luty w Longyearbyen z rdzenia lodowego z Lomonosovfonna (Divine i in., 2011); rekonstrukcja temperatury powietrza w lipcu na podstawie składu gatunkowego ochotkowatych (*Chironomidae*) z jeziora Svartvatnet w południowym Spitsbergenie (Luoto i in., 2018); rekonstrukcja temperatury głębinowej (*benthic water temperature;* BWT) z rdzenia osadów morskich w SW Svalbardzie (rdzeń OCE2019-HR7-GC; Devendra i in., 2023); rekonstrukcja temperatury wody powierzchniowej (*sea surface temperature; SST*) z rdzenia JM09-20-GC w zachodniej części Morza Barentsa (Łącka i in., 2019); rekonstrukcja temperatury wody powierzchniowej z rdzenia JM09-KA11-GC w zachodniej części Morza Barenstsa (Berben i in., 2014); rekonstrukcja temperatury

wody powierzchniowej z rdzenia OCE2019-HR7-GC (Devendra i in., 2023); $\delta^{18}O$ z rdzenia lodowego GISP2 (Grootes i in., 1993). Niebiesko-czerwona skala schematycznie przedstawia fluktuacje lodowców południowego Spitsbergenu w holocenie: recesję lodowców w okresach ocieplenia (*glacier recession*), stopniowe odbudowanie masy lodowców podczas neoglacjału (*glacier re-growth*) i okresy awansu lodowców (w tym szarż) w późnych holocenie (*glacier advances*).

Źródło: Osika i in., 2025a.

Hornsund jako fiord i cieśnina w holocenie

Ze względu na topografię podłoża lodowców Hornbreen i Hambergbreen, w szczególności obecność przegłębienia o głębokości ok. 40 m p.p.m., funkcjonowanie Hornsundu jako fiordu lub cieśniny zależy od dynamiki lodowców uchodzących do morza. Wskutek recesji lodowców, otwarcie cieśniny łączącej Morze Grenlandzkie z Morzem Barentsa nastąpi najprawdopodobniej między 2053–2065 r. (Grabiec i in., 2018; Saferna i in., 2023). Nowe i opublikowane wcześniej wyniki datowania muszli małży morskich z przedpola lodowca Hornbreen (Marks, Pękala, 1986; Tarasov i in., 1992; Birkenmajer, Olsson, 1997) wskazują recesję lodowców systemu Hornbreen-Hambergbreen we wczesnym i środkowym holocenie, która doprowadziła do otwarcia cieśniny ok. 10,9 cal ka BP (najstarsza data muszli) lub wcześniej. Podczas obserwacji w latach 70. i 80. spośród datowanych gatunków tylko jeden stwierdzono w Brepollen (Różycki, 1992). Zasięg pozostałych był ograniczony do zewnętrznej i centralnej części Hornsundu, gdzie zawartość zawieszonego materiału mineralnego dostarczanego przez lodowce uchodzące do morza jest znacznie niższa. Warto zwrócić uwagę, że najstarsze muszle z moreny dennej w wewnętrznej części Hornbukty są podobnego wieku, jak muszle z moreny dennej na płw. Treskelen (10,5 i 10,9 cal ka BP) i w obu obszarach występują muszle datowane na wczesny, środkowy i późny holocen. Awans lodowca Hornbreen i związane z nim zamknięcie cieśniny mógł nastąpić ok. 3,9 cal ka BP (wiek muszli z moreny dennej na wybrzeżu Hornbukty) lub później, ok. 2,1 cal ka BP (wiek muszli z moreny dennej na płw. Treskelen), lub nawet ok. 1,9 ± 0,3 ka (średni wiek ^{10}Be czterech próbek głazów z moreny końcowej na płw. Treskelen; Philipps i in., 2017), w zależności od dynamiki lodowców szarżujących. Recesja lodowców podczas Średniowiecznego Okresu Ciepłego najpewniej doprowadziła do ponownego otwarcia cieśniny, jak sugeruje wiek muszli z moreny dennej na płw. Treskelen (ok. 1,3 cal ka BP; Birkenmajer, Olsson, 1997). Ponowny awans Lodowca Horna po Treskelen oraz związane z nim możliwe zamknięcie cieśniny nastąpił ok. 0.7 ± 0.2 ka (Philipps i in., 2017). Po tym okresie nie stwierdziłam przesłanek ponownego otwarcia cieśniny.

Obecność cieśniny łączącej Morze Grenlandzkie z Morzem Barentsa modyfikowała cyrkulację prądów morskich w tej części Svalbardu: ciepłego Prądu Zachodniospitsbergeńskiego i zimnego Prądu Wschodniospitsbergeńskiego. Według opracowania Grabca i in. (2018), w przypadku ponownego otwarcia cieśniny, głębokość wody będzie przekraczała 40 m wzdłuż osi łączącej Morze Grenlandzkie z Morzem Barentsa. Głębokość wody w centralnej części nowego fiordu wzdłuż osi Hornbreen–Flatbreen będzie przekraczała 70 m. Zamknięcie cieśniny tej głębokości wymagało serii szarż wyprowadzających znaczne ilości lodu z obszarów rezerwuarowych. Model konceptualny zamknięcia cieśniny Hornsund poprzez szarże lodowców przedstawili Grabiec i in. (2018). Szarże lodowców najpewniej nastąpiły synchronicznie lub jedna po drugiej, podobnie jak zaobserwowano w przypadku systemu lodowcowego Nathorstbreen od 2008 r. (Sund i in., 2014). Podczas szarży, lodowiec Flatbreen mógł awansować w kierunku południowym po masyw górski Professorryggen i rozdzielić się na dwie odnogi, Hambergbreen w kierunku wschodnim i Hornbreen w kierunku zachodnim. Szarże poszczególnych lodowców uchodzących do morza w Brepollen (Svalisbreen, Mendeleevbreen, Storbreen, Chomjakovbreen, Samarinbreen) pozwoliły na rozbudowanie rozległego systemu lodowcowego w wewnętrznej części Hornsundu. Hambergbreen dodatkowo był zasilany przez lodowiec Sykorabreen wyprowadzający lód z czapy lodowej Hedgehogfonna. W ten sposób szarże lodowców doprowadziły do uformowania pomostu lodowego łączącego Torell Land na północy i Sørkapp Land na południu.

WNIOSKI

1. Fluktuacje lodowców obszaru badań przebiegały generalnie synchronicznie z pozostałą częścią Svalbardu i podobnie jak w innych regionach, odzwierciedlały zmiany bilansu masy, w tym także temperatury powietrza i wody morskiej. Z uwagi na brak danych, pytanie o rolę opadów atmosferycznych w rozwoju lodowców wymaga dalszych badań. Nisko położone strefy akumulacyjne na południowym Spitsbergenie dodatkowo sprzyjały szybkiej recesji lodowców w okresach ocieplenia i spowalniały tempo ich odbudowy w okresach chłodniejszych. Kluczową rolę w ewolucji pokrywy lodowej odgrywały szarże lodowców. Najbardziej spektakularne było kilkukrotne doprowadzenie do utworzenia pomostu lodowego łączącego Torell Land i Sørkapp Land.

2. Na podstawie kartowania geomorfologicznego, analizy materiałów historycznych oraz nowych i opublikowanych wyników datowania materiału organicznego metodą ^{14}C oraz głazów morenowych metodą ^{10}Be wyróżniłam następujące okresy fluktuacji lodowców południowego Spitsbergenu: (1) deglacjację, (2) recesję lodowców we wczesnym i środkowym holocenie, (3) rozwój lodowców w pierwszej połowie późnego holocenu, (4) awanse lodowców ok. 2,2–1,5 cal ka BP, (5) recesję lodowców ok. 1,5–1,0 cal ka BP, (6) awanse lodowców od ok. 0,7 cal ka BP oraz (7) Małą Epokę Lodową.

3. Dynamika lodowców systemu Hornbreen-Hambergbreen decyduje o funkcjonowaniu Hornsundu jako fiordu lub cieśniny między Morzem Grenlandzkim i Morzem Barentsa. Wskutek recesji lodowców, Hornsund był cieśniną w okresie wczesnego i środkowego holocenu. Nowe i opublikowane wcześniej daty ^{14}C muszli z moreny dennej lodowca Hornbreen i opublikowane daty ^{10}Be głazów morenowych z płw. Treskelen wskazują, że awans lodowców i zamknięcie cieśniny nastąpiły ok. 3,9 cal ka BP lub później, ok. 2,1 cal ka BP lub dopiero 1,9 ± 0,3 ka (Philipps i in., 2017). Ponowne otwarcie cieśniny mogło nastąpić ok. 1,3 cal ka BP do kolejnego awansu lodowców ok. 0,7 ± 0,2 ka (Birkenmajer, Olsson, 1997; Philipps i in., 2017).

4. Wyniki kartowania geomorfologicznego oraz fotografie archiwalne wskazują, że maksymalne zasięgi badanych lodowców pod koniec Małej Epoki Lodowej (MEL) były efektem szarż. Do kluczowych form rzeźby terenu, które pozwoliły zidentyfikować szarże lodowców, należą grzbiety z wyciśnięcia szczelin dennych (*crevasse-squeeze ridges, CSRs*), ozy harmonijkowe (*concertina eskers*), lineacje lodowcowe (*streamlined glacial lineations*) oraz moreny czołowe spiętrzone. Występowanie szarż w różnych obszarach Svalbardu pod koniec MEL wskazuje możliwość istnienia podobnych czynników wyzwalających szarże lodowców w tym okresie.

5. Maksymalne zasięgi zidentyfikowanych awansów w późnym holocenie były bezpośrednio związane ze zjawiskiem szarży lodowców, zwłaszcza długich, o słabo nachylonej powierzchni i rozwiniętym, rozgałęzionym systemie akumulacyjnym. Szarże były poprzedzone długotrwałym nagromadzeniem masy w strefie rezerwuarowej w warunkach chłodniejszego klimatu i wysoce prawdopodobnym wzrostem opadów śniegu na początku okresu cieplejszego. Czynnikiem wyzwalającym była najprawdopodobniej zwiększona dostawa wód ablacyjnych z powierzchni do podłoża lodowców w okresach cieplejszych, gdzie słabe nachylenie

i przegłębienia utrudniały jej szybki odpływ, zmniejszając tarcie i ułatwiając poślizg lodowca. Zmieniało się w ten sposób stale położenie geometrycznego środka ciężkości lodu i następował gwałtowny transfer masy do strefy ablacji. Skutkiem tego były wyraźne szarże lodowców. Rozciągnięcie jęzora poniżej linii równowagi przyspieszało następnie recesję lodowca. Z uwagi na niesprzyjające uwarunkowania topograficzne ograniczające tempo akumulacji śniegu i lodu, największe awanse lodowców wystąpiły nie wcześniej, niż w drugiej połowie późnego holocenu.

6. Szarże lodowców istotnie przyspieszają redukcję zlodowacenia południowego Spitsbergenu i prawdopodobnie całego Svalbardu w dobie współczesnego ocieplenia klimatu. Podobną rolę odegrały w cieplejszych okresach w przeszłości, zwiększając tempo recesji lodowców we wczesnym holocenie oraz w cieplejszych fazach późnego holocenu. Proces ten ma charakter „konwulsyjnego" zaniku zlodowacenia z cyklicznymi szarżami lodowców prowadzącymi do stosunkowo krótkotrwałego zwiększenia powierzchni zlodzonej. Następujące po sobie szarże prowadzą do odprowadzenia mas lodu ze strefy rezerwuarowej do odbierającej aż do wyczerpania strefy rezerwuarowej.

WYZWANIA I OTWARTE PYTANIA

Doświadczenia nabyte podczas analizy zmian zasięgu lodowców południowego Spitsbergenu w holocenie pozwalają wskazać obszary wymagające dalszych badań oraz wyzwania związane ze specyfiką historii zlodowacenia tej części Svalbardu w holocenie.

Fluktuacje lodowców obszaru badań przebiegały synchronicznie z pozostałą częścią Svalbardu. Niemniej, podczas badań nie stwierdziłam przesłanek awansów związanych z ochłodzeniem młodszego dryasu lub awansów dynamicznych towarzyszących deglacjacji, jakie zidentyfikowano w innych obszarach Svalbardu (np. Farnsworth i in., 2017, 2022, 2024). Odpowiedzi wymaga pytanie, czy tego typu awanse występowały w Hornsundzie, czy recesja lodowców we wczesnym holocenie miała charakter szybkiej deglacjacji frontalnej i arealnej. Ograniczone podniesienie glacjoizostatyczne w regionie Hornsundu w porównaniu np. z północno-wschodnim Svalbardem oraz nisko położone pola akumulacyjne lodowców utrudniały nagromadzenie mas lodu w strefie rezerwuarowej, który mógłby zostać odprowadzony podczas szarż. Jednocześnie wielokrotna redepozycja osadów podczas awansów lodowców w późnym holocenie ogranicza zastosowanie metody radiowęglowej w datowaniu moren.

Redepozycja osadów stanowi wyzwanie w przypadku datowania moren metodą ^{10}Be, a niedostateczna erozja podczas awansu prowadzi do „postarzenia" wieku z uwagi na obecność izotopów odziedziczonych z wczesnego i środkowego holocenu, kiedy lodowce Svalbardu były mniejsze, niż współcześnie. Niestabilność moren z uwagi na zanik jądra lodowego może prowadzić do „odmłodzenia" wieku datowanych skał wskutek redepozycji. Zastosowanie par izotopów (^{10}Be i ^{26}Al) może dostarczyć dodatkowych danych na temat historii ekspozycji i pogrzebania głazów (np. Tylmann, Moskalewicz, 2020).

Istotnym źródłem danych na temat fluktuacji lodowców pozostają rdzenie osadów morskich (np. Jang i in., 2025). Podobnie jak w przypadku datowania moren położonych na lądzie, wyzwanie w rekonstrukcji fluktuacji lodowców Hornsundu we wczesnym i środkowym holocenie na podstawie rdzeni osadów morskich stanowi wielokrotna redepozycja materiału. Jej przejawem jest zróżnicowanie wieku muszli małży w morenie dennej na płw. Treskelen, wybrzeżu Hornbukty, przedpolach lodowców Hansbreen lub Vestre Torellbreen. Awanse lodowca Hornbreen poza Treskelen doprowadziły do wymieszania osadów z wczesnego, środkowego i późnego holocenu i jego depozycji w formie moreny dennej i czołowej położonej na zachód od płw. Treskelen. Z tego względu rekonstrukcja fluktuacji z okresu poprzedzającego Małą Epokę Lodową pozostanie wyzwaniem w przypadku lodowców uchodzących do wewnętrznej części fiordu.

Dotychczas nie odtworzono minimalnego zasięgu lodowców Svalbardu w holocenie (Farnsworth i in., 2020). Możliwe dowody geomorfologiczne najpewniej zostały przemodelowane podczas rozbudowy i awansów lodowców w późnym holocenie. Z uwagi na uwarunkowania topograficzne, dowody potencjalnej obecności lodowców we wczesnym holocenie mogą znajdować się w najwyżej położonych cyrkach, szczególnie o ekspozycji północnej, gdzie mogłyby zachować się płaty lodu pokryte gruzem lub lodowce gruzowe. Jednocześnie podczas deglacjacji następuje odsłonięcie okalających grzbietów i nunataków, gdzie pokrywa lodowa jest cieńsza (Szafraniec, Dobiński, 2020). To utrudnia identyfikację obszarów o możliwie najstarszym lodzie. Źródłem informacji na temat obecności lub zaniku lodowców mogą być osady jeziorne w zlewniach zlodowaconych (np. Røthe i in., 2015). W porównaniu z liczbą lodowców, tego typu badania nadal są stosunkowo nieliczne nawet w najlepiej zbadanych obszarach Svalbardu.

W porównaniu z rekonstrukcjami temperatury powietrza lub wody morskiej, badania na temat zmian wielkości opadów w holocenie pozostają stosukowo nieliczne (np. Kjellman i in., 2024). Odpowiedzi wymaga pytanie o rolę opadów w rozwoju lodowców w późnym holocenie (Nesje i in., 2008) oraz jakie czynniki sprzyjały występowaniu szarż lodowców południowego Spitsbergenu w poszczególnych okresach holocenu.

BIBLIOGRAFIA

Allaart L., Schomacker A., Larsen N.K., Nørmark E., Rydningen T.A., Farnsworth W.R., Retelle M., Brynjólfsson S., Forwick M., Kjellman S.E., 2021: Glacial history of the Åsgardfonna Ice Cap, NE Spitsbergen, since the last glaciation. Quaternary Science Reviews 251, 106717. https://doi.org/10.1016/j.quascirev.2020.106717.

Aradóttir N., Ingólfsson Ó., Noormets R., Benediktsson Í.Ö., Ben-Yehoshua D., Håkansson L., Schomacker A., 2019: Glacial geomorphology of Trygghamna, western Svalbard - Integrating terrestrial and submarine archives for a better understanding of past glacial dynamics. Geomorphology 344, 75–89. https://doi.org/10.1016/j.geomorph.2019.07.007

Aswathy N.K., Krishnapriya P.P., Neenu P., Bijoy Nandan S., Jima M., Jayachandran P.R., Harikrishnan M., Krishnan K.P., 2023: Spatial dynamics of macrofauna with special reference to bivalve molluscs in the Arctic Kongsfjord, Svalbard, Norway. Polar Science 35, 100916. https://doi.org/10.1016/j.polar.2022.100916.

Balco G., 2011: Contributions and unrealized potential contributions of cosmogenic-nuclide exposure dating to glacier chronology, 1990–2010. Quaternary Science Reviews 30(1–2), 3–27. https://doi.org/10.1016/j.quascirev.2010.11.003.

Baranowski S., 1968: Changes of the front of Werenskioldbreen (Vestspitsbergen) and its forefield during the Holocene (preliminary report). Polish Spitsbergen Expeditions 1957–1960. Summary of Scientific Results. Polish Academy of Sciences, Warsaw, pp. 317–320.

Baranowski S., 1977: Changes of Spitsbergen glaciation at the end of the Pleistocene and in Holocene. Qauestiones Geographicae 4, 5–28.

Baranowski S., Karlén W., 1976: Remnants of Viking age tundra in Spitsbergen and northern Scandinavia. Geografiska Annaler. Series A, Physical Geography 58(1/2), 35–49. https://doi.org/10.2307/520741.

Bednarek J., Rudowski S., Zalewski S.M.W., 1993: The tectonic sketch of the offshore area within Hornsund Region, Spitsbergen. (In:) XX Polar Symposium. Man impact on polar environment (eds J. Repelewska-Pękalowa, K. Pękala), Lublin, 3–5 June 1993, 293–297.

Bellin J.N., 1758: Carte Du Spits-Berg: Suivant les Hollandois pour Servir a l'Histoire Generale des Voyages. Publisher J.N. Bellin, Paris. Dostępne na https://cartotecadigital.icgc.cat/digital/collection/europa/id/2198 (dostęp 20.09.2025)

Benn D.I., 2021: Surging glaciers in Scotland. Scottish Geographical Journal 137(1–4), 1–40. https://doi.org/10.1080/14702541.2021.1922738.

Ben-Yehoshua D., Aradóttir N., Farnsworth W.R., Benediktsson Í.Ö., Ingólfsson Ó., 2023: Formation of crevasse-squeeze ridges at Trygghamna, Svalbard. Earth Surface Processes and Landforms 48(12), 2334–2348. https://doi.org/10.1002/esp.5631

Berben S.M.P., Husum K., Cabedo-Sanz P., Belt S.T., 2014: Holocene sub-centennial evolution of Atlantic water inflow and sea ice distribution in the western Barents Sea. Climate of the Past 10, 181–198. https://doi.org/10.5194/cp-10-181-2014.

Birkenmajer K., 1990: Hornsund, Spitsbergen, geologia – geology, 1: 75 000 (Geological map and explanatory text). Committee on Polar Research. Warsaw: Polish Academy of Sciences; Katowice: Silesian University.

Birkenmajer K., Olsson I.U., 1997: Radiocarbon dating of marine bivalve shells from Holocene moraines at inner Hornsund, South Spitsbergen. Bulletin of the Polish Academy of Sciences. Earth Sciences 45(1), 59–66.

Birkenmajer K., Olsson I.U., 1998: Radiocarbon-Dated Late Pleistocene and Early Holocene Marine Shells at Werenskioldbreen, South Spitsbergen. Bulletin of the Polish Academy of Sciences. Earth Sciences 46(1), 21–34.

Błaszczyk M., Jania J.A., Ciepły M., Grabiec M., Ignatiuk D., Kolondra L., Kruss A., Luks B., Moskalik M., Pastusiak T., Strzelewicz A., Walczowski W., Wawrzyniak T., 2021: Factors Controlling Terminus Position of Hansbreen, a Tidewater Glacier in Svalbard. Journal of Geophysical Research: Earth Surface 126(2), e2020JF005763. https://doi.org/10.1029/2020JF005763.

Błaszczyk M., Jania J.A., Kolondra L., 2013: Fluctuations of tidewater glaciers in Hornsund Fjord (Southern Svalbard) since the beginning of the 20th century. Polish Polar Research 34(4), 327-352. https://doi.org/10.2478/popore−2013−0024.

Błaszczyk M., Laska M., Sivertsen A., Jawak S.D., 2022: Combined Use of Aerial Photogrammetry and Terrestrial Laser Scanning for Detecting Geomorphological Changes in Hornsund, Svalbard. Remote Sensing 14(3), 601. https://doi.org/10.3390/rs14030601.

Błaszczyk M., Moskalik M., Grabiec M., Jania J., Walczowski W., Wawrzyniak T., Strzelewicz A., Malnes E., Lauknes T.R., Pfeffer W.T., 2023: The Response of Tidewater Glacier Termini Positions in Hornsund (Svalbard) to Climate Forcing, 1992–2020. Journal of Geophysical Research: Earth Surface, 128(5), e2022JF006911. https://doi.org/10.1029/2022JF006911.

Brice C., de Vernal A., Francus P., Forwick M., Nam S.-I., 2023: Millennial-scale oscillations and an environmental regime shift around the Middle to Late Holocene transition in the North Atlantic region based on a multiproxy record from Isfjorden, West Spitsbergen. Boreas. 52, 42–59. https://doi.org/10.1111/bor.12602.

Conway W.M., 1898: With ski & sledge over Arctic glaciers. J.M. Dent & Co., London.

Copland L., Sharp M.J., Dowdeswell J.A., 2003: The distribution and flow characteristics of surge-type glaciers in the Canadian high Arctic. Annals of Glaciology 36, 73–81. https://doi.org/10.3189/172756403781816301

Ćwiąkała J., Moskalik M., Forwick M., Wojtysiak K., Giżejewski J., Szczuciński W., 2018: Submarine geomorphology at the front of the retreating Hansbreen tidewater glacier, Hornsund fjord, southwest Spitsbergen. Journal of Maps 14(2), 123–134. https://doi.org/10.1080/17445647.2018.1441757

de Geer G., 1923: Description de Ia region exploree, Geologie in Missions scientifiques pour Ia mesure d'un arc de meridien au Spitzberg, enterprises en 1899-1902 sous le auspicies de governementes suedois et russe. Mission suedois Tome II. Physique terrestre. Meteorologie. Historie naturelle -1xieme section. Topographie. Geologie. Stockholm Aktiebolagel Centraltryckeriet 1923.

Devendra D., Łącka M., Szymańska N., Szymczak-Żyła M., Krajewska M., Weiner A.K., De Schepper S., Simon M.H., Zajączkowski M., 2023: The development of ocean currents and the response of the cryosphere on the Southwest Svalbard shelf over the Holocene. Global and Planetary Change 228, 104213. https://doi.org/10.1016/j.gloplacha.2023.104213.

Divine D., Isaksson E., Martma T., Meijer H.A.J., Moore J., Pohjola V., van de Wal R.S.W., Godtliebsen F., 2011: Thousand years of winter surface air temperature variations in Svalbard and northern Norway reconstructed from ice-core data. Polar Research 30, 7379. https://doi.org/10.3402/polar.v30i0.7379.

Doncker B.H., 1663: Paskaert van Spitsbergen, met alle zijn zeekusten zoo veel tot noch toe bekent is. In: De Zee-Atlas Ofte Water-Waereld. Amsterdam, Henry Doncker, 1660. Reprod. of Spitsbergen in: Conway (1906). P. 339; Geogr. journ. Vol. 21. London 1903. P. 639; Wieder (1919). Pl. 24. No. 130.

Dowdeswell J.A., Hamilton G.S., Hagen J.O., 1991: The duration of the active phase on surge-type glaciers: contrasts between Svalbard and other regions. Journal of Glaciology 37(127), 388–400. https://doi.org/10.3189/S0022143000005827

Dowdeswell J.A., Ottesen D., Bellec V.K., 2020: The changing extent of marine-terminating glaciers and ice caps in northeastern Svalbard since the ‘Little Ice Age’ from marine-geophysical records. Holocene 30(3), 389–401. https://doi.org/10.1177/0959683619887429.

Dunér N., Nordenskiöld A.E., 1865: Karta öfver Spetsbergen, hufvudsakligast enligt iakttagelser under de svenska expeditionerna åren 1861 och 1864. Abrah. Lundquist & Cie., Stockholm. Dostępne na https://digital.library.yale.edu/catalog/15159347 (dostęp 20.09.2025)

Dzierżek J., Nitychoruk J., Rzętkowska A., 1990: Geological-geomorphological analysis and 14C dating of submoraine organogenic deposits within the Renardbreen outer margin, Wedel Jarlsberg land, Spitsbergen. Polar Research 8(2), 275–281. https://doi.org/10.3402/polar.v8i2.6817.

ESRI, 2025: ‘Imagery’ [basemap]. Scale not given, ‘world imagery vivid’. Dostępne na https://services.arcgisonline.com/ArcGIS/rest/services/World_Imagery/MapServer (dostęp 20.09.2025)

Evans D.J.A., Rea B.R., 1999: Geomorphology and sedimentology of surging glaciers: a land-systems approach. Annals of Glaciology 28, 75–82. https://doi.org/10.3189/172756499781821823

Farinotti D., Huss M., Fürst J.J., Landmann J., Machguth H., Maussion F., Pandit A., 2019: A consensus estimate for the ice thickness distribution of all glaciers on Earth. Nature Geoscience 12, 168–173. https://doi.org/10.1038/s41561-019-0300-3.

Farnsworth W. R., Ingólfsson Ó., Mannerfelt E.S., Kalliokoski M.H., Guðmundsdóttir E.R., Retelle M., Allaart L., Brynjólfsson S., Furze M.F., Hancock H.J., Kjær K.H., Pieńkowski A.J., Schomacker A., 2021: Vedde Ash constrains Younger Dryas glacier re-advance and rapid glacio-isostatic rebound on Svalbard. Quaternary Science Advances 5, 100041. https://doi.org/10.1016/j.qsa.2021.100041

Farnsworth W.R., Allaart L., Ingólfsson Ó., Alexanderson H., Forwick M., Noormets R., Retelle M., Schomacker A., 2020: Holocene glacial history of Svalbard: Status, perspectives and challenges. Earth-Science Reviews 208, 103249. https://doi.org/10.1016/j.earscirev.2020.103249.

Farnsworth W.R., Ingólfsson Ó., Brynjólfsson S., Allaart L., Kjellman S.E., Kjær K.H., Larsen N.K., Macias-Fauria M., Siggaard-Andersen M., Schomacker A., 2024: Persistence of Holocene ice cap in northeast Svalbard aided by glacio-isostatic rebound. Quaternary Science Reviews 331, 108625. https://doi.org/10.1016/j.quascirev.2024.108625.

Farnsworth W.R., Ingólfsson Ó., Noormets R., Allaart L., Alexanderson H., Henriksen M., Schomacker A., 2017: Dynamic Holocene glacial history of St. Jonsfjorden, Svalbard. Boreas 46(3), 585–603. https://doi.org/10.1111/bor.12269

Farnsworth W.R., Ingólfsson Ó., Noormets R., Allaart L., Alexanderson H., Henriksen M., Schomacker A., 2017: Dynamic Holocene glacial history of St. Jonsfjorden, Svalbard. Boreas 46(3), 585–603. https://doi.org/10.1111/bor.12269.

Farnsworth W.R., Ingólfsson Ó., Retelle M., Allaart L., Håkansson L.M., Schomacker A., 2018: Svalbard glaciers re-advanced during the Pleistocene–Holocene transition. Boreas 47(4), 1022–1032. https://doi.org/10.1111/bor.12326.

Farnsworth W.R., Ingólfsson Ó., Retelle M., Schomacker A., 2016: Over 400 previously undocumented Svalbard surge-type glaciers identified. Geomorphology 264, 52–60. https://doi.org/10.1016/j.geomorph.2016.03.025.

Flink A.E., Hill P., Noormets R., Kirchner N., 2018: Holocene glacial evolution of Mohnbukta in eastern Spitsbergen. Boreas 47(2), 390–409. https://doi.org/10.1111/bor.12277.

Forwick M., Vorren T.O., Hald M., Korsun S., Roh Y., Vogt C., Yoo K.-C., 2010: Spatial and temporal influence of glaciers and rivers on the sedimentary environment in Sassenfjorden and Tempelfjorden, Spitsbergen. Geological Society, London, Special Publications 344, 163–193. https://doi.org/10.1144/SP344.13.

Fotherby R., [1613] (reprint 1860). Narrative of a voyage to Spitzbergen in the year 1613, at the charge of the fellowship of Englishmerchants for the discovery of new trades; commonly called the Muscovy Company: with a description of the country, and the operations of the whale-fishery. Boston, Printed by J. Wilson and Son.

Geyman E.C., van Pelt W.J.J., Maloof A.C., Aas H.F., Kohler J., 2022: Historical glacier change on Svalbard predicts doubling of mass loss by 2100. Nature 601, 374–379. https://doi.org/10.1038/s41586-021-04314-4.

Gjelten H.M., Nordli Ø., Isaksen K., Førland E.J., Sviashchennikov P.N., Wyszynski P., Prokhorova U.V., Przybylak R., Ivanov B.V., Urazgildeeva A.V., 2016: Air temperature variations and gradients along the coast and fjords of western Spitsbergen. Polar Research 35, 29878. https://doi.org/10.3402/polar.v35.29878

Grabiec M., Ignatiuk D., Jania J.A., Moskalik M., Głowacki P., Błaszczyk M., Budzik T., Walczowski W., 2018: Coast formation in an Arctic area due to glacier surge and retreat: The Hornbreen-Hambergbreen case from Spitsbergen. Earth Surface Processes and Landforms 43(2), 387–400. https://doi.org/10.1002/esp.4251.

Grabiec M., Jania J.A., Puczko D., Kolondra L., Budzik T., 2012: Surface and bed morphology of Hansbreen, a tidewater glacier in Spitsbergen. Polish Polar Research 33(2), 111–138. https://doi.org/10.2478/v10183−012−0010−7.

Grant K.L., Stokes C.R., Evans I.S., 2009: Identification and characteristics of surge-type glaciers on Novaya Zemlya, Russian Arctic. Journal of Glaciology 55(194), 960–972. https://doi.org/10.3189/002214309790794940.

Grinsted A., Moore J.C., Pohjola V., Martma T., Isaksson E., 2006. Svalbard summer melting, continentality, and sea ice extent from the Lomonosovfonna ice core. Journal of Geophysical Research 111, D07110. https://doi.org/10.1029/2005JD006494.

Grootes P.M., Stuiver M., White J.W., Johnsen S., Jouzel J., 1993: Comparison of oxygen isotope records from the GISP2 and GRIP Greenland ice cores. Nature 366(6455), 552–554. https://doi.org/10.1038/366552a0

Hald M., Dahlgren T., Olsen T.-E., Lebesbye E., 2001: Late Holocene palaeoceanography in Van Mijenfjorden, Svalbard. Polar Research 20(1), 23–35. https://doi.org/10.3402/polar.v20i1.6497.

Hanssen-Bauer I., Førland E., Hisdal H., Mayer S., Sandø A.B., Sorteberg A. (eds) 2019: Climate in Svalbard 2100. A Knowledge Base for Climate Adaptation. The Norwegian Centre for Climate Services report no 1/2019.

Harland W.B., 1997: The Geology of Svalbard. London: Geological Society, Memoir No. 17.

Heaton T.J., Köhler P., Butzin M., Bard E., Reimer R.W., Austin W.E.N., Bronk Ramsey C., Grootes P.M., Hughen K.A., Kromer B., Reimer P.J., Adkins J., Burke A., Cook M.S., Olsen J., Skinner L.C., 2020: Marine20—The Marine Radiocarbon Age Calibration Curve (0–55,000 cal BP). Radiocarbon 62(4), 779–820. https://doi.org/10.1017/RDC.2020.68.

Holmes F.A., Kirchner N., Kuttenkeuler J., Krützfeldt J., Noormets R., 2019: Relating ocean temperatures to frontal ablation rates at Svalbard tidewater glaciers: Insights from glacier proximal datasets. Scientific Reports 9, 9442. https://doi.org/10.1038/s41598-019-45077-3.

Humlum O., Elberling B., Hormes A., Fjordheim K., Hansen O.H., Heinemeier J., 2005: Late-Holocene glacier growth in Svalbard, documented by subglacial relict vegetation and living soil microbes. The Holocene 15(3), 396–407. https://doi.org/10.1191/0959683605hl817rp.

Isaksson E., Hermanson M., Hicks S., Igarashi M., Kamiyama K., Moore J., Motoyama H., Muir D., Pohjola V., Vaikmäe R., Van de Wal R.S., Watanabe O., 2003: Ice cores from Svalbard––useful archives of past climate and pollution history. Physics and Chemistry of the Earth, Parts A/B/C 28(28–32), 1217–1228. https://doi.org/10.1016/j.pce.2003.08.053.

Jaklin G.S. (ed.), 2003: The Place Names of Svalbard. Rapportserie nr. 122, Norwegian Polar Institute, Tromsø

Jakobsson M., Long A., Ingólfsson Ó., Kjær K.H., Spielhagen R.F., 2010: New insights on Arctic Quaternary climate variability from palaeo-records and numerical modeling. Quaternary Science Reviews 29, 3349–3358. https://doi.org/10.1016/j.quascirev.2010.08.016

Jang K., Bayon G., Ahn Y., Joe Y.J., Son E.J., Kwon S.Y., Kim J.-H., Vogt C., Forwick M., Byun E., Nam S.-I. 2025: Geochemical and mineralogical characteristics of fjord sediments in Arctic Svalbard: insights into Holocene glacial activity and weathering variability. Journal of Sedimentary Research 95(2), 223–238. https://doi.org/10.2110/jsr.2024.088.

Jania J., 1988: Dynamiczne procesy glacjalne na południowym Spitsbergenie (w świetle badań fotointerpretacyjnych i fotogrametrycznych. Prace Naukowe Uniwersytetu Śląskiego, Katowice

Jania J., 1997: Glacjologia: nauka o lodowcach. Wydawnictwo Naukowe PWN, Warszawa.

Jania J., Głowacki P., 1996: Is the Hansbreen in South Spitsbergen (Svalbard) a surge-type glacier? (In:) Krawczyk W.E. (Ed.) 23rd Polar Symposium, Uniwersytet Śląski, Sosnowiec, 27–43.

Jiskoot H., Murray T., Boyle P., 2000: Controls on the distribution of surge-type glaciers in Svalbard. Journal of Glaciology 46(154), 412–422. https://doi.org/10.3189/172756500781833115

Joe Y.J., Jang K., Forwick M., Laberg J.S., Kong G.S., Kang M.-H., Yoon S.-H., Nam S.-I., 2022: Glacial history and depositional environments in little Storfjorden and Hambergbukta of Arctic Svalbard since the younger dryas. Frontiers in Earth Science 10, 1017594. https://doi.org/10.3389/feart.2022.1017594.

Karczewski A., Rachlewicz G., 1999: Sprawozdanie z badań prowadzonych w latach 1996-1998 w ramach projektu "Fizyczne procesy glacjalne w warunkach zmieniającego się klimatu a ich zapis w osadach i formach na przykładzie Svalbardu".

Kasprzak M., Łopuch M., Głowacki T., Milczarek W., 2020: Evolution of Near-Shore Outwash Fans and Permafrost Spreading Under Their Surface: A Case Study from Svalbard. Remote Sensing 12(3), 482. https://doi.org/10.3390/rs12030482.

Kaufman D.S., Ager T.A., Anderson N.J., Anderson P.M., Andrews J.T., Bartelein P.J., Brubaker L.B., Coats L.L., Cwynar L.C., Duvall M.L., Dyke A.S., Edwards M.E., Eisner W.R., Gajewski K., Geirsdóttir A., Hu F.S., Jennings A.E., Kaplan M.R., Kerwin M.W., Lozhkin A.V., ManDonald G.M., Miller G.H., Mock C.J., Oswald W.W., Otto-Bliesner B.L., Porinchu D.F., Rühland K., Smol J.P., Steig E.J., Wolfe B.B., 2004: Holocene thermal maximum in the western

Arctic (0–180°W). Quaternary Science Reviews 23 (5–6), 529–560. https://doi.org/10.1016/j.quascirev.2003.09.007

Kekonen T., Moore J., Perämäki P., Mulvaney R., Isaksson E., Pohjola V., van de Wal R.S.W., 2005: The 800 year long ion record from the Lomonosovfonna (Svalbard) ice core. Journal of Geophysical Research 110, D07304. https://doi.org/10.1029/2004JD005223.

Kjaer R., 1938: Nordishavet, Svalbard, Frå Sørkapp til Bellsund, Sjøkart 504, 1:200 000, Det Kongelige Departement for Handel, Sjøfart, Industri, og Håndverk. Norges Svalbard – og Ishavs-undersøkelser, Oslo. Dostępne na https://data.npolar.no/map/archive/fe263748-5917-55e8-bb0e-98e1530cdc00 (dostęp 20.09.2025)

Kjellman S.E., Thomas E.K., Farnsworth W.R., Cowling O.C., Allaart L., Brynjólfsson S., Schomacker A., 2024: Seasonal precipitation variability on Svalbard inferred from Holocene sedimentary leaf wax δ2H. Boreas, 53(3), 430–452. https://doi.org/10.1111/bor.12661

Kłysz P., Lindner L., Makowska A., Marks L., Wysokiński L., 1988: Late Quaternary glacial episodes and sea level changes in the northeastern Billefjorden region, Central Spitsbergen. Acta Geologica Polonica 38 (1–4): 107–123.

Kochtitzky W., Copland L., 2022: Retreat of Northern Hemisphere Marine-Terminating Glaciers, 2000–2020. Geophysical Research Letters 49(3), e2021GL096501. https://doi.org/10.1029/2021GL096501.

Łącka M., Cao M., Rosell-Melé A., Pawłowska J., Kucharska M., Forwick M., Zajączkowski M., 2019: Postglacial paleoceanography of the western Barents Sea: Implications for alkenone-based sea surface temperatures and primary productivity. Quaternary Science Reviews 224, 105973. https://doi.org/10.1016/j.quascirev.2019.105973.

Larocca L.J., Axford Y., 2022: Arctic glaciers and ice caps through the Holocene: a circumpolar synthesis of lake-based reconstructions. Climate of the Past 18, 579–606. https://doi.org/10.5194/cp-18-579-2022.

Larsen N.K., Søndergaard A.S., Levy L.B., Laursen C.H., Bjørk A.A., Kjeldsen K.K., Funder S., Strunk A., Olsen J., Kjær K.H., 2021: Cosmogenic nuclide inheritance in Little Ice Age moraines – A case study from Greenland. Quaternary Geochronology 65, 101200. https://doi.org/10.1016/j.quageo.2021.101200.

Lefauconnier B., Hagen J.O., 1991: Surging and calving glaciers in eastern Svalbard. Norsk Polarinstitutt Meddelelser 116, 1–130.

Liestøl O., 1969: Glacier surges in West Spitsbergen. Canadian Journal of Earth Sciences, 6(4), 895-897. https://doi.org/10.1139/e69-092.

Liestøl O., 1977: Årsmorener foran Nathorstbreen? Norsk Polarinstitutt Årbok 1976, 361–363.

Liestøl O., 1988: The glaciers in the Kongsfjorden area, Spitsbergen. Norsk Geografisk Tidsskrift 42(4), 231–238. https://doi.org/10.1080/00291958808552205.

Liestøl O., 1993: Glaciers of Svalbard, Norway. (In:) Williams Jr R.S., Ferrigno J.G. (eds) Satellite Image Atlas of Glaciers of the World. Washington, DC: US Geological Survey, pp. 127–151.

Lindner L., Marks L., 1993: Middle and Late Quaternary evolution of the Hornsund Region, South Spitsbergen. Polish Polar Research 14(3), 275–292.

Lindner L., Marks L., Pękala K., 1984: Late Quaternary glacial episodes in the Hornsund Region of Spitsbergen. Boreas 13, 35–47.

Lindner L., Marks L., Pękala K., 1986: Outline of Quaternary chronostratigraphy of the Northern Hornsund area. Southern Spitsbergen. Bulletin of the Polish Academy of Sciences. Earth Sciences 34(1), 427–436.

Lindner L., Marks L., Pękala K., 1987: Quaternary chronostratigraphy of south Spitsbergen. Polar Research 5, 273–274.

Lønne I., 2016: A new concept for glacial geological investigations of surges, based on High-Arctic examples (Svalbard). Quaternary Science Reviews 132, 74–100. https://doi.org/10.1016/j.quascirev.2015.11.009.

Lovell H., Benn D.I., Lukas S., Ottesen D., Luckman A., Hardiman M., Barr I.D., Boston C.M., Sevestre H., 2018: Multiple Late Holocene surges of a High-Arctic tidewater glacier system in Svalbard. Quaternary Science Reviews 201, 162–185. https://doi.org/10.1016/j.quascirev.2018.10.024.

Lovell H., Boston C.M., 2017: Glacitectonic composite ridge systems and surge-type glaciers: an updated correlation based on Svalbard, Norway. Arktos 3, 2. https://doi.org/10.1007/s41063-017-0028-5.

Lovell H., Fleming E.J., Benn D.I., Hubbard B., Lukas S., Naegeli K., 2015: Former dynamic behaviour of a cold-based valley glacier on Svalbard revealed by basal ice and structural glaciology investigations. Journal of Glaciology 61(226), 309–328. https://doi.org/10.3189/2015JoG14J120.

Luckman A., Benn D.I., Cottier F., Bevan S., Nilsen F., Inall M., 2015: Calving rates at tidewater glaciers vary strongly with ocean temperature. Nature Communications 6(1), 8566. https://doi.org/10.1038/ncomms9566.

Luoto T.P., Ojala A.E.K., Arppe L., Brooks S.J., Kurki E., Oksman M., Wooller M.J., Zajączkowski M., 2018: Synchronized proxy-based temperature reconstructions reveal mid- to late Holocene climate oscillations in High Arctic Svalbard. Journal of Quaternary Science 33, 93–99. https://doi.org/10.1002/jqs.3001.

Lyså A., Jennings A., Morigi C., Stokes C.R., Winsborrow M.C.M., 2022: Introduction: Processes and Palaeo-Environmental Changes in the Arctic from Past to Present (PalaeoArc) special issue. Arctic, Antarctic, and Alpine Research 54(1), 640–647. https://doi.org/10.1080/15230430.2022.2154985.

Majewski W., Szczuciński W., Zajączkowski M., 2009: Interactions of Arctic and Atlantic water-masses and associated environmental changes during the last millennium, Hornsund (SW Svalbard). Boreas 38, 529–544. https://doi.org/10.1111/j.1502-3885.2009.00091.x.

Mannerfelt E.S., Hodson A.J., Håkansson L., Lovell H., 2024: Dynamic LIA advances hastened the demise of small valley glaciers in central Svalbard. Arctic Science 10(4), 815–833. https://doi.org/10.1139/as-2024-0024.

Marks L., 1983: Late Holocene evolution of the Treskelen Peninsula (Hornsund, Spitsbergen). Acta Geologica Polonica 33, 159–168.

Marks L., Pękala K., 1986: New datings of Quaternary sediments from Bogstranda and Treskelodden, southern Spitsbergen. Bulletin of the Polish Academy of Sciences. Earth Sciences 34, 419–425.

Martín-Moreno R., Allende Álvarez F., Hagen J.O., 2017: 'Little Ice Age' glacier extent and subsequent retreat in Svalbard archipelago. The Holocene 27(9), 1379–1390. https://doi.org/10.1177/0959683617693904.

Maussion F., Hock R., Paul F., Raup B., Rastner P., Zemp M., Andreassen L., Barr I., Bolch T., Kochtitzky W., McNabb R., Tielidze L., 2023: The Randolph Glacier Inventory version 7.0 User guide (v1.0). Zenodo. https://doi.org/10.5281/zenodo.8362857

McCerery R., Davies B.J., Lovell H., Pearce D.A., Calvo-Ryan R., Małecki J., Woodward J. 2024: Terrestrial glacial geomorphology of surge-type and non-surge-type glaciers on Svalbard. Journal of Maps 20(1), 2362277. https://doi.org/10.1080/17445647.2024.2362277

Meier M.F., Post A., 1969: What are glacier surges? Canadian Journal of Earth Sciences 6(4), 807–817. https://doi.org/10.1139/e69-081.

Middelhoven M.H., 1634: 'Het nieuwe land Spits-berghen' (The new land of Spitsbergen). Kaart van Spitsbergen door M.H. Middelhoven. Reproduction: Tijdschrift. Aardrijksk. Gen., deel III. Schenking de Bas. Zie Verslag 1877, blz. 4. Facsimile van 4. VEL inv.nr. 2. Orginal volumine: https://www.nationaalarchief.nl/onderzoeken/archief/4.VELH/invnr/20 (access 31.03.2025)

Miller G.H., Brigham-Grette J., Alley R.B., Anderson L., Bauch H.A., Douglas M.S.V., Edwards M.E., Elias S.A., Finney B.P., Fitzpatrick J.J., Funder S.V., Herbert T.D., Hinzman L.D., Kaufman D.S., MacDonald G.M., Polyak L., Robock A., Serreze M.C., Smol J.P., Spielhagen R., White J.W.C., Wolfe A.P., Wolff E.W., 2010: Temperature and precipitation history of the Arctic. Quaternary Science Reviews 29, 1679–1715. https://doi.org/10.1016/j.quascirev.2010.03.001.

Nesje A., Dahl S.O., Thun T., Nordli Ø., 2008: The 'Little Ice Age' glacial expansion in western Scandinavia: summer temperature or winter precipitation? Climate Dynamics, 30, 789–801. https://doi.org/10.1007/s00382-007-0324-z.

Nordli Ø., Wyszyński P., Gjelten H., Isaksen K., Łupikasza E., Niedźwiedź T., Przybylak R., 2020: Revisiting the extended Svalbard Airport monthly temperature series, and the compiled corresponding daily series 1898–2018. Polar Research 39, 3614. https://doi.org/10.33265/polar.v39.3614.

Norwegian Polar Institute, 1921: (Kart over) Farvannet mellom Hornsund og Dunderbay 1917–1921. Dostępne na https://data.npolar.no/map/archive/066a96e0-00d8-574e-8a71-334d02ee3ca0 (dostęp 20.09.2025)

Norwegian Polar Institute, 1984: Svalbard Frå Sørkapp til Bellsund, Sjøkart 504, 1:200 000. Norsk Polarinstitutt, Oslo. Dostępne na https://data.npolar.no/map/archive/fe263748-5917-55e8-bb0e-98e1530cdc00 (dostęp 20.09.2025)

Norwegian Polar Institute, 2014: Kartdata Svalbard 1:1 000 000 (S1000 Kartdata) [data set]. Norwegian Polar Institute. https://doi.org/10.21334/NPOLAR.2014.63730E2E (dostęp 20.09.2025).

Nuth C., Kohler J., Aas H.F., Brandt O., Hagen J.O., 2007: Glacier geometry and elevation changes on Svalbard (1936–90): a baseline dataset. Annals of Glaciology 46, 106–116. https://doi.org/10.3189/172756407782871440.

Nuth C., Kohler J., Köning M., Von Deschwanden A., Hagen J.O., Kääb A., Moholdt G., Pettersson R., 2013: Decadal changes from a multi-temporal glacier inventory of Svalbard. The Cryosphere 7(5), 1603–1621. https://doi.org/10.5194/tc-7-1603-2013.

Osika A., Jania J., 2024: Geomorphological and historical records of the surge-type behaviour of Hansbreen (Svalbard). Annals of Glaciology 65, e31. https://doi.org/10.1017/aog.2024.32 – 100 pkt. MNiSW; IF: 2,1

Osika A., Jania J., Piotrowska N., Tikhomirov D., Szafraniec J., Devendra D., Christl M., Egli M., Vieli A., 2025a: Holocene glacial history of southern Spitsbergen. In preparation

Osika A., Jania J., Szafraniec J.E., 2022: Holocene ice-free strait followed by dynamic Neoglacial fluctuations: Hornsund, Svalbard. The Holocene 32(7), 664–679. https://doi.org/10.1177/09596836221088232.

Osika A., Piotrowska N., Jania J., 2025b: Radiocarbon dates of marine shells, subfossil vegetation, driftwood and a whalebone from glacial sediments in Hornsund (Spitsbergen, Svalbard) [Data set]. Zenodo. https://doi.org/10.5281/zenodo.15831642

Ottesen D., Dowdeswell J.A., 2006: Assemblages of submarine landforms produced by tidewater glaciers in Svalbard. Journal of Geophysical Research 111, F01016, https://doi.org/10.1029/2005JF000330.

Ottesen D., Dowdeswell J.A., Benn D.I., Kristensen L., Christiansen H.H., Christensen O., Hansen L., Lebesbye E., Forwick M., Vorren T., 2008; Submarine landforms characteristic of glacier surges in two Spitsbergen fjords. Quaternary Science Reviews 27(15–16), 1583–1599. https://doi.org/10.1016/j.quascirev.2008.05.007.

Ottesen D., Dowdeswell J.A., Landvik J.Y., Mienert J., 2007: Dynamics of the Late Weichselian ice sheet on Svalbard inferred from high-resolution sea-floor morphology. Boreas 36, 286–306. https://doi.org/10.1111/j.1502-3885.2007.tb01251.x.

Park H.-S., Kim S.-J., Stewart A.L., Son S.-W., Seo K.-H., 2019: Mid-Holocene Northern Hemisphere warming driven by Arctic amplification. Science advances 5(12), eaax8203. https://doi.org/10.1126/sciadv.aax8203

Pawłowska J., Łącka M., Kucharska M., Pawlowski J., Zajączkowski M., 2020: Multiproxy evidence of the Neoglacial expansion of Atlantic Water to eastern Svalbard. Climate of the Past 16, 487–501. https://doi.org/10.5194/cp-16-487-2020.

Pawłowski M., Ostafin K., 2024: Narrowing of glacial isthmus between Sørkapp Land and Torell Land, southern Spitsbergen, 1900–2023. Journal of Maps, 20(1), 2317130. https://doi.org/10.1080/17445647.2024.2317130

Pękala K., 1989: Quaternary deposits of the Hans Glacier forefield (Hornsund, Spitsbergen).(In:) Repelewska-Pękalowa J., Pękala K. (Eds.), Wyprawy geograficzne na Spitsbergen 1986–1988. UMCS, Lublin, pp. 191–204.

Peterman A., 1874: Graf Wiltschek's Nordpolarfahrt im Jahre 1872 / nach den Aufzeichnungen des Contre-Admirals Max Freiherrn Daublebsky v. Sterneck und Ehrenstein. (In:) Peterman A. (Ed.) Mittheilungen aus Justus Perthes' Geographischer Anstalt über wichtige neue Erforschungen auf dem Gesammtgebiete der Geographie, 20 Band, Justus Perthes' Geographische Anstalt Gotha, pp. 65–72.

Philipps W., Briner J.P., Gislefoss L., Linge H., Koffman T., Fabel D., Xu S., Hormes A., 2017: Late Holocene glacier activity at inner Hornsund and Scottbreen, southern Svalbard. Journal of Quaternary Science 32(4), 501–515. https://doi.org/10.1002/jqs.2944.

Pieńkowski A.J., Husum K., Furze M.F.A., Missana A.F.J.M., Irvalı N., Divine D.V., Eilertsen V.T., 2022: Revised ΔR values for the Barents Sea and its archipelagos as a pre-requisite for accurate and robust marine-based 14C chronologies. Quaternary Geochronology 68, 101244. https://doi.org/10.1016/j.quageo.2021.101244.

Porter C., Howat I., Noh M.-J., Husby E., Khuvis S., Danish E., Tomko K., Gardiner J., Negrete A., Yadav B., Klassen J., Kelleher C., Cloutier M., Bakker J., Enos J., Arnold G., Bauer G., Morin P., 2023: ArcticDEM - Mosaics, Version 4.1. Harvard Dataverse, V1. https://doi.org/10.7910/DVN/3VDC4W.

Previdi M., Smith K.L., Polvani L.M., 2021: Arctic amplification of climate change: a review of underlying mechanisms. Environmental Research Letters 16, 093003, https://doi.org/10.1088/1748-9326/ac1c29

Promińska A., Falck E., Walczowski W., 2018: Interannual variability in hydrography and water mass distribution in Hornsund, an Arctic fjord in Svalbard. Polar Research 37(1), 1495546. https://doi.org/10.1080/17518369.2018.1495546.

Przybylak R., Wyszyński P., Nordli Ø., Strzyżewski T., 2016: Air temperature changes in Svalbard and the surrounding seas from 1865 to 1920. International Journal of Climatology 36(8), 2899–2916. https://doi.org/10.1002/joc.4527

Purchas S., 1625: Greneland [map]. In: Purchas S. "Purchas His Pilgrimes" part iii. London

Rantanen M., Karpechko A.Y., Lipponen A., Nordling K., Hyvärinen O., Ruosteenoja K., Vihma T., Laaksonen A., 2022: The Arctic has warmed nearly four times faster than the globe since 1979. Communications Earth & Environment 3, 168. https://doi.org/10.1038/s43247-022-00498-3.

Raymond C.F., 1987: How do glaciers surge? A review. Journal of Geophysical Research 92(B9), 9121–9134. https://doi.org/10.1029/JB092iB09p09121.

Reimer P., Austin W., Bard E., Bayliss A., Blackwell P., Bronk Ramsey C., Butzin M., Cheng H., Edwards R., Friedrich M., Grootes P., Guilderson T., Hajdas I., Heaton T., Hogg A., Hughen K., Kromer B., Manning S., Muscheler R., Palmer J., Pearson C., van der Plicht J., Reimer R., Richards D., Scott E., Southon J., Turney C., Wacker L., Adolphi F., Büntgen U., Capano M., Fahrni S., Fogtmann-Schulz A., Friedrich R., Köhler P., Kudsk S., Miyake F., Olsen J., Reinig F., Sakamoto M., Sookdeo A., Talamo S., 2020: The IntCal20 Northern Hemisphere radiocarbon age calibration curve (0–55 cal kBP). Radiocarbon 62(4), 725-757. https://doi.org/10.1017/RDC.2020.41.

Reinthaler J., Paul F., 2023: Using a Web Map Service to map Little Ice Age glacier extents at regional scales. Annals of Glaciology 64(92), 206–224. https://doi.org/10.1017/aog.2023.39

RGI 7.0 Consortium, 2023: Randolph Glacier Inventory – A Dataset of Global Glacier Outlines, Version 7.0. Boulder, Colorado, USA: NSIDC: National Snow and Ice Data Center. https://doi.org/10.5067/f6jmovy5navz

Røthe T.O., Bakke J., Støren E.W.N., Bradley R.S., 2018: Reconstructing Holocene glacier and climate fluctuations from lake sediments in Vårfluesjøen, Northern Spitsbergen. Frontiers in Earth Science 6, 91. https://doi.org/10.3389/feart.2018.00091.

Røthe T.O., Bakke J., Vasskog K., Gjerde M., D'Andrea W. J., Bradley R.S., 2015: Arctic Holocene glacier fluctuations reconstructed from lake sediments at Mitrahalvøya, Spitsbergen. Quaternary Science Reviews 109, 111–125. https://doi.org/10.1016/j.quascirev.2014.11.017

Różycki O., 1992: Occurrence of Gastropoda and Bivalvia in Hornsund Fiord (West Spitsbergen, Svalbard). Polish Polar Research 13(1), 41–52.

Saferna D., Błaszczyk M., Grabiec M., Gądek B., 2023: Quantifying Changes in Extent and Velocity of the Hornbreen/Hambergbreen Glacial System (SW, Spitsbergen) Based on Timeseries of Multispectral Satellite Imagery. Remote Sensing 15(14), 3529. https://doi.org/10.3390/rs15143529.

Sarnthein M., Van Kreveld S., Erlenkeuser H., Grootes P.M., Kucera M., Pflaumann U., Schulz M., 2003: Centennial-to-millennial-scale periodicities of Holocene climate and sediment injections off the western Barents shelf, 75°N. Boreas 32, 447–461. https://doi.org/10.1111/j.1502-3885.2003.tb01227.x.

Schmidt L.S., Schuler T.V., Thomas E.E., Westermann S., 2023: Meltwater runoff and glacier mass balance in the high Arctic: 1991–2022 simulations for Svalbard. The Cryosphere 17, 2941–2963. https://doi.org/10.5194/tc-17-2941-2023.

Schuler T.V., Kohler J., Elagina N., Hagen J.O.M., Hodson A.J., Jania J.A., Kääb A.M., Luks B., Małecki J., Moholdt G., Pohjola V.A., Sobota I., Van Pelt W.J.J., 2020: Reconciling Svalbard Glacier Mass Balance. Frontiers in Earth Science 8, 156. https://doi.org/10.3389/feart.2020.00156.

Scoresby W., 1820: A chart of Spitzbergen or East Greenland, comprising an original survey of the west coast. Above 200 Miles in extent. An account of the Arctic regions with a history and description of the northern whale-fishery. vol. 2. Edinburgh, Pl. 7:573.

Sevestre H., Benn D.I., 2015: Climatic and geometric controls on the global distribution of surge-type glaciers: implications for a unifying model of surging. Journal of Glaciology 61(228), 646–662. https://doi.org/10.3189/2015JoG14J136.

Sevestre H., Benn D.I., Hulton N.J.R., Bælum K., 2015: Thermal structure of Svalbard glaciers and implications for thermal switch models of glacier surging. Journal of Geophysical Research: Earth Surface 120(10), 2220–2236. https://doi.org/10.1002/2015JF003517.

Skirbekk K., Kristensen D.K., Rasmussen T.L., Koç N., Forwick M., 2010: Holocene climate variations at the entrance to a warm Arctic fjord: evidence from Kongsfjorden trough, Svalbard. Geological Society, London, Special Publications 344, 289–304. https://doi.org/10.1144/SP344.20.

Ślubowska-Woldengen M., Rasmussen T.L., Koç N., Klitgaard-Kristensen D., Nilsen F., Solheim A., 2007: Advection of Atlantic Water to the western and northern Svalbard shelf since 17,500 cal yr BP. Quaternary Science Reviews 26(3–4), 463–478. https://doi.org/10.1016/j.quascirev.2006.09.009

Sund M., Eiken T., Hagen J.O., Kääb A., 2009: Svalbard surge dynamics derived from geometric changes. Annals of Glaciology 50(52), 50–60. https://doi.org/10.3189/172756409789624265.

Sund M., Lauknes T.R., Eiken T., 2014: Surge dynamics in the Nathorstbreen glacier system, Svalbard. The Cryosphere 8, 623–638. https://doi.org/10.5194/tc-8-623-2014.

Szafraniec J.E., Dobiński W., 2020: Deglaciation Rate of Selected Nunataks in Spitsbergen, Svalbard—Potential for Permafrost Expansion above the Glacial Environment. Geosciences 10(5), 202. https://doi.org/10.3390/geosciences10050202.

Szupryczyński J., 1963: Rzeźba strefy marginalnej i typy deglacjacji lodowców południowego Spitsbergenu. Prace Geograficzne 39, Instytut Geografii Polskiej Akademii Nauk, Warszawa

Tarasov G.A., Denisenko S.G., Matishov G.G., Pogodina I.A., 1992: Moraine complexes and certain questions concerning paleoecology of the Treskelen region in the Hornsund Fiord (W Spitsbergen). (In:) Repelewska-Pękalowa J., Pękala K. (Eds.), Wyprawy geograficzne na Spitsbergen 1992. UMCS, Lublin, s. 89–95.

Telesiński M.M., Przytarska J.E., Sternal B., Forwick M., Szczuciński W., Łącka M., Zajączkowski M., 2018: Palaeoceanographic evolution of the SW Svalbard shelf over the last 14 000 years. Boreas 47(2), 410–422. https://doi.org/10.1111/bor.12282.

Traczyk A., 2008: Significance of the Quaternary glaciations on the relief evolution of the western coastal zone of the Spitsbergen on example of the Hornsund area (W:) Kolwalska A., Latocha A., Marszałek H., Pereyma J. (Red.) Środowisko Przyrodnicze Obszarów Polarnych. Uniwersytet Wrocławski, Wrocław, s. 79–88.

Tylmann K., Moskalewicz D., 2020: Zastosowanie ziemskich izotopów kosmogenicznych w datowaniu glin lodowcowych: potencjał, ograniczenia i perspektywy badawcze. Przegląd Geologiczny 68 (10), 764–773. https://doi.org/10.7306/2020.32

van Keulen G., 1714: Nieuwe afteekening van Het Eyland Spits-Bergen opgegeven door de Commandeurs Giles en Outger Rep, en in't Ligt gebrat en uytgegeven. Bibliothèque nationale de France. Dostępne na https://gallica.bnf.fr/ark:/12148/btv1b5972615q (dostęp 20.09.2025)

van Pelt W., Frank T., 2025: New glacier thickness and bed topography maps for Svalbard. The Cryosphere 19(1), 1–17, https://doi.org/10.5194/tc-19-1-2025.

Walczowski W., Piechura J., 2011: Influence of the West Spitsbergen Current on the local climate. International Journal of Climatology 31(7), 1088–1093. https://doi.org/10.1002/joc.2338

Wassiliew A.S., 1925: Océan Glacial arctique. Spitzberg. Région des travaux de l'expédition de l'Académies de sciences de Russie pour la mesure d'un arc de méridien en 1899–1901. Carte dresie d'après les matériaux de l'expédition sous la rédactin de O.E. Stubendorff par A.S. Wassiliew. Échelle de 1:200 000.

Wawrzyniak T., Osuch M., 2020: A 40-year High Arctic climatological dataset of the Polish Polar Station Hornsund (SW Spitsbergen, Svalbard). Earth System Science Data 12, 805–815. https://doi.org/10.5194/essd-12-805-2020.

Werner K., Spielhagen R.F., Bauch D., Hass H.C., Kandiano E., 2013: Atlantic Water advection versus sea-ice advances in the eastern Fram Strait during the last 9 ka: Multiproxy evidence for a two-phase Holocene. Paleoceanography 28, 283–295. https://doi.org/10.1002/palo.20028

Włodarska-Kowalczuk M., 2007: Molluscs in Kongsfjorden (Spitsbergen, Svalbard): a species list and patterns of distribution and diversity. Polar Research 26(1), 48–63, https://doi.org/10.1111/j.1751-8369.2007.00003.x.

Włodarska-Kowalczuk M., Węsławski J., Kotwicki L., 1998: Spitsbergen glacial bays macrobenthos – a comparative study. Polar Biology 20, 66–73. https://doi.org/10.1007/s003000050277.

Young N.E., Schaefer J.M., Briner J.P., Goehring B.M., 2013: A 10Be production-rate calibration for the Arctic. Journal of Quaternary Science 28, 515–526. https://doi.org/10.1002/jqs.2642.

Zagórski P., Frydrych K., Jania J., Błaszczyk M., Sund M., Moskalik M., 2023: Surges in Three Svalbard Glaciers Derived from Historic Sources and Geomorphic Features. Annals of the American Association of Geographers 113(8), 1835–1855. https://doi.org/10.1080/24694452.2023.2200487.

Zemp M., Huss M., Thibert E., Eckert N., McNabb R., Huber J., Barandun M., Machguth H., Nussbaumer S. U., Thomson L., Paul F., Maussion F., Kutuzov S., Cogle, J.G., 2019: Global glacier mass changes and their contributions to sea-level rise from 1961 to 2016. Nature 568(7752), 382–386. https://doi.org/10.1038/s41586-019-1071-0

Zemp M., Jakob L., Dussaillant I., Nussbaumer S.U., Gourmelen N., Dubber S., A G., Abdullahi S., Andreassen L.M., Berthier E., Bhattacharya A., Blazquez A., Boehm Vock L.F., Bolch T., Box J., Braun M.H., Brun F., Cicero E., Colgan W., Eckert N., Farinotti D., Florentine C., Floricioiu D., Gardner A., Harig C., Hassan J., Hugonnet R., Huss M., Jóhannesson T., Liang C.-C.A., Ke C.-Q., Khan S.A., King O., Kneib M., Krieger L., Maussion F., Mattea E., McNabb R., Menounos B., Miles E., Moholdt G., Nilsson J., Pálsson F., Pfeffer J., Piermattei L., Plummer S., Richter A., Sasgen I., Schuster L., Seehaus T., Shen X., Sommer C., Sutterley T., Treichler D., Velicogna I., Wouters B., Zekollari H., Zheng W., 2025: Community estimate of global glacier mass changes from 2000 to 2023. Nature 639, 382–388. https://doi.org/10.1038/s41586-024-08545-z

Ziaja W., Ostafin K., 2015: Landscape–seascape dynamics in the isthmus between Sørkapp Land and the rest of Spitsbergen: Will a new big Arctic island form?. AMBIO 44, 332–342. https://doi.org/10.1007/s13280-014-0572-1

ZAŁĄCZNIKI

Załącznik 1. Osika A., Jania J., Szafraniec J.E., 2022: Holocene ice-free strait followed by dynamic Neoglacial fluctuations: Hornsund, Svalbard. The Holocene, 32(7), 664–679. https://doi.org/10.1177/09596836221088232.

Załączniki 2–5. Materiały dodatkowe do artykułu Osika i in. (2022), The Holocene.

Załącznik 6. Osika A., Jania J., 2024: Geomorphological and historical records of the surge-type behaviour of Hansbreen (Svalbard). Annals of Glaciology, 65, e31. https://doi.org/10.1017/aog.2024.32.

Załącznik 7. Osika A., Jania J., Piotrowska N., Tikhomirov D., Szafraniec J.E., Devendra D., Christl M., Egli M., Vieli A., 2025: Holocene glacial history of southern Spitsbergen. Złożono do *Quaternary Science Reviews* 22.09.2025 r.

Załącznik 8. Materiały dodatkowe do artykułu Osika i in. (2025).

Załącznik 9. Oświadczenie osoby ubiegającej się o własnym wkładzie w powstawanie prac.

Załączniki 10–15. Oświadczenia współautorów osoby ubiegającej się o własnym wkładzie w powstawanie prac:

- prof. dr hab. Jacek Jania (**Zał. 10–12**),
- dr Joanna Szafraniec (**Zał. 13**),
- dr hab. inż. Natalia Piotrowska, prof. PŚl (**Zał. 14**),
- dr Dhanushka Devendra (**Zał. 15**).

Załącznik 1

Research Paper

The Holocene
2022, Vol. 32(7) 664–679
© The Author(s) 2022
Article reuse guidelines:
sagepub.com/journals-permissions
DOI: 10.1177/09596836221088232
journals.sagepub.com/home/hol
SAGE

Holocene ice-free strait followed by dynamic Neoglacial fluctuations: Hornsund, Svalbard

Aleksandra Osika, Jacek Jania and Joanna Ewa Szafraniec

Abstract

The recession of the Hornbreen-Hambergbreen glaciers (Hornsund, Svalbard) will lead to the formation of a strait between the Greenland and Barents Seas within a few decades. We provide evidence for the earlier existence of this strait, in the Early–Middle Holocene and presumably since 1.3 ka cal. BP until glacier advance 0.7 ± 0.3 ka or earlier. Radiocarbon dating of mollusc shells from the ground moraines in the Hornbreen forefield indicate the existence of the marine environment at the contemporary glacierized head of Hornsund since 10.9 ka cal. BP or earlier due to glacier retreat. The gap in the radiocarbon dates between 3.9 and 1.3 ka cal. BP and the published results of ^{10}Be exposure dating on Treskelen suggest the strait's closure after glacier advance in the Neoglacial. Subsequent re-opening occurred around 1.3 ka cal. BP, but according to ^{10}Be dates from Treskelen, the strait has again been closed since ca. 0.7 ± 0.3 ka or earlier. The oldest known surge of Hornbreen occurred around 1900. Analysis of Landsat satellite images, morphometric indicators characterizing the glacier frontal zones and previous studies indicate one surge of Hambergbreen (1957–1968) and five re-advances of Hornbreen in the 20th century (after 1936, between 1958 and 1962, in 1986–1990, 1998–1999, 2011). While the warmer Holocene intervals might be a benchmark for the effects of future climate change, glacier dynamics in post-Little Ice Age climate warming seems to be an analogue of glacier retreats and re-advances in the earlier periods of the Holocene.

Keywords

glacier advance, glacier retreat, glacier surges, Holocene Climate Optimum, radiocarbon dating, Spitsbergen

Received 18 September 2021; revised manuscript accepted 14 February 2022

Introduction

Over the last 50 years, the Arctic has been warming three times faster than the global average (AMAP, 2021). For this reason, the last 20 years have witnessed exceptionally rapid deglaciation, contributing to sea level rise (Box et al., 2018; Zemp et al., 2019). In Svalbard, the maximum extent of glaciers in the last few 100 years was reached at the turn of the 19th and 20th centuries, and since the 1930s they have been receding (Martín-Moreno et al., 2017; Noël et al., 2020). As elsewhere in the Arctic, this process accelerated in the 1990s (Nuth et al., 2007). This recession has been especially rapid in the case of tidewater glaciers, which lose their mass by intensive frontal ablation (calving and submarine melt) (Błaszczyk et al., 2009, 2013, 2021; Pętlicki et al., 2015). Ongoing climate warming and deglaciation are responsible for significant changes in the Arctic environment, as exemplified by the development of paraglacial processes on recently exposed areas, the evolution of the geometry of deglacierizing fjords (Strzelecki et al., 2020) and Arctic borealization (Polyakov et al., 2020). During the first half of the Holocene, similar changes occurred in Svalbard and elsewhere in the Arctic (Bartels et al., 2017; Kaufman et al., 2004; Mangerud and Svendsen, 2018; Salvigsen and Høgvard, 2006). A growing body of evidence from the marine and terrestrial environments has demonstrated that in the Early and Middle Holocene the climate of Svalbard was warmer than today and that the glaciers receded to their minimum extents or disappeared altogether (Birks, 1991; Farnsworth et al., 2020; Mangerud and Svendsen, 2018; Røthe et al., 2015; Svendsen and Mangerud, 1997).

Despite the different causes of the warmer climate in that period and at present, the dramatically smaller extent of glaciers in the first half of the Holocene could provide a benchmark for predicting the consequences of future warming in the Arctic (Allaart et al., 2021; van der Bilt et al., 2019). On the other hand, the glacier dynamics observed in post-Little Ice Age (post-LIA) climate warming may, in accordance with uniformitarianism, be analogous to their behaviour in earlier periods of deglaciation. Although interest in the Holocene history of Svalbard is growing, our understanding of the environment of southern Spitsbergen in the warmer intervals is still insufficient (cf. Farnsworth et al., 2020). The crucial area in this region is the Hornbreen-Hambergbreen glacier isthmus, connecting Sørkapp Land with the rest of Spitsbergen and limiting the contact of warmer water masses carried by the West Spitsbergen Current (WSC) with the cold Barents Sea. GPR soundings have revealed a subglacial depression ca. 40 m below sea level (Grabiec et al., 2018), probably of a continuous nature. Hence, future decades are expected to see the opening of the Hornsund strait as a consequence of the ongoing

Institute of Earth Sciences, Faculty of Natural Sciences, University of Silesia in Katowice, Poland

Corresponding author:
Aleksandra Osika, Institute of Earth Sciences, Faculty of Natural Sciences, University of Silesia in Katowice, Będzińska 60, Sosnowiec 41-200, Poland.
Email: aosika1@us.edu.pl

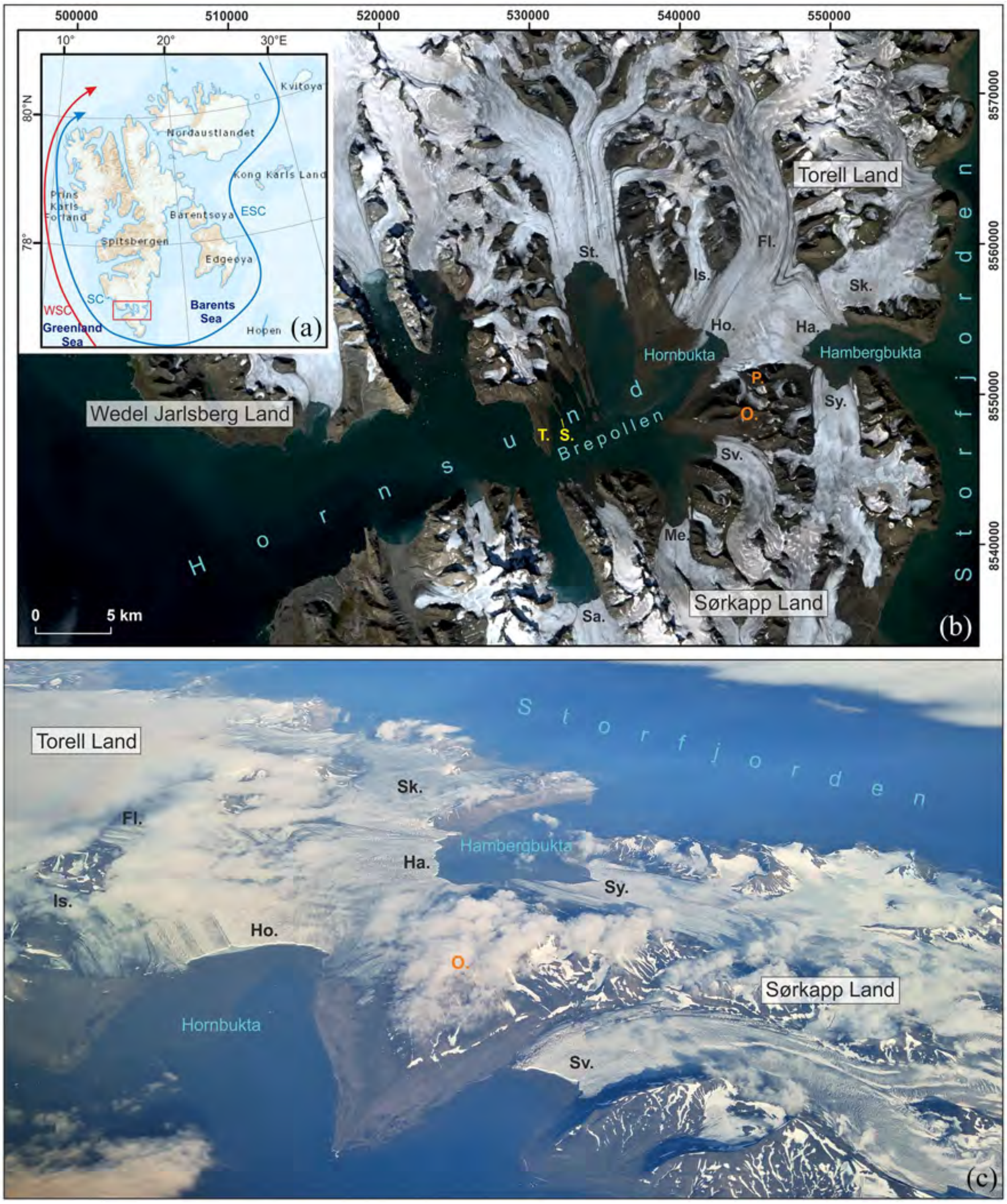

Figure 1. Overview (a) and detailed (b and c) location of the study area. Hornbreen-Hambergbreen ice bridge between the Greenland and the Barents Seas (c). Glaciers (black letters): Fl. – Flatbreen, Ha. – Hambergbreen, Ho. – Hornbreen, Is. – Isingbreen, Me. – Mendeleevbreen, Sa. – Samarinbreen, Sk. – Skjoldfonna, St. – Storbreen, Sv. – Svalisbreen, Sy. – Sykorabreen. Capes (yellow letters): T. – Treskelen, S. – Selodden. Mountains (orange letters): O. – Ostrogradskijfjella, P. – Professorryggen. Ocean currents: WSC – West Spitsbergen Current, ESC – East Spitsbergen Current, SC – Sørkapp Current. Figure map modified from TopoSvalbard © Norwegian Polar Institute 2021. Landsat-8 image ID: LC08_L1TP_210005_20200804_20200804_01_RT from 04.08.2020, USGS/NASA Landsat (U.S. Geological Survey, 2021). Photo A. Osika (26.08.2021).

retreat of these glaciers (Grabiec et al., 2018). Geomorphological investigations and analyses of bivalve shells and foraminifera from the ground moraines on the coastal areas at the head of the fjord suggest that an ice-free marine environment in the recently and contemporarily glacierized part of eastern Hornsund could also have occurred in the Early-Middle Holocene and the Medieval Warm Period (Birkenmajer and Olsson, 1997; Birkenmajer and Łuczkowska, 1996; Grabiec et al., 2018; Heintz, 1953).

This work aims to highlight the possible periods when Hornsund functioned as a fjord/strait between the Greenland and Barents Seas, depending on the fluctuations of the glaciers of the Hornbreen-Hambergbreen system. To the best of our knowledge, this is also the first study of the subfossil mollusc shells from the glacial sediments of the recently exposed coast of Hornbukta.

Study area

Hornsund is the southernmost fjord system of Spitsbergen, between Wedel-Jarlsberg Land and Torell Land in the north and Sørkapp Land in the south (Figure 1a and b). The east-west oriented fjord system is approximately 35 km long, 2–12 km wide and ca. 320 km^2 in area (Promińska et al., 2018; Strzelecki et al., 2020). Hornsund is known for its numerous glaciers, covering ca. 67% of the surrounding drainage basin of ca. 1200 km^2 (Błaszczyk

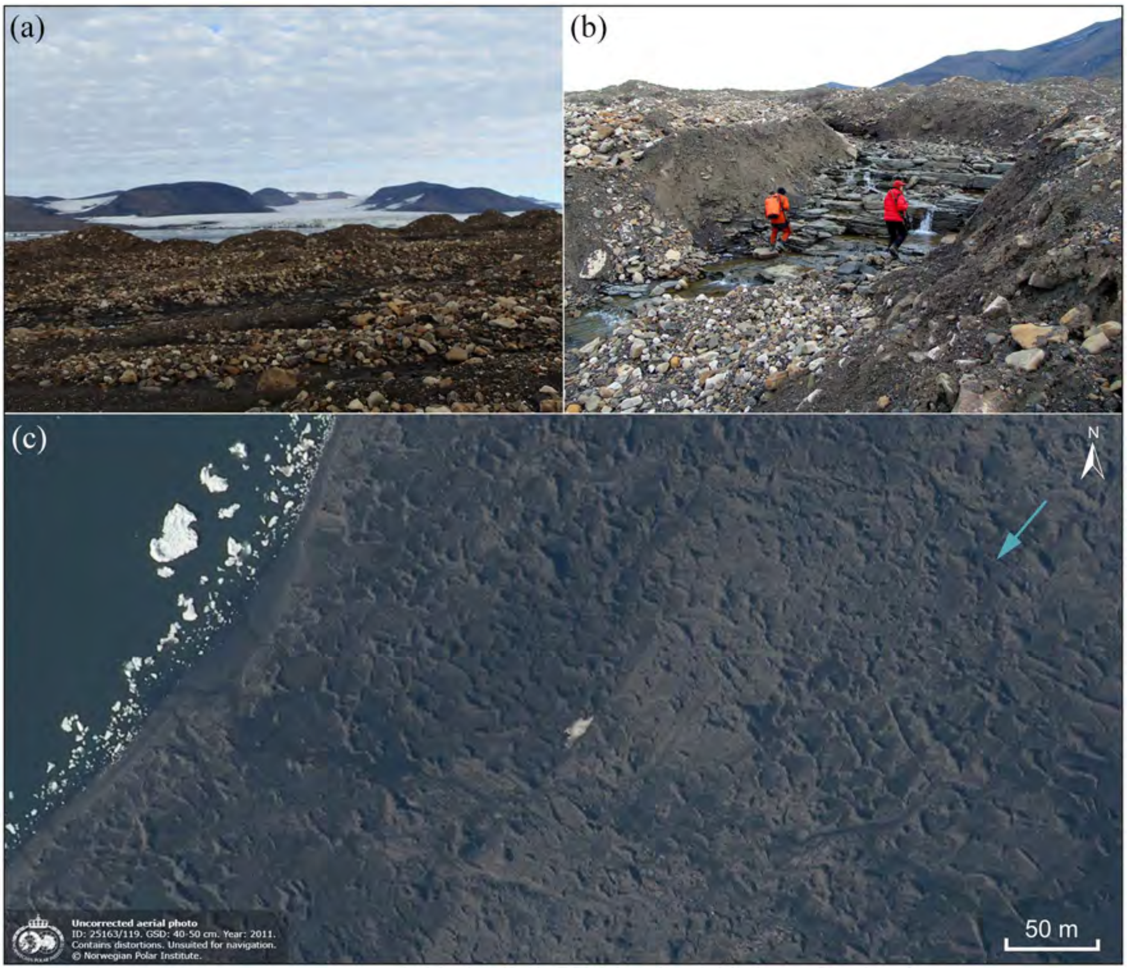

Figure 2. The ground moraine with hummocky relief from degraded crevasse-squeeze ridges (CSRs) in the Hornbreen forefield (a) dissected by streams (b). Overview of the CSR network on the aerial image from 2011 (ID: 25163/119) modified from TopoSvalbard © Norwegian Polar Institute 2021 (c). The arrow indicates the approximate direction of the glacier's movement during the surge. (a and b) – photo A. Osika (August 2020).

et al., 2013). The vast majority of them terminate in the sea (97% of the glacierized area of 781 km^2). Błaszczyk et al. (2013) point out that the tidewater glaciers in Hornsund are retreating faster than the average rate in Svalbard (ca. 70 m a^{-1} and ca. 45 m a^{-1} in 2001–2010, respectively). The glaciers of southern Spitsbergen as a whole also have one of the most negative mass balances (Nuth et al., 2010; Schuler et al., 2020; Østby et al., 2017).

The distribution of glaciers in Hornsund is governed by the topography, which, in turn, depends closely on the geological structures (Jania, 1988). The mountain ridges and major glacier valleys correspond to the longitudinal direction of the main overthrusts and faults (Birkenmajer, 1990). On the other hand, the latitudinal faults have given predestination to the course of the fjord system (Bednarek et al., 1993). Hence, fluctuations from tidewater glacier tributaries determine the shape of Hornsund. The fjord system is influenced by the warm WSC and the cooler water masses from the Barents Sea carried by the Sørkapp Current (SC) (Promińska et al., 2018). The mean annual air temperature at the Polish Polar Station in Hornsund was –3.7°C in 1979–2018 and has been increasing by 1.14°C per decade since then (Wawrzyniak and Osuch, 2020).

The study area is located at Brepollen in the inner part of Hornsund (Figure 1b). At the end of the LIA (~1900 AD), Brepollen was entirely glacierized by confluent glacier tongues. During that period, Hornbreen overpassed Treskelen and Hambergbreen advanced to Storfjorden (Vassiliev, 1907). Since then, post-LIA retreat has led to the separation of tributary glaciers and the exposure of new coastal systems (Strzelecki et al., 2020), a process that has been interrupted by surge episodes of diminishing extent (Błaszczyk et al., 2013; Jania, 1988).

Today, Hornbreen is supplied mainly by Flatbreen and, to a lesser extent, by Isingbreen. Hornbreen is about 6 km wide in the frontal zone and, together with its lateral glaciers, covers an area of 176.2 km^2 (Błaszczyk et al., 2013). Hambergbreen, in turn, is supplied by Skjoldfonna and also partly by Flatbreen. Hambergreen has a surface area of 35 km^2 and terminates in a 4.7 km long cliff. Hornbreen and Hambergbreen are separated by a several km long ice divide at ca. 180 m a.s.l. (Grabiec et al., 2018). The partly confluent Hornbreen-Hambergbreen glaciers form an ice bridge ca. 4.9 km wide (Norwegian Polar Institute, 2021) between the Greenland and Barents Seas (Figure 1b and c). The ongoing recession has given rise to the development of two bays in their forefields: Hornbukta and Hambergbukta. Surface water conditions influence glacier retreat rates in the different catchments. A lower rate of retreat has been measured in Hambergbukta (2000–2015; 71 m a^{-1} compared to 106 m a^{-1} in Hornbukta) associated with cooler waters of the East Spitsbergen Current (ESC) (Grabiec et al., 2018). The recession of the Hornbreen-Hambergbreen system will end in the collapse of the ice isthmus (Grabiec et al., 2018).

In this study, we focus on the terrestrial part of the Hornbreen forefield: the southern coast of Hornbukta at the foot of Ostrogradskijfjella and the two peninsulas – Selodden and Treskelen. The topography of the southern coast of Hornbukta is dominated by ground moraine with hummocky relief and degraded crevasse-squeeze ridge (CSR) networks, indicative of surge episodes in the 20th century (Figure 2; cf. Farnsworth et al., 2016;

Strzelecki et al., 2020). At the foot of Ostrogradskijfjella, there is also lateral moraine. During the culmination of the LIA (~1900 AD), the ice margin of Hornbreen terminated along Treskelen. The LIA push moraine is located west of Treskelen and is visible on the Hornsund bathymetry map (Moskalik et al., 2013). Both peninsulas are covered with ground moraine from degraded CSR networks. Following the LIA, Treskelen has been ice-free since the 1940s (Heintz, 1953) and Selodden was exposed in the 1950s. Deglaciation of the southern coast of Hornbukta has been progressing since the 1990s (Błaszczyk et al., 2013). At these sites, Hornbreen deposited shell-bearing diamict (Birkenmajer, 1958; Birkenmajer and Olsson, 1997; Heintz, 1953; Rodzik, 1996). On the southern coast of Hornbukta numerous sandstone cobbles and boulders are present (Figure 2a and b). During preliminary studies in 2019, no shells were found in the lateral moraines of Hornbreen or in the ground moraine on the northern coast of Hornbukta. Initial observations at Hambergbukta have not revealed any shells either in the lateral moraines of the Hambergbreen–Sykorabreen system at the foot of the steep slopes of Koval'skijfiella and Kamnova. For this reason, these sites are not included in the study area.

The bedrock of Treskelen is composed of sandstones, conglomerates, limestones and shales from the Upper Carboniferous to the Upper Triassic (Birkenmajer, 1990; Harland, 1997). The characteristic components of this area are raised marine terraces developed on structural ridges parallel to the shoreline. Detailed geomorphological descriptions and the history of deglaciation were given by for example Birkenmajer (1960), Heintz (1953), Marks (1983) and Philipps et al. (2017). The bedrock along Hornbukta and Hambergbukta is composed of Cretaceous and Palaeocene shales, siltstones, sandstones and mudstones (Birkenmajer, 1990; Harland, 1997). Submarine landforms in the forefield of Hambergbreen were described by Noormets et al. (2021) .

Materials and methods

Geomorphological observations in the forefield of Hornbreen have been carried out occasionally since 1999. During fieldwork in August 2019 and 2020, we collected samples of subfossil mollusc shells from the surface of the moraine at the foot of Ostrogradskijfjella and in the southern part of Treskelen (Treskelodden). The shells were sampled beyond the reach of the sea waves or streams so as to exclude recently redeposited specimens. Geomorphological sketch mapping was carried out in the sample collection area. Aerial images from 1936 and 2011 (Norwegian Polar Institute, 2021) and high-resolution orthoimages from 2017 (Błaszczyk et al., 2019) were used to analyse the distribution of landforms and indirectly the direction of glacier flow. After identification, the samples were submitted to the Poznań Radiocarbon Laboratory (4 samples) and the Gliwice Radiocarbon Laboratory (6 samples) for AMS radiocarbon dating. We also compiled previously published radiocarbon dates (conventional technique) of 11 shell samples from Treskelen and Selodden (Birkenmajer and Olsson, 1997; Marks and Pękala, 1986; Tarasov et al., 1992). All ^{14}C dates were calibrated (or recalibrated, in the case of previously published data) to calendar years (cal. BP; BP=AD 1950) using OxCal 4.4.4 software (Bronk Ramsey, 2009, 2017) and the Marine20 calibration curve (Heaton et al., 2020). In consultation with the Poznań Radiocarbon Laboratory (T. Goslar, 2020, personal communication), a ΔR value was calculated using the 14CHRONO Marine20 Reservoir Database (Reimer and Reimer, 2001) as a weighted mean of all available records from Spitsbergen (n = 6). We thus applied the ΔR value of –56 ± 33. The results of radiocarbon dating and (re)calibration are presented in Supplemental Material S1. The median (re)calibrated ages were used to analyse the spatio-temporal distribution of the shells. The division of the Holocene into Early, Middle and Late-Holocene together with boundaries between intervals (11,700–8236 yr b2k, 8236–4250 yr b2k and 4250 yr b2k to present) is consistent with the International Commission on Stratigraphy (Walker et al., 2019). The species names follow the World Register of Marine Species (WoRMS Editorial Board, 2021).

Landsat-5 (1985–1998), Landsat-7 (1999–2013) and Landsat-8 (2014–2020) satellite images (L5, L7 and L8, respectively) were used to determine the Hornbreen and Hambergbreen ice-cliffs positions (Supplemental Material S2). The U.S. Geological Survey (USGS) and National Aeronautics and Space Administration (NASA) share this data on the Earth Explorer portal (U.S. Geological Survey, 2021). The ice-cliffs positions in 2004 were defined using Terra ASTER © NASA satellite scene. Colour compositions (5, 4, 3 – L5 and L7 and 6, 5, 4 – L8) in the near-infrared and red channels of the visible spectrum with a resolution of 30 m × 30 m were used and loaded into QGIS version 3.16 Hannover software in the Universal Transverse Mercator (UTM) zone 33N coordinate system on the WGS84 ellipsoid (EPSG: 32633). The satellite images from L5 and L7 were additionally georeferenced using a first-order polynomial function and cubic interpolation methods. For this purpose, control points located at the summits and other topographically characteristic sites were used, depending on the cloud cover on the images. The mean transformation error was 0.54–1.44 pixels. The colour compositions enabled ice (blue) to be distinguished from water (black, navy blue) and land (red, brown). The position of the ice-cliff was manually vectorized at a scale of 1: 20,000 (cf. Aradóttir et al., 2019; Flink et al., 2015). In some cases, topographic maps (1:100,000) published by the Norwegian Polar Institute were used (Supplemental Material S2; cf. Szafraniec, 2020).

The files with the ice-cliff position allowed calculating the morphometric parameters of the glacier frontal zone of the tidewater glacier. These parameters are a glacier front dynamics indicator *CfD* and an ice-cliff balance indicator *CfE*. *CfD* is the ratio of the glacier front area contained in a circle of diameter equal to the distance between the anchoring points of the ice-cliff on land to the area of the entire circle. *CfE*, in turn, is the ratio of the diameter of the circle to the length of the ice-cliff. These indicators and the glacier frontal zone were defined and characterized by Szafraniec (2020). In that pioneering analysis, they were used to determine the beginning and end of the active phase of the surge of the tidewater glaciers in Spitsbergen. A surging glacier is considered to be one with CfD > 0.5 and positive *CfE*. The beginning and end of the active phase of the surge are considered to be a jump in the inter-annual indicator values of ca. 0.05 and higher.

Results

Geomorphological context of the shell samples

Abundant shells were detected in glacial diamict in the further part of the Hornbreen forefield (Treskelen) and on the southern coast of Hornbukta. At the foot of Ostrogradskijfjella, the shell fragments were identified even close to the dead ice margin. The shells occur up to 91 m a.s.l. on Treskelen (100 m a.s.l. according to Marks and Pękala, 1986) and up to 20 m a.s.l. on the southern coast of Hornbukta. The landscape of the coast of Hornbukta and the southern part of Treskelen is dominated by moraine with hummocky relief from degraded CSR networks. Obliteration of CSR networks increases with distance from the glacier front. The CSRs on Treskelen are now poorly preserved but visible in the aerial photo (ID: S36_2509) from 1936 (Norwegian Polar Institute, 2021). The shells were collected from compact, massive, clast-rich, matrix-supported diamict, forming the CSRs. The diamicton has a silty clay matrix. Similar to the previous studies (Heintz, 1953; Lindner and Marks, 1997; Philipps et al., 2017), the ground moraine did not reveal the differentiation into more than one unit from separate re-advances.

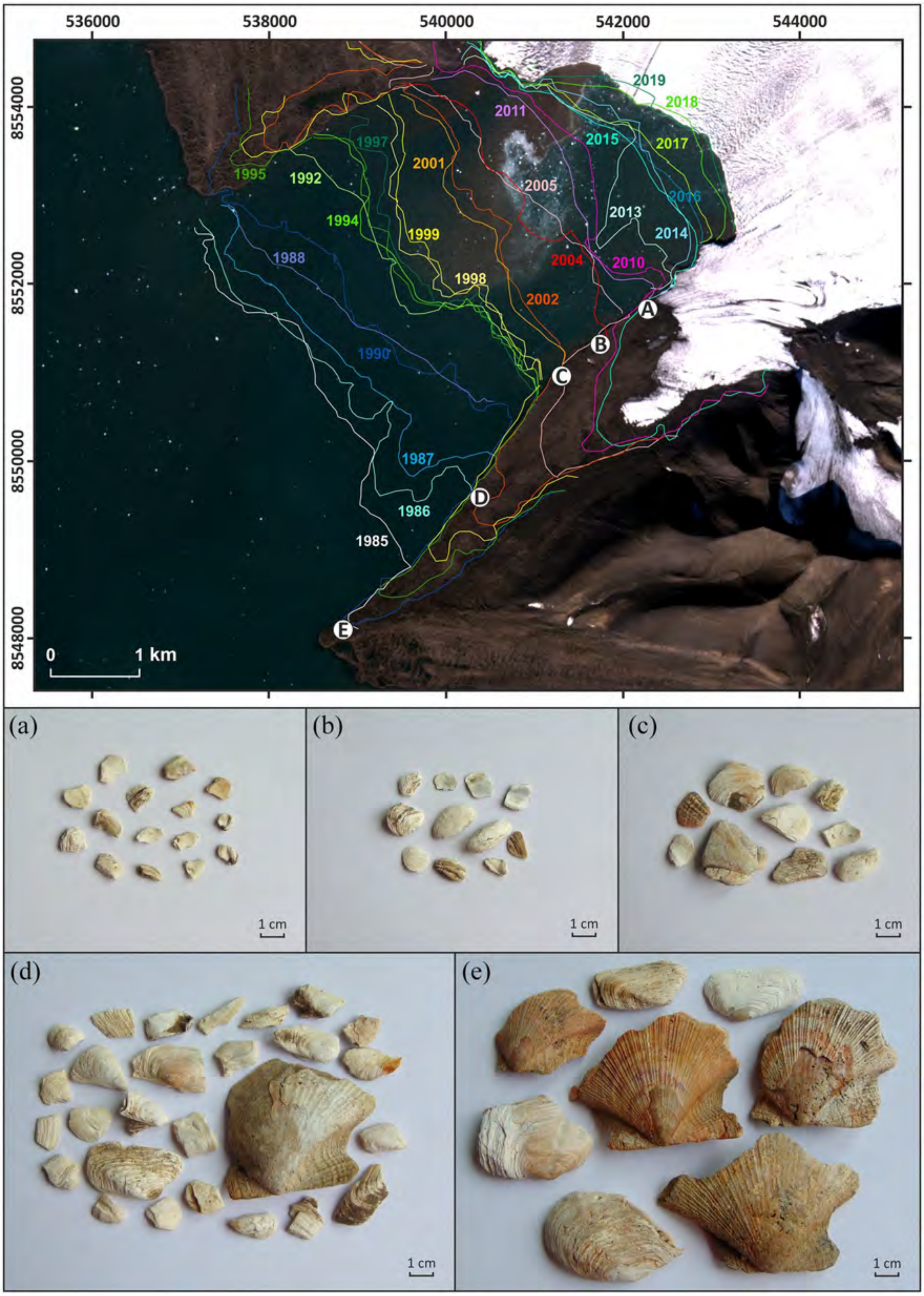

Figure 3. The extent of Hornbreen in the period 1985–2020. Sentinel-2A image ID: S2A_MSIL2A_20200825T121701_N0214_R009_T33XWF_20200825T164241.SAFE from 25.08.2020 (European Space Agency, 2021). The spatial variability of shell sizes (a–e) in the Hornbreen forefield. (a–e) photo A. Osika.

Size of the shell fragments

A characteristic feature of the shells collected in the forefield of Hornbreen is the distinct relationship between the size of the fragments and distance from the glacier front. This pattern is particularly evident on the southern coast of Hornbukta, where the fragments become gradually smaller towards the Hornbreen terminus, the tiniest ones occurring in the vicinity of dead ice (Figure 3). In the western part of this coast, the fragments are larger and numerous intact valves are present. Well-preserved shells (large fragments and undamaged valves) were also found on Treskelen, as described by for example Birkenmajer and Olsson (1997) and Heintz (1953).

Species composition

Supplemental Material S3 lists the species collected in the shell-bearing moraines, and compares them with earlier findings and

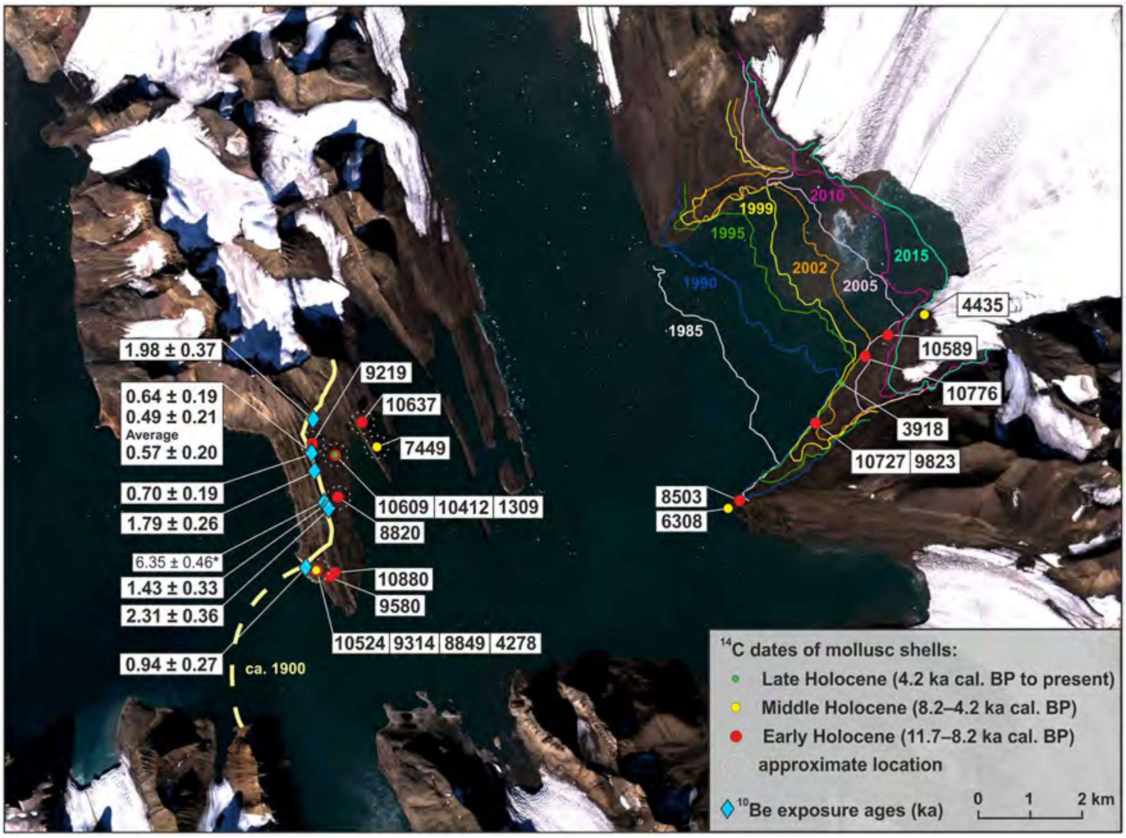

Figure 4. Location of the ^{14}C dated shell samples from the Early, Middle and Late-Holocene and median calibrated ages (cal. BP). The approximate location of previously analysed samples is based on sketches and diagrams published by Birkenmajer and Olsson (1997), Marks and Pękala (1986) and Tarasov et al. (1992). 10Be exposure ages from Philipps et al. (2017). The date 6.35 ± 0.46 ka was rejected by Philipps et al. (2017) as anomalously old and not considered in this study. The approximate extent of Hornbreen around 1900 and in 1985–2020. The approximate extent ca. 1900 is based on geomorphological evidence on aerial photo (ID: S36_2509) from 1936 (Norwegian Polar Institute, 2021) and bathymetry map (Moskalik et al., 2013). Sentinel-2A image ID: S2A_MSIL2A_20200825T121701_N0214_R009_T33XWF_20200825T164241.SAFE from 25.08.2020 (European Space Agency, 2021).

the species distribution in Hornsund in the 1970–1980s. *Mya truncata, Hiatella arctica* and *Chlamys islandica* are the dominant species from the southern coast of Hornbukta, whereas *Astarte borealis* and *A. elliptica* are less common. *M. truncata, H. arctica* and *C. islandica* can be identified in the shell debris from the marginal zone. The gastropod shell of *Boreotrophon truncatus* was found in the western part of the coast at the foot of Ostrogaskijfjella, where the shells are better preserved. These species are boreal-arctic or cosmopolitan (Różycki, 1992). Fragments of coralline algae, presumably of the *Lithothamnion* species, were also found in the research area. None of the thermophilous species for Svalbard, such as *Mytilus edulis, Modiolus modiolus, Zirfaea crispata* or *Arctica islandica* (Mangerud and Svendsen, 2018), were identified in the moraines.

^{14}C dating of mollusc shells

The results of radiocarbon dating, together with the previously published dates, range from the Early to the Late-Holocene (Figures 4 and 5, Supplemental Material S1). The majority of samples (15 out of 21) are from the Early Holocene. The oldest shell was collected from the ground moraine on Treskelen (ca. 10.9 cal. ka BP), but the oldest samples from the southern coast of Hornbukta are of a similar age (up to ca. 10.8 ka cal. BP). The range of radiocarbon dates from the coast of Hornbukta (ca. 3.9–10.8 ka cal. BP) is smaller than from Treskelen and Selodden peninsulas (ca. 1.3–10.9 ka cal. BP). The samples from the Middle (ca. 7.4, 6.3, 4.4 and 4.3 ka cal. BP) and Late-Holocene (ca. 3.9 and 1.3. ka cal. BP) are both from the distal and proximal part of the glacier forefield. There is no clear relationship between the age and distance of samples from the glacier terminus (Figure 4), as the sediments were mixed during the surges. Similarly, no association has been found between the age and elevation of the sampling sites.

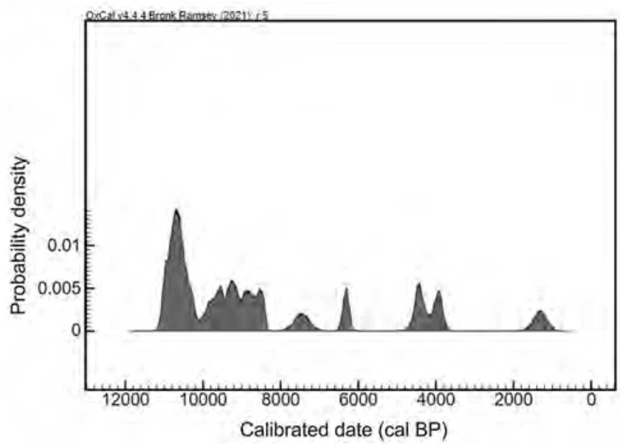

Figure 5. The summed probability density of the radiocarbon dates from the forefield of Hornbreen (n = 21), OxCal 4.4.4. (Bronk Ramsey, 2009, 2017).

Surge-type behaviour detected from the morphometric parameters of glacier frontal zones

Fluctuations in the morphometric parameters characterizing the frontal zones of Hornbreen and Hambergbreen are illustrated in Figure 6 and Supplemental Material S4. The highest values of *CfE*

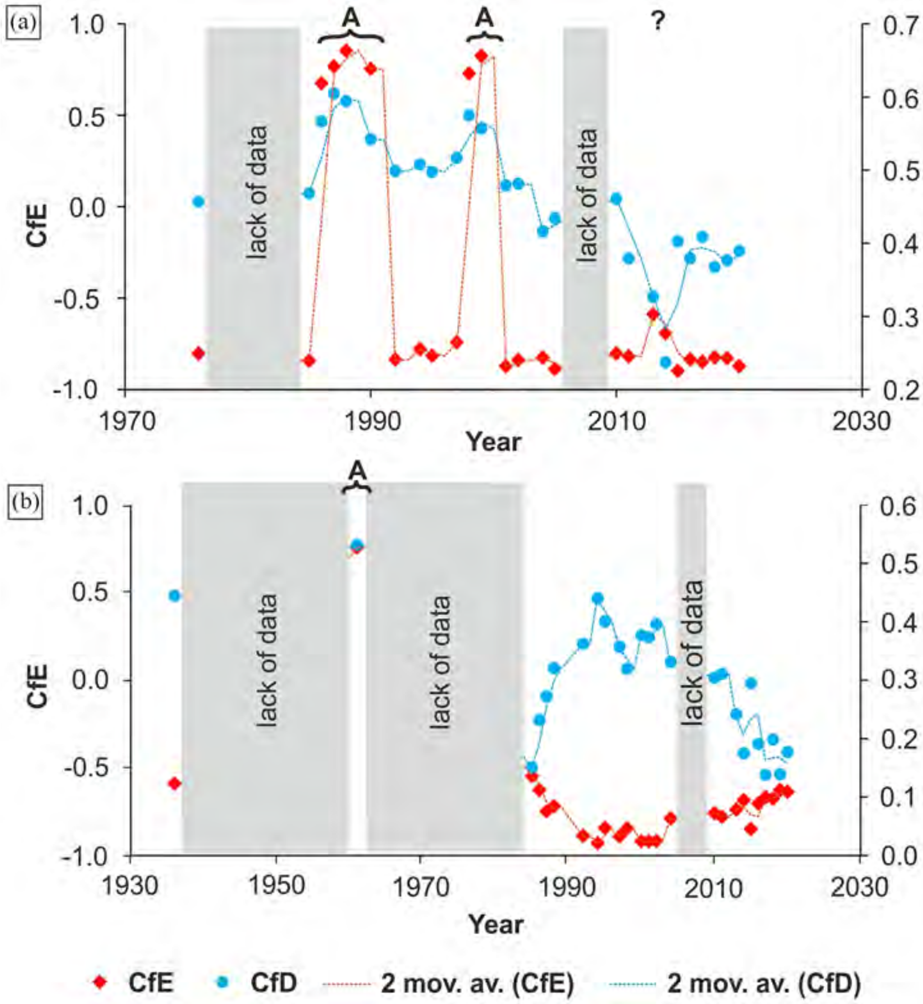

Figure 6. Calculated morphometric indicators (CfE, CfD) of the Hornbreen (a) and Hambergbreen (b) frontal zones and the 2-year moving averages. 'A' indicates the active phase of a surge. The question mark indicates the glacier advance in 2011 that is visible on the satellite images but not recorded in the coefficients.

and *CfD* for Hornbreen in the last 40 years were reached in 1986–1990 (0.675–0.853 and 0.542–0.605) and 1998–1999 (0.729–0.825 and 0.557–0.575). The glacial frontal zone was then more convex (Figure 3). *CfE* fell and stabilized at a negative level between these two peaks, while *CfD* hovered around 0.5 (Figure 6). The glacial frontal zone was concave (Figure 3). After the last maximum and a rapid decline, *CfE* stagnated with negative values, while *CfD* remained below 0.5. The highest values of *CfE* and *CfD* for Hambergbreen were recorded in 1961 (0.758 and 0.532) but there are no data from 1961–1985. In the last 40 years, *CfE* has been constantly negative, *CfD* has been lower than 0.5, and the glacial frontal zone has been concave.

Discussion

Deglaciation

During Late Weichselian, Hornsund was a pathway for an ice stream in the west part of the Svalbard–Barents Sea Ice Sheet (Ottesen et al., 2007; Rebesco et al., 2014). Cosmogenic exposure dating suggested ice-sheet thinning and deglaciation of Hornsund mouth at 17.4 ± 1.5 ka (Young et al., 2018). The central and inner parts of the fjord system were deglaciated by 13.3 ± 0.6 and 13.0 ± 0.7 ka, respectively. Presumably, the oldest reported mollusc shell from Hornsund in the Late Glacial–Early Holocene transition was collected from the raised marine terrace in the outlet of Lisbetdalen (Sørkapp Land, 30 m a.s.l.) and dated to ca. 12.6 ka cal. BP (Salvigsen and Elgersma, 1993). East of southern Spitsbergen, ice shelf and ice streams in Storfjoden decayed rapidly in the Early Bølling, ca. 15.3 ka cal. BP and at the beginning of the Holocene (Rasmussen and Thomsen, 2021). Rapid deglaciation resulted from the increased inflow of the warm Atlantic water to the Svalbard margin as well as atmospheric warming (Bartels et al., 2017; Rasmussen and Thomsen, 2021; Ślubowska et al., 2005; Ślubowska-Woldengen et al., 2007; Łącka et al., 2015).

The Late Glacial–Early Holocene transition was also a period of glacier re-advances in many regions of Svalbard (Farnsworth et al., 2017, 2018; Flink et al., 2018; Larsen et al., 2018; Lønne, 2005), although the warming climate did not favour a positive mass balance of glaciers. According to Farnsworth (2018) and Farnsworth et al. (2020), the possible advances of glaciers were temporary and unsustainable surge-type fluctuations not driven by long-term positive mass balance conditions. At that time, they caused a large volume of ice to be transposed from the upper part of the glacier to its terminus, ending in the sea and thus accelerating mass loss by calving and increased melting. Thus, the surge-type re-advances led to faster deglaciation (Farnsworth, 2018; Oerlemans and van Pelt, 2015; Szafraniec, 2013a, 2013b). These surges seem to be similar to those we are observing today, despite the negative mass balance of glaciers (e.g. Nathorstbreen; Sund et al., 2014). In the Late Glacial or Early Holocene, a surge-type advance occurred in Mohnbukta, and other glaciers on the east coast of Storfjoreden may also have re-advanced in this period (Flink et al., 2018). Considering the contemporary surge-type behaviour of the Hornbreen-Hambergbreen glaciers (see section 5.3), similar re-advances may have also occurred during deglaciation of eastern Hornsund. Noormets et al. (2021) identified a pre-LIA moraine ridge at the forefield of Hambergbreen, indicating at least two episodes of surging. However, the age of this landform is unknown.

Early–Middle Holocene ice-free strait

The radiocarbon dating results reveal that the shells from the ground moraine in the Hornbreen forefield are derived from Early, Middle and Late-Holocene marine sediments (Figures 4 and 5). It is noteworthy that the shells occur even close to the modern edge of the dead ice front of Hornbreen. The age of the shells indicates the period when the sea extended much farther eastwards, where nowadays, Hornbreen and Hambergbreen exist. Then, the shells within the marine sediments were incorporated by the advancing Hornbreen, transported westwards and deposited as shell-bearing moraines (cf. Boulton et al., 1996). Similar shell-bearing moraines, indicating glacier recession before the advance, have been reported in many regions of Svalbard (e.g. Blake, 1989b; Ronnert and Landvik, 1993; Salvigsen and Høgvard, 2006), as well as more widely in the Arctic (e.g. Ellesmere Island; Blake, 1981, 1989a).

Radiocarbon dates revealed the existence of the marine environment as a consequence of the retreat of Hornbreen-Hambergbreen glaciers in the Early and Middle Holocene, ca. 10.9–3.9 ka cal. BP (Figure 5). In this period, the glaciers of Svalbard reached their minimum extents or disappeared completely (e.g. Farnsworth et al., 2020; Røthe et al., 2018; Svendsen and Mangerud, 1997), and many tidewater glaciers retreated onto land (e.g. Allaart et al., 2021; Forwick et al., 2010). Hence, the predicted decay of Hornbreen-Hambergbreen glacier isthmus and opening of the strait in the next several decades (Grabiec et al., 2018) suggests that it was also open in the Early and Middle Holocene when the climate of Svalbard was warmer than today (e.g. de Wet et al., 2018; van der Bilt et al., 2015). Our reasoning is consistent with the findings of Nielsen and Rasmussen (2018) and Noormets et al. (2021), who indicated that the southern part of Storfjorden (SE Svalbard) was already ice-free at 11.6 ka cal. BP. At that time, the minimal deposition, if any, of ice-rafted debris (IRD) also suggests that the tidewater glaciers of this region had significantly receded or even retreated onto land after 10.0 ka cal. BP (Nielsen and Rasmussen, 2018; Noormets et al., 2021). Thus, the presence of older shells in the Hornbreen forefield cannot be ruled out and would suggest a retreat of Hornbreen-Hambergbreen and the strait opening much before the period indicated in our work (10.9 ka cal. BP). However, analysing the current dynamics of the Hornbreen-Hambergbreen system (see section 5.3), the glaciers could have surged and closed the strait during the Late Glacial-Early Holocene transition (cf. Farnsworth, 2018; Jania, 1988). The episodes of re-advances could block the strait, but the rapid recession in the warmer climate would lead to re-opening. When the glaciers receded far from the strait mouth in the Early Holocene, the blockage of the strait was less probable. Pälli et al. (2003) emphasize that Hornbreen and Hambergbreen were ‘unable to build up the reservoir-area mass and geometry for a new surge’ at the beginning of this century. The glaciers thickness and extent in the Early and Middle Holocene seem to have been much smaller, as evidenced by the strait existence. With a significant retreat of the glaciers and a small amount of mass in the accumulation zone, closure of the strait should not have been possible, even if a successive glacier surge did occur. Hence, considering other sources of data, the gaps in the spread of ^{14}C dates around 8 and 7 ka cal. BP, and between 6 and 5 ka cal. BP (Figure 5) may not result from the glacier advances and the blockage of the strait. The IRD values from Storfjorden and the Svalbard shelf west of Hornsund remained low in these periods (Nielsen and Rasmussen, 2018; Telesiński et al., 2018) and lake records have not revealed glacier advances in other regions of Svalbard (Allaart et al., 2021; de Wet et al., 2018; Røthe et al., 2015, 2018; Svendsen and Mangerud, 1997). In Hornsund, the radiocarbon dates of peat melted on the surface of Hansbreen suggest significant reduction in the glacier area around 7.9 and 5.9 ka cal. BP (Oerlemans et al., 2011) and the reconstructions from Lake Svartvatnet indicate warmer climate since 5.5 ka cal. BP (base of the core) to 5.0 ka cal. BP (Luoto et al., 2018).

The existence of the Hornsund strait in the Early and Middle Holocene is supported by the species composition of the ^{14}C dated shells. The list of species collected on the southern coast of Hornbukta is consistent with that from Treskelen (Supplemental Material S3; Birkenmajer, 1958; Birkenmajer and Olsson, 1997; Heintz, 1953; Marks and Pękala, 1986; Tarasov et al., 1992). We are aware that our list may be incomplete, as our main aim was to collect material for radiocarbon dating and identify possible thermophilic species (Mangerud and Svendsen, 2018), not to detail the species composition of the mollusc communities. Our observations and previous studies have shown that the glacigenic sediments are dominated by *Chlamys islandica, Mya truncata, Hiatella arctica, Astarte borealis* and *A. elliptica* (Birkenmajer, 1958; Birkenmajer and Olsson, 1997; Denisenko and Tarasov, 1992; Heintz, 1953). These molluscs are boreal-arctic or cosmopolitan (*Hiatella arctica*) (Różycki, 1992). Being suspension-feeding bivalves, they are not found close to tidewater glaciers because the high concentration of inorganic suspensions near the ice cliff is associated with the dilution of nutritious suspensions and would clog their filtering appendages (Görlich et al., 1987; Moore, 1977; Włodarska-Kowalczuk, 2007; Włodarska-Kowalczuk et al., 1998). The preference of these species for the outer basins of the Arctic fjords (Włodarska-Kowalczuk, 2007 and references therein) was confirmed by observations in Hornsund in the 1970s and 1980s. Only *H. arctica* of the species mentioned above was found in the heavily glacierized Brepollen; the others were found to occur only in the western and central part of Hornsund, away from the tidewater glaciers (Supplemental Material S3; Różycki, 1992). The shells or syphon holes of suspension-feeding molluscs were not detected in Hornbukta during the surveys of benthic macrofauna using a drop camera in 2016 (K. Deja, 2021, personal communication). Thus, the sediments with ^{14}C dated shells could not have accumulated near the ice cliff of Hornbreen, and the glacier must have retreated far from the area of origin of the marine sediments with molluscs, including withdrawal on land. Considering the contemporary distribution of molluscs and their sensitivity to high concentrations of inorganic suspensions, the species composition of the shells confirms the significant recession of the Horn-Hamberg glaciers, presumably associated with the strait’s opening in the warmer periods of the Holocene.

Reconstructing the coastal outline of eastern Hornsund is necessary to establish whether the strait could not have been buried shortly after deglaciation. The topography of eastern Hornsund during the Early Holocene is unknown. However, we assume that the model of the ice-free topography may shed light on the state of the glaciers in Brepollen in this warmer period. We also presume that the glacio-isostatic depression in the freshly exposed area after the extensive Weichselian glaciation was no less deep than the present depth of the glacier bed under the Hornbreen-Hambergbreen system. The subglacial topography of the glacier isthmus was studied using GPR soundings, which revealed a depression between the Greenland and Barents Seas (Grabiec et al., 2018). The approximate coastline of eastern Hornsund after the disappearance of glaciers can be delineated using the GPR data together with the results of glaciological investigations and the fjord bathymetry from a multi-beam echo-sounder (Grabiec et al., 2018; Noormets et al., 2021; Figure 7). The subglacial

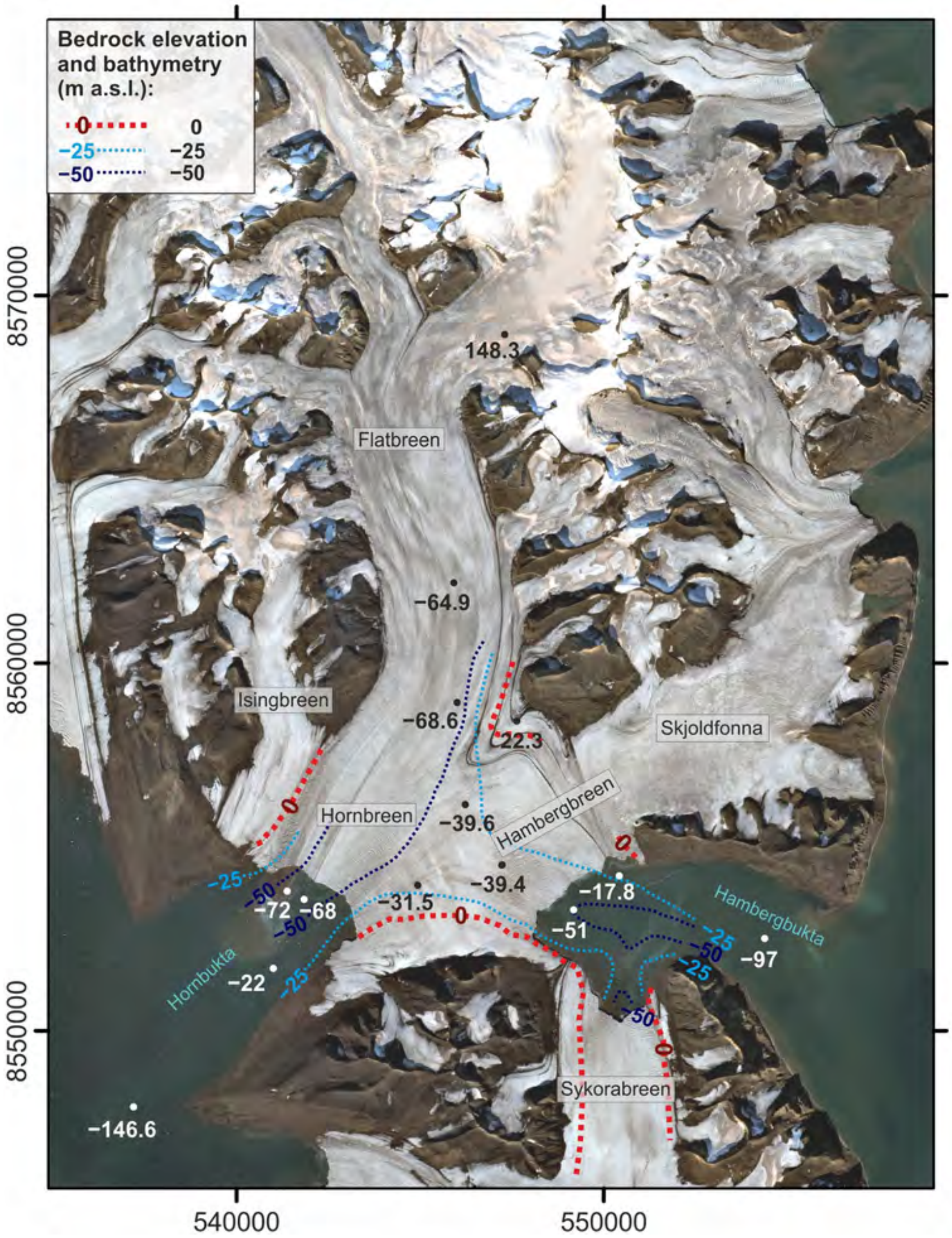

Figure 7. The approximate course of the strait's shoreline and depth below the Hornbreen-Hambergbreen ice bridge (Grabiec et al., 2018, modified). The lines represent probable contours of the subglacial topography and isobaths in the bays. Bedrock and bathymetry contour lines every 25 m. Selected points are marked. Sentinel-2A image ID: S2A_MSIL2A_20200825T121701_N0214_R009_T33XWF_20200825T164241. SAFE from 25.08.2020 (European Space Agency, 2021).

topography of this area was described by Grabiec et al. (2018). Deglaciation would lead to the uncovering of a new over-deepened branch of the fjord (below 70 m b.s.l.) along the Hornbreen-Flatbreen axis and a shallower basin in the area occupied by Hambergbreen. The section near the contemporary ice divide between Hornbreen and Hambergbreen would be a channel ca. 40 m deep linking the Greenland and the Barents Seas. In general, the sediment accumulation rate in Svalbard is higher in the inner and lower in the outer parts of the fjords (e.g. Legeżyńska et al., 2017; Renaud et al., 2007) and changes over time. In the warmer periods (the Early Holocene and nowadays), the linear accumulation rate was greater (Sternal et al., 2012; Zajączkowski et al., 2004), whereas in the colder phases of the Holocene it was significantly lower (e.g. Szczuciński et al., 2009). In the Early Holocene, after the period of rapid deglaciation and intense sediment supply, the accumulation rate in the eastern part of Hornsund may have been similar to that in the outer parts of the Svalbard fjords at present. Assuming a sedimentation rate of 0.5 cm a^{-1} (the outer part of Hornsund at present, Szczuciński et al., 2006) and ignoring sediment compaction, it would take over 8000 years for the 40-m-deep channel to fill up. In addition, the sedimentation in the open strait was presumably disturbed by local marine tidal currents between the Greenland and Barents Seas, as well as by the intensive inflow of the ESC. The latter can be suggested by the lack of thermophilic mollusc shells in Hornsund (Birkenmajer and Olsson, 1970). Thus, the strait could have been closed only by advancing glaciers.

Neoglacial and LIA dynamic activity

After 3.9 ka cal. BP there is a lack of radiocarbon dates of mollusc shells until ca. 1.3 ka cal. BP (Figure 5). This time span corresponds with significant cooling and increased glacier activity during the Neoglacial in Svalbard after ca. 5–4 ka cal. BP (Allaart et al., 2021; Philipps et al., 2017; Røthe et al., 2015; van der Bilt et al., 2015; Werner, 1993). The timing of these re-advances was diverse (de Wet et al., 2018; Farnsworth et al., 2020), and geomorphological investigations have revealed that some of them were of the surge-type (e.g. two surges of Nathorstbreen ca. 2.7 ka cal. BP; Kempf et al., 2013, the surge of Hinlopebreen before 2.6 ka cal. BP; Flink and Noormets, 2018). However, less is known about the Neoglacial in Hornsund. The palaeoclimatic reconstructions based on fossil Chironomidae assemblages from Lake Svartvatnet indicate a cooling episode at ca. 3.3 ka cal. BP (Luoto et al., 2018). Baranowski and Karlén (1976) described a subfossil tundra from the forefield of Werenskioldbreen dated to ca. 1.5–0.7 ka cal. BP. The vegetation remains were found between two layers of lodgement till and the underlying one confirms the advance before 1.5 ka cal. BP. Evidence for pre-LIA surges has been detected in the forefield of Hambergbreen (Noormets et al., 2021). Radiocarbon dates from the southern coast of Hornbukta and Treskelen reveal the existence of the marine environment at the head of Hornsund until ca. 3.9 ka cal. BP and around 1.3 ka cal. BP. Thus, the possible pre-LIA advance of Hornbreen-Hambergbreen system in the Late-Holocene could have occurred between 3.9 and 1.3 ka cal. BP. Philipps et al. (2017) proposed two periods of Hornbreen advance in the Late-Holocene: 1.9 ± 0.3 ka and 0.7 ± 0.3 ka from the ^{10}Be exposure dating of moraine boulders on Treskelen. The latter may correspond to surges of other Svalbard glaciers, such as Nathorstbreen ca. 700–890 cal. BP (Lovell et al., 2018), Paulabreen ca. 650 cal. BP (Hald et al., 2001; Larsen et al., 2018; Lyså et al., 2018) and Osbornebreen ca. 520 ± 70 cal. BP (Evans and Rea, 2005; Farnsworth et al., 2017). The glaciers presumably retreated between the two possible advances during the Medieval Warm Period (MWP; Miller et al., 2010), also known as the Little Climatic Optimum ca. 1.2–0.7 ka cal. BP (Hansen et al., 2011). The recession of Hornbreen-Hambergbreen system around 1.3 ka cal. BP or earlier is supported by the age of the youngest shell sample from Treskelen (Supplemental Material S1: sample U-2985; Birkenmajer and Olsson, 1997). Pawłowska et al. (2016) suggested a rapid retreat of tidewater glaciers in Hornsund between AD 1000–1600 based on low sediment accumulation rates (SAR) and IRD, together with changes in the foraminiferal community visible in microfossils and ancient DNA. Subfossil peat and buried soils from the forefield of Werenskioldbreen indicated this glacier's recession between ca. 1.5–0.7 ka cal. BP (Baranowski and Karlén, 1976; Kabala and Zapart, 2009). The episodes of glacier retreat were also recorded in other regions of Spitsbergen (Dzierzek et al., 1990; Furrer et al., 1991; Reusche et al., 2014; Røthe et al., 2015). As a result of glacier retreat in the Hornsund Region, the strait could also have been open during this warmer interval.

The widespread advances of Svalbard glaciers occurred in the LIA, particularly between 1890 and 1920 (Martín-Moreno et al., 2017). Many of them have been associated with surge-type dynamics. According to the map from the Russian−Swedish expedition, the surge of Hambergbreen occurred a short time before 1900 (Lefauconnier and Hagen, 1991; Vassiliev, 1907), but an extensive glacier system was indicated at the head of the Hornsund Fjord on the map prepared during the Austro−Hungarian North-Pole Expedition 1872–1874 (Daublebsky von Sterneck Zu Ehrenstein, 1874). Vassiliev's map probably captured the early quiescent phase of Hornbreen. Thus, this glacier must have surged around 1900 or earlier (Grabiec et al., 2018). Further evidence for the Hornbreen surge at the end of the 19th century stems from several relief features typical of surge-type glaciers, such as a push moraine west of Treskelen visible on the bathymetry map of Brepollen (Moskalik et al., 2013) and the CSR networks on the proximal side of this peninsula (Heintz, 1953: pp. 9 and 29). The latter are also visible in the oblique aerial photo (ID: S36_2509) from 1936 (Norwegian Polar Institute, 2021). The location and arrangement of these forms exclude the possibility of their creation during the next surge in the 1930s.

A conceptual model of the strait's blockage by surging glaciers, based on the example of LIA, was described by Grabiec et al. (2018). In the first stage, Hornsund may have been blocked from the west by surges of the vast tidewater glaciers Samarinbreen, Mendeleevbreen, Svalisbreen and Storbreen. Then, following the formation of the barrier, the easternmost part of Flatbreen could have reached the Professorryggen massif during the surge and split into two branches: Hornbreen facing west and Hambergbreen facing east. Subsequent surges of Flatbreen and Sykorabreen may have led to the filling of modern Hambergbukta with ice and the advance of Hambergbreen into Storfjorden. However, Hornsund may also have been closed first by Hambergbreen and then by Hornbreen. A thorough reconstruction of the strait's closure is not easy and will require further research.

The maximum extent of the Hornbreen-Hambergbreen system in the LIA was reached around 1900. Since then, the glaciers have been retreating with interrupting episodes of surging (Błaszczyk et al., 2013). The surge of Hornbreen occurred after 1936 (Pälli et al., 2003), and Storbreen surged in 1958 (Błaszczyk et al., 2013; K. Birkenmajer, personal communication; Jania, 1988). Flatbreen was in an active phase in the 1960s (Grabiec et al., 2018), and the last significant advance of Hornbreen took place between 1958 and 1962 (Koryakin, 1975). Our morphometric indicators characterizing the frontal zones (*CfE* and *CfD*) reveal two additional periods of possible surges of Hornbreen: 1986–1990 and 1998–1999 (Figure 6). In both, the *CfE* values are positive and $CfD > 0.5$, which is typical for the active phase of a surge (Szafraniec, 2020). The surge around 2000 is consistent with the previous findings reported by Jania (2001). Additionally, satellite images suggest an advance in 2011 (Figure 3), although this is not discernible in the morphometric parameters. Hambergbreen, in turn, surged in 1957–1968 (Lefauconnier and Hagen, 1991; Noormets et al., 2021) and the calculated morphometric indicators are also in line with the earlier results (*CfE*: 0.758, *CfD*: 0.532; Figure 6). Apart from the periods of the active phase with the peak values of the coefficients, *CfE* remains negative and $CfD < 0.5$, indicating glacier stagnation or recession (Szafraniec, 2020).

A conceptual model of sediment redeposition during surges in the Brepollen area

The shell-bearing moraines were formed by the redeposition of marine sediments during the surge of the Hornbreen glacier system. During the active phase, marine sediments were pushed up from the seafloor by ploughing and transported to the west, forming a push moraine (e.g. the submarine moraine ridge west of Treskelen). CSRs were formed by upward infilling the basal crevasses with saturated sediments during the active phase of the glacier surge and subsequent meltout (e.g. Aradóttir et al., 2019; Boulton et al., 1996; Farnsworth et al., 2016; Flink et al., 2015; Ingólfsson et al., 2016; Rea and Evans, 2011). Evidence for the glacier surge around 1900 was observed by Heintz (1953), who detected CSR networks and moraine with hummocky relief on the glacier forefield, as well as shell-bearing diamict that had been moved up along thrust planes and exposed on the surface of Hornbreen.

The exact number of surges throughout the Holocene and the detailed original location of the material is unknown. Nevertheless, the following points are worth emphasizing: (1) a wider range of the radiocarbon dates from Treskelen and Selodden (ca. 1.3–10.9 ka cal. BP) than from the southern coast of Hornbukta (ca. 3.9–10.8 ka cal. BP); (2) a small number of Late-Holocene shells among the samples; (3) the gradual decrease in shell fragment size towards the glacier terminus on the southern coast of Hornbukta in contrast to the well-preserved shells on Treskelen, regardless of their age. Considering the results of ^{10}Be exposure

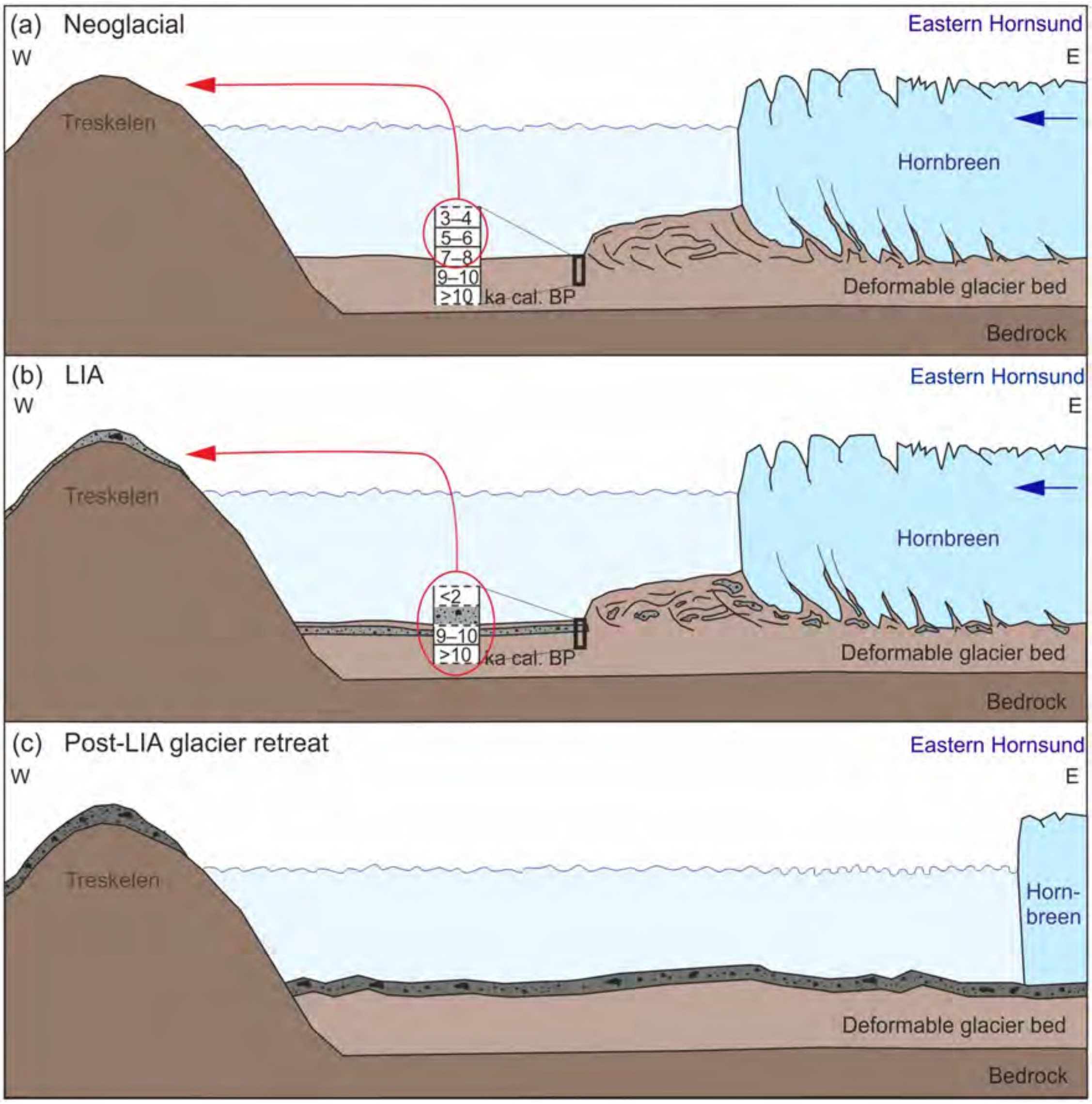

Figure 8. The conceptual model for sediment redeposition during surges in Brepollen. In the Neoglacial (a), the surge of Hornbreen may have led to the redeposition of the uppermost layers of marine sediments, perhaps from the Late-Middle Holocene. During subsequent surges in the LIA (b) the glacier may have incorporated the marine sediments accumulated in the recession phase as well as much older ones, perhaps from the Middle-Early Holocene, from deeper sedimentary levels. In the ground moraine, the younger sediments could have become covered and mixed with older ones (c).

dating on Treskelen (Philipps et al., 2017), we propose a conceptual model of sediment redeposition during the surges (Figure 8). In the first stage, for example in the Neoglacial, the surge of Hornbreen may have led to the redeposition of the uppermost layers of marine sediments, perhaps from the Late-Middle Holocene (Figure 8a). During subsequent surges, for example around 1900 or much earlier, the glacier may have incorporated the marine sediments accumulated in the recession phase as well as much older ones, perhaps from the Middle-Early Holocene, from deeper sedimentary levels (Figure 8b). Thus, the younger sediments on Treskelen, Selodden and at the foot of Ostrogradskijfjella could have become covered and mixed with older ones (Figure 8c). This may explain the dominance of Early Holocene shells among the radiocarbon-dated samples. However, more radiocarbon dates are needed to support this hypothesis, particularly from the vertical profiles.

Moreover, the small number of samples from the Middle and Late-Holocene could also be explained by the abandonment of the younger sediments in Hornbukta or Brepollen if the older surges had been less extensive. Then, during the LIA, these moraines could have been overridden by Hornbreen, with only part of the sediments being transported west to Treskelen. Nevertheless, more evidence is necessary to support this hypothesis: for instance, a detailed bathymetry map and marine geophysical surveys of the internal structure of sediments in Brepollen, which could indicate the existence of overridden pre-LIA moraine ridges.

In our study area, there is a clear relationship between the size of the shell fragments and the distance from the contemporary glacier terminus (Figure 3). Presumably, the Early Holocene shells in the ground moraine on Treskelen are well preserved because they may have been redeposited during the LIA and they were not affected by the subsequent surges in the 20th century. Heintz (1953) noted that not only were the shells contained in the ground moraine in a good condition; those melted from the supraglacial diamicton were also relatively undamaged, the sediments having protected them from disintegration during transport. In turn, the sediments deposited on the southern coast of Hornbukta were subsequently overridden, entrained and reworked during surges several times in the 20th century. The diminishing extent of surge-type re-advances is reflected by the larger shell particles and intact valves in the further part of the glacier forefield and the small fragments in the eastern part of this area, near the modern terminus. To our knowledge, a similar relationship has not been described for surging glaciers in Svalbard. For this reason, the spatial pattern of shell sizes in the ground moraine in the Hornbreen forefield is a unique, though indirect record of a series of surges of diminishing extent and is a phenomenon worth investigating in other locations.

Conclusions

- Fluctuations of the Hornbreen-Hambergbreen system determine if Hornsund functions as a fjord or a strait linking the Greenland and Barents Seas. The subfossil mollusc shells in the ground moraine at the terrestrial part of the Hornbreen forefield indicate the recession of the glacier system, which led to the subsequent collapse of this ice isthmus and opened the Hornsund strait in the Early Holocene and perhaps during the MWP.
- The glaciers' retreat is supported by the species composition of the ^{14}C dated shells. The bivalve species are suspension feeders, which generally prefer the outer basins of the Arctic fjords and they are not found in the vicinity of ice cliffs, as large amounts of inorganic suspended matter would clog the filtering apparatus.
- The opening of the strait occurred ca. 10.9 ka cal. BP or earlier and presumably around 1.3 ka cal. BP, when the glaciers in Hornsund receded. According to published ^{10}Be exposure dates, the subsequent glacier advances led to the strait's closure in the LIA (0.7 ± 0.3 ka or earlier) with a culmination in the 19th century. The closure of the strait may have also occurred in the Neoglacial between ca. 3.9 and 1.3 ka cal. BP.
- It can be assumed that surges of the glaciers near the head of Hornsund occurred one after another, as happens nowadays. At first, Hornsund may have been blocked from the west by surging glaciers. The surging Flatbreen reached the Professorryggen massif and split into two branches: Hornbreen facing west and Hambergbreen facing east. Subsequent surges may have caused Hambergbreen to advance into Storfjorden. In this way, the strait was blocked by a glacier isthmus linking Sørkapp Land with Spitsbergen.
- In our conceptual model, the first glacier surge episodes led to the redeposition of the younger marine sediments from the Late-Middle Holocene. These were subsequently covered and mixed with older sediments from deeper sedimentary levels during the successive surges (e.g. during the LIA). This may explain the dominance of Early Holocene shells among the radiocarbon-dated samples.
- Analyses of satellite images, the morphometric indicators characterizing the frontal zones and previous studies indicate six advances of Hornbreen: around 1900 or earlier, after 1936, between 1958 and 1962, in 1986–1990, 1998–1999 and 2011. The great majority of these advances were glacier surges. The confirmed surges of Hambergbreen occurred around 1900 or earlier and in 1957–1968. The diminishing extent of re-advances is reflected by the larger shell particles and intact valves in the further part of the glacier forefield and the small fragments near the modern terminus. Glacier dynamics of the Hornbreen-Hambergbreen system in post-Little Ice Age climate warming seems to be an analogue of glacier retreats and re-advances in the earlier periods of the Holocene.

Acknowledgements

We thank all the participants of the University of Silesia's expeditions to Spitsbergen in 2019 and 2020 for their support in the fieldwork, Prof. Dr Maria Włodarska-Kowalczuk (Institute of Oceanology, Polish Academy of Sciences) for her help with the identification of the shells of molluscan species, the Poznań Radiocarbon Laboratory and the Gliwice Radiocarbon Laboratory for the AMS radiocarbon dating, and Professor Tomasz Goslar and Dr Jacek Pawlyta for their valuable suggestions regarding the calibration of radiocarbon dates. We are especially grateful to Professor Maria Włodarska-Kowalczuk and Professor Jan Marcin Węsławski for their constructive comments. We thank the Editor and two anonymous Reviewers for remarks improving the quality of the manuscript.

Author contributions

A.O. structured the paper and wrote the main part of the manuscript. J.E.S. calculated the morphometric indicators (CfE, CfD) and vectorized the glacier terminus from satellite data. A.O. and J.J. conceived this research and collected the samples for radiocarbon dating. All the authors contributed to the interpretation of results and to the commenting on, reviewing and editing of the paper.

Funding

The author(s) disclosed receipt of the following financial support for the research, authorship, and/or publication of this article: This work was supported by the Centre for Polar Studies, University of Silesia – the Leading National Research Centre (KNOW) in Earth Sciences (2014–2018) [grant number 03/KNOW2/2014]. The radiocarbon dating was financed by the Institute of Earth Sciences at the University of Silesia in Katowice.

ORCID iDs

Aleksandra Osika https://orcid.org/0000-0002-4686-7203
Joanna Ewa Szafraniec https://orcid.org/0000-0002-2170-5822

Supplemental material

Supplemental material for this article is available online.

References

Allaart L, Schomacker A, Larsen NK et al. (2021) Glacial history of the Åsgardfonna ice cap, NE Spitsbergen, since the last glaciation. *Quaternary Science Reviews* 251: 106717.

AMAP (2021) *Arctic Climate Change Update 2021: Key Trends and Impacts. Summary for Policy-Makers*. Tromsø: Arctic Monitoring and Assessment Programme (AMAP).

Aradóttir N, Ingólfsson Ó, Noormets R et al. (2019) Glacial geomorphology of Trygghamna, western Svalbard - integrating terrestrial and submarine archives for a better understanding of past glacial dynamics. *Geomorphology* 344: 75–89.

Baranowski S and Karlén W (1976) Remnants of Viking age tundra in Spitsbergen and northern Scandinavia. *Geografiska Annaler. Series A, Physical Geography* 58(1/2): 35–49.

Bartels M, Titschack J, Fahl K et al. (2017) Atlantic water advection vs. glacier dynamics in northern Spitsbergen since early deglaciation. *Climate of the Past* 13: 1717–1749.

Bednarek J, Rudowski S and Zalewski SMW (1993) The tectonic sketch of the offshore area within Hornsund Region, Spitsbergen. In: *XX Polar Symposium. Man impact on polar environment* (eds J Repelewska-Pękalowa and K Pękala), Lublin, Poland, 3–5 June 1993, pp. 293–297. Lublin: UMCS Press.

Birkenmajer K (1958) Preliminary report on the raised marine features in Hornsund, Vestspitsbergen. *Bulletin de L' Academie Polonaise des Sciences, Série des Sciences Chimiques, Géologiques et Géographiques* 6(2): 151–157.

Birkenmajer K (1960) Raised marine features of the Hornsund area, Vestspitsbergen. *Studia Geologica Polonica* 5: 3–95.

Birkenmajer K (1990) *Hornsund, Spitsbergen, geologia – geology, 1: 75 000 (Geological map and explanatory text)*. Committee on Polar Research. Warsaw: Polish Academy of Sciences; Katowice: Silesian University, pp.1–42 & map sheet.

Birkenmajer K and Olsson IU (1970) Radiocarbon dating of raised marine terraces at Hornsund, Spitsbergen and the problem of land uplift. *Norsk Polarinstitutt Årbok* 1969: 17–43.

Birkenmajer K and Olsson IU (1997) Radiocarbon dating of marine bivalve shells from Holocene moraines at inner Hornsund, South Spitsbergen. *Bulletin of the Polish Academy of Sciences. Earth Sciences* 45(1): 59–66.

Birkenmajer K and Łuczkowska E (1996) Mid-Holocene foraminiferal assemblage from marine shell-bearing moraines at Hornsund, South Spitsbergen. *Bulletin of the Polish Academy of Sciences. Earth Sciences* 44(4): 227–233.

Birks HH (1991) Holocene vegetational history and climatic change in west Spitsbergen - plant macrofossils from Skardtjørna, an Arctic lake. *The Holocene* 1(3): 209–218.

Blake W (1981) Neoglacial fluctuations of glaciers, southeastern Ellesmere Island, Canadian Arctic Archipelago. *Geografiska Annaler. Series A, Physical Geography* 63(3/4): 201–218.

Blake W (1989a) Application of ^{14}C AMS dating to the chronology of Holocene glacier fluctuations in the High Arctic, with special reference to Leffert Glacier, Ellesmere Island, Canada. *Radiocarbon* 31(3): 570–578.

Blake W (1989b) Radiocarbon dating by accelerator mass spectrometry; a contribution to the chronology of Holocene events in Nordaustlandet, Svalbard. *Geografiska Annaler. Series A, Physical Geography* 71(1/2): 59–74.

Boulton GS, Van Der Meer JJM, Hart J et al. (1996) Till and moraine emplacement in a deforming bed surge — an example from a marine environment. *Quaternary Science Reviews* 15(10): 961–987.

Box JE, Colgan WT, Wouters B et al. (2018) Global sea-level contribution from Arctic land ice: 1971–2017. *Environmental Research Letters* 13(12): 125012.

Bronk Ramsey C (2009) Bayesian analysis of radiocarbon dates. *Radiocarbon* 51(1): 337–360.

Bronk Ramsey C (2017) Methods for summarizing radiocarbon datasets. *Radiocarbon* 59(6): 1809–1833.

Błaszczyk M, Ignatiuk D, Grabiec M et al. (2019) Quality assessment and glaciological applications of digital elevation models derived from space-borne and aerial images over two tidewater glaciers of Southern Spitsbergen. *Remote Sensing* 11(9): 1121.

Błaszczyk M, Jania JA, Ciepły M et al. (2021) Factors controlling terminus position of Hansbreen, a tidewater glacier in Svalbard. *Journal of Geophysical Research Earth Surface* 126(2): e2020JF005763.

Błaszczyk M, Jania JA and Hagen JO (2009) Tidewater glaciers of Svalbard: Recent changes and estimates of calving fluxes. *Polish Polar Research* 30(2): 85–142.

Błaszczyk M, Jania JA and Kolondra L (2013) Fluctuations of tidewater glaciers in Hornsund Fjord (Southern Svalbard) since the beginning of the 20th century. *Polish Polar Research* 34(4): 327–352.

Daublebsky von Sterneck Zu Ehrenstein M (1874) *Die Arktische Expedition des Grafen. Hans Wiltschek nach Spitzbergen und Novaja Semlje Juni–Sept. 1872*, Petermanns Geographische Mittheilungenvol. 20. Gotha: Justus Perthes Verlag.

Denisenko SD and Tarasov GA (1992) Fossil complexes of bivalve molluscs with prevalence of *Chlamys islandica* from coastal moraines of Treskelen area of the Hornsund Fjord (West Spitsbergen). In: Repelewska-Pekalowa J and Pekala K (eds) *Wyprawy geograficzne na Spitsbergen*. Lublin: UMCS, pp.101–106.

de Wet GA, Balascio NL, D'Andrea WJ et al. (2018) Holocene glacier activity reconstructed from proglacial lake Gjøavatnet on Amsterdamøya, NW Svalbard. *Quaternary Science Reviews* 183(1): 188–203.

Dzierzek J, Nitychoruk J and Rzętkowska A (1990) Geological-geomorphological analysis and 14C dating of submoraine organogenic deposits within the Renardbreen outer margin, Wedel Jarlsberg land, Spitsbergen. *Polar Research* 8(2): 275–281.

European Space Agency (2021) Copernicus Open Access Hub. Available at: https://scihub.copernicus.eu/ (accessed 15 June 2021).

Evans DJA and Rea BR (2005) Late Weichselian deglaciation and sea level history of St Jonsfjorden, Spitsbergen: A contribution to ice sheet reconstruction. *Scottish Geographical Journal* 121(2): 175–201.

Farnsworth WR (2018) *Holocene glacier history of Svalbard: Retracing the style of (de)glaciation*. PhD Thesis, The Arctic University of Norway, Tromsø.

Farnsworth WR, Allaart L, Ingólfsson Ó, et al. (2020) Holocene glacial history of Svalbard: Status, perspectives and challenges. *Earth-Science Reviews* 208: 103249.

Farnsworth WR, Ingólfsson Ó, Retelle M et al. (2016) Over 400 previously undocumented Svalbard surge-type glaciers identified. *Geomorphology* 264(1): 52–60.

Farnsworth WR, Ingólfsson Ó, Retelle M et al. (2018) Svalbard glaciers re-advanced during the pleistocene–Holocene transition. *Boreas* 47(4): 1022–1032.

Farnsworth WR, Ingólfsson Ó, Noormets R et al. (2017) Dynamic Holocene glacial history of St. Jonsfjorden, Svalbard. *Boreas* 46(3): 585–603.

Flink AE, Hill P, Noormets R et al. (2018) Holocene glacial evolution of Mohnbukta in eastern Spitsbergen. *Boreas* 47(2): 390–409.

Flink AE and Noormets R (2018) Submarine glacial landforms and sedimentary environments in Vaigattbogen, northeastern Spitsbergen. *Marine Geology* 402: 244–263.

Flink AE, Noormets R, Kirchner N et al. (2015) The evolution of a submarine landform record following recent and multiple surges of Tunabreen glacier, Svalbard. *Quaternary Science Reviews* 108: 37–50.

Forwick M, Vorren TO, Hald M et al. (2010) Spatial and temporal influence of glaciers and rivers on the sedimentary environment in Sassenfjorden and Tempelfjorden, Spitsbergen. In: Howe JA, Austin WEN, Forwick M et al. (eds) *Fjord Systems and Archives*. London: Geological Society, pp.165–195, Special Publications 344.

Furrer G, Stapfer A and Glaser U (1991) Zur nacheiszeitlichen Gletschergeschichte des Liefdefjords (Spitzbergen) (Ergebnisse der Geowissenschaftlichen Spitzbergenexpedition 1990). *Geographica Helvetica* 46: 147–155.

Görlich K, Węsławski JM and Zajączkowski M (1987) Suspension settling effect on macrobenthos biomass distribution in the Hornsund fjord, Spitsbergen. *Polar Research* 5(2): 175–192.

Grabiec M, Ignatiuk D, Jania JA et al. (2018) Coast formation in an Arctic area due to glacier surge and retreat: The Hornbreen-Hambergbreen case from Spistbergen. *Earth Surface Processes and Landforms* 43(2): 387–400.

Hald M, Dahlgren T, Olsen T-E et al. (2001) Late Holocene palaeoceanography in Van Mijenfjorden, Svalbard. *Polar Research* 20(1): 23–35.

Hansen J, Hanken NM, Nielsen JK et al. (2011) Late Pleistocene and Holocene distribution of *Mytilus edulis* in the Barents Sea region and its palaeoclimatic implications. *Journal of Biogeography* 38(6): 1197–1212.

Harland WB (1997) *The Geology of Svalbard*. London: Geological Society, Memoir No. 17.

Heaton TJ, Köhler P, Butzin M et al. (2020) Marine20—the marine radiocarbon age calibration curve (0–55,000 cal BP). *Radiocarbon* 62(4): 779–820.

Heintz A (1953) Non iakktagelser over isbreenes tilbakegang i Hornsund. *Norsk Geologisk Tidsskrift* 31: 7–36.

Ingólfsson Ó, Benediktsson ÍÖ, Schomacker A et al. (2016) Glacial geological studies of surge-type glaciers in Iceland — Research status and future challenges. *Earth-Science Reviews* 152: 37–69.

Jania J (1988) *Dynamiczne procesy glacjalne na południowym Spitsbergenie (w świetle badań fotointerpretacyjnych i fotogrametrycznych)* [Dynamic glacial processes in south Spitsbergen (in the light of photointerpretation and photogrammetric research)]. Prace Naukowe Uniwersytetu Śląskiego w Katowicach nr 955. Katowice (in Polish).

Jania J (2001) Evolution of the Hornbreen–Hambergbreen glacial system (SE Spitsbergen) during the 20th century. In: *Functioning of systems in varied morphological-climatic conditions – Monitoring, conservation, education* (eds A Karczewski and Z Zwoliński), Poznań, Poland, 19–20 October 2001, pp.48–49. Poznan: Association of Polish Geomorphologists. (in Polish)

Kabala C and Zapart J (2009) Recent, relict and buried soils in the forefield of Werenskiold Glacier, SW Spitsbergen. *Polish Polar Research* 30(2): 161–178.

Kaufman DS, Ager TA, Anderson NJ et al. (2004) Holocene thermal maximum in the western Arctic (0–180°W). *Quaternary Science Reviews* 23(5–6): 529–560.

Kempf P, Forwick M, Laberg JS et al. (2013) Late Weichselian and Holocene sedimentary palaeoenvironment and glacial activity in the high-arctic van Keulenfjorden, Spitsbergen. *The Holocene* 23(11): 1607–1618.

Koryakin VS (1975) The position and morphology of glaciers. In: Troitsky LS, Singer EM, Koryakin VS et al. (eds) *Glaciation of Spitsbergen (Svalbard)*. Moscow: Nauka, pp.7–41, (in Russian, English Summary).

Łącka M, Zajączkowski M, Forwick M et al. (2015) Late Weichselian and Holocene palaeoceanography of Storfjordrenna, southern Svalbard. *Climate of the Past* 11: 587–603.

Larsen E, Lyså A, Rubensdotter L et al. (2018) Lateglacial and Holocene glacier activity in the Van Mijenfjorden area, western Svalbard. *Arktos* 4: 1–21.

Lefauconnier B and Hagen JO (1991) Surging and calving glaciers in eastern Svalbard. *Norsk Polarinstitutt Meddelelser* 116: 1–130.

Legeżyńska J, Włodarska-Kowalczuk M, Gluchowska M et al. (2017) The malacostracan fauna of two Arctic fjords (west Spitsbergen): The diversity and distribution patterns of its pelagic and benthic components. *Oceanologia* 59(4): 541–564.

Lindner L and Marks L (1997) Polish Spitsbergen Bibliography: Quaternary geology. *Polish Polar Research* 18(1): 65–76.

Lovell H, Benn DI, Lukas S et al. (2018) Multiple Late Holocene surges of a High-Arctic tidewater glacier system in Svalbard. *Quaternary Science Reviews* 201: 162–185.

Luoto TP, Ojala AEK, Arppe L et al. (2018) Synchronized proxy-based temperature reconstructions reveal mid- to late Holocene climate oscillations in High Arctic Svalbard. *Journal of Quaternary Science* 33(1): 93–99.

Lyså A, Larsen EA, Høgaas F et al. (2018) A temporary glacier-surge ice-dammed lake, Braganzavågen, Svalbard. *Boreas* 47(3): 837–854.

Lønne I (2005) Faint traces of high Arctic glaciations: an early Holocene ice-front fluctuation in Bolterdalen, Svalbard. *Boreas* 34(3): 308–323.

Mangerud J and Svendsen JI (2018) The Holocene Thermal Maximum around Svalbard, Arctic North Atlantic; molluscs show early and exceptional warmth. *The Holocene* 28(1): 65–83.

Marks L (1983) Late Holocene evolution of the Treskelen Peninsula (Hornsund, Spitsbergen). *Acta Geologica Polonica* 33(1–4): 159–168.

Marks L and Pękala K (1986) New datings of Quaternary sediments from Bogstranda and Treskelodden, southern Spitsbergen. *Bulletin of the Polish Academy of Sciences. Earth Sciences* 34(4): 419–425.

Martín-Moreno R, Allende Álvarez F and Hagen JO (2017) ‘Little Ice Age’ glacier extent and subsequent retreat in Svalbard archipelago. *The Holocene* 27(9): 1379–1390.

Miller GH, Brigham-Grette J, Alley RB et al. (2010) Temperature and precipitation history of the Arctic. *Quaternary Science Reviews* 29: 1679–1715.

Moore PG (1977) Inorganic particulate suspensions in the sea and their effects on marine animals. *Oceanography and Marine Biology: An Annual Review* 15: 225–363.

Moskalik M, Grabowiecki P, Tęgowski J et al. (2013) Bathymetry and geographical regionalization of Brepollen (Hornsund, Spitsbergen) based on bathymetric profiles interpolations. *Polish Polar Research* 34(1): 1–22.

Nielsen T and Rasmussen TL (2018) Reconstruction of ice sheet retreat after the Last Glacial maximum in Storfjorden, southern Svalbard. *Marine Geology* 402: 228–243.

Noël B, Jakobs CL, van Pelt WJJ et al. (2020) Low elevation of Svalbard glaciers drives high mass loss variability. *Nature Communications* 11: 4597.

Noormets R, Flink A and Kirchner N (2021) Glacial dynamics and deglaciation history of Hambergbukta reconstructed from submarine landforms and sediment cores, SE Spitsbergen, Svalbard. *Boreas* 50(1): 29–50.

Norwegian Polar Institute (2021) TopoSvalbard. Available at: https://toposvalbard.npolar.no/ (accessed 18 July 2021).

Nuth C, Kohler J, Aas HF et al. (2007) Glacier geometry and elevation changes on Svalbard (1936–90), A baseline dataset. *Annals of Glaciology* 46: 106–116.

Nuth C, Moholdt G, Kohler J et al. (2010) Svalbard glacier elevation changes and contribution to sea level rise. *Journal of Geophysical Research* 115: F01008.

Oerlemans J, Jania J and Kolondra L (2011) Application of a minimal glacier model to Hansbreen, Svalbard. *The Cryosphere* 5: 1–11.

Oerlemans J and van Pelt WJJ (2015) A model study of Abrahamsenbreen, a surging glacier in northern Spitsbergen. *The Cryosphere* 9(2): 767–779.

Østby TI, Schuler TV, Hagen JO et al. (2017) Diagnosing the decline in climatic mass balance of glaciers in Svalbard over 1957–2014. *The Cryosphere* 11(1): 191–215.

Ottesen D, Dowdeswell JA, Landvik JY et al. (2007) Dynamics of the Late Weichselian ice sheet on Svalbard inferred from high-resolution sea-floor morphology. *Boreas* 36(3): 286–306.

Pälli A, Moore JC, Jania J et al. (2003) Glacier changes in southern Spitsbergen, Svalbard,1901–2000. *Annals of Glaciology* 37: 219–225.

Pawłowska J, Zajączkowski M, Łącka M et al. (2016) Palaeoceanographic changes in Hornsund Fjord (Spitsbergen, Svalbard) over the last millennium: new insights from ancient DNA. *Climate of the Past* 12: 1459–1472.

Pętlicki M, Ciepły M, Jania JA et al. (2015) Calving of a tidewater glacier driven by melting at the waterline. *Journal of Glaciology* 61(229): 851–863.

Philipps W, Briner JP, Gislefoss L et al. (2017) Late Holocene glacier activity at inner Hornsund and Scottbreen, southern Svalbard. *Journal of Quaternary Science* 32(4): 501–515.

Polyakov IV, Alkire MB, Bluhm BA et al. (2020) Borealization of the Arctic Ocean in response to anomalous advection from Sub-Arctic Seas. *Frontiers in Marine Science* 7: 491.

Promińska A, Falck E and Walczowski W (2018) Interannual variability in hydrography and water mass distribution in Hornsund, an Arctic fjord in Svalbard. *Polar Research* 37(1): 1495546.

Rasmussen TL and Thomsen E (2021) Climate and ocean forcing of ice-sheet dynamics along the Svalbard-Barents Sea ice sheet during the deglaciation ~20,000–10,000 years BP. *Quaternary Science Advances* 3: 100019.

Rea BR and Evans DJA (2011) An assessment of surge-induced crevassing and the formation of crevasse squeeze ridges. *Journal of Geophysical Research* 116: F04005.

Rebesco M, Laberg JS, Pedrosa MT et al. (2014) Onset and growth of Trough-Mouth Fans on the North-Western Barents Sea margin – Implications for the evolution of the Barents Sea/Svalbard Ice Sheet. *Quaternary Science Reviews* 92: 227–234.

Reimer PJ and Reimer RW (2001) A marine reservoir correction database and on-line interface. *Radiocarbon* 43(2A): 461–463.

Renaud PE, Włodarska-Kowalczuk M, Trannum H et al. (2007) Multidecadal stability of benthic community structure in a high-arctic glacial fjord (Van Mijenfjord, Spitsbergen). *Polar Biology* 30: 295–305.

Reusche M, Winsor K, Carlson AE et al. (2014) ^{10}Be surface exposure ages on the late-Pleistocene and Holocene history of Linnébreen on Svalbard. *Quaternary Science Reviews* 89: 5–12.

Rodzik J (1996) Szczelinowe formy z wyciśnięcia w strefie marginalnej Lodowca Horn (Spitsbergen). [Crevasse forms in the marginal zone of the Horn Glacier (Spitsbergen)] In: *Rzeźba i osady czwartorzędowe obszarów współczesnego i plejstoceńskiego zlodowacenia półkuli północnej* (ed A. Kostrzewski), Poznań, Poland, 17–18 October 1996, pp. 37–39. Poznań: Instytut Badań Czwartorzędu UAM (in Polish).

Ronnert L and Landvik JY (1993) Holocene glacial advances and moraine formation at Albrechtbreen, Edgeøya, Svalbard. *Polar Research* 12(1): 57–63.

Różycki O (1992) Occurrence of Gastropoda and Bivalvia in Hornsund Fiord (West Spitsbergen, Svalbard). *Polish Polar Research* 13(1): 41–52.

Røthe TO, Bakke J, Støren EWN et al. (2018) Reconstructing Holocene glacier and climate fluctuations from lake sediments in vårfluesjøen, Northern Spitsbergen. *Frontiers in Earth Science* 6: 91.

Røthe TO, Bakke J, Vasskog K et al. (2015) Arctic Holocene glacier fluctuations reconstructed from lake sediments at Mitrahalvøya, Spitsbergen. *Quaternary Science Reviews* 109: 111–125.

Salvigsen O and Elgersma A (1993) Radiocarbon dating of deglaciation and raised beaches in north-western Sørkapp Land. Zeszyty Naukowe Uniwersytetu Jagiellońskiego (Kraków). *Prace Geograficzne* 94: 39–47.

Salvigsen O and Høgvard K (2006) Glacial history, holocene shoreline displacement and palaeoclimate based on radiocarbon ages in the area of Bockfjorden, north-western Spitsbergen, Svalbard. *Polar Research* 25(1): 15–24.

Schuler TV, Kohler J, Elagina N et al. (2020) Reconciling Svalbard Glacier Mass Balance. *Frontiers in Earth Science* 8: 156.

Ślubowska MA, Koç N, Rasmussen TL et al. (2005) Changes in the flow of Atlantic water into the Arctic Ocean since the last deglaciation: Evidence from the northern Svalbard continental margin, 80°N. *Paleoceanography* 20: PA4014.

Ślubowska-Woldengen M, Rasmussen TL, Koç N et al. (2007) Advection of Atlantic Water to the western and northern Svalbard shelf since 17,500calyr BP. *Quaternary Science Reviews* 26(3–4): 463–478.

Sternal B, Szczuciński W, Forwick M et al. (2012) Sedimentary record of postglacial variability in near-bottom currents, sediment supply and ice rafting on the continental shelf off SW Spitsbergen. In: *EGU General Assembly 2012*, Vienna, Austria, 22–27 April 2012, p.5112.

Strzelecki MC, Szczuciński W, Dominiczak A et al. (2020) New fjords, new coasts, new landscapes: The geomorphology of paraglacial coasts formed after recent glacier retreat in Brepollen (Hornsund, southern Svalbard). *Earth Surface Processes and Landforms* 45(5): 1325–1334.

Sund M, Lauknes TR and Eiken T (2014) Surge dynamics in the Nathorstbreen glacier system, Svalbard. *The Cryosphere* 8: 623–638.

Svendsen JI and Mangerud J (1997) Holocene glacial and climatic variations on Spitsbergen, Svalbard. *The Holocene* 7(1): 45–57.

Szafraniec J (2013a) The glaciers of West Spitsbergen – the state of research with particular emphasis on the Hornsund region. In: Zwoliński Z, Kostrzewski A and Pulina M (eds) *Ancient and Modern Geoecosystems of Spitsbergen*. Poznań: Bogucki Wydawnictwo Naukowe, pp.245–263.

Szafraniec JE (2013b) Paleoflood marks in sandur morphometry as the result of the glacier surge (NW Poland). *Hydrology Research* 44(2): 264–280.

Szafraniec JE (2020) Ice-cliff morphometry in identifying the surge phenomenon of tidewater glaciers (Spitsbergen, Svalbard). *Geosciences* 10(9): 328.

Szczuciński W, Schellter G and Zajączkowski M (2006) Sediment accumulation rates, geochemistry and provenance in complex High Arctic fjord, Hornsund, Svalbard. In: *Fourth ESF SED- 15IFLUX science meeting & first workshop of I.A.G./A.I.G. SEDIBUD: source-to sink-fluxes and sediment budgets in cold environments* (ed AA Beylich), Trondheim, Norway, 29 October–2 November 2006, p.65.

Szczuciński W, Zajączkowski M and Scholten J (2009) Sediment accumulation rates in subpolar fjords – Impact of post-Little Ice Age glaciers retreat, Billefjorden, Svalbard. *Estuarine, Coastal and Shelf Science* 85(3): 345–356.

Tarasov GA, Denisenko SD, Matishov GG et al. (1992) Moraine complexes and certain questions concerning paleoecology of the Treskelen region in the Hornsund Fjord (Western Spitsbergen). In: Repelewska-Pekalowa J and Pekala K (eds) *Wyprawy geograficzne na Spitsbergen*. Lublin: UMCS, pp.121–154.

Telesiński MM, Przytarska JE, Sternal B et al. (2018) Palaeoceanographic evolution of the SW Svalbard shelf over the last 14 000 years. *Boreas* 47(2): 410–422.

U.S. Geological Survey (2021) Earth Explorer. Available at: https://earthexplorer.usgs.gov/ (accessed 15 June 2021).

van der Bilt WGM, Bakke J, Vasskog K et al. (2015) Reconstruction of glacier variability from lake sediments reveals dynamic Holocene climate in Svalbard. *Quaternary Science Reviews* 126: 201–218.

van der Bilt WGM, D'Andrea WJ, Werner WJ et al. (2019) Early Holocene temperature oscillations exceed amplitude of observed and projected warming in Svalbard lakes. *Geophysical Research Letters* 46: 14,732–14,741.

Vassiliev W (1907) Missions Scientifiques pour la Mesure d'un arc de Méridien au Spitsberg enterprises en 1899–1901 sous les auspices des gouvernements Russe et Suédois. Mission Russe. In: Backlund H (ed.) *Observation Geologique du Spitsberg Central*. St. Petersbourg: Imperial Academy of Sciences, pp.1–20.

Walker M, Gibbard P, Head MJ et al. (2019) Formal subdivision of the Holocene Series/Epoch: A Summary. *Journal of the Geological Society of India* 93: 135–141.

Wawrzyniak T and Osuch M (2020) A 40-year High Arctic climatological dataset of the Polish Polar Station Hornsund (SW Spitsbergen, Svalbard). *Earth System Science Data* 12: 805–815.

Werner A (1993) Holocene moraine chronology, Spitsbergen, Svalbard: lichenometric evidence for multiple Neoglacial advances in the Arctic. *The Holocene* 3(2): 128–137.

Włodarska-Kowalczuk M (2007) Molluscs in Kongsfjorden (Spitsbergen, Svalbard): a species list and patterns of distribution and diversity. *Polar Research* 26(1): 48–63.

WoRMS Editorial Board (2021) World Register of Marine Species. Available at: https://www.marinespecies.org (accessed 30 May 2021).

Włodarska-Kowalczuk M, Węsławski JM and Kotwicki L (1998) Spitsbergen glacial bays macrobenthos - a comparative study. *Polar Biology* 20: 66–73.

Young NE, Lamp J, Koffman T et al. (2018) Deglaciation of coastal south-western Spitsbergen dated with *in situ* cosmogenic ^{10}Be and ^{14}C measurements. *Journal of Quaternary Science* 33(7): 763–776.

Zajączkowski M, Szczuciński W and Bojanowski R (2004) Recent changes in sediment accumulation rates in Adventfjorden, Svalbard. *Oceanologia* 46(2): 217–231.

Zemp M, Huss M, Thibert E et al. (2019) Global glacier mass changes and their contributions to sea-level rise from 1961 to 2016. *Nature* 568: 382–386.

Załącznik 2

Supplement S1. Radiocarbon dated shells from the moraines in the Hornbreen forefield.

Lab ID	Locality	Lat. N	Long. E	Elevation (m a.s.l.)	Collection year	Dated material	Age ^{14}C (BP)	Calibrated ages BP (Marine20, ΔR = −56 ± 33)			References
								Median	68.3% Confidence interval	95.4% Confidence interval	
U-2753	Treskelen	N/A	N/A	5–10	1974	Mya truncata	9690 ± 160	10524	10725–10245 cal. BP (68.3%)	11061–10116 cal. BP (95.4%)	Birkenmajer, Olsson (1997)
U-2757	Treskelen	N/A	N/A	5–10	1974	Chlamys islandica	8770 ± 120	9314	9475–9175 cal. BP (65.1%) 9170–9151 cal. BP (3.1%)	9618–8986 cal. BP (95.4%)	Birkenmajer, Olsson (1997)
U-2755	Treskelen	N/A	N/A	5–10	1974	Hiatella arctica	8400 ± 140	8849	9052–9046 cal. BP (0.7%) 9026–8620 cal. BP (67.5%)	9261–8457 cal. BP (95.4%)	Birkenmajer, Olsson (1997)
U-2833	Treskelen	N/A	N/A	5–10	1974	Astarte borealis	4280 ± 170	4278	4519–4018 cal. BP (68.3%)	4779–3822 cal. BP (95.4%)	Birkenmajer, Olsson (1997)
U-2763	Selodden	N/A	N/A	5	1974	Mya truncata	9770 ± 150	10637	10871–10382 cal. BP (68.3%)	11101–10220 cal. BP (95.4%)	Birkenmajer, Olsson (1997)
U-2969	Treskelen	N/A	N/A	5–20	1974	Chlamys islandica	9750 ± 160	10609	10851–10338 cal. BP (68.3%)	11107–11107 cal. BP (0.2%) 11089–10117 cal. BP (95.3%)	Birkenmajer, Olsson (1997)
U-2971	Treskelen	N/A	N/A	5–20	1974	Mya truncata	9610 ± 140	10412	10619–10612 cal. BP (0.8%) 10595–10201 cal. BP (67.5%)	10877–10001 cal. BP (95.2%) 9985–9974 cal. BP (0.2%)	Birkenmajer, Olsson (1997)
U-2985	Treskelen	N/A	N/A	5–20	1974	Astarte borealis	1850 ± 150	1309	1499–1492 cal. BP (1.0%) 1483–1127 cal. BP (67.3%)	1669–1658 cal. BP (0.4%) 1651–956 cal. BP (95.0%)	Birkenmajer, Olsson (1997)
Gd-3178	Treskelen	N/A	N/A	90–100	N/A	Chlamys islandica	8680 ± 60	9219	9336–9102 cal. BP (66.3%)	9424–9005 cal. BP (95.4%)	Marks, Pękala (1986)
GIN-7083	Treskelen	N/A	N/A	5–40	1991	Chlamys islandica	8380 ± 80	8820	8974–8688 cal. BP (68.3%)	9095–8541 cal. BP (95.4%)	Tarasov et al. (1992)
GIN-7084	Selodden	N/A	N/A	N/A	1991	Chlamys islandica	7090 ± 200	7449	7649–7245 cal. BP (68.3%)	7872–7012 cal. BP (95.4%)	Tarasov et al. (1992)
Poz-125715	S coast of Hornbukta	77°01'13"	16°36'30"	1.8	2019	Chlamys islandica	9180 ± 50	9823	9950–9680 cal. BP (68.3%)	10093–9576 cal. BP (95.4%)	This study
Poz-125672	S coast of Hornbukta	77°01'13"	16°36'30"	1.8	2019	Hiatella arctica	9840 ± 50	10727	10851–10842 cal. BP (1.7%) 10834–10579 cal. BP (66.5%)	11040–11035 cal. BP (0.2%) 11016–10497 cal. BP (95.2%)	This study
Poz-125671	S coast of Hornbukta	77°01'56"	16°38'44"	1.8	2019	shell debris	9870 ± 50	10776	10927–10909 cal. BP (2.9%) 10900–10889 cal. BP (1.9%) 10883–10630 cal. BP (63.4%)	11055–10550 cal. BP (95.3%) 10542–10539 cal. BP (0.2%)	This study
Poz-125670	S coast of Hornbukta	77°02'08"	16°39'52"	2.5	2019	shell debris	9750 ± 50	10589	10708–10475 cal. BP (68.3%)	10856–10842 cal. BP (0.5%) 10835–10329 cal. BP (95.0%)	This study
GdA-6409	S coast of Hornbukta	77°01'38"	16°37'47"	2.5	2020	Astarte borealis	4010 ± 35	3918	4021–3820 cal. BP (68.3%)	4119–3713 cal. BP (95.4%)	This study
GdA-6410	S coast of Hornbukta	77°02'20"	16°41'40"	20.3	2020	Astarte borealis	4400 ± 35	4435	4529–4330 cal. BP (68.3%)	4647–4226 cal. BP (95.4%)	This study
GdA-6411	S coast of Hornbukta	77°00'28"	16°32'53"	1.6	2020	Boreotrophon truncatus	8140 ± 50	8503	8588–8404 cal. BP (68.3%)	8726–8724 cal. BP (0.1%) 8717–8326 cal. BP (95.3%)	This study
GdA-6412	S coast of Hornbukta	77°00'22"	16°32'17"	1.6	2020	Astarte elliptica	6020 ± 40	6308	6393–6220 cal. BP (68.3%)	6485–6132 cal. BP (95.4%)	This study
GdA-6413	Treskelen	76°59'46"	16°13'53"	27.8	2020	Chlamys islandica	9000 ± 50	9580	9670–9476 cal. BP (68.3%)	9817–9399 cal. BP (95.4%)	This study
GdA-6414	Treskelen	76°59'48"	16°14'03"	40.7	2020	Mya truncata	9940 ± 50	10880	11018–10755 cal. BP (68.3%)	11118–10644 cal. BP (95.4%)	This study

Załącznik 3

Supplement S2. Data sources for calculating the morphometric indicators of glacier termini.

Hornbreen		
Year	Identifier	Acquisition data
1976*	LM22300041976200AAA05	18.07.1976
1977		
1978		
1979		
1980		
1981		
1982		
1983		
1984		
1985	LT52080051985234KIS00	22.08.1985
1986	LT52070061986230KIS00	18.08.1986
1987	LT52080051987192KIS00	11.07.1987
1988	LT52070051988204KIS00	22.07.1988
1989		
1990	LT52080051990232KIS00	20.08.1990
1991		
1992	LT52070051992263KIS00	19.09.1992
1993		
1994	LT52080051994243KIS00	31.08.1994
1995	LT52080051995246KIS00	03.09.1995
1996		
1997	LT52080051997219KIS00	07.08.1987
1998	LT52080051998270KIS00	27.09.1998
1999	LE72090051999208KIS00	27.07.1999
2000		
2001	LE72110052001179EDC00	28.06.2001
2002	LE72080052002193EDC00	12.07.2002
2003		
2004	AST_L1A.003:2025232921	07.08.2004
2005	LE72130042005204EDC00	23.07.2005
2006		
2007		
2008		
2009		
2010	LE72110052010236EDC00	24.08.2010
2011	LE72110052011207ASN00	26.07.2011
2012		
2013	LE72130042013194EDC00	13.07.2013
2014	LC82100052014232LGN01	20.08.2014
2015	LC82090052015212LGN01	31.07.2015
2016	LC82090052016215LGN01	02.08.2016
2017	LC82110052017215LGN00	03.08.2017
2018	LC80272392018225LGN00	13.08.2018
2019	LC82100052019230LGN00	18.08.2019
2020	LC82100052020217LGN00	04.08.2020

Hambergbreen		
Year	Identifier	Acquisition data
1936	C12 Markhambreen	Svalbard 1:100,000 (topographic map). Oslo: Norsk Polarinstitutt; 1956
1937		
1938		
1939		
1940		
1941		
1942		
1943		
1944		
1945		
1946		
1947		
1948		
1949		
1950		
1951		
1952		
1953		
1954		
1955		
1956		
1957		
1958		
1959		
1960		
1961	C12 Markhambreen	Svalbard 1:100,000 (topographic map). Oslo: Norsk Polarinstitutt; 2008
1962		
1963		
1964		
1965		
1966		
1967		
1968		
1969		
1970		
1971		
1972		
1973		
1974		
1975		
1976		
1977		
1978		
1979		
1980		
1981		
1982		
1983		
1984		
1985	LT52080051985234KIS00	22.08.1985
1986	LT52070061986230KIS00	18.08.1986
1987	LT52080051987192KIS00	11.07.1987
1988	LT52070051988204KIS00	22.07.1988
1989		
1990	LT52080051990232KIS00	20.08.1990
1991		
1992	LT52070051992263KIS00	19.09.1992
1993		
1994	LT52080051994243KIS00	31.08.1994
1995	LT52080051995246KIS00	03.09.1995
1996		
1997	LT52080051997219KIS00	07.08.1987
1998	LT52080051998270KIS00	27.09.1998
1999		
2000		
2001	LE72110052001179EDC00	28.06.2001
2002	LE72080052002193EDC00	12.07.2002
2003		
2004	AST_L1A.003:2025232921	07.08.2004
2005		
2006		
2007		
2008		
2009		
2010	LE72110052010236EDC00	24.08.2010
2011	LE72110052011207ASN00	26.07.2011
2012		
2013	LE72130042013194EDC00	13.07.2013
2014	LC82100052014232LGN01	20.08.2014
2015	LC82090052015212LGN01	31.07.2015
2016	LC82090052016215LGN01	02.08.2016
2017	LC82110052017215LGN00	03.08.2017
2018	LC80272392018225LGN00	13.08.2018
2019	LC82100052019230LGN00	18.08.2019
2020	LC82100052020217LGN00	04.08.2020

*In 1976 the termini of Hornbreen, Storbreen, Svalisbreen and Mendeleevbreen were confluent.

Załącznik 4

Supplement S3. Species list of molluscs in the ground moraines in the Hornbreen forefield and their distribution in Hornsund Fjord in the 1970–1980s.

Taxa	Molluscs from shell-bearing moraines				Species distribution in Hornsund (1977-1985)*			
	Treskelen			Ostrogradskijfjella	Hornsund open water	Gashamna	Isbjornhamna	Brepollen
	Heintz (1953)	Birkenmajer (1958)	This study	This study				
Mya truncata (Linnaeus, 1758)	+	+	+	+	+	+	+	
Chlamys islandica (O. F. Müller, 1776)	+	+	+	+		+		
Hiatella arctica (Linnaeus, 1767)	+	+	+	+	+	+		+
Astarte borealis (Schumacher, 1817)	+	+		+	+			
Astarte elliptica (T. Brown, 1827)	+	+	+	+				
Astarte montagui		+			+			
Boreotrophon truncatus (Strøm, 1768)		+		+		+		
Macoma calcarea (Gmelin, 1790)		+			+		+	
Buccinum glaciale	+	+			+			
Balanus	+	+		+				
Lithotamnium sp.	+	+	+	+				

* After: Różycki O (1992) Occurrence of Gastropoda and Bivalvia in Hornsund Fiord (West Spitsbergen, Svalbard). *Polish Polar Research* 13(1): 41–52.

Załącznik 5

Supplement S3. Morphometric indicators (CfE, CfD) characterizing the frontal zones of Hornbreen and Hambergbreen.

Hornbreen		
Year	CfD	CfE
1976	0.457	-0.803
1977		
1978		
1979		
1980		
1981		
1982		
1983		
1984		
1985	0.468	-0.843
1986	0.567	0.675
1987	0.605	0.769
1988	0.594	0.853
1989		
1990	0.542	0.754
1991		
1992	0.499	-0.835
1993		
1994	0.508	-0.779
1995	0.497	-0.815
1996		
1997	0.517	-0.742
1998	0.575	0.729
1999	0.557	0.825
2000		
2001	0.479	-0.872
2002	0.481	-0.838
2003		
2004	0.416	-0.826
2005	0.434	-0.888
2006		
2007		
2008		
2009		
2010	0.461	-0.804
2011	0.379	-0.818
2012		
2013	0.326	-0.587
2014	0.237	-0.692
2015	0.403	-0.897
2016	0.380	-0.834
2017	0.409	-0.848
2018	0.368	-0.824
2019	0.377	-0.829
2020	0.390	-0.873

Hambergbreen		
Year	CfD	CfE
1936	0.445	-0.590
1937		
1938		
1939		
1940		
1941		
1942		
1943		
1944		
1945		
1946		
1947		
1948		
1949		
1950		
1951		
1952		
1953		
1954		
1955		
1956		
1957		
1958		
1959		
1960		
1961	0.532	0.758
1962		
1963		
1964		
1965		
1966		
1967		
1968		
1969		
1970		
1971		
1972		
1973		
1974		
1975		
1976		
1977		
1978		
1979		
1980		
1981		
1982		
1983		
1984		
1985	0.151	-0.548
1986	0.231	-0.626
1987	0.273	-0.748
1988	0.321	-0.719
1989		
1990		
1991		
1992	0.363	-0.887
1993		
1994	0.440	-0.930
1995	0.401	-0.843
1996		
1997	0.358	-0.890
1998	0.320	-0.845
1999		
2000	0.377	-0.919
2001	0.374	-0.918
2002	0.396	-0.916
2003		
2004	0.331	-0.789
2005		
2006		
2007		
2008		
2009		
2010	0.304	-0.759
2011	0.311	-0.780
2012		
2013	0.242	-0.737
2014	0.175	-0.685
2015	0.295	-0.847
2016	0.191	-0.703
2017	0.138	-0.667
2018	0.198	-0.675
2019	0.139	-0.625
2020	0.177	-0.637

Annals of Glaciology

Article

Cite this article: Osika A, Jania J (2024). Geomorphological and historical records of the surge-type behaviour of Hansbreen (Svalbard). *Annals of Glaciology* **65**, e31, 1–18. https://doi.org/10.1017/aog.2024.32

Received: 8 January 2024
Revised: 20 July 2024
Accepted: 22 July 2024

Keywords:
Arctic glaciology; glacial geomorphology; glacier surges

Corresponding author:
Aleksandra Osika;
Email: aosika1@us.edu.pl

cambridge.org/aog

Geomorphological and historical records of the surge-type behaviour of Hansbreen (Svalbard)

Aleksandra Osika and Jacek Jania

Faculty of Natural Sciences, University of Silesia, Institute of Earth Sciences, Bedzinska 60, 41-200 Sosnowiec, Poland

Abstract

This paper presents geomorphological and historical records of the surge-type behaviour of Hansbreen, one of the most studied tidewater glaciers in Svalbard. The surge-type behaviour of the glacier has not been considered before due to the lack of evidence of this phenomenon. We integrate geomorphological mapping of the terrestrial and submarine forefields with historical data from the 19th and 20th centuries to reconstruct the glacier dynamics and identify the possible timing of surging. Landform assemblages are representative of the surging glacier landsystem, including crevasse-squeeze ridges (CSRs) and submarine streamlined glacial lineations. Abundant CSRs in the outer part of the terrestrial forefield were also documented in the 1980s, but most have been obliterated since then. We suggest the identified surge landsystem was produced during a surge of Hansbreen detected from photographs taken during the Austro-Hungarian expedition in 1872. Historical photogrammetric photos from the Norwegian expedition in 1918 revealed surge-diagnostic features in the glacier surface, including a folded medial moraine and a dense, complex network of crevasses. A potential next surge remains questionable in the following decades due to the low-lying accumulation area of the main stream hindering the mass build-up, but potential surges of the tributary glaciers should not be excluded.

Introduction

Surge-type glaciers exhibit multiyear, quasi-cyclical velocity fluctuations between a prolonged quiescent phase of slow flow and a shorter active phase of fast flow, during which ice velocities can increase by 10–1000 times (Meier and Post, 1969; Raymond, 1987; Sund and others, 2009). Most surge-type glaciers concentrate in spatial clusters within an optimal climatic envelope, such as Svalbard (74–81°N) (Sevestre and Benn, 2015). Glaciers cover 57% of the land of this archipelago and more than 60% of the glaciated area is represented by tidewater glaciers (Błaszczyk and others, 2009; Nuth and others, 2013). There is general agreement that surging is a common phenomenon in Svalbard (e.g. Liestøl, 1969; Jania, 1988; Lefauconnier and Hagen, 1991; Hagen and others, 1993; Sevestre and Benn, 2015; Farnsworth and others, 2016; Benn and others, 2023), although the estimated percentage of surge-type glaciers varies from 13% (Jiskoot and others, 1998) to 90% (Hagen and Liestøl, 1990). The duration of the quiescent phase typically ranges from 30 to 150 years, but can be as long as 500 years (Dowdeswell and others, 1991; Hagen and others, 1993; Murray and others, 2003). Therefore, the length of surge cycles often exceeds the observation period, which poses a risk of misclassification of glaciers as non-surging if the active phase has not been observed and associated geomorphological and glaciological records of surging have been obliterated since then (Benn and Evans, 2010).

The frequency of surges is influenced by climatic conditions through changes in the mass balance and modification of the thermal structure of glaciers (Dowdeswell and others, 1995; Sevestre and others, 2015). In recent centuries, Svalbard glaciers reached their maximum extent during the Little Ice Age (LIA) and many of these advances were surge-related (e.g. Liestøl, 1969; Lefauconnier and Hagen, 1991; Christoffersen and others, 2005; Sevestre and others, 2015; Farnsworth and others, 2016; Zagórski and others, 2023). The main sources of data about the timing of the late LIA surges are historical observations of glaciers that have recently advanced (e.g. the surge of Kongsvegen dated to c. 1800; Liestøl, 1988) or evidence of glaciers experiencing the active phase of a surge as recorded in historical drawings and maps (e.g. Recherchebreen in 1838; Liestøl, 1993, Kongsvegen in 1869; Liestøl, 1988, Nathorstbreen and Paulabreen mapped in 1898; Ottesen and others, 2008). Although the phenomenon of glacier surges was unknown at that time, this unique photographic and cartographic documentation can be reinterpreted to identify the evidence for past surge events (e.g. Zagórski and others, 2023). However, in regions with less archival data on glacier fluctuations during the LIA, such as Hornsund, most surges have only been recorded in the second half of the 20th and in the 21st century (Błaszczyk and others, 2013). The first maps presenting glacier termini in this area were prepared during the Austro-Hungarian North Pole Expedition 1872–1874 (Peterman, 1874) and the Swedish-Russian Arc-of-Meridian Expedition to Spitsbergen 1899–1902 (Wassiliew, 1925) when the glaciers were already extensive or even at their LIA maxima. The scales of these maps and the simplified cartographic representation of glaciers on the older map do not allow the identification of evidence of

https://doi.org/10.1017/aog.2024.32 Published online by Cambridge University Press

ongoing surges, such as extensive crevassing or folded medial moraines (Copland and others, 2003). Therefore, some surges may have occurred in this area during the LIA that are not documented in existing inventories.

In the case of sparse archival data, the application of surging glacier landsystem models based on characteristic landform assemblages in the terrestrial (Evans and Rea, 1999, 2003) and submarine forefields (Ottesen and Dowdeswell, 2006; Ottesen and others, 2008, 2017) allows the detection of surge-like behaviour of glaciers with no documented surging history (Christoffersen and others, 2005; Farnsworth and others, 2016, 2017; Flink and Noormets, 2018). The landforms are a record of a fully active surge with glacier advance (stage 3 according to Sund and others, 2009) marked with pro- and supraglacial moraines and characteristic meltwater drainage patterns (Lønne, 2016). One of the key features of the surge landsystems are crevasse-squeeze ridges (CSRs), which indicate basal crevassing and saturated basal sediments during the active surge phase, while the preservation of the ridges implies abrupt surge termination and ice stagnation during the quiescent phase (Evans and Rea, 1999; Ben-Yehoshua and others, 2023). Fast ice flow during the surge can be inferred from streamlined glacial lineations (Ottesen and Dowdeswell, 2006). Glaciotectonic moraines, often associated with debris flow lobes in the marine environment, reflect an advance onto and deformation of proglacial sediments (Lovell and others, 2018). Ice-cored hummocky moraines record entrainment and transport of high volumes of sediments during the advance, and subsequent melt-out on stagnant ice (Evans and Rea, 1999). Small submarine retreat moraines reflect minor winter advances of quiescent tidewater glaciers (Flink and others, 2015).

Hansbreen (Hornsund, south Spitsbergen) is one of the most studied glaciers in Svalbard and its possible surge behaviour has long been debated (e.g. Jania, 1988; Jania and Głowacki, 1996; Rachlewicz and Szczuciński, 2000; Ćwiąkała and others, 2018). The glacier and surrounding area have been the subject of numerous investigations (e.g. Jania, 1988; Glazovskiy and others, 1992; Vieli and others, 2002; Pälli and others, 2003; Grabiec and others, 2012; De Andrés and other, 2018; Laska and others, 2022) and its contemporary dynamics are well understood (Błaszczyk and others, 2021, 2024). According to the Randolph Glacier Inventory (RGI) V7.0, there is 'no evidence' that Hansbreen is a surge-type glacier (Maussion and others, 2023; RGI 7.0 Consortium, 2023). In contrast to most medium-sized or large tidewater glaciers in Hornsund, Hansbreen has not surged since the regular monitoring of glacier dynamics initiated in 1982 and there is no unequivocal evidence for surging earlier in the 20th century (Błaszczyk and others, 2013; Szafraniec, 2020). Over the last 40 years, three tidewater glaciers in Hornsund underwent a surge: Paierlbreen (advance of 380 m in 1992–1995), Mendeleevbreen (advance of 1.5 km in 1997–2002) and Svalisbreen (advance of c. 400 m in 2016–2020; Błaszczyk and others, 2023). Evidence of an ongoing surge was also reported in the case of Mühlbacherbreen (in 1961; Sund and others, 2009) and Körberbreen (in 1938; Liestøl, 1969). Marine-terminating Storbreen, Hornbreen and Samarinbreen are also surge-type glaciers (Fig. 1b; Jiskoot and others, 2000). Minor advances (c. 100–300 m) of Hansbreen were observed in 1957–1959

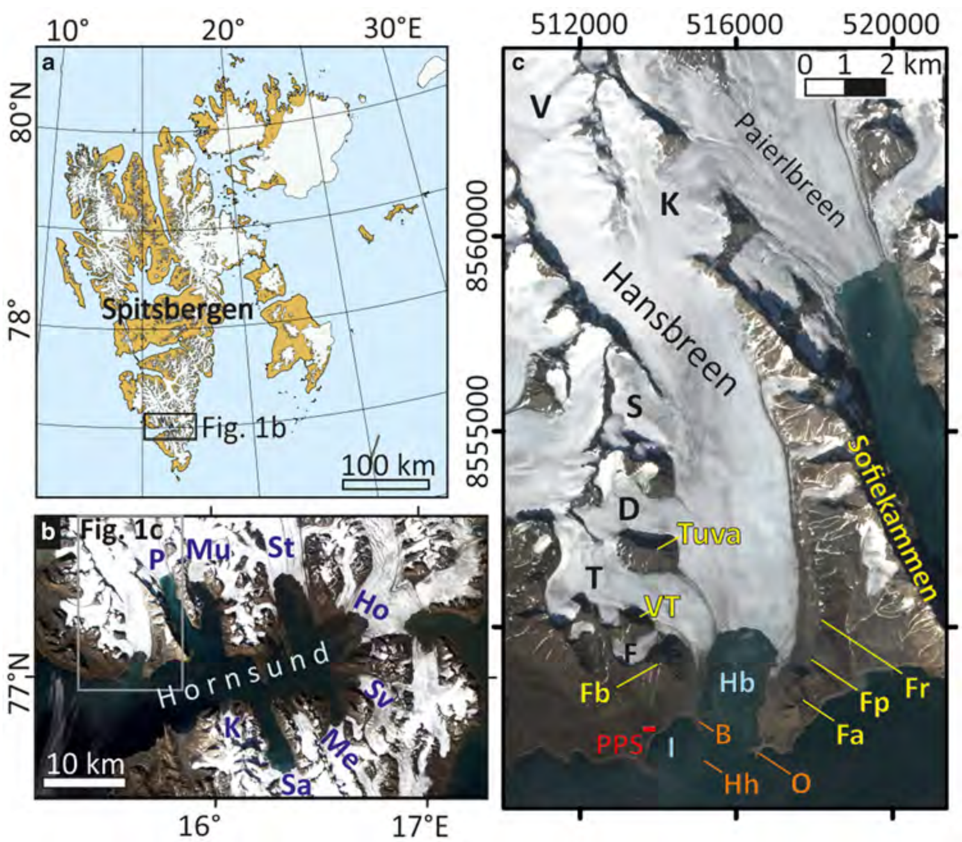

Figure 1. (a) Location of Hansbreen in the Svalbard archipelago and (b, c) Hornsund. (b) Glaciers: Ho, Hornbreen; K, Körberbreen; Me, Mendeleevbreen; Mu, Mühlbacherbreen; P, Paierlbreen; Sa, Samarinbreen; St, Storbreen; Sv, Svalisbreen. (c) Glaciers (black letters): D, Deileggbreen; F, Fuglebreen; K, Kvitungisen; S, Staszelisen; T, Tuvbreen; V, Vrangpeisbreen. Mountain ridges; peaks and saddles (yellow letters): Fa, Fannytoppen; Fb, Fugleberget; Fp, Flatpasset; Fr, Flatryggen; VT, Vesletuva. Peninsulas and islands (orange letters): B, Baranowski Peninsula (Baranowskiodden); Hh, Hansholmane; O, Oseanograftangen. Bays: Hb, Hansbukta; I, Isbjørnhamna. PPS, Polish Polar Station Hornsund. Figure map: © Norwegian Polar Institute (Norwegian Polar Institute, 2014). Sentinel-2B from 27 July 2023.

https://doi.org/10.1017/aog.2024.32 Published online by Cambridge University Press

(Kosiba, 1960), 1973–1977 and 1993–1995, and an episode of increased surface velocity occurred in the early 1990s, but these events were interpreted as 'mini-surges' rather than fully developed surges (Jania, 1988, 1998). Landforms diagnostic of surging were not detected in the submarine forefield of Hansbreen when it was mapped with multibeam echosounder in 2008 (Tegowski and others, 2016; Ćwiąkała and others, 2018). Farnsworth and others (2016) classified Hansbreen as a surge-type glacier based on the presence of CSRs in the terrestrial forefield. The geomorphology of the recently deglaciated submarine and terrestrial marginal zones presents an opportunity to investigate newly exposed geomorphological evidence for possible surging. Several studies have also demonstrated the importance of integrating terrestrial and submarine geomorphological records with historical datasets and observations in order to evaluate evidence for past surging of tidewater glaciers (e.g. Ottesen and others, 2008; Lovell and others, 2018; Aradóttir and others, 2019; Zagórski and others, 2023).

Here, we present the geomorphology of Hansbreen's terrestrial and submarine forefields and combine this with historical data to evaluate its surge-type behaviour.

Study site

Hansbreen is a polythermal tidewater glacier that terminates in Hansbukta on the northern side of Hornsund in south-west Spitsbergen (Fig. 1; Jania and others, 1996; Błaszczyk and others, 2019). The system consists of the main trunk flowing from north to south, four main tributary glaciers on the west (Fuglebreen, Tuvbreen, Deileggbreen and Staszelisen) and several minor tributaries on the east. The glacier is approximately 14 km long with a c. 2 km-long grounded calving front, 51.3 km^2 in area (as of 2015), a total ice volume of 9.6 km^3, a mean surface slope of 1.8° along the centreline and up to 5.6° along the centrelines of the tributaries (Grabiec and others, 2012; Błaszczyk and others, 2019, 2024). There is a distinct ice divide between Hansbreen and Vrangpeisbreen at the highest part of the main trunk at c. 490 m a.s.l., whereas the tributary glaciers reach up to 565 m a.s.l. (Błaszczyk and others, 2019). The delineation of the eastern border is not straightforward due to the transfluence of ice from the accumulation field of Hansbreen to Kvitungisen, a tributary of Paierlbreen. Around 2010, the mean and the maximum thickness of the glacier were 171 and 386 m, respectively, and the mean surface elevation was 306 m a.s.l. (Grabiec and others, 2012). The surface mass balance has been surveyed since 1989 and the mean annual value in 2000–2019 was −0.26 m w.e. (Schuler and others, 2020). In 2007–2015, the mean annual velocity measured c. 3.5 km from the calving front varied from 49.3 to 88.2 m a^{-1} and the central part of the front was 4–5 times faster. The average retreat rate in 1992–2015 was 38 m a^{-1} with a maximum of 311 m a^{-1} (Błaszczyk and others, 2021). The bedrock of the main trunk is overdeepened below sea level for 10 km from the calving front, and this overdeepening corresponds to a quarter of the total bedrock area beneath the glacier system (Grabiec and others, 2012; Otero and others, 2017). The geological structure is complex and diverse with several stratigraphic units of N-S orientation. The main valley has developed within Middle and Late Proterozoic phyllites, dolomites and conglomerates as well as Cambrian dolomites and quartzites. The west tributary glaciers have eroded Middle Proterozoic quartzites, marbles, phyllites and schists (Birkenmajer, 1990; Ohta and Dallmann, 1999). In 1979–2018, mean annual air temperature and precipitation measured at the nearby Polish Polar Station were −3.7°C and 235 mm with increase trends of +1.14°C and +61.6 mm per decade (Wawrzyniak and Osuch, 2019, 2020).

Similar to other glaciers in Hornsund, the first maps of the Hansbreen frontal position were based on surveys by the Austro-Hungarian (1872–1874) and Swedish-Russian expeditions (1899–1902) (Peterman, 1874; Wassiliew, 1925). At this time, Hansbreen occupied Hansbukta, the Baranowski Peninsula (Baranowskiodden), part of Isbjørnhamna, Oseanograftangen and raised marine terraces at the foot of Fugleberget and Fannytoppen. The geomorphology of the forefield was investigated by Birkenmajer (1960), Karczewski and others (1984), Pękala (1989), Lindner and others (1992), Rachlewicz and Szczuciński (2000). Since that time, there have been no new studies of the entire terrestrial forefield. The submarine geomorphology of Hansbukta was outlined by Jania (1988, 1998) and Tegowski and others (2016), and described in detail by Ćwiąkała and others (2018).

Materials and methods

We mapped the terrestrial forefield by combining field investigations with remote sensing data, as recommended by Chandler and others (2018). Field observations were carried out in 2021–2023 with detailed mapping in August 2022. Our map is based on a very high-resolution orthophotomosaic and DEM generated and published by Błaszczyk and others (2022) from aerial photos acquired on 22 June 2020 using a Dornier DO228 aircraft. The resolution of the orthophotomosaic and the DEM are 0.0843 and 0.169 m, with a maximal vertical DEM error of 0.54 m. Mapping of the submarine forefield was based on two datasets of bathymetric data. We mapped most of the forefield using a high-resolution DEM (1 m) based on multibeam bathymetric data from the Norwegian Hydrographic Service collected in 2008 (The Norwegian Mapping Authority, Kartverket). This dataset was used in the previous geomorphological studies of Hansbukta (Tegowski and others, 2016; Ćwiąkała and others, 2018). In addition, we used a DEM generated by Błaszczyk and others (2021) from multiple data sources to map the areas not surveyed in 2008. The DEM was based on measurements from a small boat using a Norbit Wideband Multibeam Sonar with a positioning system (2014, 2016, 2017) and data collected from a small boat with a single beam echosounder Lowrance HDS5 with positioning (2015). The assessed accuracy of these bathymetric data was ±5 m (Błaszczyk and others, 2021). We mapped the landforms in QGIS using the WGS84/UTM33N spatial reference system. Some small areas of the forefields were not covered by the bathymetry data or the orthophotomap and a small part of the seafloor with a surveyed topography remained unclassified in the geomorphological map (Figs 2 and 3). Changes in the frontal position of Hansbreen were taken from supplementary data to Błaszczyk and others (2013, 2021) and vectorized from Sentinel-2 images in natural colour compositions for the period 2016–2018.

To characterize the changing glacier and its forefield over time, we used historical maps and photographs from 1872 (Austro-Hungarian North Pole expedition, Peterman, 1874), a map from 1899 (Swedish-Russian Arc-of-Meridian Expedition, Wassiliew, 1925), a map and archival photographs from the Norwegian expedition to Spitsbergen in 1918 (Hoel, 1929), oblique aerial photographs from 1936 by the Norwegian Polar Institute and the orthophotomap from these data (Geyman and others, 2022), terrophotogrammetric documentation of the Hansbreen forefield in 1982–1996 from the archives of the University of Silesia (Jania and Kolondra, 1982) and the orthophotomap based on vertical aerial photographs from 2011 by the Norwegian Polar Institute, available in the TopoSvalbard online archive (https://toposvalbard.npolar.no/). The historical photographs from 1872 were acquired from the Austrian National Library Digital Image Archive (https://onb.digital/) and from 1918 from the digital image archive of the Norwegian Polar Institute (https://bildearkiv.npolar.no/fotoweb/). The

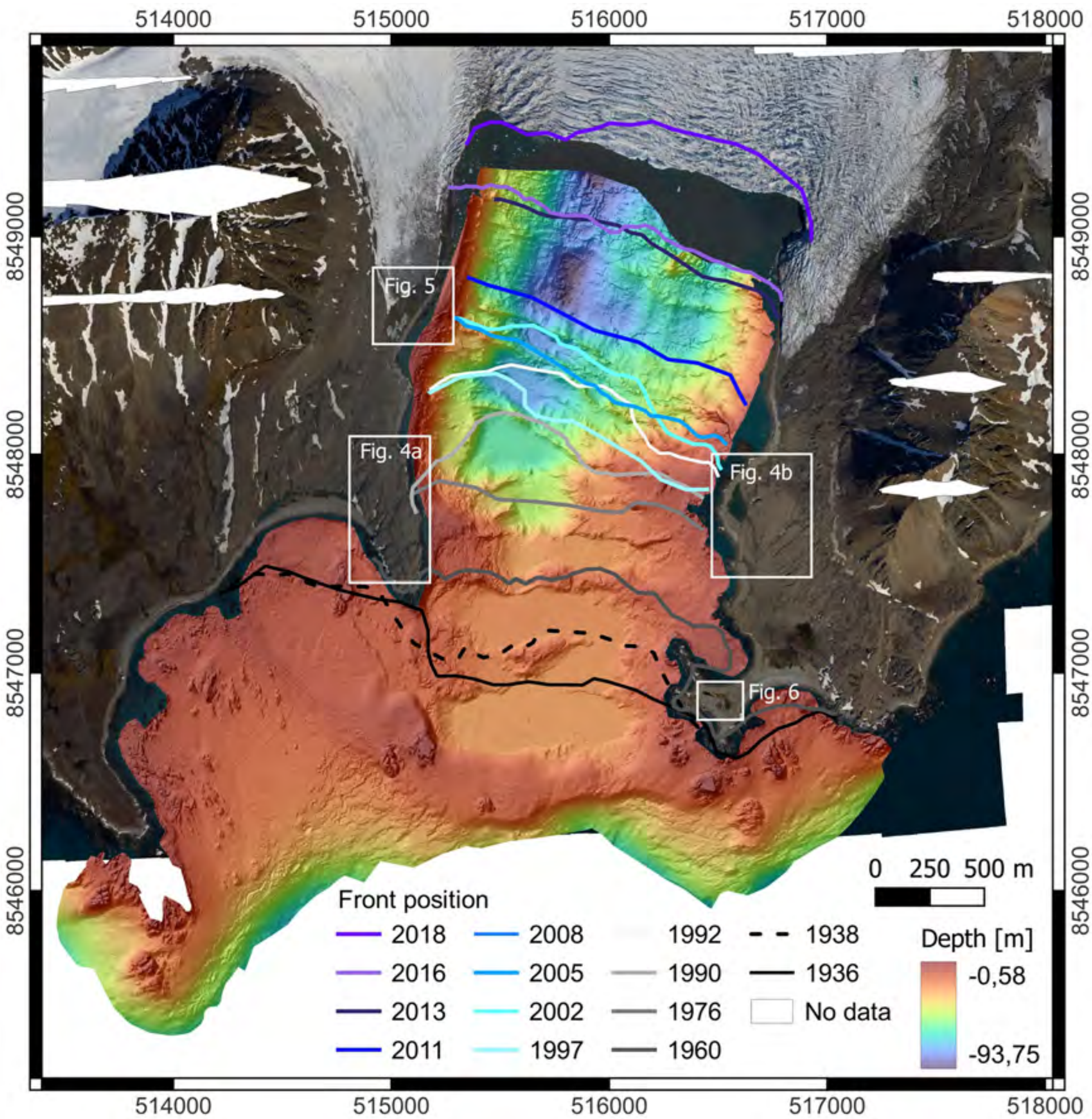

Figure 2. Hansbreen and its forefield. Orthophotomap from June 2020 after Błaszczyk and others (2022) and bathymetric map based on the Norwegian Hydrographic Service multibeam data (2008) combined with bathymetric data (2014–2017) after Błaszczyk and others (2021) were used to produce the geomorphological map (Fig. 3). Changes in the frontal position of Hansbreen after Błaszczyk and others (2013, 2021), Sentinel-2A from 2 August 2016 and 18 September 2018, and Jania (1988). The dashed line marks the glacier extent in 1938 based on terraphotogrammetric measurements conducted by Pillewizer (1939).

purpose of the historical data was to help interpret the formation of landforms and to assess past glacier frontal positions and any geomorphological or glaciological evidence for surging. As the surge criteria, we considered (1) looped moraines, (2) deformed ice structures, (3) heavy surface crevassing, (4) a surge bulge and (5) shear margins on the glacier surface (Lefauconnier and Hagen, 1991; Copland and others, 2003; Grant and others, 2009).

Hansbreen surging glacier landsystem

Glacial and glacifluvial landforms are classified according to their origin and morphological features and presented in the context of their associations (subglacial, supraglacial, ice-marginal, proglacial, glacimarine). We describe the terrestrial and submarine marginal zones separately to highlight the similarities and contrasts between landform assemblages in different environments.

Glacier ice and debris covered glacier ice

The main tongue of Hansbreen is densely crevassed at the active calving front, and similarly crevassed at the confluence zone between Tuvbreen and the main trunk (Figs 1 and 2). The dominant crevasse pattern is transverse with additional sigmoidal crevasses near the confluence zone. A dense network of crevasses with different orientations and crevasse traces (healed crevasses) can be observed in the eastern lateral zone of Hansbreen, including the land-terminating part, which transitions into the ice-cored hummocky moraine. The extensively crevassed central and eastern parts of Hansbreen contrast with the almost uncrevassed surfaces of Tuvbreen and Fuglebreen, which are dominated by crevasse traces and exhibit a few supraglacial streams and moulins.

Two medial moraines can be traced on the western part of the glacier (Figs 1 and 2). The medial moraine between the main trunk of Hansbreen and Tuvbreen takes the form of a wide belt of highly dispersed debris a few centimetres thick, with fine clasts of metamorphic rocks from the nunatak Tuva. Snow patches partially mask a scattered medial moraine between Tuvbreen and Fuglebreen composed of fine-grained, homogeneous debris sourced from the metamorphic rocks of the Vesletuva mountain. We interpret the former as an ice-stream interaction medial moraine and the latter as an ablation-dominant moraine.

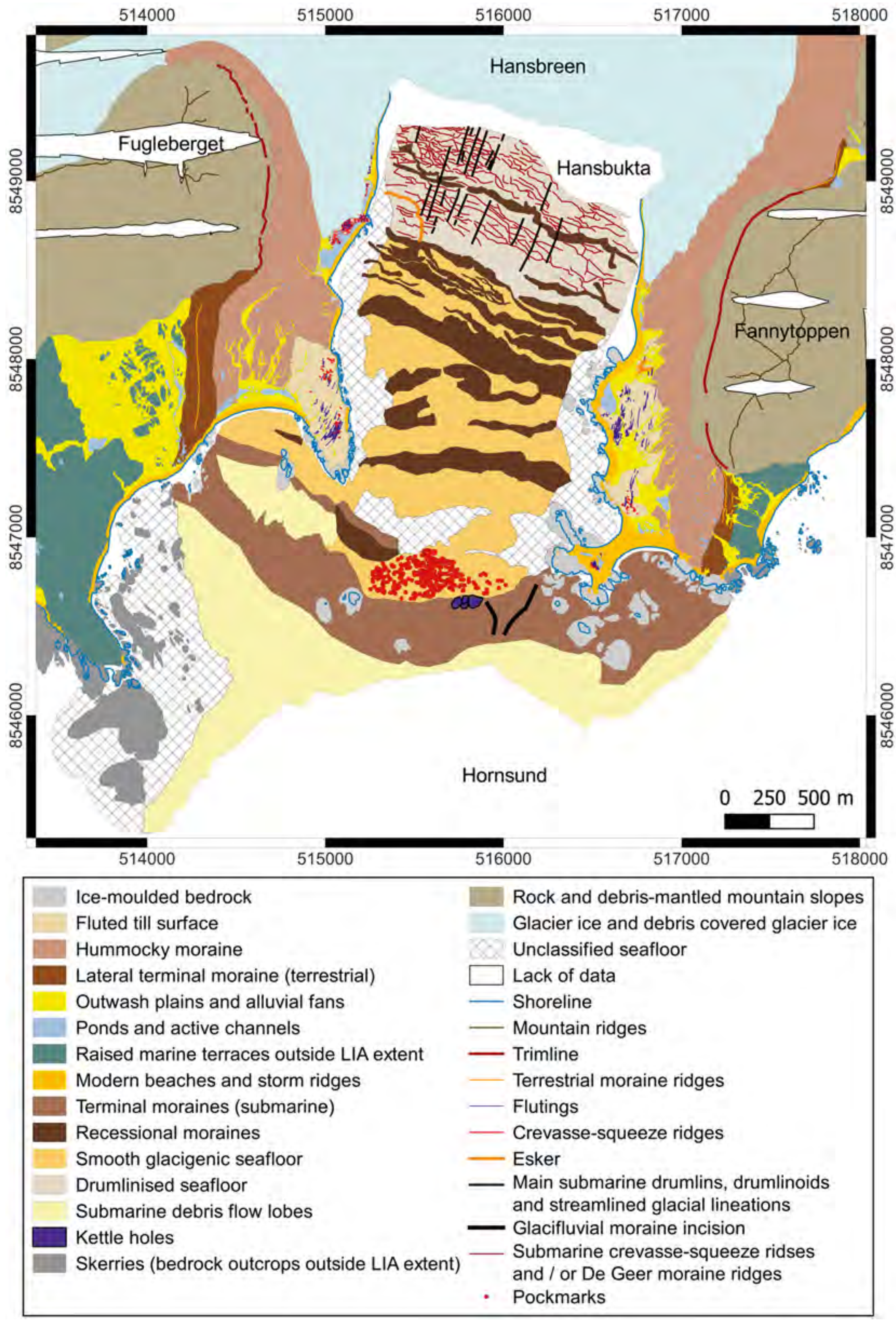

Figure 3. Geomorphological map of the forefield of Hansbreen. Glacier extent on 22 June 2020.

Terrestrial forefield

Ice-moulded bedrock: Ice-moulded bedrock is exposed on abundant glacially eroded skerries and capes in Hansbukta and Isbjørnhamna, which often take the form of roches moutonnées (Fig. 3). The most prominent of these features is the Baranowski Peninsula, which is covered by a thin, discontinuous layer of fluted till with numerous bedrock outcrops of amphibolites. The surface of the peninsula is streamlined with minor roches moutonnées and rock drumlins (Fig. 4a). Similarly, streamlined bedrock with a fluted till surface occurs at the foot of Fannytoppen, across Hansbukta from the Baranowski Peninsula (Fig. 4b). A large, 9.5 m high roche moutonné, partially draped with a thin layer of fluted till is located in the north-western forefield near the glacier terminus (Figs 5a and c). In the south-eastern forefield, ice-moulded bedrock is also represented by glacio-isostatically uplifted marine abrasive terraces and sea stacks covered with till.

Fluted till surface: Ice-moulded bedrock is strewn with a thin layer of coarse-grained, matrix-supported diamicton interpreted

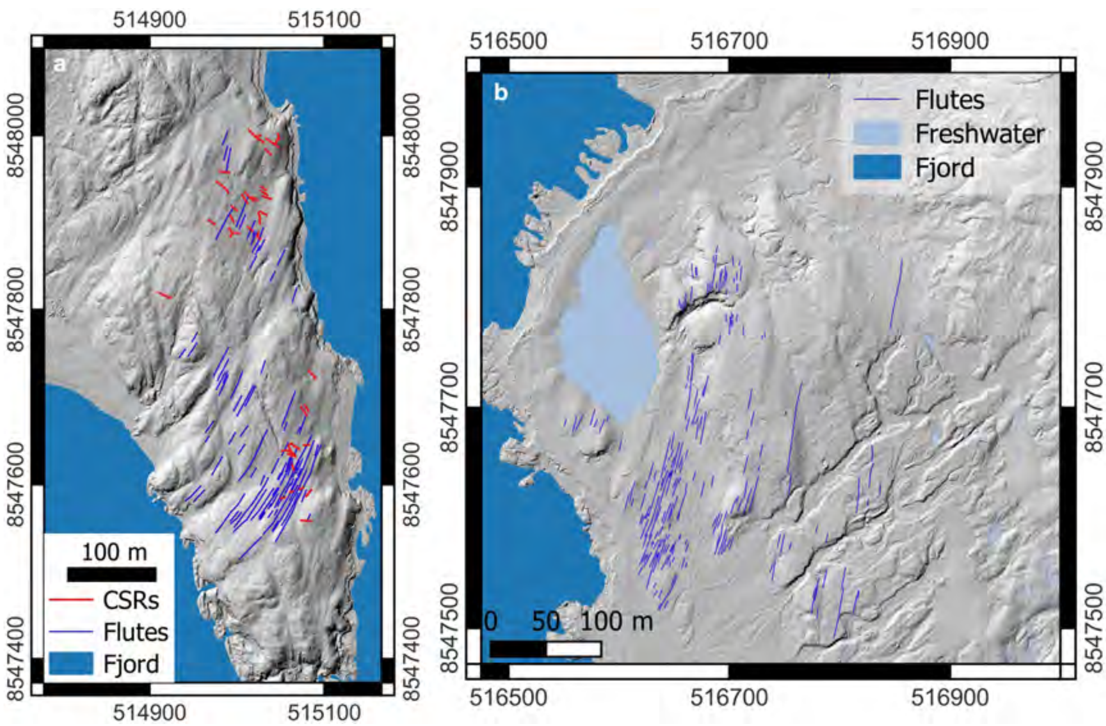

Figure 4. Streamlined topography of (a) the Baranowski Peninsula and (b) at the foot of Fannytoppen with parallel-sided flutings on a thin layer of till. Note CSRs transverse and oblique to flutes on the Baranowski Peninsula. Shaded relief maps after Błaszczyk and others (2022).

as subglacial traction till and a discontinuous layer of supraglacial diamicton of subglacial origin with similar properties (Skolasińska and others, 2016). The clasts are sub-angular to sub-rounded, ranging from gravels to boulders up to 2 m in diameter. The total thickness of diamictons is usually less than 0.5–1 m (Rachlewicz and Szczuciński, 2000).

The till surface is densely fluted, except in areas reworked by meltwater streams, where only the most prominent flutes can be recognized. Flutes are low, flow-parallel ridges composed of till similar to the till plain, but with significantly smaller clasts. Their formation is connected with infilling of till into a subglacial cavity in the lee-side of a boulder (e.g. Boulton, 1976; Benn, 1994; Ives and Iverson, 2019). Flutings concentrate in four spatial clusters: (1) the streamlined topography of the Baranowski Peninsula (Fig. 4), (2) the recently exposed north-western part of the forefield, at the foot of Fugleberget (Fig. 5), (3) raised marine terraces at the foot of Fannytoppen (Fig. 4) and (4) remnants of till plain on Oseanograftangen (Fig. 6). Most of the flutings are parallel-sided and up to 84 m long with nearly constant width between 0.3 and 2.4 m and height below 0.3 m, commonly with a boulder lodged on the stoss-side of the flute. There is a second group of short tapering flutes up to 14 m long, with boulders embedded at their heads and decreasing width and height in a downstream direction. The assemblages of long flutings associated with CSRs, which can be observed in the Hansbreen forefield, are vital components of the surging glacier landsystems (e.g. Evans and Rea, 1999, 2003; Christoffersen and others, 2005; Benn and Evans, 2010; Aradóttir and others, 2019; Ives and Iverson, 2019).

Crevasse-squeeze ridges (CSRs): Low, diamicton ridges oriented transverse or oblique to ice-flow direction and superimposed on flutes are interpreted as CSRs. CSRs are composed of the same till as flutings and their formation involves till infilling of basal crevasses that have opened during a surge and subsequent emergence of ridges from stagnating ice during the quiescent phase (e.g. Boulton and others, 1996; Rea and Evans, 2011; Farnsworth and others, 2016; Ben-Yehoshua and others, 2023). The landforms are a key characteristic of the geomorphological record produced by surging glaciers and have been reported in the forefields of numerous glaciers in Svalbard with both confirmed and undocumented surge histories (e.g. Heintz, 1953; Boulton and others, 1996; Glasser and others, 1998; Ottesen and Dowdeswell, 2006; Farnsworth and others, 2016; Ottesen and others, 2017; Flink and Noormets, 2018; Aradóttir and others, 2019). The morphology of CSRs in the forefield of Hansbreen ranges from distinct, intersecting ridges c. 0.5 m high to remnants of ridges or mounds and sediment trails reflecting the characteristic criss-cross pattern of CSRs. A network of well-defined cross-cutting ridges c. 0.5 m high, up to 3.5 m wide and up to 50 m long that overlay dense flutes can be seen emerging from the downwasting glacier snout in the northwestern part of the forefield (Fig. 5). The most prominent ridges approach the height of 0.8 m (Fig. 5d). In contrast, CSRs on the Baranowski Peninsula appear as indistinct ridges in the field and are best identified on the orthophotomaps. However, in the 1980s they were visible as abundant, distinct diamicton ridges transverse or oblique to underlying flutes (Fig. 7). In the eastern forefield, CSRs occur less frequently and are mostly individual diamicton ridges and mounds 6–40 m long and 0.3–0.5 m high overprinted on highly degraded flutes (Figs 6 and 8). The ridges are located among numerous cross-cutting diamicton trails a few centimetres high, which mimic the networks of CSRs and flutings. Similar features interpreted as the remains of CSRs were described in western Svalbard by Ben-Yehoshua and others (2023). In the southernmost forefield, transverse and oblique CSRs are superimposed on fluted till draped on two roches moutonnées (Fig. 6). Their morphology ranges from distinct, short ridges and mounds approaching 0.3–0.5 m in height, to degraded, intersecting ridges a few centimetres high taking the form of diamicton trails.

Eskers: Low, locally eroded sinuous eskers are visible in the eastern forefield on the till plain with fluvial overprinting. The ridges are 70–90 m long, 1–3 m wide, up to 0.5 m high and dissected by meltwater channels. They can be recognized by their surface of compact, sub-angular to rounded clasts ranging from fine gravels to 30 cm boulders with absent finer fractions. Based

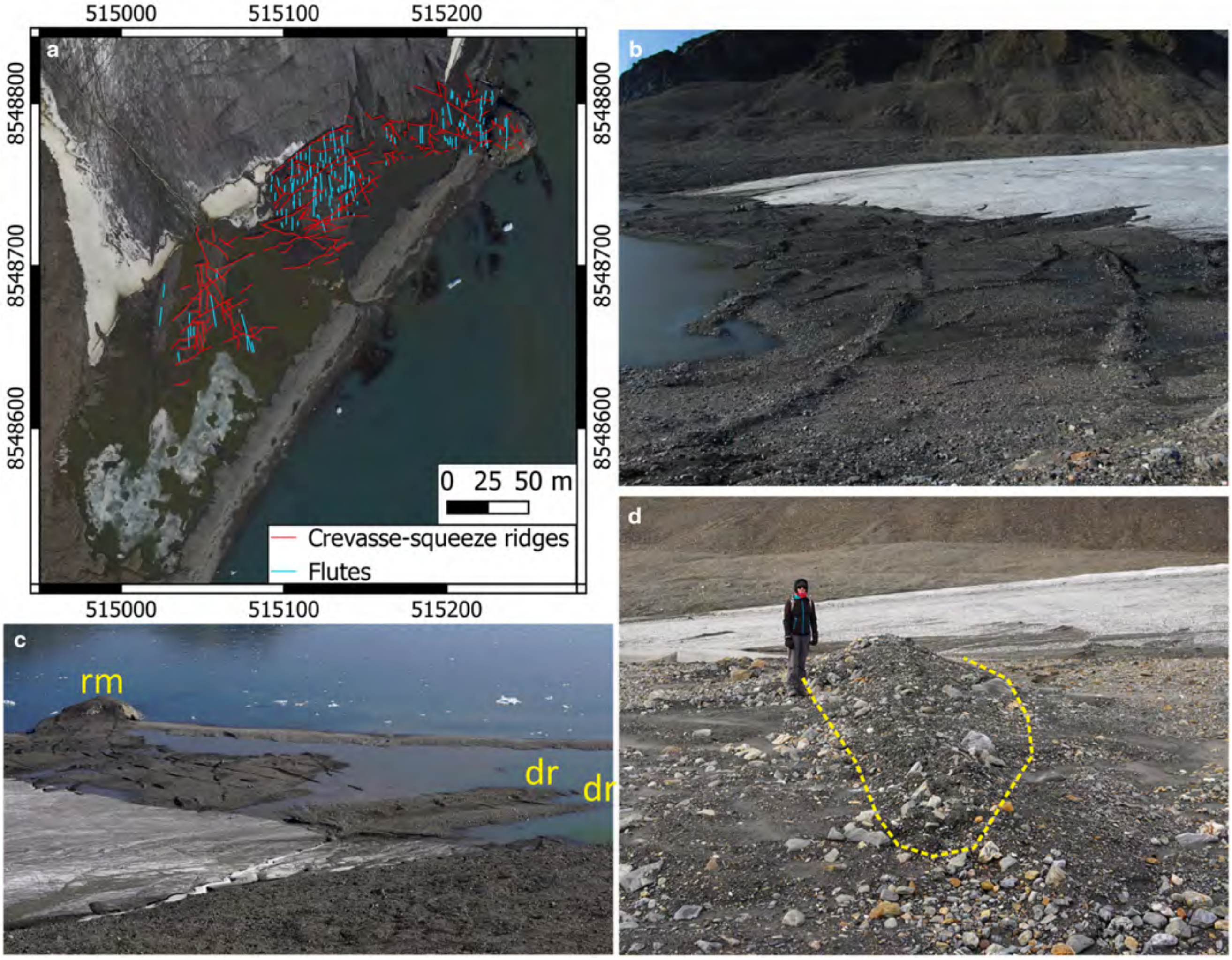

Figure 5. Fluted till surface with CSRs at the foot of Fugleberget in the north-western part of the forefield. (a) Overview of the flutings and CSRs networks on the orthophotomap from 2020 (Błaszczyk and others, 2022). (b) Flutings and CSRs emerging from downwasting glacier ice in August 2020. Hummocky moraine and trimline on the Fugleberget slopes in the background. (c) The same area in September 2023. Note two drumlins (dr) and a roche moutonné (rm) overprinted with flutings and well-developed CSRs. (d) A prominent CSR c. 0.8 m high with the extent marked with the dashed line. (b–d) Photos A. Osika.

on their sinuous morphology, we interpret them as landforms developed in stagnant ice during the quiescent phase.

Hummocky moraine: Hummocky moraine occurs on the ice-proximal side of the lateral terminal moraine (Fig. 3). In the western part of the forefield, it takes the form of low, ice-cored, aligned hummocks, depressions and ponds, transitioning to the north into regular, ice-cored, low-amplitude linear ridges, interpreted as controlled moraine (Evans, 2009). The formation of hummocky and controlled moraines involves entrainment, transport and melt-out of debris on a stagnant glacier snout, leading to the accumulation of supraglacial debris cover (Boulton, 1968; Rachlewicz and Szczuciński, 2000; Schomacker and Kjær, 2008; Evans, 2009; Ewertowski and others, 2011). In controlled moraine, the supraglacial debris retains distinct linearity reflecting the inherited pattern of englacial debris concentrations (Evans, 2009). In the eastern forefield, hummocky moraine occurs as a complex of irregular, partly ice-cored, low-amplitude mounds and depressions at the proximal zone of the lateral terminal moraine (Fig. 8). The second assemblage is a complex of low, recently exposed ice-cored hummocky moraines adjacent to the slopes of Fannytoppen and Flatryggen. The surficial sediments are clast-rich, matrix-supported diamictons with large clasts of metamorphic and sedimentary rocks (Skolasińska and others, 2016). Abundant fragments of marine mollusc shells can be found up to the Flatpasset saddle between Fannytoppen and Flatryggen at c. 150 m a.s.l. (Fig. 2). The development of hummocky moraines requires entrainment and transport of large volumes of debris, which is particularly effective and widespread during the active phase of surging (Evans and Rea, 1999; Lovell and others, 2015a). Therefore, they are an important component of the surging glacier landsystems, although they are not independently diagnostic of surge-type behaviour (Evans and Rea, 2003).

Lateral terminal moraine: The outer, most prominent moraine belts are interpreted as lateral terminal moraines that extend underwater as a frontal terminal moraine (Fig. 3). In the western forefield, the lateral terminal moraine occurs as a conspicuous controlled moraine belt with sub-parallel units reflecting the former englacial structures in the glacier snout (cf. Evans, 2009). The outer moraine belt is 1130 m long, up to 200 m wide, 30 m high and ice-cored as evidenced by electrical resistivity tomography (Glazer and others, 2020), but the internal structure is unknown. The transverse profile is asymmetric with a steeper distal slope. In the south-eastern forefield, the lateral terminal moraine takes the form of two arcuate ridges 570 and 580 m long, 30–50 m wide and up to 8 m high, dissected by proglacial channels. The ridges are probably ice-cored based on the evidence of ongoing de-icing processes. The relief of their southern margins is subdued and resembles the adjacent hummocky moraine. In turn, the lateral terminal moraine on Flatpasset (Fig. 8c) occurs as a distinct,

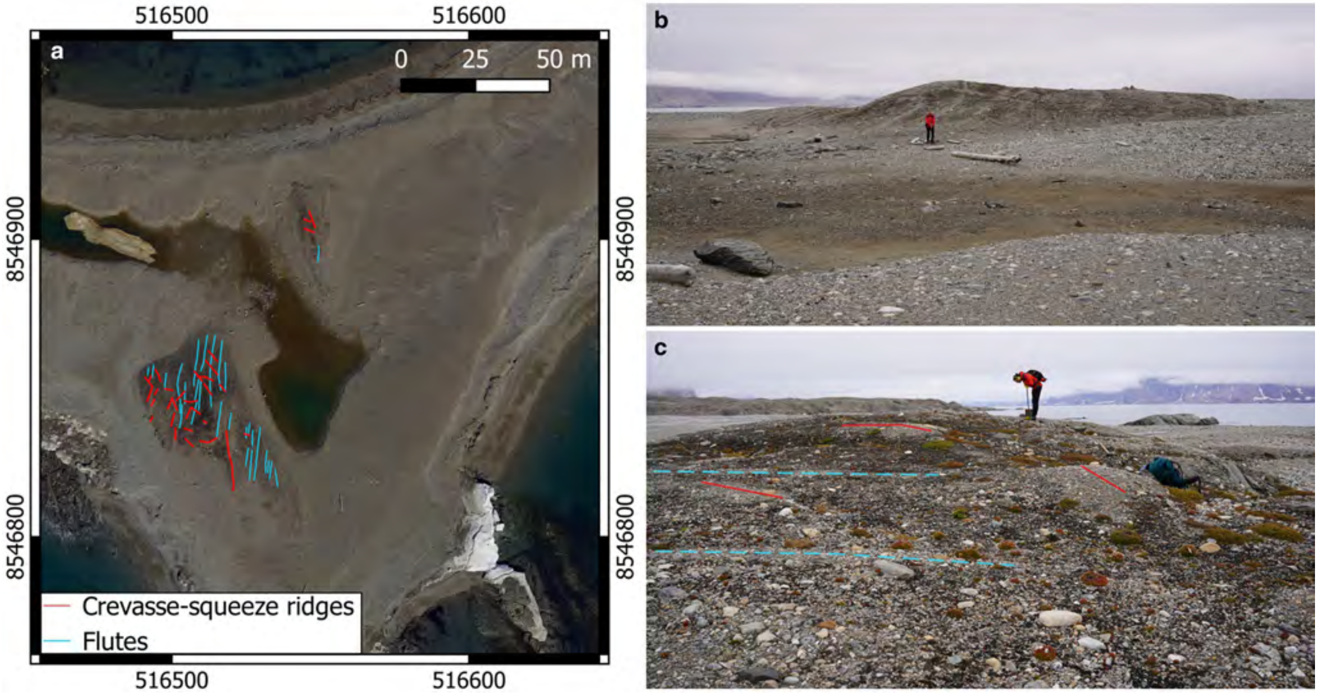

Figure 6. (a, b) Roches moutonnées on Oseanograftangen overprinted with fluted till and CSRs. Note the extensive beaches and storm ridges around the hills and remaining of the plain south of the lake, indicating the flutes and CSRs reworking by coastal processes. (c) Levelled flutes (parallel; blue lines) and CSRs (oblique and transverse; red lines). The latter take the form of low ridges (0.3–0.5 m) or diamicton trails a few centimetres high.

arcuate ridge 420 m long, up to 30 m wide, 6 m high and probably ice-cored. The northern part merges with ice-cored hummocky moraine, whereas the south-western part is associated with a trimline on the adjacent Fannytoppen slope. The lateral terminal moraines are composed of clast-rich diamicton with sub-angular to sub-rounded, and occasionally angular large clasts of metamorphic and sedimentary rocks. We interpret them as the outer and oldest ridges of controlled moraines, formed by debris entrainment during glacier advance and supraglacial melt-out of sediments from stagnating ice, preserving the ice core from degradation (cf. Evans, 2009).

Trimline: Trimlines can be traced on the eastern and south-eastern slopes of Fugleberget at 174–70 m a.s.l. and the western slopes of Fannytoppen at 173–32 m a.s.l. (Figs 3 and 8). We interpret them as the maximum thickness of Hansbreen during the surge (cf. Yde and others, 2019). The imprint is discontinuous due to paraglacial reworking and formation of talus cones. A gradual elevation decline corresponds to widening and lateral spread-out of the glacier tongue. Well-developed trimlines from the LIA are typical for Svalbard glaciers and their formation and distribution are primarily controlled by bedrock erodibility (Rootes and Clark, 2022). According to their study, erosional trimlines are slightly more common among surging and tidewater glaciers in Svalbard compared to land-terminating glaciers or glaciers with no known surge history.

Submarine forefield

Drumlinized seafloor and streamlined glacial lineations: The drumlinized seafloor comprises c. 750 m wide zone in the proximal part of the submarine forefield, taking the form of streamlined topography with drumlinoids, low-amplitude streamlined ridges and grooves (Figs 2 and 3). In the central zone, an oval, symmetrical ridge 260 m long and 90 m wide, interpreted as a

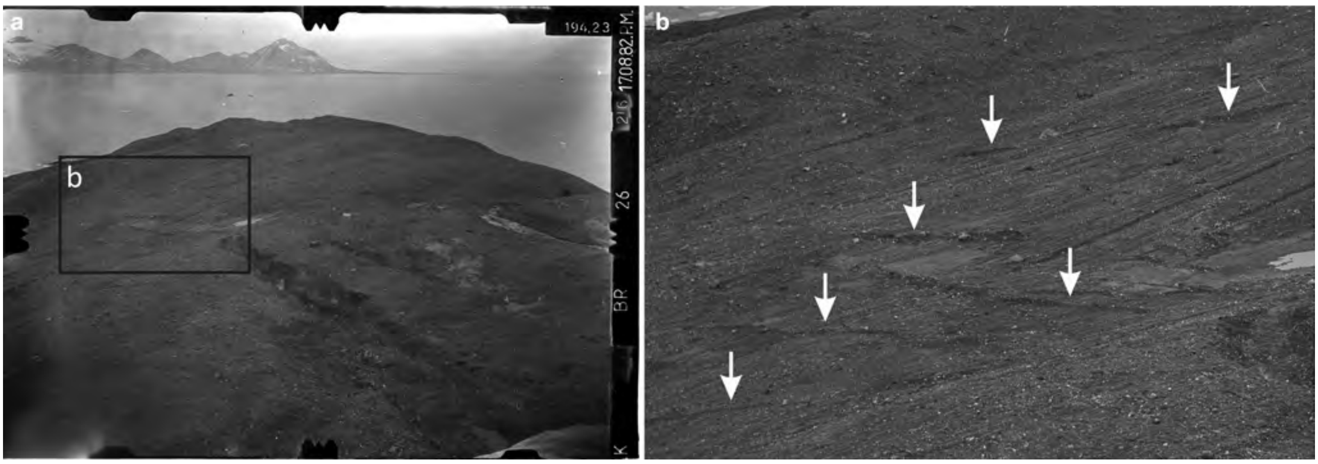

Figure 7. (a, b) Terrestrial photogrammetric photograph of the Baranowski Peninsula from 1982. Note long, parallel-sided flutings and low CSRs (white arrows) oblique and transverse to the flutes. Today, CSRs in this site are sparse and have an indistinct appearance in the field.

https://doi.org/10.1017/aog.2024.32 Published online by Cambridge University Press

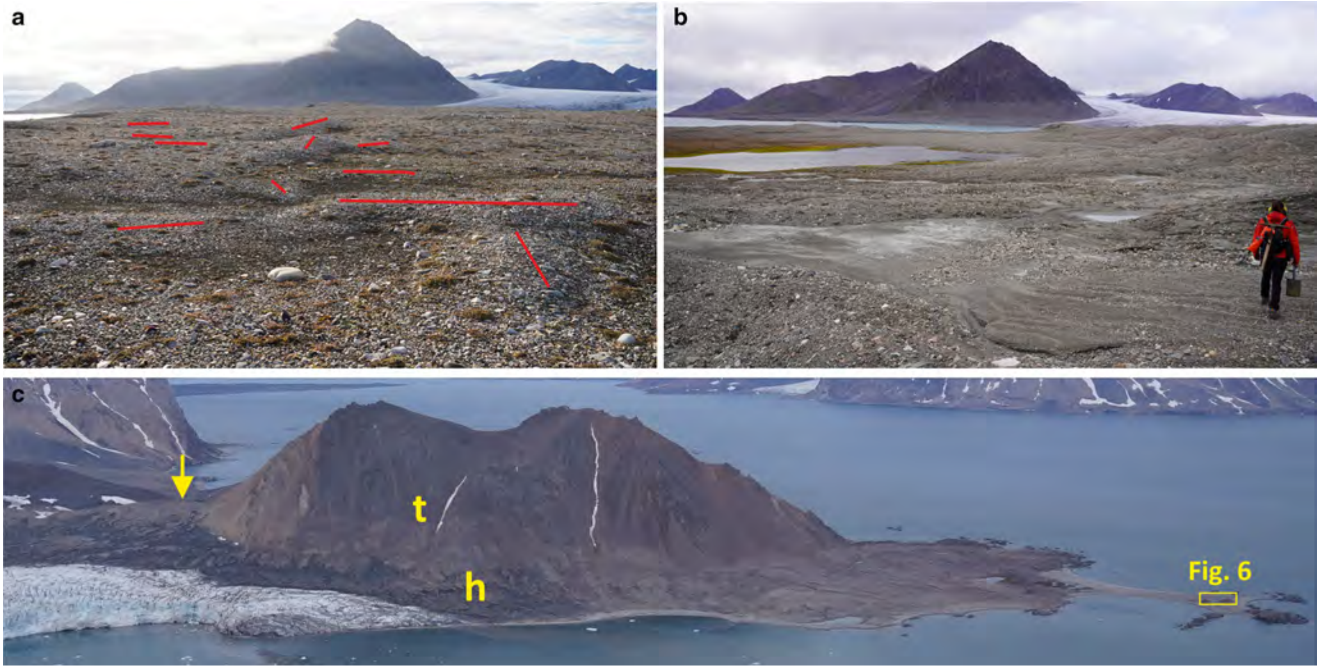

Figure 8. (a) Low, obliterated CSRs c. 0.3–0.5 m high among sediment trails reflecting the cross-cutting pattern of CSRs and flutings at the foot of Fannytoppen. (b) Ice-cored hummocky moraine in this area. In the background, hummocky moraine and trimline on the slopes of Fugleberget. (c) Hummocky moraine (h) and trimline (t) on the Fannytoppen slopes. The arrow marks the lateral terminal moraine and the rectangle illustrates the location of the roches moutonnées with CSRs on Oseanograftangen. (a–c) Photos A. Osika.

drumlin, can be observed between a similar ridge with an indistinct appearance and a prominent drumlinoid 190 m wide. In the western part, an assemblage of distinct, flow-parallel, low-amplitude ridges and grooves up to 430 m long can be observed on the slopes of an overdeepening that extends to a depth of 94 m. The ridges are up to 5 m high, 30 m wide and the distance between their crests is usually 40–60 m. We interpret these as streamlined glacial lineations, which indicate high velocities during glacier advance and are a key characteristic of the submarine forefields of tidewater surge-type glaciers in Svalbard (e.g. Flink and others, 2015, 2018; Dowdeswell and Ottesen, 2016; Ottesen and others, 2017; Streuff and others, 2018). Based on their morphology and elongation ratios, the ridges represent a continuum between elongated drumlins and mega-scale glacial lineation, indicating subglacial streamlining (MSGL; Stokes and Clark, 2002; Spagnolo and others, 2014).

Esker: A single, sinusoidal ridge in the inner part of the forefield, which can be traced to an R channel in the nearby land-terminating part of the glacier is interpreted as an esker, resulting from the infilling of the subglacial conduit with sediments during decreasing meltwater discharge (Ottesen and others, 2008). The ridge is 390 m long, up to 10 m wide, 2 m high and faces east for the first 185 m before turning south. The distinct morphology of the first segments contrasts with blurred distal part c. 90 m long ending at the recessional moraine. Eskers have been documented in the forefields of many tidewater glaciers in Svalbard and, in the case of surge-type glaciers, inferred to have developed after surge termination (Ottesen and others, 2008; Dowdeswell and Ottesen, 2016; Flink and others, 2018; Noormets and others, 2021).

Small moraine ridges – CSRs and / or De Geer moraines: Small ridges oriented subparallel to the calving front and overprinting the flow-parallel ridges of streamlined bedforms can be traced across the inner part of Hansbukta. The transverse, locally branching and cross-cutting ridges approach 10–20 m in width and 3 m in height with spacing of 15–50 m. Their spatial pattern and abundance compared with the number of winter glacier advances (Błaszczyk and others, 2021) and the proximity of CSRs in the terrestrial forefield (Fig. 3) imply that the ridges are probably submarine CSRs formed during a surge (e.g. Ottesen and others, 2008; Dowdeswell and Ottesen, 2016). Based on a similar appearance, some ridges could be De Geer moraines, also known as small annual retreat moraines or push moraines (e.g. Streuff and others, 2015; Flink and Noormets, 2018). The formation of De Geer moraines involves the pushing of sediments during seasonal winter advances (Boulton, 1986; Ottesen and Dowdeswell, 2006). The landforms are widespread in the proximal but not visible in the central or outer parts of the forefield, possibly because they have been buried by sediments from meltwater plumes.

Recessional moraines: Several distinct transverse ridges, larger than those described above, can be observed primarily in the central and outer parts of the forefield. The ridges are oriented subparallel to the calving front, up to 10–15 m high and partly buried in glacimarine sediments (Ćwiąkała and others, 2018). In the proximal forefield, a chain of crescent ridges c. 5 m high corresponds to several winter advances to a similar position in 2013–2015. The most conspicuous ridges correspond with glacier advances in 1957–1959, 1973–1977 and during the 1990s (Jania, 1998; Ćwiąkała and others, 2018; Błaszczyk and others, 2021). We interpret the ridges as recessional moraines associated with minor readvances interrupting the overall glacier retreat (Robinson and Dowdeswell, 2011; Flink and others, 2015; Streuff and others, 2018).

Terminal moraines: Two terminal moraines can be observed in the submarine forefield of Hansbreen, each of them associated with a debris flow lobe. The outermost terminal moraine takes the form of a large, crescent, transverse ridge beyond Hansbukta, emerging onshore as the ice-cored lateral terminal moraines and marking the LIA maximum of Hansbreen (Figs 2 and 3). The total length of the LIA terminal moraine approaches 5100 m with a submarine part of c. 3300 m. The arcuate form indicates the radial splaying of the glacier beyond the constraining mountain ridges. The indentation in the distal flank is related to the abrupt break in the slope into a deeper fjord basin, which has

https://doi.org/10.1017/aog.2024.32 Published online by Cambridge University Press

prevented the full development of the moraine (cf. Dowdeswell and others, 2020). The outermost terminal moraine of Hansbreen was described in detail by Ćwiąkała and others (2018). The submarine ridge is plain-topped, c. 13 m high, with clear margins in the central, but extensively blurred in the lateral parts and located in a water depth of 10–25 m. Rock outcrops, fields of megaripples, iceberg pits and ploughmarks can be identified on the moraine surface (Ćwiąkała and others, 2018). On the proximal flank, four oval, flat-floored depressions 28–55 m in diameter and 2 m deep are interpreted as kettle holes. Near Oseanograftangen, the moraine surface is eroded by a channel-like feature interpreted as a glacifluvial incision, 2–7 m deep, 160–250 m wide, and with blurred margins reworked by sediment flows (Figs 2 and 3). In Isbjørnhamna, the outermost terminal moraine is subdued and overprinted with a debris flow lobe associated with an inner terminal moraine.

The inner terminal moraine occurs as transverse ridge segments up to 3 m high, semi-parallel to the outer terminal moraine and corresponding to the glacier extent in 1938 (Figs 2 and 3). We imply that terminal moraines have been formed by surges based on their resemblance to surge terminal moraines of Svalbard tidewater glaciers, in particular the association with well-developed debris flow lobes (e.g. Flink and others, 2015; Burton and others, 2016; Noormets and others, 2021). The morphology of the inner terminal moraine of Hansbreen is similar to the moraines of Tunabreen or Blomstrandbreen, corresponding to surges in the 20th century (Flink and others, 2015; Burton and others, 2016). In each site, the terminal moraines of subsequent surges are significantly smaller than the LIA terminal moraine and often discontinuous across the fjord. The formation of submarine terminal moraines involves thrusting and pushing of sediments during glacier advances as well as depositional processes during glacier stillstand, which may be long-lasting on a sill (e.g. Benn and Evans, 2010; Ottesen and others, 2017; Lovell and others, 2018).

Debris flow lobes: We identified two glacigenic debris flow lobes in the forefield of Hansbreen. The outermost lobe overprints the distal flank of the large terminal moraine, the adjacent flat-floored area of Isbjørnhamna and a steep northern side of the Hornsund Fjord beyond the outermost terminal moraine (Figs 2 and 3). In Isbjørnhamna, the lobe is flat-surfaced with clear outer margins, several rock outcrops and small, circular depressions, which are probably iceberg pits. Towards the break in slope into a deeper part of Hornsund, the lobe surface becomes hummocky with abundant iceberg pits, ploughmarks and minor sediment slides and flows. Similar topography can be observed beyond the central and eastern parts of the outermost terminal moraine with several prominent downslope-oriented flow structures. The ice-proximal margins of the moraine are clear, apart from the area adjacent to the moraine incision affected by mass-wasting processes. The second debris flow lobe is associated with the inner terminal moraine and superimposed on the top of the outermost, large terminal moraine in Isbjørnhamna. The landform has distinct margins and flow direction to the south-west (Figs 2 and 3). According to published backscattering data, the sediment flow lobes are composed of fine-grained or mixed material contrasting with coarse-grained surficial sediments of the terminal moraines (Ćwiąkała and others, 2018). Glacigenic debris flow lobes result from the bulldozing or pushing of seafloor sediments in front of the advancing terminus during surging and subsequent slope failure on the distal side of the glaciotectonic moraine (Dowdeswell and Ottesen, 2016; Lovell and others, 2018). The steep topography beyond the outermost terminal moraine has presumably controlled the development of the associated debris flow lobe, as they usually take the form of extensive gently sloped lobes in flat-floored areas (e.g. Dowdeswell and others, 2016; Flink and others, 2018; Streuff and others, 2018).

Smooth glacigenic seafloor: Smooth seafloor with flat-floored depressions separated by transverse moraine ridges comprises a major part of the submarine forefield (Figs 2 and 3). The maximum depth of depressions increases towards the current glacier front. We interpret these as glacially overdeepened basins filled with sediments from meltwater plumes, previously described by Tegowski and others (2016) and Ćwiąkała and others (2018). The basin-fill sediments partly bury the moraine ridges from minor readvances of Hansbreen. The sediment thickness ranges from 10 m in the central to 25 m in the southernmost part of the submarine forefield and the estimated mean sediment accumulation rate in particular basins ranged between 0.25 and 0.4 m a^{-1} (Ćwiąkała and others, 2018). In the topography of the smooth seafloor, Ćwiąkała and others (2018) documented fields of megaripples, pockmarks, iceberg pits and ploughmarks.

Pockmarks: Pockmarks occur in the southernmost part of the forefield as small, circular depressions with diameters and depths approaching 15 and 1 m, respectively. The distribution of pockmarks in the basin adjacent to the frontal terminal moraine was documented by Ćwiąkała and others (2018), who suggested their possible origin as gas migration along faults or seepage of pore water due to very high sedimentation rate. Widespread craters and mounds related to methane release develop in the Arctic seabed after deglaciation (Andreassen and others, 2017). Apart from geological factors (e.g. Weniger and others, 2019), pockmarks in Svalbard fjords may form as a result of water escape from rapidly deposited glacigenic debris flow lobes related to surging (Ottesen and others, 2008; Forwick and others, 2009). Pockmarks in Hansbukta may be of similar origin considering the high sediment accumulation rate in the basins (cf. smooth glacigenic seafloor; Ćwiąkała and others, 2018). In addition, we infer that their formation may be associated with the burying of organic-rich sediments during glacier advance.

Hansbreen on archival maps and photographs (1872–1936)

Historical maps

The first published sketch map of the Hansbreen snout (scale 1: 200 000) was prepared in 1872 during the Austro-Hungarian North Pole Expedition (Peterman, 1874). The glacier was also presented on a 1: 200 000 map from the Russian–Swedish expedition in 1899–1901 (Wassiliew, 1925). The frontal position can be traced on a 1: 100 000 map based on reconnaissance photogrammetric surveys of the Hornsund area in 1918 during the Norwegian expeditions in 1917–1921 (Fig. 9a; Hoel, 1929). In these maps, Hansbreen occupies Hansbukta and the north-eastern part of Isbjørnhamna, covering the Baranowski Peninsula and Oseanograftangen. However, the maps are not detailed enough to accurately assess the extent and possible fluctuations of the glacier. Hence, our study is primarily based on archival photographs documenting the extent and surface morphology of Hansbreen.

Archival photographs

Unique photographic documentation of Hansbreen from the late 19th and early 20th centuries was collected by the Austro-Hungarian expedition in 1872 and the Norwegian expedition in 1918. In 1936, Hansbreen was documented on oblique aerial photographs during the Norwegian mapping campaign of Svalbard (Luncke, 1936). The photographs provide data on the glacier extent, surface morphology, ice structure in the ice cliff and geomorphological features, which shed light on the glacier dynamics. In addition, they are a vital source of data on geomorphological processes.

1872: Photographs from the Austro-Hungarian expedition in 1872 documented the terrestrial margins of Hansbreen and part

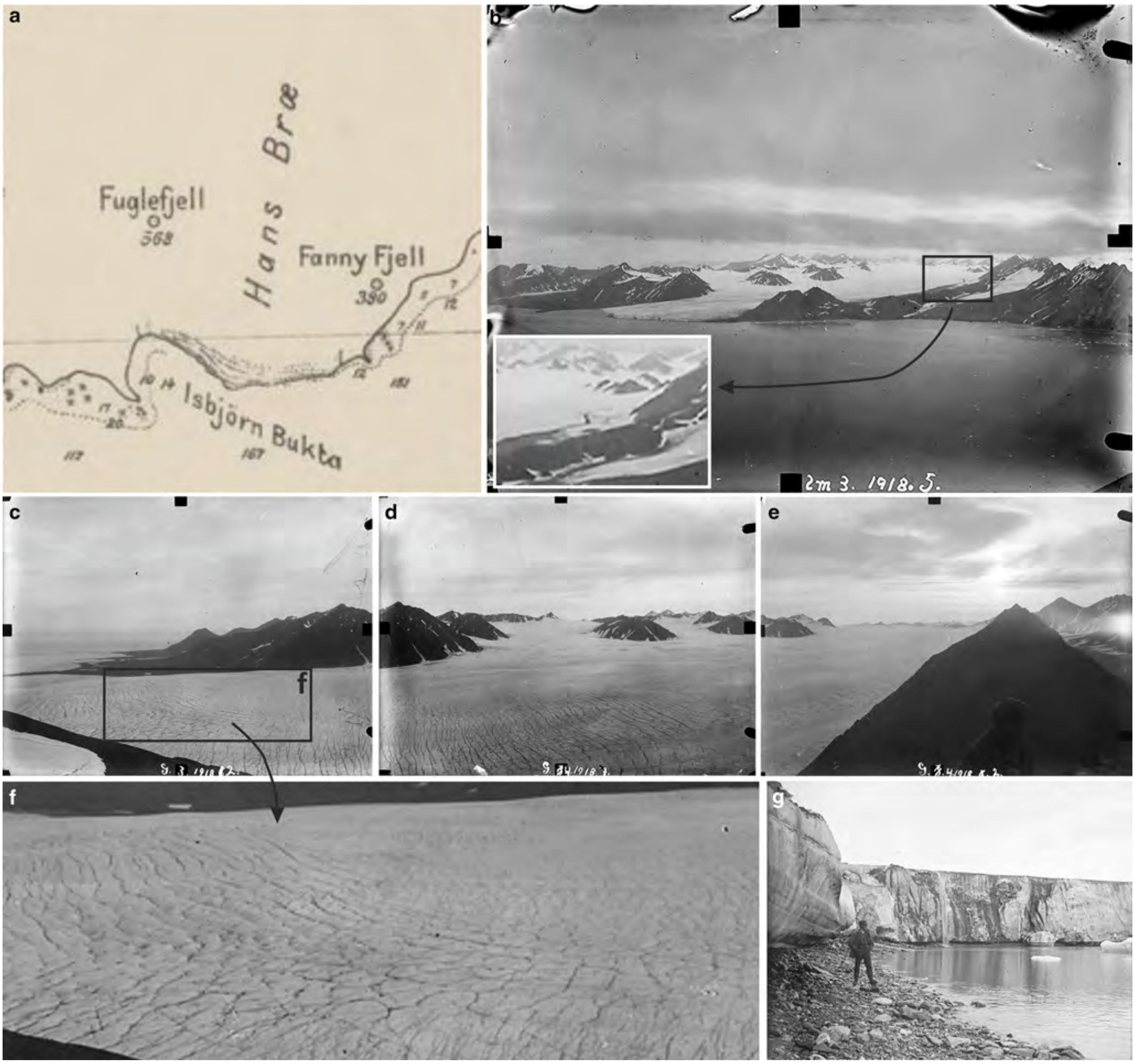

Figure 9. (a) Hansbreen on a 1: 100 000 map 'Spitsbergens Kyst, Hornsund til Dunder Bay' based on the Norwegian Spitsbergen expeditions in 1917–1921 with photogrammetric measurements in Hornsund in 1918 (public domain, https://data.npolar.no). (b–g) Terrestrial photogrammetric documentation of Hansbreen from 1918. (b) The radially expanded glacier snout after surge advance. Note a folded medial moraine in the eastern part of the glacier. (c–f) A complex network of narrow, cross-cutting crevasses and crevasse traces documented from Fannytoppen. (g) The glacier front in Isbjørnhamna. Note a waterfall from an active supraglacial channel in the background. (b) © Olaf Holtedahl, Norsk Polarinstitutt (modified), (c–f) © Jørgen Gløersen, Norsk Polarinstitutt (modified), (g) © Adolf Hoel, Norsk Polarinstitutt (cropped and modified).

of the calving front. In the western terrestrial zone, the glacial terminus had already reached its LIA maximum position (Fig. 10a). The marine-terminating zone was densely and chaotically crevassed with a conspicuous surface bulge (Fig. 10b). At the foot of Fannytoppen, the terrestrial margin of Hansbreen terminated as a steep ice cliff, exposing inclined and folded debris layers. The photograph also documented top-down and bottom-up crevasses and a convex surface profile (Figs 10c and d). In this part of the glacier, the terminus had not yet reached the LIA maximum, today marked by the lateral terminal moraine adjacent to rocky raised marine terraces. The proglacial outwash plains mapped outside the terminal moraine were also absent in this photograph (Figs 3 and 10c).

1918: The Norwegian Spitsbergen expedition in 1918, led by Adolf Hoel and Sverre Røvig, conducted reconnaissance photogrammetric measurements in Hornsund. The comprehensive documentation, including photogrammetric photos, overlays the entire glacier. At that time, the glacier front was anchored on the small Hansholmane islands and Oseanograftangen (Figs 9a and b). The extent of the terrestrial margins was similar to that of 1872, but the calving front positions are difficult to compare due to insufficient data from the previous photographs. Glacier-free unnamed islands within the terminal moraine belt suggest a slight retreat from the maximum LIA position. A photograph from the southern side of Hornsund revealed a folded median moraine between Hansbreen and one of the eastern tributaries (Fig. 9b). The two black features on the calving front can be observed in other photographs and could be interpreted as the mouths of subglacial channels. The photos from Fannytoppen documented a dense, complex network of intersecting crevasses and crevasse traces extending high up on the main trunk of the glacier (Figs 9c–f). Most crevasses were narrow, which allowed

https://doi.org/10.1017/aog.2024.32 Published online by Cambridge University Press

Figure 10. Photographs of Hansbreen from the Austro-Hungarian expedition in 1872. (a) The western terrestrial margin of the glacier. (b) Crevassed marine-terminating zone with a conspicuous surface bulge. (c, d) The eastern terrestrial margin, where the glacier had not yet reached the maximum extent. Note folded and inclined debris layers, top-down and bottom-up crevasses exposed on the ice cliff and a convex surface profile of the glacier. © ÖNB Vienna: Image ID 00299043, 00480587 and 00444839 (cropped and modified).

the expedition to cross the glacier (Hoel, 1929). The photographs also documented a steep ice cliff in Isbjørnhamna with supra- and englacial sediments and a waterfall at the ice front (Fig. 9g). Compared to 1872, this part of the glacier had a smooth topography in 1918.

1936: By 1936, the glacier had retreated beyond Hansholmane, but the terminus was still anchored on Oseanograftangen and the Baranowski Peninsula (Fig. 11). The glacier front was relatively straight and slightly expanded in the central zone. The downwasting of the stagnant terrestrial margins had led to the development of the ice-cored moraine complexes. The lateral moraines of the eastern tributary glaciers had merged into a wide belt along the glacier margin. As a result, the folded moraine of the 1918 photo was no longer visible as it was probably squeezed to the eastern lateral moraine. The surface morphology was dominated by crevasse traces and wide transverse crevasses in the frontal zone. Some crevasse traces reflected the intersecting pattern of crevasses documented in 1918.

Discussion

Geomorphological records of surging

The forefield of Hansbreen with CSRs, fluted till plains, hummocky moraines, high trimlines, drumlinized seafloor, glacial lineations, De Geer moraines, terminal moraines with debris flow lobes and other components (Fig. 3) indicates at least one surge event. Such landform assemblages are consistent with surging glacier landsystem models in terrestrial and submarine environments (Evans and Rea, 1999, 2003; Ottesen and Dowdeswell, 2006; Ottesen and others, 2008, 2017; Flink and others, 2015; Aradóttir and others, 2019).

The key features diagnostic for the surges of Hansbreen are CSRs, glacial lineations and two glacitectonic terminal moraines with debris flow lobes. Terrestrial CSRs and flutings occur up to the southernmost part of field (Figs 2–8). In Svalbard, CSRs networks emerging from stagnating ice may be related to surge episodes from years to over a century ago (Lovell and others, 2015a; Farnsworth and others, 2016). CSRs and flutings in the terrestrial forefield of Hansbreen correspond with the submarine features. The rapid ice flow during the surge is evidenced by the streamlined glacial lineations (Figs 2 and 3; Ottesen and others, 2008, 2017; Streuff and others, 2018), although their absence would not preclude a surge event (Aradóttir and others, 2019). The submarine CSRs and glacial lineations appear only in the inner part of Hansbukta, but they might have been more widespread in the past and buried later with glacimarine sediments. A restricted extent or absence of CSRs on the fjord floor, but occurrence on land, were evidenced in the forefield of surge-type Blomstrandbreen (Burton and others, 2016; Farnsworth and others, 2016) and the glacial system of Trygghamna (Aradóttir

https://doi.org/10.1017/aog.2024.32 Published online by Cambridge University Press

Figure 11. Hansbreen in the oblique aerial photograph from 1936. © Norwegian Polar Institute.

and others, 2019). Hansbreen has not developed a terrestrial thrust-block moraine diagnostic of surging, but such landforms are not widespread in the lateral forefields of surge-type tidewater glaciers in Svalbard (Lønne, 2016; Lovell and Boston, 2017). The slightly curvilinear ridges of the lateral terminal moraines and the submarine large terminal moraine indicate the radial expansion of the glacier snout when entering the Hornsund Fjord (Figs 2, 3, 9). The occurrence of terrestrial CSRs up to the southernmost part of the forefield (Figs 3 and 6), the dimensions of the submarine terminal moraine and the occurrence of a debris flow lobe on its distal flank imply that the maximum LIA extent of Hansbreen was related to a surge. The lateral terminal moraine on the Flatpasset saddle (Figs 2 and 3) marks the glacier's attempt to pass the mountain ridge during this surge advance when the glacier entrained marine sediments with mollusc shells and deposited with diamicton up to 150 m a.s.l.

The inner terminal moraine with a debris flow lobe is the main evidence of a possible second surge. The lobe has overprinted the large terminal moraine and the flow direction of sediment was to the south-west, perpendicular to the inner moraine (Figs 2 and 3). The inner moraine corresponds to the frontal position of Hansbreen in 1938, which was similar or, in some parts, slightly more extensive than in 1936 (Fig. 2). The dimensions of the moraine and the sediment lobe are notably smaller than those from the LIA maximum. However, in Svalbard, surge terminal moraines from the 20th century tend to be less prominent than surge moraines from the LIA and may have similar morphology to recessional moraines (Burton and others, 2016). Surge end moraines of Tunabreen from 1930, 1971 and 2004 are much lower than the outermost moraine belt from the 1870s surge and only two surge moraines have adjacent debris flow lobes (Flink and others, 2015). The younger debris flow lobe of Hansbreen has similar dimensions to debris flow lobes on the outermost surge moraines of Blomstrandbreen (Streuff and others, 2015, 2022). This glacier has not developed debris flow lobes at all during the subsequent surges in the 20th century (Burton and others, 2016). The formation of the inner surge moraine of Hansbreen may have been limited by the scarce supply of sediment from resistant metamorphic rocks in the glacier basin that had been redeposited during the older surge. Low surge end moraines with small or without debris flow lobes may also reflect a short-active surge phase, which limits the sediment supply to the glacier terminus (Flink and others, 2015). In addition, most of the moraine ridges in the central and southern Hansbukta have been partly buried with glacimarine sediments, which mask their primary size. If the inner terminal moraine had a continuation across Hansbukta, it also might have been buried and subdued.

Historical records of surging

1872 – ongoing surge: The photographs of Hansbreen from the Austro-Hungarian expedition in 1872 reveal characteristic features of an active surge phase (Fig. 10). The glacier surface was densely crevassed with a conspicuous bulge, which we interpret as a surge front propagating downglacier (e.g. Sund and others, 2009; Lovell and Fleming, 2023). A surge bulge reflects the mass displacement from the reservoir area and builds up in a high friction zone near the glacier front (Haga and others, 2020). The ice thickness at the south-western margin corresponded to the trimline on edge between the eastern and southern slopes of Fugleberget (Fig. 2). Most of the southern slope is overprinted with talus cones and it was not possible to identify a clear trimline over there (Figs 2, 3, 10a). The vertical ice extent in 1872 was not documented on the other mountain slopes. The south-eastern margin of Hansbreen had a convex surface profile and a steep ice cliff with debris-rich structures (Figs 10c, d). Similar features are typical for the termini of surging glaciers (e.g. Lovell and others, 2015a; Ingólfsson and others, 2016; Sobota and others, 2016; Lovell and Fleming, 2023) and we suggest they fed the subsequent controlled moraines in this area (Fig. 3). The glacier extent in this area was smaller than marked by the LIA lateral terminal moraine. Hence, we imply that the surge was underway and the glacier was advancing to the maximum LIA position.

1918 – quiescent phase: Photographic documentation from the Norwegian Spitsbergen expedition in 1918 provides evidence for a glacier in the quiescent phase. The radially expanded snout was anchored on capes and small islands, and the glacier extent corresponded to the outermost submarine terminal moraine and

https://doi.org/10.1017/aog.2024.32 Published online by Cambridge University Press

the lateral terminal moraines. The ice thickness was similar to the trimlines mapped on the Fugleberget slopes and the southern slope of Fannytoppen (Figs 3 and 9). The frontal position did not change significantly between 1872 and 1918 (Koryakin, 1974; Jania, 1988). We suggest it was linked to anchoring the terminus on the terminal moraine and skerries with the prevailing thinning of the glacier tongue by the surface ablation rather than limited frontal ablation in shallow water. The water depth on the terminal moraine ranges from 2 to 15 m and does not exceed 25 m on the ice-proximal side of the belt (Fig. 2). The southernmost extent of the calving front was on the Hansholmane islands, which were probably one of the pinning points within the moraine belt (Figs 1, 2, 3, 9a and b). The mouths of subglacial channels could be observed on the calving front (Figs 9a and b) and the location of one of them seemed to correspond with an incision in the submarine terminal moraine (Figs 2 and 3), which suggests possible glacifluvial origin of this feature. The surface morphology of Hansbreen revealed compelling evidence for a surge before 1918, such as a folded medial moraine and a dense, complex network of intersecting crevasses and crevasse traces extending high up on the main trunk of the glacier (Fig. 9). We infer that abundant healed crevasses and their cross-cutting pattern were associated with rapid ice flow while surging in 1872. In 1918, the glacier terminus in Isbjørnhamna had a smooth topography and an active supraglacial channel with a waterfall at the ice cliff, which suggests closed crevasses in this part of the glacier during the quiescent phase (Fig. 9g). Similar spectacular features can be observed on the front of Bråsvellbreen (https://toposvalbard.npolar.no/) after decades of the quiescent phase in the aftermath of its surge in 1938 when the glacier tongue was badly crevassed (Schytt, 1969).

Late 1930s – limited evidence for a subsequent surge: In the western part of the forefield, the inner terminal moraine with a debris flow lobe suggests a younger surge of Hansbreen, which might have occurred in the first half of the 20th century (Fig. 2). Oblique aerial photographs from 1936 do not indicate a fully active surge (stage 3 according to Sund and others, 2009) as the surface morphology was dominated by crevasse traces, wide transverse crevasses were confined to the frontal zone, the terrestrial margins were stagnant, and the calving front was relatively straight and slightly expanded only in the central zone (Fig. 11). These data alone do not allow a qualitative assessment of the upper part of the glacier for evidence for the first two stages of the active surge phase expressed by changes in the glacier thickness (Sund and others, 2009). In August 1938, Pillewizer (1939) measured the unusually high surface velocity of Hansbreen using the terrestrial photogrammetric method of Finsterwalder (1931), which could suggest an active surge phase, and his map indicates an advance in some parts of the glacier front compared to 1936 (Fig. 2). If such event occurred, it may have been related to the inner terminal moraine with a debris flow lobe. However, additional evidence is necessary to support this interpretation in its current state.

Reconciling glacial geomorphology and past dynamics of Hansbreen

The possible surge-type behaviour of Hansbreen has long been debated for the lack of evidence of an ongoing surge in the observation period (e.g. Jania, 1988; Jania and Głowacki, 1996; Rachlewicz and Szczuciński, 2000; Ćwiąkała and others, 2018). We present the records of at least one surge event. Photographic documentation of the glacier extent, surface morphology and ice structure in the ice cliff revealed characteristic features for the active surge phase in 1872 (Fig. 10) and quiescence in 1918 (Fig. 9). This advance was marked by the outermost terminal moraine, trimlines and the lateral terminal moraines (Figs 2 and 3). Sparse historical data may suggest a minor surge episode in the 1930s, but further investigation is necessary to confirm this event. The imprints of the possible younger surge are much weaker than the LIA surge and the only compelling geomorphological evidence is the inner terminal moraine with a debris flow lobe (Fig. 3).

Our interpretation differs from previous investigations, which did not conclude that surges had occurred. Ćwiąkała and others (2018) analysed the submarine forefield and excluded the possibility of surging in the last c. 120 years based on the absence of streamlined glacial lineations, overridden recessional moraines, CSRs or a surge moraine with a debris flow lobe. However, drumlinized seafloor, streamlined glacial lineations and CSRs are not visible in the multibeam data collected in 2008, which they used for geomorphological mapping. Such landforms occur in the inner zone of Hansbukta surveyed in 2014–2017 (Fig. 3). CSRs were also not identified in the terrestrial forefield of Hansbreen (Skolasińska and others, 2016 and references therein), but part of the debris-rich structures in the passive ice cliff described by Rachlewicz and Szczuciński (2000) resembled CSRs at the base of surge-type glaciers (e.g. Evans and Rea, 2003; Lovell and others, 2015a). Apart from the north-western forefield, most CSRs are subdued and take the form of low ridges or sediment trails (Figs 6 and 8), similar to those described in Trygghamna (Aradóttir and others, 2019; Ben-Yehoshua and others, 2023). CSRs in the Hansbreen forefield are less abundant, lower and worse preserved than in many surge-type glaciers in Svalbard, e.g. Nathorstbreen (Lovell and others, 2018), Sefströmbreen (Boulton and others, 1996), Tunabreen, Von Postbreen (Lovell and others, 2015a) or the Hornbreen-Hambergbreen glacier system (Osika and others, 2022). Therefore, previous investigations could have omitted them without high-resolution remote sensing data.

Our study shows the importance of compiling terrestrial and submarine geomorphology with historical records for reconstructing past glacier dynamics. However, if the archival data are sparse, the identification of surge-type glaciers is impeded by the low preservation potential of surge-diagnostic landforms or topographic or geological conditions meaning that they do not form in the first place (e.g. Hansen, 2003; Farnsworth and others, 2016; Ingólfsson and others, 2016; Gądek and others, 2022). Therefore, we infer that the number of Svalbard surge-type glaciers or decaying glaciers that surged in the past can be underestimated if the geomorphological fingerprints have been obliterated and historical records are lacking or unrecognized. One example may be a cold-based valley Tellbreen, which was thought not to have ever surged (Bælum and Benn, 2011). However, the basal sequence and glaciological structures revealed that it had experienced warm-based conditions and dynamic ice flow, most probably during the LIA (Lovell and others, 2015b).

Interestingly, the 1870s surge of Hansbreen occurred in a period of numerous surge events in Svalbard between 1860s–1900s (e.g. Fridtjovbreen in 1861; Liestøl, 1993, Kronebreen, Kongsvegen and Kongsbreen in 1869; Liestøl, 1988, Von Postbreen in 1870; Liestøl, 1993, Nathorstbreen in the 1870s or 1880s; Liestøl, 1977; Ottesen and others, 2008, Sefströmbreen in 1882–1886; De Geer, 1910, Recherchebreen and Renardbreen at the turn of the 1870s and 1880s; Zagórski and others, 2023, Scottbreen in 1880s; Zagórski and others, 2023, Hambergbreen c. 1900; Wassiliew, 1925 or Paulabreen before 1898; Ottesen and others, 2008). The 1930s was another decade of apparent surge clustering (e.g. Bråsvellbreen in 1936–1938; Schytt, 1969, Negribreen in 1935–1936; Liestøl, 1969, Körberbreen in 1938; Liestøl, 1969, Markhambreen in 1930–1936; Hagen and others, 1993, Arnesenbreen in 1925–1935; Hagen and others, 1993 or

Etonbreen, Rijpbreen and Clasebreen in 1938; Hagen and others, 1993), although, despite some evidence, a surge of Hansbreen in this period remains questionable. Such synchronicity of surge advances might suggest regional factors affecting glacier dynamics. The reconstructed winter surface air temperatures in Longyearbyen were higher in the 1860s and early 1870s than in the 1850s or late 1870s (Divine and others, 2011). The 1920s and 1930s corresponded to the early 20th-century climate warming in Svalbard (Nordli and others, 2020) and we speculate that these surges may have been related to increased water content at the glacier beds from enhanced summer melt and produced by frictional heating (cf. enthalpy balance theory by Benn and others, 2019). However, this observation requires further studies on the LIA climate conditions and investigation into triggering factors of glacier surges (e.g. Benn and others, 2023).

Repeated surge events of many Svalbard glaciers with different durations of the quiescent phase (e.g. Tunabreen; Flink and others, 2015, Blomstrandbreen; Burton and others, 2016, Negribreen; Haga and others, 2020) raise the question about a potential future surge of Hansbreen. In our opinion, the surface topography of Hansbreen, i.e. the low-lying accumulation area of the main trunk and significant ice supply by the western tributary glaciers, as well as the subglacial topography with overdeepenings along the centreline, will hinder the build-up of mass and triggering the next surge. A dramatic increase in solid precipitation will be critical to fill up the reservoir area(s) and allow the rapid transfer of large amounts of ice to the receiving zone. We can speculate that such conditions will not be fulfilled in the following decades under projected climatic conditions in Svalbard (Hanssen-Bauer and others, 2019). However, one should not exclude possible dynamic advances of the western tributary glaciers after retreat of the main trunk. The loose of the back-stress from the Hansbreen main tongue may lead to re-organization of the surface profiles of the tributary glaciers through re-advances (Farnsworth and others, 2017).

Conclusions

We present a reconstruction of the past dynamics of Hansbreen by combining geomorphological mapping of the terrestrial and submarine forefields with historical data from Spitsbergen expeditions in the 19th and 20th centuries. Landform assemblages, including CSRs, flutings, glacial lineations and terminal moraines with debris flow lobes are consistent with the published surging glacier landsystem models and indicate at least one surge of Hansbreen.

Photographic documentation from the Austro-Hungarian expedition in 1872 revealed evidence of an ongoing active surge phase, such as a surge bulge, extensive surface crevassing, top-down and bottom-up crevasses and a convex surface profile of the terrestrial margin. The terminus had not yet reached the surge maximum. This surge corresponded to the maximum LIA extent of Hansbreen, marked by the outermost submarine terminal moraine with a debris flow lobe, terrestrial lateral terminal moraines and trimlines.

In 1918, the glacier was in the quiescent phase and the calving front was anchored on small islands and capes. The photogrammetric photos from the Norwegian expedition revealed further evidence of the surge before 1918, including a folded medial moraine and a dense, complex network of intersecting healed crevasses extending high up on the main trunk of Hansbreen. There may have been a subsequent surge in the 1930s based on a minor submarine terminal moraine with a debris flow lobe but this potential event requires further investigation.

Under projected climatic conditions, the low-lying accumulation area of the main trunk will hinder the mass build-up, and a potential next surge will probably remain questionable in the following decades. However, surges of the western tributary glaciers should not be excluded, in particular as a dynamic response when they lose the back-stress from the receding main tongue.

Acknowledgements. This study was funded by the National Science Centre of Poland (grant no. 2021/41/N/ST10/02070). The publication was co-financed by the Institute of Earth Sciences at the University of Silesia in Katowice. We sincerely thank Joanna Szafraniec for her comments, and Małgorzata Błaszczyk, Michał Ciepły, Dawid Saferna and Kamil Kachniarz (University of Silesia in Katowice) for their support during the fieldwork. We thank the crew of the Polish Polar Station Hornsund for logistic support and hospitality. The research and logistic equipment of the Polar Laboratory of the University of Silesia in Katowice was used during the fieldwork. We thank the Norwegian Hydrographic Service for the bathymetric data from Hansbukta and Isbjørnhamna. We are especially grateful to Österreichische Nationalbibliothek and Norsk Polarinstitutt for providing historical photographs from the polar expeditions to Hornsund in 1872 and 1918. We thank the Editor Andrew Fowler and in particular Harold Lovell for constructive comments and the insightful review, which significantly improved this manuscript.

Author contributions. A.O.: conceptualization, field investigation, data analysis. J.J.: conceptualization, field investigation, data analysis, supervision. A.O. structured the paper and wrote the manuscript with support from J.J.

Conflict of interest. The authors declare none.

Data availability. We re-used several published datasets available at individual databases. A very high-resolution orthophotomap of the Hansbreen forefield is available at https://ppdb.us.edu.pl/geonetwork/srv/eng/catalog.search#/metadata/9b980572-2bcb-401f-a2e6-2a7a16428dd7 (supplementary data to Błaszczyk and others, 2022). A DEM of these areas is available at https://ppdb.us.edu.pl/geonetwork/srv/eng/catalog.search#/metadata/69987fe3-f0ed-4fdc-b597-41dd5ae7d21a (supplementary data to Błaszczyk and others, 2022). The bathymetric data of Hansbukta are available at https://ppdb.us.edu.pl/geonetwork/srv/eng/catalog.search#/metadata/27151f9a-b3c4-4955-8db7-0365861f3dd6 (supplementary data to Błaszczyk and others, 2021). Front positions of Hansbreen are available at https://ppdb.us.edu.pl/geonetwork/srv/eng/catalog.search#/metadata/05e2c69a-5645-4488-bc88-630beb03a462 and https://ppdb.us.edu.pl/geonetwork/srv/eng/catalog.search#/metadata/77c6fbd4-1a07-47b1-a663-559970517841 (supplementary data to Błaszczyk and others, 2013, 2021). Archival photographs from 1872 are available at https://onb.digital/search/766393 and from 1918 at https://bildearkiv.npolar.no/fotoweb/. Upon publication, the vector layers (shapefiles) of the geomorphological map will be available in the open database ZENODO: https://doi.org/10.5281/zenodo.13646525.

References

Andreassen K and 11 others (2017) Massive blow-out craters formed by hydrate-controlled methane expulsion from the Arctic seafloor. *Science (New York, N.Y.)* **356**(6341), 948–953. doi: 10.1126/science.aal4500

Aradóttir N and 6 others (2019) Glacial geomorphology of Trygghamna, western Svalbard – Integrating terrestrial and submarine archives for a better understanding of past glacial dynamics. *Geomorphology* **344**, 75–89. doi: 10.1016/j.geomorph.2019.07.007

Bælum K and Benn DI (2011) Thermal structure and drainage system of a small valley glacier (Tellbreen, Svalbard), investigated by ground penetrating radar. *Cryosphere* **5**, 139–149. doi: 10.5194/tc-5-139-2011

Benn DI (1994) Fluted moraine formation and till genesis below a temperate valley glacier: Slettmarkbreen, Jotunheimen, southern Norway. *Sedimentology* **41**(2), 279–292. doi: 10.1111/j.1365-3091.1994.tb01406.x

Benn DI and Evans DJA (2010) *Glaciers & Glaciation*, 2nd Edn. London: Routledge. doi:10.5860/choice.35-6240

Benn DI, Fowler AC, Hewitt I and Sevestre H (2019) A general theory of glacier surges. *Journal of Glaciology* **65**(253), 701–716. doi: 10.1017/jog.2019.62

Benn DI, Hewitt I and Luckman A (2023) Enthalpy balance theory unifies diverse glacier surge behaviour. *Annals of Glaciology* **63**, 88–94. doi: 10.1017/aog.2023.23

Ben-Yehoshua D, Aradóttir N, Farnsworth WR, Benediktsson ÍÖ and Ingólfsson Ó (2023) Formation of crevasse-squeeze ridges at

Trygghamna, Svalbard. *Earth Surface Processes and Landforms* **48**(12), 2334–2348. doi: 10.1002/esp.5631
Birkenmajer K (1960) Raised marine features of the Hornsund area, Vestspitsbergen. *Studia Geologica Polonica* **5**, 3–95.
Birkenmajer K (1990) *Geological map of the Hornsund Area 1:75 000*. Katowice: Uniwersytet Śląski.
Błaszczyk M, Jania JA and Hagen JO (2009) Tidewater glaciers of Svalbard: recent changes and estimates of calving fluxes. *Polish Polar Research* **30**(2), 85–142.
Błaszczyk M, Jania JA and Kolondra L (2013) Fluctuations of tidewater glaciers in Hornsund Fjord (Southern Svalbard) since the beginning of the 20th century. *Polish Polar Research* **34**(4), 327–352. doi: 10.2478/popore-2013-0024
Błaszczyk M and 10 others (2019) Quality assessment and glaciological applications of digital elevation models derived from space-borne and aerial images over two tidewater glaciers of southern Spitsbergen. *Remote Sensing* **11**(9), 1121. doi: 10.3390/rs11091121
Błaszczyk M and 12 others (2021) Factors controlling terminus position of Hansbreen, a tidewater glacier in Svalbard. *Journal of Geophysical Research: Earth Surface* **126**(2), e2020JF005763. doi: 10.1029/2020JF005763
Błaszczyk M, Laska M, Sivertsen A and Jawak SD (2022) Combined use of aerial photogrammetry and terrestrial laser scanning for detecting geomorphological changes in Hornsund, Svalbard. *Remote Sensing* **14**(3), 601. doi: 10.3390/rs14030601
Błaszczyk M and 9 others (2023) The response of tidewater glacier termini positions in Hornsund (Svalbard) to climate forcing, 1992–2020. *Journal of Geophysical Research: Earth Surface* **128**(5), e2022JF006911. doi: 10.1029/2022JF006911
Błaszczyk M and 7 others (2024) High temporal resolution records of the velocity of Hansbreen, a tidewater glacier in Svalbard. *Earth Syst. Sci. Data* **16**(4), 1847–1860. doi: 10.5194/essd-16-1847-2024
Boulton GS (1968) Flow tills and related deposits on some Vestspitsbergen glaciers. *Journal of Glaciology* **7**(51), 391–412. doi: 10.3189/S0022143000020608
Boulton GS (1976) The origin of glacially fluted surfaces – Observations and theory. *Journal of Glaciology* **17**(76), 287–309. doi: 10.3189/S0022143000013605
Boulton GS (1986) Push-moraines and glacier-contact fans in marine and terrestrial environments. *Sedimentology* **33**(5), 677–698. doi: 10.1111/j.1365-3091.1986.tb01969.x
Boulton GS and 6 others (1996) Till and moraine emplacement in a deforming bed surge – an example from a marine environment. *Quaternary Science Reviews* **15**(10), 961–987. doi: 10.1016/0277-3791(95)00091-7
Burton DJ, Dowdeswell JA, Hogan KA and Noormets R (2016) Marginal fluctuations of a Svalbard surge-type tidewater glacier, Blomstrandbreen, since the little ice age: a record of three surges. *Arctic, Antarctic, and Alpine Research* **48**(2), 411–426. doi: 10.1657/AAAR0014-094
Chandler BMP and 17 others (2018) Glacial geomorphological mapping: a review of approaches and frameworks for best practice. *Earth-Science Reviews* **185**, 806–846. doi: 10.1016/j.earscirev.2018.07.015
Christoffersen P, Piotrowski JA and Larsen NK (2005) Basal processes beneath an Arctic glacier and their geomorphic imprint after a surge, Elisebreen, Svalbard. *Quaternary Research* **64**(2), 125–137. doi: 10.1016/j.yqres.2005.05.009
Copland L, Sharp MJ and Dowdeswell JA (2003) The distribution and flow characteristics of surge-type glaciers in the Canadian high Arctic. *Annals of Glaciology* **36**, 73–81. doi: 10.3189/172756403781816301
Ćwiąkała J and 5 others (2018) Submarine geomorphology at the front of the retreating Hansbreen tidewater glacier, Hornsund fjord, southwest Spitsbergen. *Journal of Maps* **14**(2), 123–134. doi: 10.1080/17445647.2018.1441757
De Andrés E and 5 others (2018) A two-dimensional glacier–fjord coupled model applied to estimate submarine melt rates and front position changes of Hansbreen, Svalbard. *Journal of Glaciology* **64**(247), 745–758. doi: 10.1017/jog.2018.61
De Geer G (1910) Guide de l'excursion au Spitzberg. XIe Congrés Géologique Internationale, Stockholm.
Divine D and 7 others (2011) Thousand years of winter surface air temperature variations in Svalbard and northern Norway reconstructed from ice core data. *Polar Research* **30**, 7379. doi: 10.3402/polar.v30i0.7379
Dowdeswell JA and Ottesen D (2016) Submarine landform assemblage for Svalbard surge-type tidewater glaciers. *Geological Society, London, Memoirs* **46**, 151–154. doi: 10.1144/M46.160
Dowdeswell JA, Hamilton GS and Hagen JO (1991) The duration of the active phase on surge-type glaciers: contrasts between Svalbard and other regions. *Journal of Glaciology* **37**(127), 388–400. doi: 10.3189/S0022143000005827
Dowdeswell JA, Hodgkins R, Nuttall M, Hagen JO and Hamilton GS (1995) Mass balance change as a control on the frequency and occurrence of glacier surges in Svalbard, Norwegian High Arctic. *Geophysical Research Letters* **22**(21), 2909–2912. doi: 10.1029/95GL02821
Dowdeswell JA, Ottesen D and Plassen L (2016) Debris-flow lobes on the distal flanks of terminal moraines in Spitsbergen fjords. *Geological Society, London, Memoirs* **46**(1), 77–78. doi: 10.1144/M46.97
Dowdeswell JA, Ottesen D and Bellec VK (2020) The changing extent of marine-terminating glaciers and ice caps in northeastern Svalbard since the 'Little Ice Age' from marine-geophysical records. *The Holocene* **30**(3), 389–401. doi: 10.1177/0959683619887429
Evans DJA (2009) Controlled moraines: origins, characteristics and palaeoglaciological implications. *Quaternary Science Reviews* **28**(3–4), 183–208. doi: 10.1016/j.quascirev.2008.10.024
Evans DJA and Rea BR (1999) Geomorphology and sedimentology of surging glaciers: a land-systems approach. *Annals of Glaciology* **28**, 75–82. doi: 10.3189/172756499781821823
Evans DJA and Rea BR (2003) Surging glacier landsystem. In Evans DJA (ed.), *Glacial Landsystems*. London: Arnold, pp. 259–288.
Ewertowski M, Kasprzak L, Szuman I and Tomczyk AM (2011) Controlled, ice-cored moraines: sediments and geomorphology. An example from Ragnarbreen, Svalbard. *Zeitschrift für Geomorphologie* **56**(1), 53–74. doi: 10.1127/0372-8854/2011/0049
Farnsworth WR, Ingólfsson Ó, Retelle M and Schomacker A (2016) Over 400 previously undocumented Svalbard surge-type glaciers identified. *Geomorphology* **264**, 52–60. doi: 10.1016/j.geomorph.2016.03.025
Farnsworth WR and 6 others (2017) Dynamic Holocene glacial history of St. Jonsfjorden, Svalbard. *Boreas* **46**(3), 585–603. doi: 10.1111/bor.12269
Finsterwalder R (1931) Geschwindigkeitsmessungen an Gletschern mittels Photogrammetrie. *Z. Gletscherk* **19**(4–5), 251–262.
Flink AE and Noormets R (2018) Submarine glacial landforms and sedimentary environments in Vaigattbogen, northeastern Spitsbergen. *Marine Geology* **402**, 244–263. doi: 10.1016/j.margeo.2017.07.019
Flink AE and 5 others (2015) The evolution of a submarine landform record following recent and multiple surges of Tunabreen glacier, Svalbard. *Quaternary Science Reviews* **108**, 37–50. doi: 10.1016/j.quascirev.2014.11.006
Flink AE, Hill P, Noormets R and Kirchner N (2018) Holocene glacial evolution of Mohnbukta in eastern Spitsbergen. *Boreas* **47**, 390–409. doi: 10.1111/bor.12277
Forwick M, Baeten NJ and Vorren TO (2009) Pockmarks in Spitsbergen fjords. *Norwegian Journal of Geology* **89**, 65–77.
Gądek B, Rojan E and Suska-Malawska M (2022) Surge-type Uisu glacier and its undisturbed forefield relief, Eastern Pamir, Tajikistan. *Misc. Geogr* **26**(4), 227–236. doi: 10.2478/mgrsd-2022-0009
Geyman EC, van Pelt WJJ, Maloof AC, Aas HF and Kohler J (2022) Historical glacier change on Svalbard predicts doubling of mass loss by 2100. *Nature* **601**(7893), 374–379. doi: 10.1038/s41586-021-04314-4
Glasser NF, Hambrey MJ, Crawford KR, Bennett MR and Huddart D (1998) The structural glaciology of Kongsvegen, Svalbard, and its role in landform genesis. *Journal of Glaciology* **44**(146), 136–148. doi: 10.3189/S0022143000002422
Glazer M, Dobiński W, Marciniak A, Majdański M and Błaszczyk M (2020) Spatial distribution and controls of permafrost development in non-glacial Arctic catchment over the Holocene, Fuglebekken, SW Spitsbergen. *Geomorphology* **358**, 107128. doi: 10.1016/j.geomorph.2020.107128
Glazovskiy AF, Kolondra L, Moskalevskiy MY and Jania J (1992) Studies on the tidewater glacier Hansbreen on Spitsbergen. *Polar Geography and Geology* **16**, 243–252. doi: 10.1080/10889379209377492
Grabiec M, Jania JA, Puczko D, Kolondra L and Budzik T (2012) Surface and bed morphology of Hansbreen, a tidewater glacier in Spitsbergen. *Polish Polar Research* **33**(2), 111–138. doi: 10.2478/v10183-012-0010-7
Grant KL, Stokes CR and Evans IS (2009) Identification and characteristics of surge-type glaciers on Novaya Zemlya, Russian Arctic. *Journal of Glaciology* **55**(194), 960–972. doi: 10.3189/002214309790794940
Haga ON and 5 others (2020) From high friction zone to frontal collapse: dynamics of an ongoing tidewater glacier surge, Negribreen, Svalbard. *Journal of Glaciology* **66**(259), 742–754. doi: 10.1017/jog.2020.43

Hagen JO and Liestøl O (1990) Long-term glacier mass-balance investigations in Svalbard, 1950–88. *Annals of Glaciology* **14**, 102–106. doi: 10.3189/S0260305500008351

Hagen JO, Liestøl O, Roland E and Jørgensen T (1993) Glacier atlas of Svalbard and Jan Mayen. Nor. Polarinst. Medd. 129.

Hansen S (2003) From surge-type to non-surge-type glacier behaviour: midre Lovénbreen, Svalbard. *Annals of Glaciology* **36**, 97–102. doi: 10.3189/172756403781816383

Hanssen-Bauer I and 5 others (eds) (2019) Climate in Svalbard 2100 – a knowledge base for climate adaptation. Norwegian Centre of Climate Services (NCCS) for Norwegian Environment Agency (Miljødirektoratet). doi: 10.25607/OBP-888

Heintz A (1953) Non iakktagelser over isbreenes tilbakegang i Hornsund. *Norsk Geografisk Tidsskrift* **31**, 7–36.

Hoel A (1929) *The Norwegian Svalbard Expeditions 1906-1926*, vol. **1**. Oslo: Skrifter om Svalbard og Ishavet.

Ingólfsson Ó and 7 others (2016) Glacial geological studies of surge-type glaciers in Iceland – research status and future challenges. *Earth-Science Reviews* **152**, 37–69. doi: 10.1016/j.earscirev.2015.11.008

Ives LRW and Iverson NR (2019) Genesis of glacial flutes inferred from observations at Múlajökull, Iceland. *Geology* **47**(5), 387–390. doi: 10.1130/G45714.1

Jania J (1988) *Dynamiczne procesy glacjalne na południowym Spitsbergenie (w świetle badań fotointerpretacyjnych i fotogrametrycznych) [Dynamic glacial processes in south Spitsbergen (in the light of photointerpretation and photogrammetric research)]*. Katowice: Wydawnictwo Uniwersytetu Śląskiego (in Polish with English summary).

Jania J (1998) Dynamika Lodowca Hansa (Spitsbergen, Svalbard), a wybrane elementy rzeźby na jego przedpolu [Dynamics of the Hans Glacier (Spitsbergen, Svalbard) and selected elements of relief in its forefield. In Kostrzewski A (ed.), *Rzeźba i osady czwartorzędowe obszarów współczesnego i plejstoceńskiego zlodowacenia półkuli północnej*. Poznań: Wydawnictwo Naukowe UAM, pp. 81–96 (In Polish with English summary).

Jania J and Głowacki P (1996) Is the Hansbreen in South Spitsbergen (Svalbard) a surge-type glacier? In Krawczyk WE ed. 23rd Polar Symposium, Uniwersytet Śląski, Sosnowiec, 27–43.

Jania J and Kolondra L (1982) Field investigations performed during the Glaciological Spitsbergen Expedition in the Summer of 1982. Interim Report, Uniwersytet Śląski, Katowice.

Jania J, Mochnacki D and Gądek B (1996) The thermal structure of Hansbreen, a tidewater glacier in southern Spitsbergen, Svalbard. *Polar Research* **15**, 53–66. doi: 10.1111/j.1751-8369.1996.tb00458.x

Jiskoot H, Boyle P and Murray T (1998) The incidence of glacier surging in Svalbard: evidence from multivariate statistics. *Computers & Geosciences* **24**(4), 387–399. doi: 10.1016/S0098-3004(98)00033-8

Jiskoot H, Murray T and Boyle P (2000) Controls on the distribution of surge-type glaciers in Svalbard. *Journal of Glaciology* **46**(154), 412–422. doi: 10.3189/172756500781833115

Karczewski A and 13 others (1984) *Hornsund, Spitsbergen – Geomorphology, 1:75000*. Katowice: University of Silesia.

Koryakin VM (1974) Izmjenienje razmerov lednikov Szpicbergena (Svalnarda). *Materials of the Investigations in the Glaciation Region of the Spitsbergen* (*Svalbard*). Moscow: AN SSSR [Acad. of Sci. of the USSR], pp. 29–44.

Kosiba A (1960) *Some Results of Glaciological Investigations in SW-Spitsbergen Carried Out During the Polish I. G. Y. Spitsbergen Expeditions in 1957, 1958 and 1959*. Wrocław: Uniwersytet Wrocławski.

Laska M and 8 others (2022) Hansbreen snowpit dataset – over 30-year of detailed snow research on an Arctic glacier. *Scientific Data* **9**, 656. doi: 10.1038/s41597-022-01767-8

Lefauconnier B and Hagen JO (1991) Surging and calving glaciers in eastern Svalbard. *Nor. Polarinst. Medd* **116**, 1–130.

Liestøl O (1969) Glacier surges in West Spitsbergen. *Canadian Journal of Earth Sciences* **6**(4), 895–897. doi: 10.1139/e69-092

Liestøl O (1977) Årsmorener foran Nathorstbreen? *Nor. Polarinst. Årb* **1976**, 361–363.

Liestøl O (1988) The glaciers in the Kongsfjorden area, Spitsbergen. *Nor. Geogr. Tidsskr* **42**(4), 231–238. doi: 10.1080/00291958808552205

Liestøl O (1993) Glaciers of Svalbard, Norway. In Williams Jr RS and Ferrigno JG (eds), *Satellite Image Atlas of Glaciers of the World*. Washington, DC: US Geological Survey, pp. 127–151.

Lindner L, Marks L and Szczęsny R (1992) Quaternary landforms, sediments and morphogenetic evolution of Hansbreen-Sofiekammen region, Wedel Jarlsberg Land, Spitsbergen. *Polish Polar Research* **13**(2), 91–101.

Lønne I (2016) A new concept for glacial geological investigations of surges, based on high-Arctic examples (Svalbard). *Quaternary Science Reviews* **132**, 74–100. doi: 10.1016/j.quascirev.2015.11.009

Lovell H and Boston CM (2017) Glacitectonic composite ridge systems and surge-type glaciers: an updated correlation based on Svalbard, Norway. *Arktos* **3**, 2. doi: 10.1007/s41063-017-0028-5

Lovell H and Fleming E (2023) Structural evolution during a surge in the Paulabreen glacier system, Svalbard. *Journal of Glaciology* **69**(273), 141–152. doi: 10.1017/jog.2022.53

Lovell H and 7 others (2015a) Debris entrainment and landform genesis during tidewater glacier surges. *Journal of Geophysical Research: Earth Surface* **120**(8), 1574–1595. doi: 10.1002/2015JF003509

Lovell H and 5 others (2015b) Former dynamic behaviour of a cold-based valley glacier on Svalbard revealed by basal ice and structural glaciology investigations. *Journal of Glaciology* **61**(226), 309–328. doi: 10.3189/2015JoG14J120

Lovell H and 8 others (2018) Multiple Late Holocene surges of a high-Arctic tidewater glacier system in Svalbard. *Quaternary Science Reviews* **201**, 162–185. doi: 10.1016/j.quascirev.2018.10.024

Luncke B (1936) Luftkartlegningen på Svalbard 1936. *Norsk Geogr. Tidsskr* **6**, 145–154.

Maussion F and 11 others (2023) The Randolph Glacier Inventory version 7.0, User guide v1.0. doi: 10.5281/zenodo.8362857

Meier MF and Post A (1969) What are glacier surges? *Canadian Journal of Earth Sciences* **6**(4), 807–817. doi: 10.1139/e69-081

Murray T, Strozzi T, Luckman A, Jiskoot H and Christakos P (2003) Is there a single surge mechanism? Contrasts in dynamics between glacier surges in Svalbard and other regions. *Journal of Geophysical Research: Solid Earth* **108**(B5), 2237. doi: 10.1029/2002JB001906

Noormets R, Flink A and Kirchner N (2021) Glacial dynamics and deglaciation history of Hambergbukta reconstructed from submarine landforms and sediment cores, SE Spitsbergen, Svalbard. *Boreas* **50**, 29–50. doi: 10.1111/bor.12488

Nordli Ø and 6 others (2020) Revisiting the extended Svalbard Airport monthly temperature series, and the compiled corresponding daily series 1898–2018. *Polar Research* **39**, 3614. doi: 10.33265/polar.v39.3614

Norwegian Polar Institute (2014) *Kartdata Svalbard 1:1 000 000 (S1000 Kartdata) [Data set]*. Tromsø: Norwegian Polar Institute. doi: 10.21334/npolar.2014.63730e2e

Nuth C and 7 others (2013) Decadal changes from a multi-temporal glacier inventory of Svalbard. *Cryosphere* **7**, 1603–1621. doi: 10.5194/tc-7-1603-2013

Ohta Y and Dallmann WK (eds) (1999) Geological map of Svalbard 1:100 000. Sheet B12 G Torellbreen. Norsk Polarinstitutt Temakart Nr. 29.

Osika A, Jania J and Szafraniec JE (2022) Holocene ice-free strait followed by dynamic Neoglacial fluctuations: Hornsund, Svalbard. *The Holocene* **32**(7), 664–679. doi: 10.1177/09596836221088232

Otero J and 5 others (2017) Modeling the controls on the front position of a tidewater glacier in Svalbard. *Frontiers in Earth Science* **5**, 243157. doi: 10.3389/feart.2017.00029

Ottesen D and Dowdeswell JA (2006) Assemblages of submarine landforms produced by tidewater glaciers in Svalbard. *Journal of Geophysical Research: Earth Surface* **111**, F01016. doi: doi:10.1029/2005JF000330

Ottesen D and 9 others (2008) Submarine landforms characteristic of glacier surges in two Spitsbergen fjords. *Quaternary Science Reviews* **27**(15–16), 1583–1599. doi: 10.1016/j.quascirev.2008.05.007

Ottesen D, Dowdeswell J, Bellec V and Bjarnadóttir L (2017) The geomorphic imprint of glacier surges into open-marine waters: examples from eastern Svalbard. *Marine Geology* **392**, 1–29. doi: 10.1016/j.margeo.2017.08.007

Pälli A, Moore JC, Jania J, Kolondra L and Glowacki P (2003) The drainage pattern of Hansbreen and Werenskioldbreen, two polythermal glaciers in Svalbard. *Polar Research* **22**(2), 355–371. doi: 10.3402/polar.v22i2.6465

Pękala K (1989) Quaternary deposits of the Hans Glacier forefield (Hornsund, Spitsbergen). *Polar Session. Natural Environment Research of West Spitsbergen*. Lublin: Wydawnictwo UMCS, pp. 191–204.

Peterman A (1874) Graf Wiltschek's Nordpolarfahrt im Jahre 1872 / nach den Aufzeichnungen des Contre-Admirals Max Freiherrn Daublebsky v. Sterneck und Ehrenstein. In Peterman A ed. Mittheilungen aus Justus Perthes' Geographischer Anstalt über wichtige neue Erforschungen auf dem

Gesammtgebiete der Geographie, 20 Band, Justus Perthes' Geographische Anstalt Gotha, 65–72.
Pillewizer W (1939) Die kartographischen und gletscherkundlichen Ergebnisse der deutschen Spitzbergen-Expedition 1938, Justus Perthes Verlag Gotha.
Rachlewicz G and Szczuciński W (2000) Ice tectonics and bedrock relief control on glacial sedimentation – an example from Hansbreen, Spitsbergen. In Grześ M, Lankauf KR and Sobota I eds. Polish Polar Studies. 27th Polar Symposium, 1–3 December 2000, Toruń, Pracownia Sztuk Plastycznych, 259–275.
Raymond CF (1987) How do glaciers surge? A review. *Journal of Geophysical Research: Solid Earth* **92**(B9), 9121–9134. doi: 10.1029/JB092iB09p09121
Rea BR and Evans DJA (2011) An assessment of surge-induced crevassing and the formation of crevasse squeeze ridges. *Journal of Geophysical Research: Earth Surface* **116**, F04005. doi: 10.1029/2011JF001970
RGI 7.0 Consortium (2023) *Randolph Glacier Inventory – A Dataset of Global Glacier Outlines, Version 7.0.* Boulder, Colorado, USA: NSIDC: National Snow and Ice Data Center. doi: 10.5067/f6jmovy5navz
Robinson P and Dowdeswell JA (2011) Submarine landforms and the behavior of a surging ice cap since the last glacial maximum: the open-marine setting of eastern Austfonna, Svalbard. *Marine Geology* **286**(1–4), 82–94. doi: 10.1016/j.margeo.2011.06.004
Rootes CM and Clark CD (2022) On the expression and distribution of glacial trimlines: a case study of Little Ice Age trimlines on Svalbard. *E&G Quaternary Science Journal* **71**, 111–122. doi: 10.5194/egqsj-71-111-2022
Schomacker A and Kjær KH (2008) Quantification of dead-ice melting in ice-cored moraines at Holmströmbreen. *Svalbard. Boreas* **37**(2), 211–225. doi: 10.1111/j.1502-3885.2007.00014.x
Schuler TV and 12 others (2020) Reconciling Svalbard glacier mass balance. *Frontiers in Earth Science* **8**, 523648. doi: 10.3389/feart.2020.00156
Schytt V (1969) Some comments on glacier surges in eastern Svalbard. *Canadian Journal of Earth Sciences* **6**(4), 867–873. doi: 10.1139/e69-088
Sevestre H and Benn D (2015) Climatic and geometric controls on the global distribution of surge-type glaciers: implications for a unifying model of surging. *Journal of Glaciology* **61**(228), 646–662. doi: 10.3189/2015JoG14J136
Sevestre H, Benn DI, Hulton NJR and Bælum K (2015) Thermal structure of Svalbard glaciers and implications for thermal switch models of glacier surging. *Journal of Geophysical Research: Earth Surface* **120**(10), 2220–2236. doi: 10.1002/2015JF003517
Skolasińska K, Rachlewicz G and Szczuciński W (2016) Micromorphology of modern tills in southwestern Spitsbergen – insights into depositional and post-depositional processes. *Polish Polar Research* **37**(4), 435–456. doi: 10.1515/popore-2016-0023
Sobota I, Weckwerth P and Nowak M (2016) Surge dynamics of Aavatsmarkbreen, Svalbard, inferred from the geomorphological record. *Boreas* **45**(2), 360–376. doi: 10.1111/bor.12160
Spagnolo M and 7 others (2014) Size, shape and spatial arrangement of mega-scale glacial lineations from a large and diverse dataset. *Earth Surface Processes and Landforms* **39**(11), 1432–1448. doi: 10.1002/esp.3532
Stokes CR and Clark CD (2002) Are long subglacial bedforms indicative of fast ice flow? *Boreas* **31**(3), 239–249. doi: 10.1111/j.1502-3885.2002.tb01070.x
Streuff K, Forwick M, Szczuciński W, Andreassen K and Cofaigh CÓ (2015) Submarine landform assemblages and sedimentary processes related to glacier surging in Kongsfjorden, Svalbard. *Arktos* **1**, 14. doi: 10.1007/s41063-015-0003-y
Streuff K, Cofaigh CÓ, Noormets R and Lloyd J (2018) Submarine landform assemblages and sedimentary processes in front of Spitsbergen tidewater glaciers. *Marine geology* **402**, 209–227. doi: 10.1016/j.margeo.2017.09.006
Streuff KT, Cofaigh CÓ and Wintersteller P (2022) Glacidat – a GIS database of submarine glacial landforms and sediments in the Arctic. *Boreas* **51**(3), 517–531. doi: 10.1111/bor.12577
Sund M, Eiken T, Hagen JO and Kääb A (2009) Svalbard surge dynamics derived from geometric changes. *Annals of Glaciology* **50**(52), 50–60. doi: 10.3189/172756409789624265
Szafraniec JE (2020) Ice-cliff morphometry in identifying the surge phenomenon of tidewater glaciers (Spitsbergen, Svalbard). *Geosciences* **10**, 328. doi: 10.3390/geosciences10090328
Tegowski J, Trzcinska K, Kasprzak M and Nowak J (2016) Statistical and spectral features of corrugated seafloor shaped by the Hans glacier in Svalbard. *Remote Sensing* **8**(9), 744. doi: 10.3390/rs8090744
Vieli A, Jania J and Kolondra L (2002) The retreat of a tidewater glacier: observations and model calculations on Hansbreen, Spitsbergen. *Journal of Glaciology* **48**(163), 592–600. doi: 10.3189/172756502781831089
Wassiliew AS (1925) Océan Glacial arctique. Spitzberg. Région des travaux de l'expédition de l'Académies de sciences de Russie pour la mesure d'un arc de méridien en 1899–1901. Carte dresie d'après les matériaux de l'expédition sous la rédactin de O.E. Stubendorff par A.S. Wassiliew. Échelle de 1:200 000.
Wawrzyniak T and Osuch M (2019) A consistent high Arctic climatological dataset (1979-2018) of the Polish polar station Hornsund (SW Spitsbergen, Svalbard). *PANGAEA*. doi: 10.1594/PANGAEA.909042
Wawrzyniak T and Osuch M (2020) A 40-year high Arctic climatological dataset of the Polish polar station Hornsund (SW Spitsbergen, Svalbard). *Earth Syst. Sci. Data* **12**, 805–815. doi: 10.5194/essd-12-805-2020
Weniger P and 6 others (2019) Origin of near-surface hydrocarbon gases bound in northern Barents Sea sediments. *Marine and Petroleum Geology* **102**, 455–476. doi: 10.1016/j.marpetgeo.2018.12.036
Yde JC and 5 others (2019) Kuannersuit Glacier revisited: constraining ice dynamics, landform formations and glaciomorphological changes in the early quiescent phase following the 1995–98 surge event. *Geomorphology* **330**, 89–99. doi: 10.1016/j.geomorph.2019.01.012
Zagórski P and 5 others (2023) Surges in three Svalbard glaciers derived from historic sources and geomorphic features. *Annals of the American Association of Geographers* **113**(8), 1835–1855. doi: 10.1080/24694452.2023.2200487

Załącznik 7

Quaternary Science Reviews

Holocene glacial history of southern Spitsbergen

--Manuscript Draft--

Manuscript Number:	JQSR-D-25-00716
Article Type:	Research Paper
Keywords:	glacier fluctuations; glacier surges; glacial geomorphology; Holocene Thermal Maximum; Medieval Warm Period; Little Ice Age; Svalbard; Hornsund
Corresponding Author:	Aleksandra Osika University of Silesia in Katowice Institute of Earth Sciences POLAND
First Author:	Aleksandra Osika
Order of Authors:	Aleksandra Osika
	Jacek Jania
	Natalia Piotrowska
	Dmitry Tikhomirov
	Joanna Ewa Szafraniec
	Dhanushka Devendra
	Marcus Christl
	Markus Egli
	Andreas Vieli
Abstract:	Climate change affects the extent of glaciers in Svalbard, and warmer periods of the Holocene may serve as analogues for predicting their future decay. While the Holocene glacial history of central, western and northern Svalbard is relatively well-studied, knowledge of glacier fluctuations in southern Spitsbergen remains limited. We reconstruct the Holocene glacier dynamics in Hornsund and adjacent areas, using geomorphological, geochronological, and historical data. New and published radiocarbon (14C) and cosmogenic nuclide (10Be) dates were combined with historical maps dating back to the 1600s and photographs from 1872–1936. The ages of mollusc shells from till deposits and Little Ice Age (LIA) moraines suggest glacier retreat in the Early Holocene, enabling colonisation of glacier-free branches of Hornsund. During the first half of the Late Holocene, the extent of tidewater glaciers remained reduced compared to their LIA maxima. Their limited advance was likely constrained by increasing sea-surface temperatures and atmospheric warming between c. 2.2–1.8 and 1.5–0.7 cal ka BP. The maximum Late Holocene glacier extents were associated with surges, probably preceded by ice mass accumulation due to climatic cooling and increased precipitation. However, many surges may also have occurred under warmer conditions. Most glaciers in southern Spitsbergen are highly sensitive to climatic changes, both through mass balance and surging, due to their specific topographic settings (low-elevation, gently sloping, long, multi-branched glaciers with overdeepenings in the bedrock). The interaction between climate variability and glacier surging played a crucial role in glacier evolution throughout the Holocene.

Aleksandra Osika

Institute of Earth Sciences
Faculty of Natural Sciences
University of Silesia in Katowice
Bedzinska 60
41-200 Sosnowiec, Poland
e-mail: aosika1@us.edu.pl;
1aleksandra.osika@gmail.com

September 22, 2025

To **Dr. Miryam Bar-Matthews**
Editor-in-chief
Quaternary Science Reviews

Dear Dr. Miryam Bar-Matthews,

We would like to present our manuscript **"Holocene glacial history of southern Spitsbergen"** by Aleksandra Osika, Jacek Jania, Natalia Piotrowska, Dmitry Tikhomirov, Joanna Ewa Szafraniec, Dhanushka Devendra, Marcus Christl, Markus Egli and Andreas Vieli, and propose it for publication as a research paper in *Quaternary Science Reviews*.

We reconstruct the fluctuations of selected marine-terminating and land-based glaciers in southern Spitsbergen in the Holocene, combining geomorphological, geochronological and historical data. So far, knowledge of the Holocene glacial history of this part of Svalbard has been limited, compared to well-investigated northern and central Spitsbergen. We provide 57 new radiocarbon dates of marine mollusc shells, driftwood, subfossil soils and a whalebone collected from glacial sediments of Hansbreen, Hornbreen, Vestre Torellbreen and Werenskioldbreen. In particular, we focus on the role of surges in past glacial dynamics. We found that the main glacial advances in the Late Holocene, including the maximum extents from the Little Ice Age, were associated with glacier surges. Glacier surges at the end of the Little Ice Age have been documented in the maps and photographs from expeditions to Spitsbergen in 1872 and 1918, which captured the evidence of ongoing surges or the early quiescent phase.

We believe that our findings will find interest in *Quaternary Science Reviews* Readers. The Holocene history of this part of the Arctic is still not thoroughly recognised. The studies on the spatio-temporal scale of glacier fluctuations in the past also provide essential data for prediction the consequences of the ongoing climate warming in this sensitive region.

We confirm this manuscript has not been published elsewhere and is not being considered for publication in another journal. All authors have contributed substantially to this work, approved the manuscript and agree with its submission to *Quaternary Science Reviews*. The individual contribution of each co-author, stated also in the manuscript, is as follows:

AO: conceptualization, data curation, formal analysis, funding acquisition, investigation, methodology, project administration, visualization, writing. JJ: conceptualization, funding acquisition, investigation, methodology, resources, supervision, writing. NP: data curation, formal analysis, investigation, methodology, resources, writing. DT: data curation, formal analysis, investigation, methodology, resources, writing. JES: conceptualization, supervision, visualization, writing – review and editing. DD: visualization, writing – review and editing. MC: data curation, investigation. ME: data curation, methodology, resources. AV = writing – review and editing, resources.

AO = Aleksandra Osika, JJ = Jacek Jania, NP = Natalia Piotrowska, DT = Dmitry Tikhomirov, JES = Joanna Ewa Szafraniec, DD = Dhanushka Devendra, MC = Marcus Christl, ME = Markus Egli, AV = Andreas Vieli

On behalf of the authors,

Aleksandra Osika

Highlights

- Widespread glacier recession in the Early Holocene and significant reduction of glacier extents in the Middle Holocene
- High sensitivity of S Spitsbergen glaciers to climate changes throughout the Holocene
- Late Holocene glacier expansion hindered by warmer Atlantic water and atmospheric warming
- Glacier surges were crucial for reaching the maximum glacier extents in the Little Ice Age and probably in the transition from colder to warmer phases of the Holocene

Holocene glacial history of southern Spitsbergen

Aleksandra Osika[a]*, Jacek Jania[a], Natalia Piotrowska[b], Dmitry Tikhomirov[c], Joanna Ewa Szafraniec[a], Dhanushka Devendra[d], Marcus Christl[e], Markus Egli[c], Andreas Vieli[c]

[a] Institute of Earth Sciences, Faculty of Natural Sciences, University of Silesia in Katowice, Bedzinska 60, 41-200 Sosnowiec, Poland

[b] Institute of Physics, Silesian University of Technology, Stanislawa Konarskiego 22B/217, 44-100 Gliwice, Poland

[c] Department of Geography, University of Zurich, Zurich, Switzerland

[d] Department of Palaeoceanography, Institute of Oceanology, Polish Academy of Sciences, 81-712 Sopot, Poland

[e] Laboratory of Ion Beam Physics, ETH, Zurich, Switzerland

*Corresponding author: 1aleksandra.osika@gmail.com

Abstract. Climate change affects the extent of glaciers in Svalbard, and warmer periods of the Holocene may serve as analogues for predicting their future decay. While the Holocene glacial history of central, western and northern Svalbard is relatively well-studied, knowledge of glacier fluctuations in southern Spitsbergen remains limited. We reconstruct the Holocene glacier dynamics in Hornsund and adjacent areas, using geomorphological, geochronological, and historical data. New and published radiocarbon (^{14}C) and cosmogenic nuclide (^{10}Be) dates were combined with historical maps dating back to the 1600s and photographs from 1872–1936. The ages of mollusc shells from till deposits and Little Ice Age (LIA) moraines suggest glacier retreat in the Early Holocene, enabling colonisation of glacier-free branches of Hornsund. During the first half of the Late Holocene, the extent of tidewater glaciers remained reduced compared to their LIA maxima. Their limited advance was likely constrained by increasing sea-surface temperatures and atmospheric warming between c. 2.2–1.8 and 1.5–0.7 cal ka BP. The maximum Late Holocene glacier extents were associated with surges, probably preceded by ice mass accumulation due to climatic cooling and increased precipitation. However, many surges may also have occurred under warmer conditions. Most glaciers in southern Spitsbergen are highly sensitive to climatic changes, both through mass balance and surging, due to their specific topographic settings (low-elevation, gently sloping, long, multi-branched glaciers with overdeepenings in the bedrock). The interaction between climate variability and glacier surging played a crucial role in glacier evolution throughout the Holocene.

Keywords: glacier fluctuations, glacier surges, glacial geomorphology, Holocene Thermal Maximum, Medieval Warm Period, Little Ice Age, Svalbard, Hornsund

1. Introduction

Svalbard glaciers covered 33,750 km^2 in ~2010, which corresponded to 57% of the terrestrial area of the archipelago (Nuth et al., 2013). Located at the edge of the retreating sea ice and affected by contrasting oceanic and air regimes, since 1979, Svalbard has warmed almost twice as fast as the Arctic and seven times faster than the global average (Nordli et al., 2020; Rantanen et al., 2022). Glacier recession has been observed since the maximum of the Little Ice Age (LIA) at the turn of the 19th and 20th centuries and dramatically accelerated in the 1990s (Nuth et al., 2007; Martín-Moreno et al., 2017). Schuler et al. (2020) estimated the total mass balance of Svalbard glaciers in 2000–2019 as –8 ± 6 Gt a^{-1}. The retreat rate is higher for marine-terminating glaciers, which also lose mass by frontal ablation (Błaszczyk et al., 2013). They represent more than 60% of the glaciated area in Svalbard (Błaszczyk et al., 2009), although the number of tidewater glaciers that became land-terminating increased in the last decade (Kochtitzky and Copland, 2022).

The present-day fluctuations of Svalbard glaciers reflect an increase in air and sea-water temperatures, and their dynamics, including glacier surges (Luckman et al., 2015; Holmes et al., 2019; Błaszczyk et al., 2023). Considering surge-type behaviour as one of the key factors of rapid changes in glacier extent could improve our understanding of their past behaviour, current dynamics and projections for the future environment in the warmer Arctic (Hanssen-Bauer et al., 2019). The pattern of climatic and glacier changes throughout the Holocene has been consistent in different parts of the Arctic, despite spatial and temporal variability of the phases of warming in the Early and Middle Holocene and cooling in the Late Holocene (Larocca and Axford, 2022). Geochronological records from Svalbard indicate glacier retreat in the Early Holocene corresponding to the Holocene Thermal Maximum (HTM), which led to the glacial minimum between c. 8.0 and 6.0 cal ka BP (Røthe et al., 2018; Allaart et al., 2020; Farnsworth et al., 2020). A decrease in summer insolation, climate cooling and glacier advances occurred in the Neoglacial after 4.0 cal ka BP (Werner, 1993; Miller et al., 2017; Farnsworth et al., 2020), including the LIA (Martín-Moreno et al., 2017). However, climate cooling was punctuated by warmer phases with glacier retreat, such as the Medieval Warm Period (MWP) c. 1.2–0.7 cal ka BP (Dzierżek et al., 1990; Divine et al., 2011). The Holocene glacier advances have reflected the combination of climatic drivers and surges (Lefauconnier and Hagen, 1991; Dowdeswell et al., 2020). Glacier surges are quasi-cyclical, brief periods of rapid ice flow with velocities 10–1000 times higher than usual, i.e. the balance flow through the equilibrium line altitude (ELA) cross section of the tongue, often associated with extensive advances (Meier and Post, 1969; Raymond, 1987; Sund et al., 2009). Svalbard is a well-defined cluster of surging glaciers (Sevestre and Benn, 2015), and every larger glacier in south Spitsbergen is surge-type (Jania, 1988; Lefauconnier and Hagen, 1991; Błaszczyk et al., 2013, 2023). Geological records over the archipelago revealed surge advances also earlier in the Holocene (e.g. Farnsworth et al., 2016; Flink et al., 2018; Larsen et al., 2018; Lovell et al., 2018; Zagórski et al., 2023). One of the hypotheses tested in this work is recognizing the importance of surging for changes in glacier extent in southern Spitsbergen in the Holocene. Relatively rich data on the interplay between climate change and glacier surge dynamics during and after the LIA have been collected and interpreted (e.g. Dowdeswell et al., 1995; Lønne, 2014; Sund et al., 2014; Dunse et al., 2015; Zagórski et al., 2023), and they may serve as analogues for glacier behaviour in the past.

Compared with well-studied central, western and northern Svalbard (Farnsworth et al., 2020), knowledge of the Holocene glacier changes in southern Spitsbergen is still limited. Previous investigations have provided evidence of glacier retreat in the Early Holocene and the MWP, and advances in the Late Holocene (Baranowski and Karlén, 1976; Lindner et al., 1984; Dzierżek et al., 1990; Birkenmajer and Olsson, 1997; Philipps et al., 2017; Osika et al., 2022; Osika and Jania, 2024; Jang et al., 2025). Lindner et al. (1986, 1987) and Lindner and Marks (1993) reconstructed the Quaternary chronostratigraphy of this part of Svalbard, but the time constraints of glacier advances are still debated (Baranowski, 1977; Birkenmajer and Olsson, 1997; Osika et al., 2022; Jang et al., 2025). Here, we reconstruct the Holocene fluctuations of tidewater and land-terminating glaciers in southern Spitsbergen using a compilation of new and published radiocarbon and cosmogenic exposure dates, and historical data from Svalbard expeditions in the 1600s–1900s. We link climatic conditions with glacier surge dynamics (e.g. Dowdeswell et al., 1995; Sund et al., 2014; Dunse et al., 2015) to support a more realistic reconstruction of past glacier activity. In addition, we assess the similarities and differences in how the glaciers of southern Spitsbergen responded to climatic changes throughout the Holocene, compared to the rest of Svalbard.

2. Study area

2.1. Regional setting

Southern Spitsbergen is a relatively small region of Svalbard in the form of an upturned triangle, located between the cold East Spitsbergen Current (–1.5°C to 2.0°C) and warm West Spitsbergen Current transporting Atlantic Waters (AW; > 3°C) towards the Arctic Ocean (Promińska et al., 2018; Błaszczyk et al., 2021), and exposed to the direct inflow of warmer and wetter air masses from the SW

(Migała et al., 2023). Thus, weather changes are frequent and climatic conditions are of the oceanic type. The regional topography with tectonically predefined main valleys of dominant N-S orientations determines the pattern of glacierisation as a network of low-elevated interconnected ice masses – mainly tidewater glaciers, which are particularly susceptible to an increase in ablation and the ELA rise (Jania, 1988; Noël et al., 2020). The subglacial topography with extensive zones below sea level amplifies their retreat when the calving fronts reach the glacier-bed overdeepenings (Grabiec et al., 2012b; Fürst et al., 2018; Błaszczyk et al., 2021). Glaciers in this region have one of the most negative mass balances in Svalbard (Nuth et al., 2010; Østby et al., 2017; Schuler et al., 2020), and many of them are surge-type (Jania, 1988; Lefauconnier and Hagen, 1991; Noormets et al., 2021; Zagórski et al., 2023).

The Hornsund region, Recherchefjorden and the Barents Sea shore are the most investigated areas of southern Spitsbergen, based on intensive field studies supported by historical cartography, photography and remote sensing data (e.g. Jania, 1988; Błaszczyk et al., 2013; Kavan et al., 2022; Zagórski et al., 2023). Hornsund is a west-east oriented fjord system, c. 35 km long and 320 km^2 in area, separating Wedel-Jarlsberg Land and Torell Land in the north from Sørkapp Land in the south (Fig. 1). Glaciers cover c. 67% of the Hornsund drainage basin, and most terminate in the sea (c. 97% of the glacierized area; Błaszczyk et al., 2013). Mean annual air temperature and precipitation at the Polish Polar Station Hornsund (77°00′ N, 15°33′ E) were –3.7°C and 478 mm in 1979–2018, with increasing trends of +1.14°C and +61.6 mm per decade (Wawrzyniak and Osuch, 2020).

2.2. Glaciers and glacial geomorphology

Here, we focus on four glaciers and terrestrial parts of their forefields: Hornbreen, Hansbreen, Vestre Torellbreen (tidewater) and Werenskioldbreen (land-terminating). All of them underwent at least one glacier surge based on current observations or geomorphological and historical records (Sund et al., 2009; Grabiec et al., 2012a; Szafraniec, 2013; Osika et al., 2022; Osika and Jania, 2024).

Hornbreen is a tidewater glacier at the head of Hornsund, supplied by Flatbreen and Isingbreen and separated from neighbouring Hambergbreen with an ice divide at c. 180 m a.s.l. Hornbreen and Hambergbreen form an ice isthmus c. 4 km wide between the Greenland and the Barents Seas (Fig. 1c; Osika et al., 2022; Saferna et al., 2023). During the LIA, Hornbreen was confluent with several tidewater glaciers in Brepollen. The bed of the Hornbreen-Hambergbreen system is overdeepened c. 40 m b.s.l., and glacier recession will lead to the collapse of the ice bridge and presumably opening of the Hornsund strait between 2055 and 2065 (Grabiec et al., 2018; Saferna et al., 2023). The water depth at Hornbreen within the 1992 extent and the range of bathymetric data is on average 52 m, but exceeds 140 m in the central part of Brepollen (Błaszczyk et al., 2023). The geomorphology of the glacier forefield is representative of surging glacier landsystems, including fluted moraine, crevasse-squeeze ridges (CSRs) and a large submarine terminal moraine west of Treskelen (Evans and Rea, 1999; Moskalik et al., 2013; Osika et al., 2022). The diamicton of CSRs and underlying till contain abundant mollusc shells from the Early to the Late Holocene (Osika et al., 2022, and references therein).

Hansbreen is a tidewater glacier near the Hornsund mouth and one of the most investigated glaciers in Svalbard (e.g. Jania, 1988; Vieli et al., 2002; Otero et al., 2017; Błaszczyk et al., 2021), including monitoring of the surface mass balance since 1989 (Grabiec et al., 2012b). Apart from the main flow unit with a low-lying accumulation area of up to 500 m a.s.l., the glacier is supplied by four tributaries on the west (Fuglebreen, Tuvbreen, Deileggbreen and Staszelisen; Fig. 1c). The maximal water depth at the calving front was 94 m in 2014 (Błaszczyk et al., 2021). The subglacial topography of the main tongue is overdeepened below sea level for 10 km from the calving front (Grabiec et al., 2012b; Otero et al., 2017). Hansbreen has not surged during regular observations since 1982, but geomorphological and historical data indicate a surge advance in the 1870s and a possible minor surge in the late 1930s (Osika and Jania, 2024). The found landform assemblages are typical for surging glaciers, including CSRs, glacial lineations and a large submarine terminal moraine with a debris flow lobe (Evans and Rea, 1999; Osika and Jania, 2024).

Vestre Torellbreen is a tidewater glacier in SW Wedel Jarlsberg Land, supplied by Høgstebreen draining Amundsenisen, Profilbreen and Skoddebreen on the east and Lifjellfonna on the west (Fig. 1c; Hagen et al., 1993), and grounded below sea level besides the eastern tributaries and the ice divide (Macheret, 1981; van Pelt and Frank, 2025). The central part terminates in Isfjellbukta, whereas the west and east flanks are land-based. Within the range of bathymetric data and the LIA terminal moraine, the average water depth does not exceed 10 m (https://toposvalbard.npolar.no/). Previous investigations addressed glacier dynamics and geometry (Jania, 1988; Řehak et al., 2004), ice thickness and subglacial topography (Macheret et al., 1985), and geomorphology of the terrestrial forefield (Karczewski et al., 1984; Pękala et al., 1985; Szafraniec, 2013). To our knowledge, the western part of the forefield has only been described by Szafraniec (2013) based on remote sensing data, and there is not much known about the Holocene history of this glacier. The forefield of Vestre Torellbreen is a palimpsest of glacial and glaciofluvial landforms reflecting surge advances, including push moraines (Szafraniec, 2013).

Werenskioldbreen is a land-terminating glacier on the west coast of Spitsbergen (Fig. 1c). The glacier is divided by a distinct medial moraine into the northern part, Skilryggbreen, and the southern part with the Slyngfjellbreen and Angellkroken trunks. Werenskioldbreen and its forefield have been the subject of numerous investigations, including multi-annual series of glaciological, meteorological and hydrological data (e.g. Kosiba, 1960; Pälli et al., 2003; Majchrowska et al., 2015; Ignatiuk et al., 2022; Stachniak et al., 2022). A looped medial moraine visible in the photogrammetric photos from 1936 indicates that the glacier surged sometime before (https://toposvalbard.npolar.no/, photo S36_2646). Since then, surge-type behaviour has not been observed. The glacier has developed on a raised marine terrace from the Early Holocene (Birkenmajer and Olsson, 1998), and a small part of the subglacial topography (0.25% of the area) is overdeepened slightly below sea level (Fürst et al., 2017). The forefield is dominated by an ice-cored terminal moraine with a low ridge of proglacial push moraine (Kasprzak et al., 2020). The ages of marine shells from the terminal moraine, sediments melted out on the glacier surface, and sediments of the raised marine terrace within the forefield indicated the reduced glacier extent before the Last Glacial Maximum and during the Late Glacial-Holocene transition (Birkenmajer and Olsson, 1998; Traczyk, 2008). The ages of plant remains from the ground moraine suggested glacier advances before 1.5 cal ka BP and after 0.7 cal ka BP (Baranowski and Karlén, 1976), the latter of which was also inferred from the ages of subfossil tundra in the push moraine (Kasprzak et al., 2020). Here, these results are integrated with new dates to compare the fluctuations of Werenskioldbreen with other glaciers around Hornsund.

3. Methods

3.1. Geomorphological mapping

Geomorphological mapping and sample collection for ^{14}C and ^{10}Be dating were conducted in 2019–2024. The mapping was focused on the identification of glacier surge evidence (Figs. 2 and 3). We combined analysis of remote sensing data and field investigation, as recommended by Chandler et al. (2018). For Hansbreen and Werenskioldbreen, we used high-resolution DEMs and orthophotomaps generated from aerial images collected by Dornier DO228 aircraft in June 2020, produced and published by Błaszczyk et al. (2022). The horizontal resolution of these products for Hansbreen and Werenskioldbreen is 8.43 cm and 8.7 cm for orthomosaics and 16.9 cm and 17.4 cm for DEMs. To map the forefields of Vestre Torellbreen and Hornbreen, we used the ESRI World Imagery basemap (ESRI, 2025) with a horizontal resolution of 1.2 m, 2-meter resolution DEMs from ArcticDEM version 4.1 (Porter et al., 2023) and related hillshades with an azimuth of 315°. In the clouded and shaded areas, we also used a 0.4-meter resolution orthophotomap from aerial photographs captured in 2010 and 2011, available as WMTS from the Norwegian Polar Institute Map Data and Services (https://geodata.npolar.no/). Detailed maps with an extended description will be presented in a separate study.

3.2. Radiocarbon dating

We collected marine mollusc shells, paleosoils and driftwood from glacial sediments for radiocarbon dating for the time constraints on glacier changes. Mollusc shells were sampled from the surficial part of the ground and terminal moraines, excluding coastlines and channels. Two samples of subfossil soils below glacial diamict were taken on Oseanograftangen in the outer part of the Hansbreen forefield (Fig. 2c and d). We also sampled two shell fragments from a basal till layer on sediment-laden icebergs at Hansbreen. A broken whale rib with traces of subglacial transport (scratches like striations) was collected from the hummocky moraine on the Baranowski Peninsula in 1985.

Fifty-four samples of marine shells, two samples of paleosoils, three samples of driftwood and the whalebone were submitted to the Gliwice Radiocarbon Laboratory for accelerator mass spectrometry (AMS) radiocarbon dating. The pretreatment of each sample was tailored to its specific material. The shell samples were mechanically cleaned, washed in an ultrasonic bath in demineralised water for c. 0.5 hours. The outermost layer, potentially including secondary carbonates, was removed by subjecting it to 0.5 M HCl for 0.5 hours at room temperature. The samples were then crushed and subjected to hydrolysis using concentrated H_3PO_4 in a vacuum line. The resulting CO_2 was dried using an ethanol-dry ice trap at -70 °C, and a subsample equivalent to 1 mg of carbon was transferred to an AGE-3 automated graphitisation instrument in a quartz tube to produce elemental graphite (Němec et al., 2010; Wacker et al., 2010a). Pretreatment of organic samples was performed following the ABA (acid-base-acid) protocol. The first step was treatment with 0.5 M HCl for 1 hour at 85 °C. It was followed by treatment with 0.1 M NaOH for 1 hour at 85 °C to remove the humic compounds. The samples were then subjected to 0.5 M HCl for 1 hour at 85 °C. For driftwood samples, after the ABA treatment, the holocellulose was extracted using 5% $NaClO_2$ acidified to pH 2 by adding HCl at 70 °C for 1 hour. After each step, the samples were rinsed with demineralised water until a neutral pH was reached. The final step was drying at 60 °C. The whalebone sample underwent collagen extraction following the protocol by Piotrowska and Goslar (2002). The acid treatment (0.5 M HCl at room temperature) was applied to remove the apatite fraction, followed by a base wash (0.1 M NaOH at room temperature for 0.5 hours). Then, the collagen was extracted at pH 3 for 8 hours at 85 °C. The obtained supernatant was separated using Eeze syringe filters and freeze-dried. The prepared organic material was then packed into tin capsules and combusted using a Vario Micro Cube (Elementar™) elemental analyser. The CO_2 was then transferred to an AGE-3 system. The graphite, which had been pressed into cathodes, was analysed for its ^{14}C concentration using the MICADAS spectrometer, as described by Ustrzycka et al. (2025). Oxalic Acid II (NIST SRM-4990C) was used as a modern reference material. As background material, the phthalic anhydride (Sigma-Aldrich) was used for organic samples, while marble was used for shell samples. The radiocarbon ages and their uncertainties were calculated using BATS software (Wacker et al., 2010b), including correction for isotopic fractionation based on δ^{13}C values measured in MICADAS.

New and previously reported dates (in total 88 dates) were (re)calibrated to calendar years (cal BP; BP = 1950 CE) in OxCal 4.4.4 software (Bronk Ramsey, 2009, 2017, 2021) using Intcal20 calibration curve for the terrestrial material (Reimer et al., 2020) and the Marine20 for the mollusc shells and the whalebone (Heaton et al., 2020). In the case of published radiocarbon dates of molluscs based on the conventional technique with separate ages of the "inner" and "outer" fractions, we used the ^{14}C ages of the "inner" fractions for further analysis (e.g. Birkenmajer and Olsson, 1998). We applied the ΔR values recommended for western Svalbard, −61 ± 37 for molluscs and −160 ± 41 ^{14}C yrs for the whalebone (Pieńkowski et al., 2022). New results and published ^{14}C dates (AMS and conventional technique) are available in an open dataset (Osika et al., 2025). We present median values in Figs. 4 and 5, and refer to the median values rounded to the nearest century in the discussion.

3.3. ^{10}Be dating

Due to the lack of large boulders of non-carbonate rocks, in 2021 and 2022, we collected ten cobbles of dolomitic sandstones, quartzite and schist from the lateral terminal moraine of Hansbreen (Fig. 6a and b). Three samples were collected from the moraine ridges at the Flatpasset saddle c. 160 m a.s.l. and seven from the moraine ridges on a raised marine terrace at the foot of Fanytoppen c. 20–30 m a.s.l. In addition, one cobble of quartzite was collected from a trimline on Fanytoppen (Fig. 2e). We used a 2–4.5 cm thick top layer, cut from each sample with a saw, hammer, and chisel. The dip and dip directions were measured with a geological compass, and the topographic shielding was calculated using a point-based topographic shielding ArcGIS toolbox developed by Li (2018) and a 5-m DEM generated and published by the Norwegian Polar Institute (2014b) from aerial photographs from 2010 and 2011. Physical and chemical preparation was conducted at the Cosmogenic and Fallout Radioisotope Analysis Laboratory at the University of Zurich.

Due to different sample lithology, the density of every sample was measured in the laboratory, giving an average of 2.60 ± 0.05 g cm^{-3}. The samples were crushed and sieved to a 250–600 µm fraction. Quartz separation and purification included froth flotation, heavy liquid separation and leaching in diluted hydrofluoric acid. Because some samples required a longer time to extract 60 g of pure quartz, chemical isolation of beryllium was done in two batches following an adapted procedure of Kohl and Nishiizumi (1992). The ^{10}Be/^{9}Be ratio of the samples was measured with the MILEA AMS system at ETH Zurich (Maxeiner et al., 2019). Nuclide ratios were normalised to in-house secondary standards S2007N and S2010N (Christl et al., 2013). The final concentration of ^{10}Be in quartz was corrected to the background of preparation blank samples, while its error includes errors of AMS standards and blanks.

Exposure age of the samples was calculated with the "Cronus-Earth" online calculator ver. 3 (https://hess.ess.washington.edu, Balco et al., 2008). The local production rate of ^{10}Be was derived with the calibration sets of Baffin Bay and Arctic by Young et al. (2013) and the classic non-time-dependent scaling scheme by Lal (1991) and Stone (2000). We assumed that the effects of glacio-isostatic uplift, snow/vegetation cover and rock erosion on the exposure age are negligible. Final exposure ages and the data used to calculate them are presented in Table 1a and b, and Fig. 6a and b.

3.4. Historical maps and photographs

We used a set of historical maps and photographs from Spitsbergen expeditions in the 1600s–1900s (Table 2; Figs. 7, A.1, A.2, A.3 and A.4) as a source of qualitative data on changes in glacier extent over time and to identify surge evidence in their surface morphology. We considered the following glacier surge criteria: a rapid advance of the glacier terminus, looped moraines and deformed ice structures, a steepened and bulging terminus, heavy and extensive surface crevassing and shear margins on the glacier surface (Lefauconnier and Hagen, 1991; Copland et al., 2003; Grant et al., 2009). The historical photographs were acquired from the Austrian National Library Digital Image Archive (https://onb.digital/), the digital image archive of the Norwegian Polar Institute (https://bildearkiv.npolar.no/fotoweb/), the digital Archive of the Nikolai Aleksandrovich Morozov – the Russian Academy of Sciences (https://www.ras.ru/namorozovarchive/about.aspx) and the TopoSvalbard online archive (https://toposvalbard.npolar.no/). Descriptions by Sir Martin Conway (1897, 1898) from his expedition to Hornsund in 1897 provided additional information about the state of glaciers at the end of the LIA.

4. Results

4.1. Outline of glacial geomorphology

4.1.1. Hansbreen

The forefield of Hansbreen reveals typical features for surge-type glaciers, including fluted till plains with crevasse-squeeze ridges (CSRs) and terminal moraine on the Flatpasset saddle, marking the attempt to overpass the mountain ridge (Fig. 2a and b). Detailed description of the surge landsystem was provided by Osika and Jania (2024). We collected fine shell debris, fragments and a few intact marine mollusc shells from the till plain on the Baranowski Peninsula, Oseanograftangen and at the foot of Fannytoppen. Shell fragments and fine shell debris were also sampled from the surficial part of the terminal and hummocky moraines, including moraine ridges at the Flatpasset saddle, up to 160 m a.s.l.

In the outer forefield, we identified subfossil soil below glacial diamicton (Fig. 2c and d). The soil occurs within a short incision in schists of Oseanograftangen (N76° 59.998' E15° 39.091') as a dark brown layer 10 cm thick below 45 cm of massive, matrix-supported diamicton. C. 20 m to the NE (N77° 00.002' E15° 39.138'), we found a layer of organic material 0.3–0.5 cm thick below 45 cm of similar diamicton. From each site, we sampled the soils for AMS radiocarbon dating.

4.1.2. Hornbreen

The forefield of Hornbreen is dominated by fluted moraine and CSRs in the form of cross-cutting ridges and sediment mounds (Fig. 2f). On the Treskelen Peninsula, we also mapped terminal moraine (Fig. 2g). At Chomjakovbreen, eroded flutings, oriented W-E, contrast with an assemblage of distinct flutes oriented NW-SE, associated with well-defined CSR networks (Fig. A.5). We identified and collected shell fragments from the diamicton of CSRs, till plain and hummocky moraine on Treskelen, on the eastern coast of Selbukta and the southern coast of Hornbukta (Osika et al., 2022).

4.1.3. Vestre Torellbreen

The topography at Vestre Torellbreen forefield with flutings, CSRs, concertina eskers, overridden moraine ridges, and elongated drumlins (Fig. 3a and b) is typical for surging glaciers (e.g. Evans and Rea, 1999; Jónsson et al., 2014). We mapped three surge end moraines dissected by channels with braided outwash fans (Fig. 3c). In the southern part of the forefield, the outer controlled moraine is associated with a proglacial composite ridge system (Lovell and Boston, 2017). We sampled mollusc shell fragments, fine shell debris and driftwood from the surficial diamicton layer of the middle surge end moraine, LIA terminal moraine and the ice-cored hummocky moraine in the outer forefield. One shell fragment was collected from the surface diamicton layer, 1 cm thick, covering fluvioglacial sediments of an esker.

4.1.4. Werenskioldbreen

The forefield of Werenskioldbreen can be divided into the southern zone with drumlins and fluted till plains, and the northern part with outwash plains and kame terraces. We identified sparse, low CSRs overprinting the fluted moraine in the south-eastern forefield (Fig. 3 d and e). The topography reveals the remnants of two medial moraines, continuing on the glacier ice between Werenskioldbreen and Angellkroken and between Skilryggbreen and Slyngfjellbreen. Within the multi-crested terminal moraine, one can recognise the inner moraine ridge associated with the remnants of the Skilryggbreen-Slyngfjellbreen medial moraine and piggybacked on the outer part of the terminal moraine system, partly dissected with several channels. Fragments and intact mollusc shells occur sporadically in the till plain and terminal moraine.

4.2. Radiocarbon dating

4.2.1. Hansbreen

Radiocarbon ages of mollusc shells in the Hansbreen forefield range from the Early to the Late Holocene (Fig. 4a). Most samples are from the Early Holocene, including two shell fragments from sediment-laden icebergs from Hansbreen. One of them is the oldest dated shell in this forefield (GdA-7027; c. 11.3 cal ka BP). Three samples were dated to the Middle and two to the Late Holocene. The youngest shell was collected from the hummocky moraine at the foot of Fannytoppen and dated to c. 1.6 cal ka BP (GdA-6643). There is no relation between the ages of molluscs and the distance from the glacier terminus or elevation above sea level, presumably due to reworking and redeposition during glacier advances. The median age of collagen extracted from a whalebone collected from glacial diamict on the Baranowski Peninsula indicates the 17th century (median: 1683 CE, 1 sigma: 1599–1779 and 1792–1795 CE).

Radiocarbon dating of subfossil soils in the outer forefield reveals a few hundred calendar years discrepancy between the fractions above and below 250 µm (Osika et al., 2025). The age of moss phyllids from the soil in the erosional incision (GdA-7032) is similar to the age of the fraction below 250 µm (c. 0.6 cal ka BP; Osika et al., 2025). The sample from the second site (GdA-7033) contained traces of seeds and husks, which were too sparse for ^{14}C dating. Subfossil soil from this peninsula was dated by Pękala (1989) to a similar age of c. 2.75 cal ka BP obtained for our fraction >150 µm (GdA-7033.2).

4.2.2. Hornbreen

Our results and reported ^{14}C dates of marine shells at Hornbreen (Osika et al., 2022, and references therein) range from the Early to the Late Holocene (Fig. 4b). Most samples (18 from 29) are from the Early Holocene, with the oldest c. 10.8 and 10.9 cal ka BP collected on Treskelen. Three specimens from the east coast of Selbukta are younger than 1950 CE. Apart from these, the youngest samples are dated to c. 1.3 cal ka BP (Birkenmajer and Olsson, 1997), 2.1 and 2.6 cal ka BP. They were all collected on Treskelen.

4.2.3. Vestre Torellbreen

^{14}C dates of marine shells from the forefield of Vestre Torellbreen (7 samples) span the Early and Late Holocene (Fig. 5a). The oldest sample of shell debris was dated to c. 10.5 cal ka BP, similar to the ages of single shell fragments from the inner and outer forefield (c. 10.0 and 10.2 cal ka BP). The age of one shell from the LIA terminal moraine (GdA-6637) extends beyond the Marine20 calibration curve (Heaton et al., 2020) and is probably younger than 1950 CE. Three driftwood samples from diamicton on the top of moraine ridges were dated to the Late Holocene with median values of 702, 636 and 173 cal BP, although the youngest's 1 and 2 sigma confidence intervals exceed 1950 CE (Osika et al., 2025). There is no correlation between the ^{14}C ages and the location of sampling sites in particular end moraines.

4.2.4. Werenskioldbreen

New and published ^{14}C dates of molluscs from the Werenskioldbreen forefield form two clusters of ages, at the turn of the Late Glacial and Early Holocene and before the Last Glacial Maximum (Fig. 5b). Two younger shell fragments collected in 2020 are c. 11.7 and 12.5 cal ka BP, whereas two older shells predate the Last Glacial Maximum. The oldest shells are from the outer part, and the youngest from the inner part of the forefield and terminal moraine.

4.3. ^{10}Be dating

The ^{10}Be ages of cobbles from the moraine ridges of Hansbreen range from $0.07^{+0.11}_{-0.07}$ ka to 10.07 ± 0.56 ka (Table 1 a and b, Fig. 6 a and b). The quartzite boulder from the trimline on Fannytoppen yields an age of 0.2 ± 0.04 ka. Most ages do not exceed 1.2 ka, although two samples are from the Early Holocene (10.07 ± 0.56 ka and 6.75 ± 0.36 ka) and two from the late Middle Holocene (4.68 ± 0.27 ka and 4.65 ± 0.27 ka). There are no spatial patterns of ages at the Flatpasset saddle or the foot of Fanytoppen. In the former, the ^{10}Be ages range from 0.45 ± 0.04 ka to 10.07 ± 0.56 ka. In the latter, the ^{10}Be ages range from $0.07^{+0.11}_{-0.07}$ ka to 4.68 ± 0.27 ka (the outer moraine ridge) and from 1.08 ± 0.07 ka to 6.75 ± 0.36 ka (the inner ridge).

4.4. Historical data

4.4.1. 1613–1820

The maps from the 1600s and 1700s are highly generalised, but the approximate calving front positions can be estimated from changes in the shoreline. The maps outline the main branches of Hornsund, which appear more extensive than during the late LIA (Fig. A.1a). However, the accuracy is insufficient for a detailed comparison with subsequent works from the 1800s (Middelhoven, 1634; Doncker, 1663; van Keulen, 1714; Bellin, 1758). A more detailed map by William Scoresby from 1820 shows the confluent termini of Vestre and Austre Torellbreen marked as the “Iceberg Mount”. It presents two distinct fjord branches in the northern, two in the southern Hornsund, and one in the inner part of the fjord, which could correspond to Brepollen.

4.4.2. 1861–1900

The map from the Swedish expedition in 1861–1864 (Fig. A.1b; Dunér and Nordenskiöld, 1865) shows the termini of Werenskioldbreen, Hornbreen and two marine-terminating glaciers in northern Hornsund, probably Hansbreen and Paierlbreen or Mühlbacherbreen. The fjord branches are significantly shorter, and glaciers are more advanced than in the maps from the 1600s or 1700s. The terminus of Hornbreen appears more expanded in the southern part than in the subsequent maps from 1872, 1897 or 1899 (Figs. 7b and A.1; Peterman, 1874; Conway, 1898; Wassiliew, 1925). This map also shows a large glacier corresponding to the confluent lobes of Austre and Vestre Torellbreen (Fig. A.1b).

The photographs from the Austro-Hungarian expedition in 1872 documented most of the tidewater glaciers in Hornsund (Figs. 7 and A.2). The photos of Hansbreen described in detail by Osika and Jania (2024) revealed extensive surface crevassing, basal crevasses and debris-rich englacial structures exposed in the ice cliff. The terminus was bulging, steep and less advanced than the LIA terminal moraine position. The glaciers of Brepollen were confluent into a large system, Hornbreen, which had overpassed the southern part of Treskelen and was heavily crevassed in 1872 (Fig. 7). At this time, the terminus of Paierlbreen appears thickened, chaotically crevassed and radially splayed beyond Vestre Burgerbukta, in contrast to the smooth and subdued surface topography of Mühlbacherbreen (Figs. 7a and A.2b). In the map from 1897 (Fig. A.1d; Conway, 1898), Mühlbacherbreen appears to have a steep terminus and heavily crevassed surface on the confluence with Kvalfangarbreen and Wibebreen. In 1897, the surface of Körberbreen was also densely crevassed, and its terminus was expanded beyond constraining mountain ridges (Conway, 1898). A similar front position is presented in the Arc of Meridian expedition's map from 1900 (Fig. 7b; Wassiliew, 1925). Gåsbreen, the largest land-terminating glacier in Hornsund, was documented in the photograph and mapped in 1899 with a smooth surface topography and a debris-covered terminus at the terminal moraine (de Geer, 1923).

4.4.3. 1917–1918

The photographs and maps from Norwegian expeditions documented surface morphology and glacier extent in 1917 and 1918 (Figs. 7c, A.1e, f and A.3; Norwegian Polar Institute, 1921, 1938). By 1917, Hansbreen had splayed radially beyond Hansbukta, and its surface revealed a dense network of narrow cross-cutting crevasses and crevasse traces (Fig. A.3a; Osika and Jania, 2024). Compared with the maps from 1861–1899, the calving front of Hornbreen has slightly retreated (Figs. 7 and A.1f). The surface of Storbreen appears to be more crevassed and thicker than other flow units of Hornbreen . The medial moraine between Chomjakovbreen and Mendelejevbreen was folded and pushed to the north (Fig. 7c). By 1918, the eastern margin of Paierlbreen had slightly retreated, whereas Mühlbacherbreen had expanded beyond the fjord (Fig. A.3b). Compared with the map from 1897 (Conway, 1898), Kvalfangarbreen and Wibebreen were more advanced and pushed their medial moraines to the west. The photos from 1918 documented the crevassed surface of Werenskioldbreen with two looped medial moraines (Fig. A.3c and d). At that time, the extensive lobes of Vestre and Austre Torellbreen were at their terrestrial terminal moraines from the LIA (Fig. A.3e and f).

4.4.4. 1936

Aerial photographs from 1936 reveal widespread glacier retreat compared to 1918 and the late 1800s. The recession of Hornbreen has led to the development of Brepollen in the southeast from Treskelen (Fig. A.4a). Chomjakovbreen was still expanded and heavily crevassed. Samarinbreen had retreated over 1 km at the centreline since 1918. Chaotic crevassing can also be observed on Storbreen, the widest flow unit at the terminus of the glacier system in Brepollen, compared to the very narrow units of Mendeleevbreen, Svalisbreen and Hornbreen (Fig. A.4a). Wibebreen and Kvalfangarbreen retreated by 1936 and were dominated by the main trunk of Mühlbacherbreen (Fig. A.4b). The downwasting terminus of Werenskioldbreen exposed most of the terminal moraine (Fig. A.4c).

5. Glacier changes throughout the Holocene

5.1. Interpretation of the ^{14}C and ^{10}Be dates

Radiocarbon-dated mollusc shells and a whalebone redeposited in the moraines, and paleosoils below glacial diamict are evidence of glacier recession and subsequent advances. The spread ages of reworked marine shells ranging from the Early to the Late Holocene indicate reduced glacier extent and ice-free environments in recently or currently glacierized areas (Blake, 1989; Salvigsen and Høgvard, 2006; Osika et al., 2022). Our mollusc specimens represent suspension-feeding species sensitive to the high amounts of suspended inorganic material typical for the forefields of tidewater glaciers (Moore, 1977; Włodarska-Kowalczuk et al., 1998; Włodarska-Kowalczuk, 2007). They exhibit a preference for the outer and central basins of the Arctic fjords with lower glacial sedimentation (Włodarska-Kowalczuk, 2007) that was also observed in Hornsund and Kongsfjorden (Różycki, 1992;

Aswathy et al., 2023). In turn, the gaps in the mollusc chronologies may suggest glacier expansion (Osika et al., 2022). The limiting ages of glacier advances can be inferred from ^{14}C dates of subfossil vegetation layers embedded between or overlaid by glacial diamicton (e.g. Baranowski and Karlén, 1976) or driftwood redeposited inland during advance (e.g. Marks and Pękala, 1986).

More precise time constraints on glacier advances require cosmogenic exposure dating, yielding the timing of moraine abandonment (Balco, 2011; Philipps et al., 2017). However, the spread ^{10}Be dates on the moraine ridges of Hansbreen (Fig. 6a and b), in particular the Early and Middle Holocene ages, are not supported by the ^{14}C ages from this forefield, reported ^{10}Be ages from terminal moraines in southern Spitsbergen (Fig. 6c; Philipps et al., 2017) or changes in the ice-rafted debris (IRD) flux near the Hornsund mouth (Fig. 8; Devendra et al., 2023). We infer that most, if not all, of the ^{10}Be ages from the Hansbreen moraines are anomalously old and reflect nuclide inheritance from the previous exposure during the Early and Middle Holocene when Svalbard glaciers were smaller than present (Farnsworth et al., 2020). A similar scenario was described for the apparent ^{10}Be ages at the LIA moraine at Gletscherlukket, SE Greenland, ranging from 10.2 to 1.6 ka (Larsen et al., 2021). The youngest sample may reflect redeposition during the LIA advance or subsequent remobilisation. Hence, the ^{10}Be dates from the Hansbreen forefield are not considered in further discussion on glacier changes in the Holocene.

5.2. Late Pleistocene/Holocene transition – deglaciation

In the Late Weichselian, Hornsund was a pathway for an ice stream draining the Svalbard–Barents Sea Ice Sheet (Ottesen et al., 2007). Surface exposure dating with ^{10}Be, ^{26}Al, and *in situ* ^{14}C suggested coastal deglaciation of SW Spitsbergen between 18 and 16 ka, whereas the central and inner part of Hornsund were deglaciated by 13.3 ± 0.6 and 13.0 ± 0.7 ka (Young et al., 2018). East of Hornsund, the Storfjorden Ice Stream decayed after 15.3 cal ka BP and during the Younger Dryas–Holocene transition in response to advection of warm AW and atmospheric warming (Rasmussen and Thomsen, 2021; Joe et al., 2022). The shell ages at the Werenskioldbreen forefield indicate glacier retreat by 12.5 cal ka BP and emergence of a raised marine terrace after 10.0 cal ka BP (Fig. 5b; Birkenmajer and Olsson, 1998; Traczyk, 2008). We have not found the evidence for glacier re-advances in Hornsund during the Late Glacial–Early Holocene transition, which have been detected in Svalbard (Farnsworth et al., 2017, 2018, 2022, 2024). However, Joe et al. (2022) suggested a short still stand of re-advance of marine-terminating glaciers or ice streams in the nearby Little Storfjorden (eastern Svalbard) between 13–12 cal ka BP.

5.3. Early and Middle Holocene glacier retreat

Deglaciation was followed by glacier recession in the Early and Middle Holocene. The oldest fragment from a sediment-laden iceberg at Hansbreen (Osika et al., 2025) suggests that the glacier was smaller than present, at 11.3 cal ka BP. The oldest shells collected at Hornbreen and Vestre Torellbreen demonstrate extensive retreat by 10.9 cal ka BP and 10.4 cal ka BP. Based on the ages of molluscs, the reduced glacier extents persisted throughout the Early and Middle Holocene, as in the circumpolar Arctic (Farnsworth et al., 2020; Larocca and Axford, 2022). The mean summer air temperatures in Svalbard reconstructed from lake records were up to 7 °C higher in the Early Holocene than the 1850–

1900 CE preindustrial baseline (van der Bilt et al., 2019). The increased air temperature and the enhanced inflow of warm AW to Svalbard fjords led to glacier recession to their Holocene minima between 8.0–6.0 cal ka BP (Farnsworth et al., 2020). At the inner shelf outside of Hornsund, the highest flux of AW and associated maxima of the surface and bottom water temperatures occurred between 10–7 ka BP (Fig. 8; Devendra et al., 2023). From the circum-Arctic perspective, the vast majority of glaciers (>90% of 66 records) were smaller than present or entirely disappeared at 7–6 cal ka BP (Larocca and Axford, 2022). In Svalbard, lake archives indicate that small glaciers in their catchments were considerably smaller than present or absent in the Early and Middle Holocene (Snyder et al., 2000; Røthe et al., 2015, 2018; de Wet et al., 2018; Farnsworth et al., 2020). According to marine records, tidewater glaciers have retreated to the inner part of their fjords or even onto land (e.g. Bartels et al., 2017; Nielsen and Rasmussen, 2018; Allaart et al., 2020). However, Early Holocene re-advances of some glaciers were also recorded (Lønne, 2005; Forwick et al., 2010; Larsen et al., 2018; Farnsworth et al., 2024). A very low sedimentation rate and limited terrestrial input near Hornsund in 9–7 cal ka BP were linked to the reduced extent of tidewater glaciers (Devendra et al., 2023). Oerlemans et al. (2011) suggested that Hansbreen, the nearest tidewater glacier, retreated onto land by c. 8 cal ka BP based on the ages of subfossil vegetation reworked and melted out on the glacier surface. The minimum extent of southern Spitsbergen glaciers remains unknown, although recent investigation implies the persistence of the Åsgardfonna Ice Cap (NE Spitsbergen) in the Early Holocene due to glacio-isostatic rebound after deglaciation (Farnsworth et al., 2024). The postglacial relative sea level curves suggest that the rebound in Hornsund was significantly lower than in the NE Spitsbergen (Farnsworth et al., 2020), but the modelling of glacio-isostatic rebound showed that the largest glaciers in southern Spitsbergen survived the HTM (Fjeldskaar et al., 2018). It was also suggested that some glaciers in NE Spitsbergen persisted due to increased precipitation (Auer et al., 2025). However, with low elevations of southern Spitsbergen glaciers, such an effect may have been limited to the highest parts of the Amundsenisen ice field rather than tidewater glaciers with low-lying accumulation areas.

Fluctuations of the Hornbreen-Hambergbreen system determine whether Hornsund is a fjord or a strait between the Greenland Sea and the Barents Sea. The ages of molluscs from the Hornbreen forefield imply that glacier retreat led to the opening of the Hornsund strait in the Early Holocene (Fig. 4b). The passage was glacier-free presumably during most of the Holocene, as suggested by the ^{14}C shell dates ranging from the Early to the Late Holocene, and the Late Holocene ^{10}Be ages from terminal moraine on Treskelen (Figs. 4b and 6c; Philipps et al., 2017; Osika et al., 2022, 2025). However, the Late Glacial–Early Holocene glacial advances identified in the central and northern Spitsbergen (e.g. Lønne, 2005; Forwick et al., 2010; Farnsworth et al., 2017, 2020, 2024; Larsen et al., 2018) suggest the possibility of similar short-lived re-advances punctuating the glaciers' retreat, which could block the strait until the final collapse of the Hornbreen-Hambergbreen system (Osika et al., 2022). Previous investigations into the glacial history of Hornsund discussed the possibility of wide-range glacier advances around 8 ka BP (Grönfjorden Stage; Lindner et al., 1986; Lindner and Marks, 1993). This discrepancy with our results may be related to the limited number of samples used for dating the terminal moraine of Hornbreen (Marks and Pękala, 1986). The result of radiocarbon dating (c. 8 ka ^{14}C BP) was interpreted as the limiting age of Hornbreen advance up to Treskelen, and other glacier advances in Hornsund. Further works provided more ages from this moraine, ranging from the Early to Late Holocene, and excluded the hypothesis of an extensive Early Holocene advance (e.g. Birkenmajer and Olsson, 1997). Increased summer air temperatures during the HTM did not favour the positive mass balance of glaciers (Farnsworth et al., 2020), and we suggest that the possible advances at that time were glacier surges, which may have blocked the strait for a short time during the overall glacier recession.

5.4. Glacier re-growth in the first half of the Late Holocene

During the Late Holocene, the weakened advection of the warm AW and the sea surface temperature (SST) decrease were recorded in different parts of Svalbard (Ślubowska et al., 2005; Skirbekk et al., 2010; Łącka et al., 2019; Rasmussen and Thomsen, 2021), including the shelf outside Hornsund after c. 6 cal ka BP (Telesiński et al., 2018; Devendra et al., 2023). Glacier re-growth occurred in response to the reduced surface ablation due to lower summer air temperatures (e.g. Allaart et al., 2021) and a decline in SST, which controls the frontal ablation of tidewater glaciers (Luckman et al., 2015; Błaszczyk et al., 2023). The increase in IRD content in marine sediments suggested the growth of Tunabreen c. 5.6 cal ka BP (Forwick et al., 2010) and Nordenskiöldbreen c. 5.4 cal ka BP (Baeten et al., 2010), and overall increase in the glacial activity in Svalbard, e.g. in Kongsfjorden since c. 3.5 cal ka BP (Skirbekk et al., 2010) or Wahlenbergfjorden since c. 3.1 cal ka BP (Bartels et al., 2018). Lake sedimentary archives indicate the reapperance of glaciers in their catchments after c. 3.5 cal ka BP (Röthe et al., 2015, 2018; Allaart et al., 2021). Around 2.7 cal ka BP, marine-terminating Nathorstbreen surged twice (Kempf et al., 2013). We have not found evidence for glacier surges in Hornsund at this time, although low AW influx to the inner shelf west of Hornsund and increased iceberg rafting, probably from fluctuating glacier margins, occurred between 3.5–2.2 cal ka BP (Devendra et al., 2023).

The period of the Late Holocene glacier advances prior to the LIA was often called a Revdalen Stage in Hornsund around 2.5–3 ka BP (Karczewski et al., 1981; Marks, 1983; Lindner et al., 1986; Lindner and Marks, 1993). Although Hornsund glaciers expanded seaward by c. 4 cal ka BP (Jang et al., 2025), our ^{14}C-dating results (Figs. 4 and 5) show they were less extensive in this interval than their LIA maxima. Suspension-feeding molluscs were present within the maximum LIA extent of Hansbreen at c. 2.8 cal ka BP and Vestre Torellbreen at c. 2.1 cal ka BP. Mollusc shells collected at the Treskelen Peninsula are of similar ages (c. 2.1 and 2.5 cal ka BP; Osika et al., 2025). The outer part of the Hansbreen forefield was ice-free in the first half of the Late Holocene based on the ages of subfossil soil below glacial diamict (c. 3.6, 2.8 and 2.1 cal ka BP; Pękala, 1989; Osika et al., 2025). The extent of Hambergbreen and glaciers in Brepollen was still reduced at c. 2.4 and 2.1 cal ka BP, as indicated by the ages of benthic foraminifera and molluscs (Noormets et al., 2021). Based on the ^{14}C and ^{10}Be ages, Hornsund was a strait until 3.9 cal ka BP (the age of shell debris from Hornbukta) or longer, up to c. 2.1 cal ka BP (the oldest shell from Treskelen), or c. 1.9 ± 0.3 ka (average ^{10}Be moraine ages (n=4) on Treskelen in Philipps et al., 2017), depending on the intricate dynamics of surge-type glaciers of the Hornbreen-Hambergbreen system (Osika et al., 2022). The interval between 2.2–1.8 cal ka BP evidenced a stronger inflow of AW and higher SST and benthic water temperature (BWT) at the southwestern Svalbard inner shelf (Fig. 8; Devendra et al., 2023), similarly to Isfjorden (Brice et al., 2023), eastern Svalbard (Pawłowska et al., 2020) and in the western Barents Sea (Sarnthein et al., 2003; Łącka et al., 2019). Moreover, an increase in the mean annual and July air temperatures is visible in paleoclimate reconstructions from Svartvatnet lake in the Hornsund region (Fig. 8; Luoto et al., 2018). Hence, we imply that substantial tidewater glacier expansion in the early Late Holocene was hindered during higher SST and summer air temperatures.

5.5. Glacier advances in c. 2.2–1.5 cal ka BP

Glacier advances in southern Spitsbergen occurred between c. 2.2 and 1.5 cal ka BP. Based on the ^{10}Be ages, Hornbreen expanded to the Treskelen Peninsula by 1.9 ± 0.3 ka (Fig. 6c; n=4; Philipps et al., 2017), and this advance could correspond to the peak of IRD at the entrance to Hornsund and in the central basin of the fjord around 2.2 cal ka BP (Fig. 8; Devendra et al., 2023; Jang et al., 2025). Jang et al. (2025) linked this IRD peak with the overall glacier expansion or the collapse of tidewater glaciers. Notably, the advance of Hornbreen and the IRD peak coincided with increased mean annual and July air temperatures in Hornsund c. 2.2–1.9 cal ka BP (Fig. 8; Luoto et al., 2018) and the SST rise between 2.2–1.8 cal ka BP (Devendra et al., 2023). Hornbreen and its former tributary tidewater glaciers are surge-type, and rapid advance to the Treskelen Peninsula, suggested by mollusc shells only slightly older and of a similar age to the ^{10}Be moraine ages, indicate a surge event in this warmer interval. However, due to reworking during the LIA, mapping of the terrestrial forefield did not reveal geomorphic imprints of the pre-LIA advances of Hornbreen (Marks, 1983; Philipps et al., 2017; Osika et al., 2022).

Apart from Hornbreen, the ages of subfossil vegetation between two units of lodgement till indicate the advance of Werenskioldbreen before 1.5 cal ka BP, with the maximum extent probably comparable to the LIA culmination (Baranowski and Karlén, 1976). Similarly, the pre-LIA moraines of land-terminating glaciers in northern Wedel Jarlsberg Land (southern Spitsbergen) were deposited around 1.7 ± 0.1 ka (Scottbreen) and before 1.1 cal ka BP (Renardbreen) when the glaciers reached their Late Holocene maxima, 50–100 m outside the LIA terminal moraines (Dzierżek et al., 1990; Philipps et al., 2017). Glacier advances between 2.0 and 1.5 cal ka BP were also identified in other parts of Svalbard. According to ^{10}Be exposure dating of terminal moraines, a valley glacier, Linnébreen (W Spitsbergen), advanced and began to recede from its maximal Late Holocene extent at 1.6 ± 0.2 ka (Reusche et al., 2014) while the reconstructed ELA of a small valley glacier, Karlbreen (NW Spitsbergen), dropped c. 1.7 cal ka BP (Røthe et al., 2015). Based on the lichenometric method, one of several periods of moraine stabilisation in central and northern Spitsbergen occurred around 1500 years ago (Werner, 1993).

5.6. Glacier retreat in 1.5–1.0 cal ka BP

After the culmination of glacier advances, the following interval, c. 1.5–0.7 cal ka BP, corresponding to the MWP (Miller et al., 2010; Divine et al., 2011), brought glacier retreat. Radiocarbon ages of marine shells indicate the recession of Hansbreen (c. 1.6 cal ka BP) and Hornbreen (c. 1.3 cal ka BP; Fig. 4). One sample of mollusc evidences a smaller area of Vestre Torellbreen c. 0.7 cal ka BP than the LIA maximum (Fig. 5a). The ages of moss phyllids and bulk sediment from paleosoil (Fig. 4a; Osika et al., 2025) suggest that the outer part of the Hansbreen forefield was ice-free until 0.6 cal ka BP or longer. The decay of the Hornbreen-Hambergbreen system could lead to the re-opening of the Hornsund strait around 1.3 cal ka BP (Osika et al., 2022). Glacier retreat coincided with the enhanced influx of AW and SST increase at the SW Svalbard inner shelf between 1.5–1.0 cal ka BP (Fig. 8; Devendra et al., 2023), which was also recorded in Isfjorden (2.0–1.2 cal ka BP; Brice et al., 2023), eastern Svalbard (c. 1.7 cal ka BP; Pawłowska et al., 2020) or western Barents Sea (c. 1.6 cal ka BP; Sarnthein et al., 2003). Mean annual and July air temperatures inferred from the Svartvatnet lake were also higher around 1.5 cal ka BP (Fig. 8; Luoto et al., 2018).

Widespread recession has also affected land-terminating glaciers, including Werenskioldbreen in 1.5–0.7 cal ka BP (the ages of subfossil vegetation below two moraine units; Baranowski and Karlén, 1976), Renardbreen c. 1.1–0.6 cal ka BP (the ages of organogenic deposits between two moraine ridges; Dzierżek et al., 1990) and Longyearbreen c. 1.9–1.1 cal ka BP (the ages of subfossil bryophytes from a relict soil below glacier surface; Humlum et al., 2005). Climate warming was also evidenced by the return of the thermophilous mollusc *Mytilus edulis* to Isfjorden c. 0.9 cal ka BP (Samtleben, 1985; Salvigsen et al., 1992) as well as in the mean December-February temperatures in c. 800–1200 CE inferred from the Lomonosovfonna ice core (Divine et al., 2011). However, Devendra et al. (2023) identified a distinct peak of IRD c. 1.0 cal ka BP at the SW Svalbard inner shelf, which they linked with glacial activity based on an increase in terrigenous biomarkers and total organic carbon (TOC). Higher IRD flux values were also recorded at the Hornsund mouth at 1075 CE (Majewski et al., 2009) and in the central basin of the fjord system (Jang et al., 2025). Such sharp peaks of IRD may indicate enhanced calving after glacier surges (e.g. Paulabreen c. 1300 CE; Hald et al., 2001). Indeed, Jang et al. (2025) identified glacial advances in Hornsund at 940 and 1380 CE based on fluctuations of detrital neodymium isotopes values, although they linked them with a probable shorter duration of the MWP or a limited glacier response to this warmer period.

5.7. Glacier advances after c. 0.7 cal ka BP

In Svalbard, most Late Holocene glacier advances were dated to 1.0–0.5 cal ka BP (Farnsworth et al., 2020). This time span corresponds to moraine stabilisation in central and northern Svalbard c. 1000 and 650 years ago (Werner, 1993). According to the ^{10}Be ages of moraine abandonment, Hornbreen advanced to the Treskelen Peninsula around 0.7 ± 0.2 ka (Fig. 6c; Philipps et al., 2017). The limiting age of this advance can also be inferred from the age of driftwood from glacial diamicton on Treskelen, dated to 810 ± 70 ^{14}C yr BP (median 731 cal yr BP; Marks and Pękala, 1986). Therefore, tidewater glaciers blocked the Hornsund strait again if it had been reopened during the MWP (Osika et al., 2022). Radiocarbon ages of subfossil vegetation indicate an advance of Werenskioldbreen after 0.7 cal ka BP (Baranowski and Karlén, 1976; Kasprzak et al., 2020). The moss phyllids from the subfossil soil suggest a limiting age of the Hansbreen advance as c. 0.6 cal ka BP, which agrees well with the period of glacial advances c. 0.57 cal ka BP (1380 CE) inferred from IRD peak and detrital neodymium isotopes in the central basin of Hornsund (Jang et al., 2025). Similarly, the ages of organic material indicate that Renardbreen advanced sometime after 0.6 cal ka BP (Dzierżek et al., 1990). Surges of large glacier systems have also occurred c. 0.8–0.6 cal ka BP, such as Paulabreen c. 1300 CE (Hald et al., 2001; Larsen et al., 2018) or Nathorstbreen c. 1160 CE (Lovell et al., 2018), which advanced to their Late Holocene maxima. Notably, since 0.65 cal. ka BP Paulabreen has surged four times, with two surges between 0.65 cal. ka BP and c. 1898 CE, the surge c. 1898 CE and the last event in 2003–2005 CE (Larsen et al., 2018; Lovell and Fleming, 2023). Therefore, glacier surges in the Late Holocene were frequent, and glacier extents reflected coupled climatic conditions with dynamic advances. The winter temperatures until the 1200s CE were comparable to those in the warmer decades of the 1930s and 1990s (Fig. 8; Divine et al., 2011), and the period 1130–1300 CE witnessed intensive summer melt exceeding that from the 1990s (Grinsted et al., 2006).

We suggest that the increased meltwater delivery to glacier beds could have promoted glacier surges in Svalbard, as observed nowadays (Dunse et al., 2015). Surge events around and after 0.7 cal ka BP may have also occurred in Hornsund. The advance of Hornbreen dated to c. 0.7 ± 0.2 ka (Philipps et al., 2017) coincided with warmer conditions inferred from the Lomonosovfonna ice core (Grinsted et al., 2006; Divine et al., 2011). Joe et al. (2022) implied that the large terminal moraine complex in

Hambergbukta is a product of glacier surges after 0.7 cal ka BP based on the increased IRD content in marine sediments. A proglacial push moraine of Werenskioldbreen (Fig. 3f) contains a deformed layer of subfossil tundra dated to a similar age (c. 0.7 and 0.6 cal ka BP; Kasprzak et al., 2020). This single ridge, c. 4 m high, adjacent to a prominent ice-cored terminal moraine, is rather inconspicuous compared to multi-crested composite moraine ridges associated with Svalbard surge-type glaciers (Lovell and Boston, 2017). However, such a moraine system might have been eroded by meltwater or storm surges (Szupryczyński, 1963), or it may not have developed due to topographic conditions (Lønne, 2016). Although our geochronological data show no direct evidence of pre-LIA advances of Vestre Torellbreen, the overridden moraine ridges imply glacier advances sometime before the LIA maximum.

5.8. Little Ice Age and glacier surges

The tributary fjords of Hornsund appear more extensive in the maps from the 1600s and 1700s (Table 2) than during the 1800s. A similar observation was noted by Zagórski et al. (2023) for Recherchefjorden and interpreted as the reduced tidewater glaciers extent compared to the LIA maximum in the 1800s. The age of a whale bone in the terrestrial forefield of Hansbreen (median 1683 CE, 1 sigma: 1599–1779 and 1792–1795 CE) suggests that tidewater glaciers in Hornsund were less advanced at that time than at the LIA maximum. Subfossil vegetation from the lateral terminal moraine of Hansbreen was dated to a similar age (Pękala, 1989; Osika et al., 2025). A slightly different scenario for glacier development in Hornsund during the LIA was proposed by Jang et al. (2025) based on the fluctuations of detrital neodymium isotopes and bulk mineralogical data from the fjord sediments. They identified limited glacial activity at the onset of the LIA, glacier advances between 1580 and 1620 CE, followed by glacier retreat, and the second period of glacier advances around 1900 CE. A peak of IRD shortly before 1600 CE was recorded in the outer basin of Hornsund and interpreted as evidence for glacier surges or climatic advances (Majewski et al., 2009). In turn, the age of the whalebone from the Hansbreen forefield could correspond to the period of glacier recession after 1620 CE (Jang et al., 2025), which may have allowed for whaling in Hansbukta or at least colonisation of this fjord. Glacier retreat after c. 1620 CE agrees well with more extensive fjords in the historical maps (Table 2) compared to the late LIA.

According to the reconstruction from the Lomonosovfonna ice core, the clear onset of the LIA is challenging to define, and the temperature decline was gradual, with the coldest period around 1850 CE (Fig. 8; Divine et al., 2011). However, the cooling signal has been visible since 1600 CE in the oxygen isotopes and chemistry (Isaksson et al., 2003; Kekonen et al., 2005; Grinsted et al., 2006). Evidence for the LIA in the marine archives from Hornsund can be seen since c. 1600 CE, although the timing of glacier advances has been debated (Majewski et al., 2009; Pawłowska et al., 2016; Jang et al., 2025). The shift to the glacier-proximal conditions after c. 1800 CE (Pawłowska et al., 2016) corresponds to glacier surges in the late LIA. Extensive crevassing and a steepened, bulging terminus with open basal crevasses in the photographs from 1872 indicate that Hansbreen was surging and had not yet advanced to the LIA maximum marked by the terminal moraine (Osika and Jania, 2024). Chaotic, widespread crevassing and a thick, radially splayed terminus extended to the LIA terminal moraine imply a surge of Paierlbreen at or shortly before 1872 (Fig. 7a). The neighbouring Mühlbacherbreen appears less expanded in the map from 1872 (Fig. A.1c; Peterman, 1874), and a smooth surface topography in the photographs from this expedition implies a quiescent phase (Fig. A.2b). The splayed front of

Körberbreen in this map and the description of a glacier "full of hidden crevasses" from 1897 (Conway, 1898) imply a surge in the late 1800s. The terminus of Hornbreen appears radially splayed in the southern part in the map from 1861–1864 (Fig. A.1b; Dunér and Nordenskiöld, 1865) and heavily crevassed in the photos from 1872, which suggest a surge in or before 1860s. The Swedish-Russian Arc of Meridian Expedition map shows that Hambergbreen underwent a surge around 1900, and Hornbreen had slightly receded (Wassiliew, 1925). Land-terminating Gåsbreen was already extensive in the map from 1872 (Peterman, 1874), and the timing of its LIA maximum is difficult to define. In the photograph from 1899, the glacier surface appears to be smooth, with a debris-covered terminus at the LIA terminal moraine. Folded medial moraines and cross-cutting narrow crevasses and crevasse traces in the photographs from 1918 indicate that Werenskioldbreen was in the quiescent phase after a surge sometime before 1918 (Fig. A.3e and f). In 1918, Chomjakovbreen was during or shortly after a surge, pushing the medial moraine with Mendeleevbreen to the north. This surge event corresponds to the assemblage of flutings oriented NW-SE, overprinting older flutes from the late LIA surge of Hornbreen (Fig. A.5). By 1918, the calving front of Hornbreen had slightly retreated. However, a surface bulge and extensive crevassing suggested an ongoing surge of Storbreen, which pushed the other flow units of the Hornbreen system to the south by 1936. A surge-type Mühlbacherbreen had also advanced sometime before 1918 and expanded beyond Austre Burgerbukta (Fig. A.3b). A thickened terminus and extensive crevassing in the map from 1897 (Conway, 1898) imply a glacier surge in the 1890s. The timing of the LIA maximum of Vestre and Austre Torellbreen is difficult to estimate, as they were already expanded in the maps from 1820 and the 1860s (Scoresby, 1820; Dunér and Nordenskiöld, 1865) and in the photographs from 1918 (Fig. A.3e and f).

Many more glaciers in southern Spitsbergen and Svalbard experienced surge advances in the late 1800s. In south Spitsbergen, Recherchebreen and Renardbreen surged in the late 1870s or early 1880s, Scottbreen in the 1880s (Zagórski et al., 2023) and Hambergbreen c. 1900 (Wassiliew, 1925). Surges also affected the Kongsbreen, Kongsvegen- Kronebreen system (1869, Liestøl, 1988), Nathorstbreen (c. 1870; Liestøl, 1977), Von Postbreen (1870, Liestøl, 1993), Paulabreen (before 1898; Ottesen et al., 2008), and even small valley glaciers in central Spitsbergen (Mannerfelt et al., 2024). Geomorphological and historical records show that the maximum LIA extents often correspond to surge events (Liestøl, 1969; Lefauconnier and Hagen, 1991; Lovell et al., 2018; Dowdeswell et al., 2020; Zagórski et al., 2023; Mannerfelt et al., 2024; Osika and Jania, 2024). Such clustering of glacier surges in different parts of Svalbard suggests some supra-regional factors controlling these dynamic advances. December–February surface air temperature values inferred from the Lomonosovfonna ice core suggest that some surge events coincided with warmer winters (e.g., in the 1860s, early 1870s or 1890–1910) compared to the 1850s or 1880s (Divine et al., 2011). The surges of valley land-terminating glaciers were linked to the thermal switch from cold-based to polythermal conditions (Lovell et al., 2015; Sevestre et al., 2015). We think that the widespread surges of larger, warm-based land-terminating and tidewater glaciers, where such thermal transition would not be a trigger mechanism (Sevestre et al., 2015), could have been related to increased water content at the glacier beds delivered from the surface and produced by frictional heating, as pointed out in the enthalpy balance theory (Benn et al., 2019). The question arises about the mean summer temperatures or the role of winter precipitation in glaciers' re-growth during the LIA (e.g. Nesje et al., 2008; D'Andrea et al., 2012). Therefore, further investigations into the LIA climate conditions and glacier surge mechanisms are necessary to identify the triggering factors of the widespread late LIA surges. Such works may also improve our understanding of the role of surging in the pre-LIA glacier advances and predictions of further decay of land ice masses.

5.9. Glacier retreat punctuated by surge advances in the 20th and 21st centuries

The LIA was followed by rapid climate warming in Svalbard in the 1920s and 1930s and glacier retreat interrupted by glacier surges (Martín-Moreno et al., 2017; Nordli et al., 2020). In Hornsund, Körberbreen surged in 1938 (Liestøl, 1969). In the photos from 1936 (Fig. A.4a), Storbreen appears to be after a surge, evidenced by an extensively crevassed and thickened terminus contrasting with dead ice on Treskelen. Interestingly, more Svalbard glaciers experienced surges in the 1930s, including Negribreen (1935–1936; Liestøl, 1969), Bråsvellbreen (1936–1938; Schytt, 1969), Etonbreen, Rijpbreen and Clasebreen (1938, Hagen et al., 1993) or Scott Turnerbreen (sometime in c. 1914–1936; Mannerfelt et al., 2024). The 1920s and 1930s were much warmer than the 1910s, and the 1930s witnessed frequent winter-warming events with positive temperatures between October and April (Nordli et al., 2020). We suggest that these surges in Svalbard may have occurred in response to increased water content at the glacier bed from enhanced summer melt and more frequent winter melt days in this decade.

Glacier surges in Hornsund occurred in the 1960s (e.g. Mühlbacherbreen; Błaszczyk et al., 2013, and Hambergbreen; Lefauconnier and Hagen, 1991). Vestre Torellbreen was surging in the 1960s (Jania, 1988), with the maximal extent marked by the middle surge end moraines. The 1950s were the second warmer period in Svalbard in the twentieth century, and like the 1930s, they witnessed frequent positive temperatures in winter (Nordli et al., 2020). The 1960s were another period of glacier surge clustering in Svalbard, including Blomstrandbreen (1956–1966; Burton et al., 2016), Tunabreen (1966–1971; Richard and Dowdeswell, 1994) or Marmorbreen (1965–1970; Hagen et al., 1993). The latest surge advances in Hornsund were experienced by Paierlbreen in 1992–1995, Mendeleevbreen in 1997/98–2002 and Svalisbreen in 2016–2020 (Szafraniec, 2020; Błaszczyk et al., 2023). In southern Spitsbergen, surges also affected Nathorstbreen with tributiaries, which advanced over 15 km in 2008–2016 (Sund et. al., 2014; Lovell et al., 2018) or Recherchebreen in 2018–2020 (Zagórski et al., 2023). In 2007–2013, Vestre Torellbreen advanced due to the surge of its tributary glacier Profilbreen since 2007 (Sund et al., 2009). These events were one of many glacier surges in Svalbard this century (e.g. Sund et al., 2009; Kääb et al., 2023). Their advances were usually smaller than previous ones, which might suggest reduced reservoir filling by ice masses, and more abundant penetration of meltwater to glacier beds or subglacial sediments in the periods of progressive warming. Tunabreen in Tempelfjorden is a good example of a surge-type glacier with a short recurrence interval (40 years) and smaller advances during successive active phases (Flink et al., 2015). This type of “convulsive” retreat appears to be increasingly common (e.g. Recherchebreen; Zagórski et al., 2023) and should not be excluded from reconstructions of deglaciation processes during earlier warmer periods of the Holocene.

5.10. Glacier fluctuations in southern Spitsbergen in a pan-regional perspective

Reconstructing glacier changes in southern Spitsbergen raises the question of their similarity or difference to the rest of Svalbard. Data on the Holocene glacier fluctuations in the entire archipelago are limited, but the timing of warmer and colder phases has been generally consistent in different parts of Svalbard (Fig. 8; Farnsworth et al., 2020). Location between the warmer waters of the eastern Greenland Sea to the west, the cold Arctic Ocean to the north, and the cool Barents Sea to the east determines the contrasts in contemporary climatic conditions across the archipelago (e.g. Gjelten et al., 2016; Hanssen-Bauer et al., 2019). Climatic gradients also result from differences in the extent and duration of sea ice (Nihoul and Kostianoy, 2009; Bintanja and Selten, 2014; Gjelten et al., 2016), which affects air temperature and precipitation patterns. Southern Spitsbergen is more exposed to the advection of warmer and wetter air masses from the southwest, and to the variable influence of the ocean currents and sea ice extent (Migała et al., 2023). Assuming that the regional climate gradients were similar earlier in the Holocene, this region may have experienced slightly higher snow accumulation, as is the case today (van Pelt et al., 2016; Østby et al., 2017; Schmidt et al., 2023), which may have contributed to glacier development during the transition from warmer to colder phases of the Holocene.

The development, persistence, and evolution of glacierisation depend on topographic conditions controlling glacier extent and morphological type, which determine their vulnerability to changes in mass balance components (e.g. Oerlemans, 1989; Benn and Evans, 2010). The presence of tidewater glaciers implies additional significant mass loss due to frontal ablation, making marine-terminating glaciers more sensitive to changes in climate and the thermal and dynamic properties of seawater at the calving front (e.g. Błaszczyk et al., 2013; Li et al., 2025). Ground-penetrating radar studies of ice thickness (e.g. Grabiec et al., 2012b) and inversion models (Fürst et al., 2018; van Pelt and Frank, 2025) indicate that long sections of glacierized valley floors in southern Spitsbergen are lower than those in the other regions of Svalbard, including extensive overdeepenings below sea level. Such subglacial topography has presumably hastened frontal ablation during the increased inflow of warm AW and the SST rise. The bed of Amundsenisen, the largest and highest accumulation area of the glacier system of the Wedel Jarlsberg Land, is also close to the sea level (Glowacki et al., 2008). The regional glacier hypsometry (Fig. 1b) shows that the widest surface area of the S Svalbard glaciers is significantly lower than in the other parts of Svalbard (Østby et al., 2017 – Fig. 2; van Pelt and Frank, 2025 – Fig. 6), which has presumably promoted their recession in the Holocene, also influencing the highest sections due to the glacier surface lowering (Szafraniec and Dobiński, 2020). Today, southern Spitsbergen appears to be more sensitive to mass balance changes (Schuler et al., 2020; Schmidt et al., 2023; van Pelt and Frank, 2025) than other regions of Svalbard. Considering the regional glacier surface mass balance data (Schmidt et al., 2023 – Fig. 7), one can observe that during the second decade of the 21st century, the mean annual accumulation rate in southern Spitsbergen was higher by a factor of 1.26 compared to north-western Spitsbergen, and the mean summer surface ablation rate was higher by a factor of 1.58. The amplitude between accumulation and surface ablation is also higher for southern Spitsbergen than for the north-western region (approximately 1.86 m w.e. y^{-1} and 1.28 m w.e. y^{-1}, respectively). A comparison with other regions of Svalbard reveals similar differences. Therefore, a more pronounced and rapid response of southern Spitsbergen glaciers to climate change, particularly warming, can be expected.

6. Conclusions

We integrated geomorphological, geochronological, and historical data to reconstruct the glacial history of southern Spitsbergen with a special focus on Hansbreen, Hornbreen, Werenskioldbreen and Vestre Torellbreen.

- The Early Holocene retreat of tidewater glaciers allowed colonisation of new ice-free branches of Hornsund. The oldest marine mollusc shell from the Hansbreen forefield suggests that the glacier was smaller than present at 11.3 cal ka BP. Glacier recession was linked to increased summer insolation driven by orbital forcing, and SST rise. The collapse of the Hornbreen-Hambergbreen glacier system led to the opening of the Hornsund strait by 10.9 cal ka BP.

- The Late Holocene climate cooling led to glacier re-growth. However, the extent of tidewater glaciers in Hornsund in the first half of the Late Holocene was still reduced compared to their LIA maxima. The expansion of tidewater glaciers was probably hindered by SST rise and the atmospheric warming.

- The climate cooling was interrupted by a short warm interval with glacier retreat between c. 1.5–0.7 cal ka BP, as evidenced by the radiocarbon ages of marine mollusc shells and subfossil vegetation.

- The Late Holocene glacier maxima corresponded to glacier surges. The surge events from the late LIA were documented in the photographs from 1872, 1917 and 1918, which captured ongoing glacier surges or the early quiescent phase. The dynamic advances in the Late Holocene were preceded by mass build-up due to climate cooling and probable increase of snow precipitation at the beginning of the warmer period. Still, they occurred in probably warmer intervals, according to published paleoclimatic data.

- New ^{14}C dates of marine shells from Treskelen and published ^{10}Be ages from this peninsula (Philipps et al., 2017) suggest that Hornsund may have been an open strait even until 1.9 ± 0.3 ka when Hornbreen advanced to Treskelen. Subsequent re-opening was possible around 1.3 cal ka BP until the second re-advance c. 0.7 ± 0.3 ka.

- Surge-type behaviour of glaciers in southern Spitsbergen appears to be characteristic of transitions from colder to warmer intervals, leading to significant frontal advances after the climatic thermal minimum. Glaciers are a system for transporting mass, water, and heat, striving to reduce flow resistance and maximise mass transport efficiency through the shape evolution during the active phase of glacial surge (extension of the glacier tongue). Glacier surge is a natural response to increased heat transfer in the global atmospheric and oceanic circulation system. Although initially providing stability and energy efficiency to the glacier, it later causes accelerated recession, as mass transfer consistent with the gravitational gradient pulls a significant portion of the glacier toward the ablation zone. We suggest that "convulsive" deglaciation involving glacier surges is climatically driven and accelerates the decay of land-based ice masses. As surge-type glaciers are widespread across the archipelago, coupling climate change with glacier dynamics should be considered as a normal process affecting the Holocene glaciation history of Svalbard. Surging glaciers may also be regarded as climatically controlled systems, leaving distinct imprints in the geological records.

- The general pattern of the Holocene glacier fluctuations in southern Spitsbergen is similar to that observed in the other regions of Svalbard (Farnsworth et al., 2020). However, the specific topography with large, low-inclined tidewater glaciers, and the proximity of the West Spitsbergen Current transporting warmer Atlantic Waters, combined with exposure to warmer air masses, make this area more sensitive to changes in glaciation, in particular during warmer periods of the Holocene.

- Today, southern Spitsbergen has a more negative climatic mass balance with higher summer ablation and winter accumulation than in most of Svalbard (Schmidt et al., 2023). High mass loss in summer is promoted by low hypsometry and subglacial topography with overdeepenings below sea level, which hasten frontal ablation once the glacier termini retreat into deeper water. These topographic conditions have presumably fostered glacier recession earlier in the Holocene.

Acknowledgements

We thank the participants of the expeditions to Spitsbergen in 2019–2024, organised by the University of Silesia in Katowice, for their support in fieldwork. The infrastructure of the Polish Polar Station Hornsund, managed by the Institute of Geophysics, Polish Academy of Sciences was used during field campaigns. We thank Mateusz Strzelecki for providing access to the Stanislaw Baranowski Polar Station of the University of Wrocław. The studies were carried out using logistic equipment of the Polar Laboratory of the University of Silesia in Katowice. We thank Janusz Godziek for his help with the point-based topographic shielding toolbox. We are especially grateful to Maria Włodarska-Kowalczuk and Jan Marcin Węsławski (Institute of Oceanology, Polish Academy of Sciences) for their constructive comments on the ecology of suspension feeding species. The internship of A.O. at the University of Zurich under the supervision of Andreas Vieli in 2022 was supported by the Polish National Agency for Academic Exchange (grant no. BPN/BEK/2021/1/00412/U/00001).

Funding

This work was supported by the National Science Centre of Poland (grant no. 2021/41/N/ST10/02070); the Research Council of Norway (Arctic Field Grant no. 310661); the Centre for Polar Studies, University of Silesia – the Leading National Research Centre (KNOW) in Earth Sciences (2014–2018) [grant number 03/KNOW2/2014]; and the Institute of Earth Sciences, University of Silesia in Katowice. The ^{10}Be dating analysis was funded by the Department of Geography at the University of Zurich.

Author contributions

AO: conceptualization, data curation, formal analysis, funding acquisition, investigation, methodology, project administration, visualization, writing. JJ: conceptualization, funding acquisition, investigation, methodology, resources, supervision, writing. NP: data curation, formal analysis, investigation, methodology, resources, writing. DT: data curation, formal analysis, investigation, methodology, resources, writing. JES: conceptualization, supervision, visualization, writing – review and editing. DD: visualization, writing – review and editing. MC: data curation, investigation. ME: data curation, methodology, resources. AV = writing – review and editing, resources.

AO = Aleksandra Osika, JJ = Jacek Jania, NP = Natalia Piotrowska, DT = Dmitry Tikhomirov, JES = Joanna Ewa Szafraniec, DD = Dhanushka Devendra, MC = Marcus Christl, ME = Markus Egli, AV = Andreas Vieli

References

Allaart, L., Müller, J., Schomacker, A., Rydningen, T.A., Håkansson, L., Kjellman, S.E., Mollenhauer, G., Forwick, M., 2020. Late Quaternary glacier and sea-ice history of northern Wijdefjorden, Svalbard. Boreas. 49, 417-437. https://doi.org/10.1111/bor.12435.

Allaart, L., Schomacker, A., Larsen, N.K., Nørmark, E., Rydningen, T.A., Farnsworth, W.R., Retelle, M., Brynjólfsson, S., Forwick, M., Kjellman, S.E., 2021. Glacial history of the Åsgardfonna Ice Cap, NE Spitsbergen, since the last glaciation. Quat. Sci. Rev. 251, 106717. https://doi.org/10.1016/j.quascirev.2020.106717.

Aswathy, N.K., Krishnapriya, P.P., Neenu, P., Bijoy Nandan, S., Jima, M., Jayachandran, P.R., Harikrishnan, M., Krishnan, K.P., 2023. Spatial dynamics of macrofauna with special reference to bivalve molluscs in the Arctic Kongsfjord, Svalbard, Norway. Polar Sci. 35, 100916. https://doi.org/10.1016/j.polar.2022.100916.

Auer, A. G., van der Bilt, W.G.M., Schomacker, A., Bakke, J., Støren, E.W., Buckby, J.M., Cederstrøm, J.M., van der Plas, S., 2025. Hydroclimate intensification likely aided glacier survival on Svalbard in the Early Holocene. Commun. Earth Environ. 6, 100. https://doi.org/10.1038/s43247-025-02064-z.

Baeten, N.J., Forwick, M., Vogt, C., Vorren, T.O., 2010. Late Weichselian and Holocene sedimentary environments and glacial activity in Billefjorden, Svalbard. Geol. Soc. Lond. Spec. Publ. 344, 207-223. https://doi.org/10.1144/SP344.15.

Balco, G., 2011. Contributions and unrealized potential contributions of cosmogenic-nuclide exposure dating to glacier chronology, 1990–2010. Quat. Sci. Rev. 30(1-2), 3-27. https://doi.org/10.1016/j.quascirev.2010.11.003.

Balco, G., Stone, J.G., Lifton, N.A., Dunai, T.J.A, 2008. A complete and easily accessible means of calculating surface exposure ages or erosion rates from 10Be and 26Al measurements. Quat. Geochronol. 3(3), 174-195. https://doi.org/10.1016/j.quageo.2007.12.001.

Baranowski, S., 1977. Changes of Spitsbergen glaciation at the end of the Pleistocene and in Holocene. Quaest. Geogr. 4, 5-28.

Baranowski, S., Karlén, W., 1976. Remnants of Viking age tundra in Spitsbergen and northern Scandinavia. Geogr. Ann. Ser. A. 58(1/2), 35-49. https://doi.org/10.2307/520741.

Bartels, M., Titschack, J., Fahl, K., Stein, R., Hebbeln, D., 2018. Wahlenbergfjord, eastern Svalbard: A glacier-surrounded fjord reflecting regional hydrographic variability during the Holocene? Boreas. 47(4), 1003-1021. https://doi.org/10.1111/bor.12325.

Bartels, M., Titschack, J., Fahl, K., Stein, R., Seidenkrantz, M.-S., Hillaire-Marcel, C., Hebbeln, D., 2017. Atlantic Water advection vs. glacier dynamics in northern Spitsbergen since early deglaciation. Clim. Past. 13, 1717-1749. https://doi.org/10.5194/cp-13-1717-2017.

Bellin, J.N., 1758. Carte Du Spits-Berg: Suivant les Hollandois pour Servir a l'Histoire Generale des Voyages. Publisher J.N. Bellin, Paris. Available at https://cartotecadigital.icgc.cat/digital/collection/europa/id/2198 (access 12.09.2025)

Benn, D.I., Fowler, A.C., Hewitt, I., Sevestre, H., 2019. A general theory of glacier surges. J. Glaciol. 65(253), 701-716. https://doi.org/10.1017/jog.2019.62.

Benn, D.L., Evans, D.J.A 2010: Glaciers and Glaciation. 2nd edition. Routledge, London. https://doi.org/10.4324/9780203785010.

Berben, S.M.P., Husum, K., Cabedo-Sanz, P., Belt, S.T., 2014. Holocene sub-centennial evolution of Atlantic water inflow and sea ice distribution in the western Barents Sea. Clim. Past. 10, 181-198. https://doi.org/10.5194/cp-10-181-2014.

Bintanja, R., Selten, F., 2014. Future increases in Arctic precipitation linked to local evaporation and sea-ice retreat. Nature. 509, 479-482. https://doi.org/10.1038/nature13259.

Birkenmajer, K., Olsson, I.U., 1997. Radiocarbon dating of marine bivalve shells from Holocene moraines at inner Hornsund, South Spitsbergen. Bull. Pol. Acad. Sci. Earth Sci. 45(1), 59-66.

Birkenmajer, K., Olsson, I.U., 1998. Radiocarbon-Dated Late Pleistocene and Early Holocene Marine Shells at Werenskioldbreen, South Spitsbergen. Bull. Pol. Acad. Sci. Earth Sci. 46(1), 21-34.

Blake, W., 1989. Radiocarbon Dating by Accelerator Mass Spectrometry; A Contribution to the Chronology of Holocene Events in Nordaustlandet, Svalbard. Geogr. Ann. Ser. A. 71(1-2), 59-74. https://doi.org/10.1080/04353676.1989.11880273.

Błaszczyk, M., Jania, J.A., Ciepły, M., Grabiec, M., Ignatiuk, D., Kolondra, L., Kruss, A., Luks, B., Moskalik, M., Pastusiak, T., Strzelewicz, A., Walczowski, W., Wawrzyniak, T., 2021. Factors Controlling Terminus Position of Hansbreen, a Tidewater Glacier in Svalbard. J. Geophys. Res. Earth Surf. 126(2), e2020JF005763. https://doi.org/10.1029/2020JF005763.

Błaszczyk, M., Jania, J.A., Hagen, J.O., 2009. Tidewater glaciers of Svalbard: Recent changes and estimates of calving fluxes. Pol. Polar Res. 30(2), 85-142.

Błaszczyk, M., Jania, J.A., Kolondra, L., 2013. Fluctuations of tidewater glaciers in Hornsund Fjord (Southern Svalbard) since the beginning of the 20th century. Pol. Polar Res. 34(4), 327-352. https://doi.org/10.2478/popore−2013−0024.

Błaszczyk, M., Laska, M., Sivertsen, A., Jawak, S.D., 2022. Combined Use of Aerial Photogrammetry and Terrestrial Laser Scanning for Detecting Geomorphological Changes in Hornsund, Svalbard. Remote Sens. 14(3), 601. https://doi.org/10.3390/rs14030601.

Błaszczyk, M., Moskalik, M., Grabiec, M., Jania, J., Walczowski, W., Wawrzyniak, T., Strzelewicz, A., Malnes, E., Lauknes, T.R., Pfeffer, W.T., 2023. The Response of Tidewater Glacier Termini Positions in Hornsund (Svalbard) to Climate Forcing, 1992–2020. J. Geophys. Res. Earth Surf. 128(5), e2022JF006911. https://doi.org/10.1029/2022JF006911.

Brice, C., de Vernal, A., Francus, P., Forwick, M., Nam, S.-I., 2023. Millennial-scale oscillations and an environmental regime shift around the Middle to Late Holocene transition in the North Atlantic region based on a multiproxy record from Isfjorden, West Spitsbergen. Boreas. 52, 42-59. https://doi.org/10.1111/bor.12602.

Bronk Ramsey, C. 2021. OxCal v.4.4.4 [software]. Available at https://c14.arch.ox.ac.uk/oxcal.html (access 12.09.2025)

Bronk Ramsey, C., 2009. Bayesian Analysis of Radiocarbon Dates. Radiocarbon. 51(1), 337-360. https://doi.org/10.1017/S0033822200033865.

Bronk Ramsey, C., 2017. Methods for Summarizing Radiocarbon Datasets. Radiocarbon. 59(6), 1809-1833. https://doi.org/10.1017/RDC.2017.108.

Burton, D.J., Dowdeswell, J.A., Hogan, K.A., Noormets, R., 2016. Marginal fluctuations of a Svalbard surge-type tidewater glacier, Blomstrandbreen, since the little ice age: a record of three surges. Arct. Antarct. Alp. Res. 48(2), 411-426. https://doi.org/10.1657/AAAR0014-094.

Chandler, B.M., Lovell, H., Boston, C.M., Lukas, S., Barr, I.D., Benediktsson, Í.Ö., Benn, D.I., Clark, C.D., Darvill, C.M., Evans, D.J., Ewertowski, M.W., Loibl, D., Margold, M., Otto, J., Roberts, D.H., Stokes, C.R., Storrar, R.D., Stroeven, A.P., 2018. Glacial geomorphological mapping: A review of approaches and frameworks for best practice. Earth-Sci. Rev. 185, 806-846. https://doi.org/10.1016/j.earscirev.2018.07.015.

Christl, M., Vockenhuber, C., Kubik, P.W., Wacker, L., Lachner, J., Alfimov, V., Synal, H.A., 2013. The ETH Zurich AMS facilities: Performance parameters and reference materials. Nucl. Instrum. Methods Phys. Res., B. 294, 29-38. https://doi.org/10.1016/j.nimb.2012.03.004.

Conway, W.M., 1897. The first crossing of Spitsbergen. J.M. Dent & Co., London.

Conway, W.M., 1898. With ski & sledge over Arctic glaciers. J.M. Dent & Co., London.

Copland, L., Sharp, M.J., Dowdeswell, J.A., 2003. The distribution and flow characteristics of surge-type glaciers in the Canadian high Arctic. Ann. Glaciol. 36, 73-81. https://doi.org/10.3189/172756403781816301.

D'Andrea, W.J., Vaillencourt, D.A., Balascio, N.L., Werner, A., Roof, S.R., Retelle, M., Bradley, R.S., 2012. Mild Little Ice Age and unprecedented recent warmth in an 1800 year lake sediment record from Svalbard. Geology. 40 (11), 1007-1010. https://doi.org/10.1130/G33365.1.

de Geer, G., 1923. Description de Ia region exploree, Geologie in Missions scientifiques pour Ia mesure d'un arc de meridien au Spitzberg, enterprises en 1899-1902 sous le auspicies de governementes suedois et russe. Mission suedois Tome II. Physique terrestre. Meteorologie. Historie naturelle -1xieme section. Topographie. Geologie. Stockholm Aktiebolagel Centraltryckeriet 1923.

de Wet, G.A., Balascio, N.L., D'Andrea, W.J., Bakke, J., Bradley, R.S., Perren, B., 2018. Holocene glacier activity reconstructed from proglacial lake Gjøavatnet on Amsterdamøya, NW Svalbard. Quat. Sci. Rev. 183, 188-203. https://doi.org/10.1016/j.quascirev.2017.03.018.

Devendra, D., Łącka, M., Szymańska, N., Szymczak-Żyła, M., Krajewska, M., Weiner, A.K., De Schepper, S., Simon, M.H., Zajączkowski, M., 2023. The development of ocean currents and the response of the cryosphere on the Southwest Svalbard shelf over the Holocene. Glob. Planet. Change. 228, 104213. https://doi.org/10.1016/j.gloplacha.2023.104213.

Divine, D., Isaksson, E., Martma, T., Meijer, H.A.J., Moore, J., Pohjola, V., van de Wal, R.S.W., Godtliebsen, F., 2011. Thousand years of winter surface air temperature variations in Svalbard and northern Norway reconstructed from ice-core data. Polar Res. 30, 7379. https://doi.org/10.3402/polar.v30i0.7379.

Doncker, B.H., 1663. Paskaert van Spitsbergen, met alle zijn zeekusten zoo veel tot noch toe bekent is. In: De Zee-Atlas Ofte Water-Waereld. Amsterdam, Henry Doncker, 1660. Reprod. of Spitsbergen in: Conway (1906). P. 339; Geogr. journ. Vol. 21. London 1903. P. 639; Wieder (1919). Pl. 24. No. 130.

Dowdeswell, J.A., Hodgkins, R., Nuttall, M., Hagen, J.O., Hamilton, G.S., 1995. Mass balance change as a control on the frequency and occurrence of glacier surges in Svalbard, Norwegian High Arctic. Geophys. Res. Lett., 22(21), 2909-2912. https://doi.org/10.1029/95GL02821.

Dowdeswell, J.A., Ottesen, D., Bellec, V.K., 2020. The changing extent of marine-terminating glaciers and ice caps in northeastern Svalbard since the ‘Little Ice Age’ from marine-geophysical records. Holocene. 30(3), 389-401. https://doi.org/10.1177/0959683619887429.

Dunér, N., Nordenskiöld, A.E., 1865. Karta öfver Spetsbergen, hufvudsakligast enligt iakttagelser under de svenska expeditionerna åren 1861 och 1864. Abrah. Lundquist & Cie., Stockholm. Available at https://digital.library.yale.edu/catalog/15159347 (access 12.09.2025)

Dunse, T., Schellenberger, T., Hagen, J.O., Kääb, A., Schuler, T.V., Reijmer, C.H., 2015. Glacier-surge mechanisms promoted by a hydro-thermodynamic feedback to summer melt. Cryosphere. 9, 197-215. https://doi.org/10.5194/tc-9-197-2015.

Dzierżek, J., Nitychoruk, J., Rzętkowska, A., 1990. Geological-geomorphological analysis and ^{14}C dating of submoraine organogenic deposits within the Renardbreen outer margin, Wedel Jarlsberg land, Spitsbergen. Polar Res. 8(2), 275,281. https://doi.org/10.3402/polar.v8i2.6817.

ESRI, 2025. ‘Imagery’ [basemap]. Scale not given, ‘world imagery vivid’. Available at https://services.arcgisonline.com/ArcGIS/rest/services/World_Imagery/MapServer (access 12.09.2025)

Evans, D., Rea, B., 1999. Geomorphology and sedimentology of surging glaciers: A land-systems approach. Ann. Glaciol. 28, 75-82. https://doi.org/10.3189/172756499781821823.

Farnsworth, W. R., Ingólfsson, Ó., Retelle, M., Schomacker, A., 2016. Over 400 previously undocumented Svalbard surge-type glaciers identified. Geomorphology. 264, 52-60. https://doi.org/10.1016/j.geomorph.2016.03.025.

Farnsworth, W.R., Allaart, L., Ingólfsson, Ó., Alexanderson, H., Forwick, M., Noormets, R., Retelle, M., Schomacker, A., 2020. Holocene glacial history of Svalbard: Status, perspectives and challenges. Earth-Sci. Rev. 208, 103249. https://doi.org/10.1016/j.earscirev.2020.103249.

Farnsworth, W.R., Ingólfsson, Ó., Brynjólfsson, S., Allaart, L., Kjellman, S.E., Kjær, K.H., Larsen, N.K., Macias-Fauria, M., Siggaard-Andersen, M., Schomacker, A., 2024. Persistence of Holocene ice cap in northeast Svalbard aided by glacio-isostatic rebound. Quat. Sci. Rev. 331, 108625. https://doi.org/10.1016/j.quascirev.2024.108625.

Farnsworth, W.R., Ingólfsson, Ó., Mannerfelt, E.S., Kalliokoski, M.H., Guðmundsdóttir, E.R., Retelle, M., Allaart, L., Brynjólfsson, S., Furze, M.F., Hancock, H.J., Kjær, K.H., Pienkowski, A.J., Schomacker, A., 2022. Vedde Ash constrains Younger Dryas glacier re-advance and rapid glacio-isostatic rebound on Svalbard. Quat. Sci. Adv. 5, 100041. https://doi.org/10.1016/j.qsa.2021.100041.

Farnsworth, W.R., Ingólfsson, Ó., Noormets, R., Allaart, L., Alexanderson, H., Henriksen, M., Schomacker, A., 2017. Dynamic Holocene glacial history of St. Jonsfjorden, Svalbard. Boreas. 46(3), 585-603. https://doi.org/10.1111/bor.12269.

Farnsworth, W.R., Ingólfsson, Ó., Retelle, M., Allaart, L., Håkansson, L.M., Schomacker, A., 2018. Svalbard glaciers re-advanced during the Pleistocene–Holocene transition. Boreas. 47(4), 1022-1032. https://doi.org/10.1111/bor.12326.

Fjeldskaar, W., Bondevik, S., Amantov, A., 2018. Glaciers on Svalbard survived the Holocene thermal optimum. Quat. Sci. Rev. 199, 18-29. https://doi.org/10.1016/j.quascirev.2018.09.003.

Flink, A.E., Hill, P., Noormets, R., Kirchner, N., 2018. Holocene glacial evolution of Mohnbukta in eastern Spitsbergen. Boreas. 47(2), 390-409. https://doi.org/10.1111/bor.12277.

Forwick, M., Vorren, T.O., Hald, M., Korsun, S., Roh, Y., Vogt, C., Yoo, K.-C., 2010. Spatial and temporal influence of glaciers and rivers on the sedimentary environment in Sassenfjorden and Tempelfjorden, Spitsbergen. Geol. Soc. Lond., Spec. Publ. 344, 163–193. https://doi.org/10.1144/SP344.13.

Fotherby, R., [1613] (reprint 1860). Narrative of a voyage to Spitzbergen in the year 1613, at the charge of the fellowship of Englishmerchants for the discovery of new trades; commonly called the Muscovy Company: with a description of the country, and the operations of the whale-fishery. Boston, Printed by J. Wilson and Son.

Fürst, J.J., Gillet-Chaulet, F., Benham, T.J., Dowdeswell, J.A., Grabiec, M., Navarro, F., Pettersson, R., Moholdt, G., Nuth, C., Sass, B., Aas, K., Fettweis, X., Lang, C., Seehaus, T., Braun, M., 2017. Application of a two-step approach for mapping ice thickness to various glacier types on Svalbard. Cryosphere. 11, 2003-2032. https://doi.org/10.5194/tc-11-2003-2017.

Fürst, J.J., Navarro, F., Gillet-Chaulet, F., Huss, M., Moholdt, G., Fettweis, X., Lang, C., Seehaus, T., Ai, S., Benham, T.J., Benn, D.I., Björnsson, H., Dowdeswell, J.A., Grabiec, M., Kohler, J., Lavrentiev, I., Lindbäck, K., Melvold, K., Pettersson, R., Rippin, D., Saintenoy, A., Sánchez-Gámez, P., Schuler, T.V., Sevestre, H., Vasilenko, E., Braun, M.H., 2018. The ice-free topography of Svalbard. Geophys. Res. Lett. 45(21), 11760-11769. https://doi.org/10.1029/2018GL079734.

Geyman, E.C., van Pelt, W.J.J., Maloof, A.C., Aas, H.F., Kohler, J., 2022. Historical glacier change on Svalbard predicts doubling of mass loss by 2100. Nature. 601, 374-379. https://doi.org/10.1038/s41586-021-04314-4.

Gjelten, H.M., Nordli, Ø., Isaksen, K., Førland, E.J., Sviashchennikov, P.N., Wyszynski, P., Prokhorova, U.V., Przybylak, R., Ivanov, B.V., Urazgildeeva, A.V., 2016. Air temperature variations and gradients along the coast and fjords of western Spitsbergen. Polar Res. 35, 29878. https://doi.org/10.3402/polar.v35.29878.

Glowacki, P., Vasilenko, E.B., Glazovsky, A.F., Macheret, Y.Y., Navarro, F.H., Moore, J.K., Hagen, J.O., 2008. Stroyenye i gidrotermicheskaya struktura lednikovo plato Amundsena na Szpitsbergenye po dannym nazyemnogo radiozondirowanya. Mater. Glacjoł. Issled. 105, 97-104.

Grabiec, M., Budzik, T., Głowacki, P., 2012a. Modeling and Hindcasting of the Mass Balance of Werenskioldbreen (Southern Svalbard). Arct. Antarct. Alp. Res. 44(2), 164-179. https://doi.org/10.1657/1938-4246-44.2.164.

Grabiec, M., Ignatiuk, D., Jania, J.A., Moskalik, M., Głowacki, P., Błaszczyk, M., Budzik, T., Walczowski, W., 2018. Coast formation in an Arctic area due to glacier surge and retreat: The Hornbreen-

Hambergbreen case from Spitsbergen. Earth Surf. Process. Landf. 43(2), 387-400. https://doi.org/10.1002/esp.4251.

Wpisz tektaj

Grabiec, M., Jania, J.A., Puczko, D., Kolondra, L., Budzik, T., 2012b. Surface and bed morphology of Hansbreen, a tidewater glacier in Spitsbergen. Pol. Polar Res. 33(2), 111-138. https://doi.org/10.2478/v10183−012−0010−7.

Grant, K.L., Stokes, C.R., Evans, I.S., 2009. Identification and characteristics of surge-type glaciers on Novaya Zemlya, Russian Arctic. J. Glaciol. 55(194), 960-972. https://doi.org/10.3189/002214309790794940.

Grinsted, A., Moore, J.C., Pohjola, V., Martma, T., Isaksson, E., 2006. Svalbard summer melting, continentality, and sea ice extent from the Lomonosovfonna ice core. J. Geophys. Res. 111, D07110. https://doi.org/10.1029/2005JD006494.

Grootes, P. M., Stuiver, M., White, J. W., Johnsen, S., Jouzel, J., 1993. Comparison of oxygen isotope records from the GISP2 and GRIP Greenland ice cores. Nature. 366(6455), 552-554. https://doi.org/10.1038/366552a0

Hagen, J.O., Liestøl, O., Roland, E., Jørgensen, T., 1993. Glacier Atlas of Svalbard and Jan Mayen. Norsk Polarinstitutt Meddelelser 129, Oslo.

Hald, M., Dahlgren, T., Olsen, T.-E., Lebesbye, E., 2001. Late Holocene palaeoceanography in Van Mijenfjorden, Svalbard. Polar Res. 20(1), 23-35. https://doi.org/10.3402/polar.v20i1.6497.

Hanssen-Bauer, I., Førland, E., Hisdal, H., Mayer, S., Sandø, A.B., Sorteberg, A., 2019. Climate in Svalbard 2100. A Knowledge Base for Climate Adaptation.

Heaton, T.J., Köhler, P., Butzin, M., Bard, E., Reimer, R.W., Austin, W.E.N., Bronk Ramsey, C., Grootes, P.M., Hughen, K.A., Kromer, B., Reimer, P.J., Adkins, J., Burke, A., Cook, M.S., Olsen, J., Skinner, L.C., 2020. Marine20—The Marine Radiocarbon Age Calibration Curve (0–55,000 cal BP). Radiocarbon. 62(4), 779-820. https://doi.org/10.1017/RDC.2020.68.

Holmes, F.A., Kirchner, N., Kuttenkeuler, J., Krützfeldt, J., Noormets, R., 2019. Relating ocean temperatures to frontal ablation rates at Svalbard tidewater glaciers: Insights from glacier proximal datasets. Sci. Rep. 9, 9442. https://doi.org/10.1038/s41598-019-45077-3.

Humlum, O., Elberling, B., Hormes, A., Fjordheim, K., Hansen, O.H., Heinemeier, J., 2005. Late-Holocene glacier growth in Svalbard, documented by subglacial relict vegetation and living soil microbes. Holocene. 15(3), 396-407. https://doi.org/10.1191/0959683605hl817rp.

Ignatiuk, D., Błaszczyk, M., Budzik, T., Grabiec, M., Jania, J.A., Kondracka, M., Laska, M., Małarzewski, Ł., Stachnik, Ł., 2022. A decade of glaciological and meteorological observations in the Arctic (Werenskioldbreen, Svalbard). Earth Syst. Sci. Data. 14, 2487-2500. https://doi.org/10.5194/essd-14-2487-2022.

Isaksson, E., Hermanson, M., Hicks, S., Igarashi, M., Kamiyama, K., Moore, J., Motoyama, H., Muir, D., Pohjola, V., Vaikmäe, R., Van de Wal, R.S., Watanabe, O., 2003. Ice cores from Svalbard—useful archives of past climate and pollution history. Phys. Chem. Earth (Pt AB,C). 28(28-32), 1217-1228. https://doi.org/10.1016/j.pce.2003.08.053.

Jang, K., Bayon, G., Ahn, Y., Joe, Y.J., Son, E.J., Kwon, S.Y., Kim, J.-H., Vogt, C., Forwick, M., Byun, E., Nam, S.-I. 2025. Geochemical and mineralogical characteristics of fjord sediments in Arctic Svalbard: insights into Holocene glacial activity and weathering variability. J. Sediment. Res. 95(2), 223-238. https://doi.org/10.2110/jsr.2024.088.

Jania, J., 1988. Dynamiczne procesy glacjalne na południowym Spitsbergenie (w świetle badań fotointerpretacyjnych i fotogrametrycznych) [Dynamic glacial processes in south Spitsbergen (in the light of photointerpretation and photogrammetric research)]. Pr. Nauk. Uniw. Śl. Katowice. 955. Uniwersytet Śląski, Katowice (in Polish).

Joe, Y.J., Jang, K., Forwick, M., Laberg, J.S., Kong, G.S., Kang, M.-H., Yoon, S.-H., Nam, S.-I., 2022. Glacial history and depositional environments in little Storfjorden and Hambergbukta of Arctic Svalbard since the younger dryas. Front. Earth Sci. 10, 1017594. https://doi.org/10.3389/feart.2022.1017594.

Jónsson, S.A., Schomacker, A., Benediktsson, Í.Ö., Ingólfsson, Ó., Johnson, M.D., 2014. The drumlin field and the geomorphology of the Múlajökull surge-type glacier, central Iceland. Geomorphology. 207, 213-220. https://doi.org/10.1016/j.geomorph.2013.11.007.

Kääb, A., Bazilova, V., Leclercq, P.W., Mannerfelt, E.S., Strozzi, T., 2023. Global clustering of recent glacier surges from radar backscatter data, 2017–2022. J. Glaciol. 69(277), 1515-1523. https://doi.org/10.1017/jog.2023.35.

Karczewski, A., Andrzejewski, L., Chmal, H., Jania, J., Kłysz, P., Kostrzewski, A., Lindner, L., Marks, L., Pękala, K., Pulina, M., Rudowski, S., Stankowski, W., Szczypek, T., Wiśniewski, E., 1984. Hornsund, Spitsbergen. Geomorfologia — geomorphology. 1:75,000. Silesian University, Katowice.

Karczewski, A., Kostrzewski, A., Marks, L., 1981. Late Holocene glacier advances in Revdalen, Spitsbergen. Pol. Polar Res. 2(112), 51-61.

Kasprzak, M., Łopuch, M., Głowacki, T., Milczarek, W., 2020. Evolution of Near-Shore Outwash Fans and Permafrost Spreading Under Their Surface: A Case Study from Svalbard. Remote Sens. 12(3), 482. https://doi.org/10.3390/rs12030482.

Kavan, J., Tallentire, G.D., Demidionov, M., Dudek, J., Strzelecki, M.C., 2022. Fifty Years of Tidewater Glacier Surface Elevation and Retreat Dynamics along the South-East Coast of Spitsbergen (Svalbard Archipelago). Remote Sens. 14(2), 354. https://doi.org/10.3390/rs14020354.

Kekonen, T., Moore, J., Perämäki, P., Mulvaney, R., Isaksson, E., Pohjola, V., van de Wal, R.S.W., 2005. The 800 year long ion record from the Lomonosovfonna (Svalbard) ice core. J. Geophys. Res. 110, D07304. https://doi.org/10.1029/2004JD005223.

Kempf, P., Forwick, M., Laberg, J.S., Vorren, T.O., 2013. Late Weichselian and Holocene sedimentary palaeoenvironment and glacial activity in the high-arctic van Keulenfjorden, Spitsbergen. Holocene. 23(11), 1607-1618. https://doi.org/10.1177/0959683613499055.

Kjaer, R., 1938. Nordishavet, Svalbard, Frå Sørkapp til Bellsund, Sjøkart 504, 1:200 000, Det Kongelige Departement for Handel, Sjøfart, Industri, og Håndverk. Norges Svalbard – og Ishavs-undersøkelser, Oslo. Available at https://data.npolar.no/map/archive/fe263748-5917-55e8-bb0e-98e1530cdc00 (access 12.09.2025)

Kochtitzky, W., Copland, L., 2022. Retreat of Northern Hemisphere Marine-Terminating Glaciers, 2000–2020. Geophys. Res. Lett. 49(3), e2021GL096501. https://doi.org/10.1029/2021GL096501.

Kohl, C.P., Nishiizumi, K., 1992. Chemical isolation of quartz for measurement of in-situ-produced cosmogenic nuclides. Geochim. Cosmochim. Acta. 56, 3583-3587. https://10.1016/0016-7037(92)90401-4.

Kosiba, A., 1960. Some Results of Glaciological Investigations in SW-Spitsbergen Carried Out During the Polish I. G. Y. Spitsbergen Expeditions in 1957, 1958 and 1959. Zesz. Nauk. Uniw. Wroc. B. 4, 1-30.

Łącka, M., Cao, M., Rosell-Melé, A., Pawłowska, J., Kucharska, M., Forwick, M., Zajączkowski, M., 2019. Postglacial paleoceanography of the western Barents Sea: Implications for alkenone-based sea surface temperatures and primary productivity. Quat. Sci. Rev. 224, 105973. https://doi.org/10.1016/j.quascirev.2019.105973.

Lal, D., 1991. Cosmic ray labeling of erosion surface: in situ nuclide production rates and erosion models. Earth Planet. Sci. Lett. 104, 424-439. https://doi.org/10.1016/0012-821X(91)90220-C.

Larocca, L.J., Axford, Y., 2022. Arctic glaciers and ice caps through the Holocene: a circumpolar synthesis of lake-based reconstructions. Clim. Past. 18, 579-606, https://doi.org/10.5194/cp-18-579-2022.

Larsen, E.A., Lyså, A., Rubensdotter, L., Farnsworth, W.R., Jensen, M., Nadeau, M.J., Ottesen, D., 2018. Late-Glacial and Holocene glacier activity in the Van Mijenfjorden area, western Svalbard. Arktos, 4, 9. https://doi.org/10.1007/s41063-018-0042-2.

Larsen, N.K., Søndergaard, A.S., Levy, L.B., Laursen, C.H., Bjørk, A.A., Kjeldsen, K.K., Funder, S., Strunk, A., Olsen, J., Kjær, K.H., 2021. Cosmogenic nuclide inheritance in Little Ice Age moraines - A case study from Greenland. Quat. Geochronol. 65, 101200. https://doi.org/10.1016/j.quageo.2021.101200.

Lefauconnier, B., Hagen, J.O., 1991. Surging and calving glaciers in eastern Svalbard. Nor. Polarinst. Medd 116, 1-130.

Li, T., Hofer, S., Moholdt, G., Igneczi, A., Heidler, K., Zhu, X.X., Bamber, J., 2025. Pervasive glacier retreats across Svalbard from 1985 to 2023. Nat. Commun. 16, 705. https://doi.org/10.1038/s41467-025-55948-1.

Li, Yk., 2018. Determining topographic shielding from digital elevation models for cosmogenic nuclide analysis: a GIS model for discrete sample sites. J. Mt. Sci. 15, 939-947. https://doi.org/10.1007/s11629-018-4895-4.

Liestøl, O., 1969. Glacier surges in West Spitsbergen. Can. J. Earth Sci. 6(4), 895-897. https://doi.org/10.1139/e69-092.

Liestøl, O., 1977. Årsmorener foran Nathorstbreen? Nor. Polarinst. Årb. 1976, 361-363.

Liestøl, O., 1988. The glaciers in the Kongsfjorden area, Spitsbergen. Nor. Geogr. Tidsskr. 42(4), 231-238. https://doi.org/10.1080/00291958808552205.

Liestøl, O., 1993. Glaciers of Svalbard, Norway. In: Williams Jr R.S., Ferrigno J.G. (eds) Satellite Image Atlas of Glaciers of the World. Washington, DC: US Geological Survey, pp. 127–151.

Lindner, L., Marks, L., 1993. Middle and Late Quaternary evolution of the Hornsund Region, South Spitsbergen. Pol. Polar Res. 14(3), 275-292.

Lindner, L., Marks, L., Pękala, K., 1984. Late Quaternary glacial episodes in the Hornsund Region of Spitsbergen. Boreas. 13, 35-47.

Lindner, L., Marks, L., Pękala, K., 1986. Outline of Quaternary chronostratigraphy of the Northern Hornsund area. Southern Spitsbergen. Bull. Pol. Acad. Sci. Earth Sci. 34(1), 427-436.

Lindner, L., Marks, L., Pękala, K., 1987. Quaternary chronostratigraphy of south Spitsbergen. Polar Res. 5, 273-274.

Lønne, I., 2005. Faint traces of high Arctic glaciations: An early Holocene ice-front fluctuation in Bolterdalen, Svalbard. Boreas. 34(3), 308-323. https://doi.org/10.1111/j.1502-3885.2005.tb01103.x.

Lønne, I., 2016. A new concept for glacial geological investigations of surges, based on High-Arctic examples (Svalbard). Quat. Sci. Rev. 132, 74-100. https://doi.org/10.1016/j.quascirev.2015.11.009.

Lønne, I.,(2014. The influence of climate during and after a glacial surge — A comparison of the last two surges of Fridtjovbreen, Svalbard. Geomorphology. 207, 190-202. https://doi.org/10.1016/j.geomorph.2013.11.005.

Lovell, H., Benn, D.I., Lukas, S., Ottesen, D., Luckman, A., Hardiman, M., Barr, I.D., Boston, C.M., Sevestre, H., 2018. Multiple Late Holocene surges of a High-Arctic tidewater glacier system in Svalbard. Quat. Sci. Rev. 201, 162-185. https://doi.org/10.1016/j.quascirev.2018.10.024.

Lovell, H., Boston, C.M., 2017. Glacitectonic composite ridge systems and surge-type glaciers: an updated correlation based on Svalbard, Norway. Arktos. 3, 2. https://doi.org/10.1007/s41063-017-0028-5.

Lovell, H., Fleming, E.J., 2023. Structural evolution during a surge in the Paulabreen glacier system, Svalbard. J. Glaciol. 69(273), 141-152. https://doi.org/10.1017/jog.2022.53.

Lovell, H., Fleming, E.J., Benn, D.I., Hubbard, B., Lukas, S., Naegeli, K., 2015. Former dynamic behaviour of a cold-based valley glacier on Svalbard revealed by basal ice and structural glaciology investigations. J. Glaciol. 61(226), 309-328. https://doi.org/10.3189/2015JoG14J120.

Luckman, A., Benn, D.I., Cottier, F., Bevan, S., Nilsen, F., Inall, M., 2015. Calving rates at tidewater glaciers vary strongly with ocean temperature. Nat. Commun. 6(1), 8566. https://doi.org/10.1038/ncomms9566.

Luoto, T.P., Ojala, A.E.K., Arppe, L., Brooks, S.J., Kurki, E., Oksman, M., Wooller, M.J., Zajączkowski, M., 2018. Synchronized proxy-based temperature reconstructions reveal mid- to late Holocene climate oscillations in High Arctic Svalbard. J. Quat. Sci. 33, 93-99. https://doi.org/10.1002/jqs.3001.

Macheret, Yu.Ya., 1981. Forms of Glacial Relief of Spitsbergen Glaciers. Ann. Glaciol. 2, 45-51. https://doi.org/10.3189/172756481794352405.

Macheret, Yu.Ya., Zhuravlev, A.B., Bobrova, L.I., 1985. Thickness, subglacial relief and volume of Svalbard glaciers based on radio echo-sounding data. Polar Geogr. Geol. 9(3), 224-243. https://doi.org/10.1080/10889378509377254.

Majchrowska, E., Ignatiuk, D., Jania, J., Marszałek, H., Wąsik, M., 2015. Seasonal and interannual variability in runoff from the Werenskioldbreen catchment, Spitsbergen. Pol. Polar Res. 36(3), 197-224. https://doi.org/10.1515/popore−2015−0014.

Majewski, W., Szczuciński, W., Zajączkowski, M., 2009. Interactions of Arctic and Atlantic water-masses and associated environmental changes during the last millennium, Hornsund (SW Svalbard). Boreas. 38, 529-544. https://doi.org/10.1111/j.1502-3885.2009.00091.x.

Mannerfelt, E.S., Hodson, A.J., Håkansson, L., Lovell, H., 2024. Dynamic LIA advances hastened the demise of small valley glaciers in central Svalbard. Arct. Sci. 10(4), 815-833. https://doi.org/10.1139/as-2024-0024.

Marks, L., 1983. Late Holocene evolution of the Treskelen Peninsula (Hornsund, Spitsbergen). Acta Geol. Polon. 33, 159-168.

Marks, L., Pękala, K., 1986. New datings of Quaternary sediments from Bogstranda and Treskelodden, southern Spitsbergen. Bull. Pol. Acad. Sci. Earth Sci. 34, 419-425.

Martín-Moreno, R., Allende Álvarez, F., Hagen, J.O., 2017. 'Little Ice Age' glacier extent and subsequent retreat in Svalbard archipelago. Holocene. 27(9), 1379-1390. https://doi.org/10.1177/0959683617693904.

Maxeiner, S., Synal, H.A., Christl, M., Suter, M., Müller, A., Vockenhuber, C., 2019. Proof-of-principle of a compact 300 kV multi-isotope AMS facility. Nucl. Instrum. Methods Phys. Res. Sect. B. 439, 84-89. https://doi.org/10.1016/j.nimb.2018.11.028.

Meier, M.F., Post, A., 1969. What are glacier surges?. Can. J. Earth Sci. 6(4), 807-817. https://doi.org/10.1139/e69-081.

Middelhoven, M.H., 1634. 'Het nieuwe land Spits-berghen' (The new land of Spitsbergen). Kaart van Spitsbergen door M.H. Middelhoven. Reproduction: Tijdschrift. Aardrijksk. Gen., deel III. Schenking de Bas. Zie Verslag 1877, blz. 4. Facsimile van 4. VEL inv.nr. 2. Orginal volumine: https://www.nationaalarchief.nl/onderzoeken/archief/4.VELH/invnr/20 (access 31.03.2025)

Migała, K., Łepkowska, E., Osuch, M., Stachnik, Ł., Wawrzyniak, T., Ignatiuk, D., Owczarek, P., 2023. Climate indices of environmental change in the High Arctic: Study from Hornsund, SW Spitsbergen, 1979–2019. Pol. Polar Res. 44(2), 91-126. https://doi.org/10.24425/ppr.2022.143316.

Miller, G.H., Brigham-Grette, J., Alley, R.B., Anderson, L., Bauch, H.A., Douglas, M.S.V., Edwards, M.E., Elias, S.A., Finney, B.P., Fitzpatrick, J.J., Funder, S.V., Herbert, T.D., Hinzman, L.D., Kaufman, D.S., MacDonald, G.M., Polyak L., Robock, A., Serreze, M.C., Smol, J.P., Spielhagen, R., White, J.W.C., Wolfe, A.P., Wolff, E.W., 2010. Temperature and precipitation history of the Arctic. Quat. Sci. Rev. 29, 1679-1715. https://doi.org/10.1016/j.quascirev.2010.03.001.

Miller, G.H., Landvik, J.Y., Lehman, S.J., Southon, J.R., 2017. Episodic Neoglacial snowline descent and glacier expansion on Svalbard reconstructed from the ^{14}C ages of ice-entombed plants. Quat. Sci. Rev. 155, 67-78. http://dx.doi.org/10.1016/j.quascirev.2016.10.023.

Moore, P.G., 1977. Inorganic particulate suspensions in the sea and their effects on marine animals. Oceanogr. Mar. Biol. Ann. Rev. 15, 225-363.

Moskalik, M., Grabowiecki, P., Tęgowski, J., Żulichowska, M., 2013. Bathymetry and geographical regionalization of Brepollen (Hornsund, Spitsbergen) based on bathymetric profiles interpolations. Pol. Polar Re. 34(1), 1-22. https://doi.org/10.2478/popore−2013−0001.

Němec, M., Wacker, L., Gäggeler, H., 2010. Optimization of the graphitization process at AGE-1. Radiocarbon 52(3), 1380–1393. https://doi.org/10.1017/S0033822200046464.

Nesje, A., Dahl, S.O., Thun, T., Nordli, Ø., 2008. The 'Little Ice Age' glacial expansion in western Scandinavia: summer temperature or winter precipitation? Clim. Dyn. 30, 789-801. https://doi.org/10.1007/s00382-007-0324-z.

Nielsen, T., Rasmussen, T.L., 2018. Reconstruction of ice sheet retreat after the Last Glacial maximum in Storfjorden, southern Svalbard. Mar. Geol. 402, 228-243. https://doi.org/10.1016/j.margeo.2017.12.003.

Nihoul, J.C.J., Kostianoy A.G., 2009. Influence of Climate Change on the Changing Arctic and Sub-Arctic Conditions. Springer Dordrecht. https://doi.org/10.1007/978-1-4020-9460-6.

Noël, B., Jakobs, C.L., van Pelt, W.J.J., Lhermitte, S., Wouters, B., Kohler, J., Hagen, J.O., Luks, B., Reijmer, C.H., van de Berg, W.J., van den Broeke, M.R., 2020. Low elevation of Svalbard glaciers drives high mass loss variability. Nat. Commun. 11(1), 4597. https://doi.org/10.1038/s41467-020-18356-1.

Noormets, R., Flink, A., Kirchner, N., 2021. Glacial dynamics and deglaciation history of Hambergbukta reconstructed from submarine landforms and sediment cores, SE Spitsbergen, Svalbard. Boreas. 50(1), 29-50. https://doi.org/10.1111/bor.12488.

Nordli, Ø., Wyszyński, P., Gjelten, H., Isaksen, K., Łupikasza, E., Niedźwiedź, T., Przybylak, R., 2020. Revisiting the extended Svalbard Airport monthly temperature series, and the compiled corresponding daily series 1898–2018. Polar Res. 39, 3614. https://doi.org/10.33265/polar.v39.3614.

Norwegian Polar Institute, 1921. (Kart over) Farvannet mellom Hornsund og Dunderbay 1917–1921. Available at https://data.npolar.no/map/archive/066a96e0-00d8-574e-8a71-334d02ee3ca0 (access 12.09.2025)

Norwegian Polar Institute, 1984. Svalbard Frå Sørkapp til Bellsund, Sjøkart 504, 1:200 000. Norsk Polarinstitutt, Oslo. Available at https://data.npolar.no/map/archive/fe263748-5917-55e8-bb0e-98e1530cdc00 (access 12.09.2025)

Norwegian Polar Institute, 2014a. Kartdata Svalbard 1:1 000 000 (S1000 Kartdata) [data set]. Norwegian Polar Institute. https://doi.org/10.21334/NPOLAR.2014.63730E2E.

Norwegian Polar Institute, 2014b. Terrengmodell Svalbard (S0 Terrengmodell) [dataset]. Norwegian Polar Institute. https://doi.org/10.21334/npolar.2014.dce53a47.

Nuth, C., Kohler, J., Aas, H.F., Brandt, O., Hagen, J.O., 2007. Glacier geometry and elevation changes on Svalbard (1936–90): a baseline dataset. Ann. Glaciol. 46, 106-116. https://doi.org/10.3189/172756407782871440.

Nuth, C., Kohler, J., Köning, M., Von Deschwanden, A., Hagen, J.O., Kääb, A., Moholdt, G., Pettersson, R., 2013. Decadal changes from a multi-temporal glacier inventory of Svalbard. Cryosphere. 7(5), 1603-1621. https://doi.org/10.5194/tc-7-1603-2013.

Nuth, C., Moholdt, G., Kohler, J., Hagen, J.O., Kääb, A., 2010. Svalbard glacier elevation changes and contribution to sea level rise. J. Geophys. Res. 115, F01008. https://doi.org/10.1029/2008JF001223.

Oerlemans, J., 1989. On the Response of Valley Glaciers to Climatic Change, in: Oerlemans, J. (Ed.) Glacier Fluctuations and Climatic Change. Glaciology and Quaternary Geology, 6. Springer, Dordrecht. https://doi.org/10.1007/978-94-015-7823-3_23.

Oerlemans, J., Jania, J., Kolondra, L., 2011. Application of a minimal glacier model to Hansbreen, Svalbard. Cryosphere. 5, 1-11. https://doi.org/10.5194/tc-5-1-2011.

Osika, A., Jania, J., 2024. Geomorphological and historical records of the surge-type behaviour of Hansbreen (Svalbard). Ann. Glaciol. 65, e31. https://doi.org/10.1017/aog.2024.32.

Osika, A., Jania, J., Szafraniec, J.E., 2022. Holocene ice-free strait followed by dynamic Neoglacial fluctuations: Hornsund, Svalbard. Holocene. 32(7), 664-679. https://doi.org/10.1177/09596836221088232.

Osika, A., Piotrowska, N., Jania, J., 2025. Radiocarbon dates of marine shells, subfossil vegetation, driftwood and a whalebone from glacial sediments in Hornsund (Spitsbergen, Svalbard) [Data set]. Zenodo. https://doi.org/10.5281/zenodo.15831642

Østby, T.I., Schuler, T.V., Hagen, J.O., Hock, R., Kohler, J., Reijmer, C.H., 2017. Diagnosing the decline in climatic mass balance of glaciers in Svalbard over 1957–2014. Cryosphere. 11(1), 191-215. https://doi.org/10.5194/tc-11-191-2017.

Otero, J., Navarro, F.J., Lapazaran, J.J., Welty, E., Puczko, D., Finkelnburg, R., 2017. Modeling the Controls on the Front Position of a Tidewater Glacier in Svalbard. Front. Earth Sci. 5, 243157. https://doi.org/10.3389/feart.2017.00029.

Ottesen, D., Dowdeswell, J.A., Benn, D.I., Kristensen, L., Christiansen, H.H., Christensen, O., Hansen, L., Lebesbye, E., Forwick, M., Vorren, T., 2008. Submarine landforms characteristic of glacier surges in two Spitsbergen fjords. Quat. Sci. Rev. 27(15-16), 1583-1599. https://doi.org/10.1016/j.quascirev.2008.05.007.

Ottesen, D., Dowdeswell, J.A., Landvik, J.Y., Mienert, J., 2007. Dynamics of the Late Weichselian ice sheet on Svalbard inferred from high-resolution sea-floor morphology. Boreas. 36, 286-306. https://doi.org/10.1111/j.1502-3885.2007.tb01251.x.

Pälli, A., Moore, J.C., Jania, J., Kolondra, L., Glowacki, P., 2003. The drainage pattern of Hansbreen and Werenskioldbreen, two polythermal glaciers in Svalbard. Polar Res. 22(2), 355-371. https://doi.org/10.3402/polar.v22i2.6465.

Pawłowska, J., Łącka, M., Kucharska, M., Pawlowski, J., Zajączkowski, M., 2020. Multiproxy evidence of the Neoglacial expansion of Atlantic Water to eastern Svalbard. Clim. Past. 16, 487-501. https://doi.org/10.5194/cp-16-487-2020.

Pawłowska, J., Zajączkowski, M., Łącka, M., Lejzerowicz, F., Esling, P., Pawlowski, J., 2016. Palaeoceanographic changes in Hornsund Fjord (Spitsbergen, Svalbard) over the last millennium: new insights from ancient DNA. Clim. Past. 12, 1459-1472. https://doi.org/10.5194/cp-12-1459-2016.

Pękala, K., 1989. Quaternary deposits of the Hans Glacier forefield (Hornsund, Spitsbergen), in: Repelewska-Pękalowa J., Pękala K. (Eds.), Wyprawy geograficzne na Spitsbergen 1986-1988. UMCS, Lublin, pp. 191-204.

Pękala, K., Lindner, L., Marks, L., Szczęsny, R., 1985. Evolution of the Interlobal Zone of the Torell Glacier (Torellbreen), Spitsbergen. Ann. Univ. Mariae Curie-Skłodowska, Sect. B. 40, 1–19.

Peterman, A., 1874. Graf Wiltschek's Nordpolarfahrt im Jahre 1872 / nach den Aufzeichnungen des Contre-Admirals Max Freiherrn Daublebsky v. Sterneck und Ehrenstein, in: Peterman, A. (Ed.) Mittheilungen aus Justus Perthes' Geographischer Anstalt über wichtige neue Erforschungen auf dem Gesammtgebiete der Geographie, 20 Band, Justus Perthes' Geographische Anstalt Gotha, pp. 65–72.

Philipps, W., Briner, J.P., Gislefoss, L., Linge, H., Koffman, T., Fabel, D., Xu, S., Hormes, A., 2017. Late Holocene glacier activity at inner Hornsund and Scottbreen, southern Svalbard. J. Quat. Sci. 32(4), 501-515. https://doi.org/10.1002/jqs.2944.

Pieńkowski, A.J., Husum, K., Furze, M.F.A., Missana, A.F.J.M., Irvalı, N., Divine, D.V., Eilertsen, V.T., 2022. Revised ΔR values for the Barents Sea and its archipelagos as a pre-requisite for accurate and robust marine-based ^{14}C chronologies. Quat. Geochronol. 68, 101244. https://doi.org/10.1016/j.quageo.2021.101244.

Piotrowska, N., Goslar, T., 2002. Preparation of bone samples in the Gliwice radiocarbon laboratory for AMS radiocarbon dating. Isot. Environ. Health Stud. 38(4), 267–275. https://doi.org/10.1080/10256010208033272.

Porter, C., Howat, I., Noh, M.-J., Husby, E., Khuvis, S., Danish, E., Tomko, K., Gardiner, J., Negrete, A., Yadav, B., Klassen, J., Kelleher, C., Cloutier, M., Bakker, J., Enos, J., Arnold, G., Bauer, G., Morin, P., 2023. ArcticDEM - Mosaics, Version 4.1. [dataset] Harvard Dataverse, V1. https://doi.org/10.7910/DVN/3VDC4W.

Promińska, A., Falck, E., Walczowski, W., 2018. Interannual variability in hydrography and water mass distribution in Hornsund, an Arctic fjord in Svalbard. Polar Res. 37(1), 1495546. https://doi.org/10.1080/17518369.2018.1495546.

Purchas, S., 1625. Greneland [map]. In: Purchas, S. "Purchas His Pilgrimes" part iii. London

Rantanen, M., Karpechko, A.Y., Lipponen, A., Nordling, K., Hyvärinen, O., Ruosteenoja, K., Vihma, T., Laaksonen, A., 2022. The Arctic has warmed nearly four times faster than the globe since 1979. Commun. Earth Environ. 3, 168. https://doi.org/10.1038/s43247-022-00498-3.

Rasmussen, T.L., Thomsen, E., 2021. Climate and ocean forcing of ice-sheet dynamics along the Svalbard-Barents Sea ice sheet during the deglaciation ∼20,000–10,000 years BP. Quat. Sci. Adv. 3, 100019. https://doi.org/10.1016/j.qsa.2020.100019.

Raymond, C.F., 1987. How do glaciers surge? A review. J. Geophys. Res. 92(B9), 9121-9134. https://doi.org/10.1029/JB092iB09p09121.

Řehak, J. Sr., Řehak, J. Jr., Řehak, S., 2004. The recession of Vestre and Austre Torellbreen ice cliffs (SW Spitsbergen). Probl. Klim. Polar. 14, 87-94. [in Polish with English summary]

Reimer, P., Austin, W., Bard, E., Bayliss, A., Blackwell, P., Bronk Ramsey, C., Butzin, M., Cheng, H., Edwards, R., Friedrich, M., Grootes, P., Guilderson, T., Hajdas, I., Heaton, T., Hogg, A., Hughen, K., Kromer, B., Manning, S., Muscheler, R., Palmer, J., Pearson, C., van der Plicht, J., Reimer, R., Richards, D., Scott, E., Southon, J., Turney, C., Wacker, L., Adolphi, F., Büntgen, U., Capano, M., Fahrni, S., Fogtmann-Schulz, A., Friedrich, R., Köhler, P., Kudsk, S., Miyake, F., Olsen, J., Reinig, F., Sakamoto, M., Sookdeo, A., Talamo, S., 2020. The IntCal20 Northern Hemisphere radiocarbon age calibration curve (0–55 cal kBP). Radiocarbon. 62(4), 725-757. https://doi.org/10.1017/RDC.2020.41.

Reusche, M., Winsor, K., Carlson. A.E., Marcott. S.A., Rood, D.H., Novak, A., Roof, S., Retelle, M., Werner, A., Caffee, M., Clark, P.U., 2014. ^{10}Be surface exposure ages on the late-Pleistocene and Holocene history of Linnébreen on Svalbard. Quat. Sci. Rev. 89, 5-12. https://doi.org/10.1016/j.quascirev.2014.01.017.

Richard, H., Dowdeswell, J.A., 1994. Tectonic processes in Svalbard tide-water glacier surges: evidence from structural glaciology. J. Glaciol. 40(136), 553-560. https://doi.org/10.3189/S0022143000012430.

Røthe, T.O., Bakke, J., Støren, E.W.N., Bradley, R.S., 2018. Reconstructing Holocene glacier and climate fluctuations from lake sediments in Vårfluesjøen, Northern Spitsbergen. Front. Earth Sci. 6, 91. https://doi.org/10.3389/feart.2018.00091.

Røthe, T.O., Bakke, J., Vasskog, K., Gjerde, M., D'Andrea, W.J., Bradley, R.S., 2015. Arctic Holocene glacier fluctuations reconstructed from lake sediments at Mitrahalvøya, Spitsbergen. Quat. Sci. Rev. 109, 111-125. https://doi.org/10.1016/j.quascirev.2014.11.017.

Różycki, O., 1992. Occurrence of Gastropoda and Bivalvia in Hornsund Fiord (West Spitsbergen, Svalbard). Pol. Polar Res. 13(1), 41-52.

Saferna, D., Błaszczyk, M., Grabiec, M., Gądek, B., 2023. Quantifying Changes in Extent and Velocity of the Hornbreen/Hambergbreen Glacial System (SW, Spitsbergen) Based on Timeseries of Multispectral Satellite Imagery. Remote Sens. 15(14), 3529. https://doi.org/10.3390/rs15143529.

Salvigsen O., Høgvard K., 2006: Glacial history, Holocene shoreline displacement and palaeoclimate based on radiocarbon ages in the area of Bockfjorden, north-western Spitsbergen, Svalbard. Polar Research, 25, 15-24. https://doi.org/10.1111/j.1751-8369.2006.tb00147.x

Salvigsen, O., Forman, S.L., Miller, G.H., 1992. Thermophilous molluscs on Svalbard during the Holocene and their paleoclimatic implications. Polar Res. 11(1), 1-10. https://doi.org/10.3402/polar.v11i1.6712.

Samtleben, C., 1985. Climatic influence on shell microstructure in Mytilus edulis from Spitsbergen. In: Paper presented at the 75. Jahrestagung der Geologischen Vereinung, Kiel.

Sarnthein, M., Van Kreveld, S., Erlenkeuser, H., Grootes, P.M., Kucera, M., Pflaumann, U., Schulz, M., 2003. Centennial-to-millennial-scale periodicities of Holocene climate and sediment injections off the western Barents shelf, 75°N. Boreas. 32, 447-461. https://doi.org/10.1111/j.1502-3885.2003.tb01227.x.

Schmidt, L.S., Schuler, T.V., Thomas, E.E., Westermann, S.. 2023. Meltwater runoff and glacier mass balance in the high Arctic: 1991–2022 simulations for Svalbard. Cryosphere. 17, 2941-2963. https://doi.org/10.5194/tc-17-2941-2023.

Schuler, T.V., Kohler, J., Elagina, N., Hagen, J.O.M., Hodson, A.J., Jania, J.A., Kääb, A.M., Luks, B., Małecki, J., Moholdt, G., Pohjola, V.A., Sobota, I., Van Pelt, W.J.J., 2020. Reconciling Svalbard Glacier Mass Balance. Front. Earth Sci. 8, 156. https://doi.org/10.3389/feart.2020.00156.

Schytt, V., 1969. Some comments on glacier surges in eastern Svalbard. Can. J. Earth Sci. 6(4), 867-873. https://doi.org/10.1139/e69-088.

Scoresby, W., 1820. A chart of Spitzbergen or East Greenland, comprising an original survey of the west coast. Above 200 Miles in extent. An account of the Arctic regions with a history and description of the northern whale-fishery. vol. 2. Edinburgh, Pl. 7:573.

Sevestre, H., Benn, D.I., 2015. Climatic and geometric controls on the global distribution of surge-type glaciers: implications for a unifying model of surging. J. Glaciol. 61(228), 646-662. https://doi.org/10.3189/2015JoG14J136.

Sevestre, H., Benn, D.I., Hulton, N.J.R., Bælum, K., 2015. Thermal structure of Svalbard glaciers and implications for thermal switch models of glacier surging. J. Geophys. Res. Earth Surf. 120(10), 2220-2236. https://doi.org/10.1002/2015JF003517.

Skirbekk, K., Kristensen, D.K., Rasmussen, T.L., Koç, N., Forwick, M., 2010. Holocene climate variations at the entrance to a warm Arctic fjord: evidence from Kongsfjorden trough, Svalbard. Geol. Soc. Lond., Spec. Publ. 344, 289-304. https://doi.org/10.1144/SP344.20.

Ślubowska, M.A., Koç, N., Rasmussen, T.L., Klitgaard-Kristensen, D., 2005. Changes in the flow of Atlantic water into the Arctic Ocean since the last deglaciation: Evidence from the northern Svalbard continental margin, 80°N. Paleoceanography. 20, PA4014, https://doi.org/10.1029/2005PA001141.

Snyder, J.A., Werner, A., Miller, G.H., 2000. Holocene cirque glacier activity in western Spitsbergen, Svalbard: sediment records from proglacial Linnévatnet. Holocene 10, 555-563. https://doi.org/10.1191/095968300667351.

Stachniak, K., Sitek, S., Ignatiuk, D., Jania, J., 2022. Hydrogeological Model of the Forefield Drainage System of Werenskioldbreen, Svalbard. Water. 14(9), 1514. https://doi.org/10.3390/w14091514.

Stone, J.O., 2000. Air pressure and cosmogenic isotope production. J. Geophys. Res. 105, 23753-23759. https://doi.org/10.1029/2000jb900181.

Sund, M., Eiken, T., Hagen, J.O., Kääb, A., 2009. Svalbard surge dynamics derived from geometric changes. Ann. Glaciol. 50(52), 50-60. https://doi.org/10.3189/172756409789624265.

Sund, M., Lauknes, T.R., Eiken, T., 2014. Surge dynamics in the Nathorstbreen glacier system, Svalbard, Cryosphere. 8, 623-638, https://doi.org/10.5194/tc-8-623-2014.

Szafraniec, J., 2013. The glaciers of West Spitsbergen – the current state of research with particular emphasis on the Hornsund region. (In:) Zwoliński, Z., Kostrzewski, A., Pulina, M. (Eds), Ancient and modern geoecosystems of Spitsbergen. Bogucki Wydawnictwo Naukowe, Poznań, 245–263.

Szafraniec, J.E., 2020. Ice-Cliff Morphometry in Identifying the Surge Phenomenon of Tidewater Glaciers (Spitsbergen, Svalbard). Geosciences. 10(9), 328. https://doi.org/10.3390/geosciences10090328.

Szafraniec, J.E., Dobiński, W., 2020. Deglaciation Rate of Selected Nunataks in Spitsbergen, Svalbard—Potential for Permafrost Expansion above the Glacial Environment. Geosciences. 10(5), 202. https://doi.org/10.3390/geosciences10050202.

Szupryczyński, J., 1963. Relief of marginal zones of glaciers and types of deglaciation of Southern Spitsbergen glaciers. Prace Geograficzne. 39, Inst. Geogr. Pol. Akad. Nauk, Warsaw (in Polish with English summary).

Tarasov G.A., Denisenko S.G., Matishov G.G., Pogodina I.A., 1992: Moraine complexes and certain questions concerning paleoecology of the Treskelen region in the Hornsund Fiord (W Spitsbergen). (In:) Repelewska-Pękalowa, J., Pękala, K. (Eds.), Wyprawy geograficzne na Spitsbergen UMCS, Lublin, pp. 89–95.

Telesiński, M.M., Przytarska, J.E., Sternal, B., Forwick, M., Szczuciński, W., Łącka, M., Zajączkowski, M., 2018. Palaeoceanographic evolution of the SW Svalbard shelf over the last 14 000 years. Boreas. 47(2), 410-422. https://doi.org/10.1111/bor.12282.

Traczyk, A., 2008. Significance of the Quaternary glaciations on the relief evolution of the western coastal zone of the Spitsbergen on example of the Hornsund area. (In:) Kolwalska, A., Latocha, A., Marszałek, H., Pereyma, J. (Eds.), Środowisko Przyrodnicze Obszarów Polarnych. Uniwersytet Wrocławski, Wrocław, pp. 79–88 (in Polish with English abstract).

Ustrzycka, A., Piotrowska, N., Kłusek, M., Pawełczyk, F., Michczyńska, D. J., Michczyński, A., Kozioł, A., Jędrzejowski, M., 2025. Performance of the new MICADAS spectrometer at the Radiocarbon and Mass Spectrometry Laboratory, Gliwice, Poland. Radiocarbon 67(2), 365-377. https://doi.org/10.1017/RDC.2024.126

van der Bilt, W.G.M., D'Andrea, W.J., Werner, J.P., Bakke, J., 2019. Early Holocene temperature oscillations exceed amplitude of observed and projected warming in Svalbard lakes. Geophys. Res. Lett. 46, 14732–14741. https://doi.org/10.1029/2019GL084384.

van Keulen, G., 1714. Nieuwe afteekening van Het Eyland Spits-Bergen opgegeven door de Commandeurs Giles en Outger Rep, en in't Ligt gebrat en uytgegeven. Bibliothèque nationale de France. Available at https://gallica.bnf.fr/ark:/12148/btv1b5972615q (access 13.09.2025)

van Pelt, W., Frank, T., 2025. New glacier thickness and bed topography maps for Svalbard. Cryosphere. 19(1), 1-17, https://doi.org/10.5194/tc-19-1-2025.

van Pelt, W.J.J., Kohler, J., Liston, G.E., Hagen, J.O., Luks, B., Reijmer, C.H., Pohjola, V.A., 2016. Multidecadal climate and seasonal snow conditions in Svalbard. J. Geophys. Res. Earth Surf. 121, 2100-2117. https://doi.org/10.1002/2016JF003999.

Vieli, A., Jania, J., Kolondra, L., 2002. The retreat of a tidewater glacier: observations and model calculations on Hansbreen, Spitsbergen. J. Glaciol. 48(163), 592-600. https://doi.org/10.3189/172756502781831089.

Wacker L., Christl M., Synal H.-A., 2010b. BATS: A new tool for AMS data reduction. Nucl. Instrum. Methods Phys. Res. B 268(7–8), 976–979. https://doi.org/10.1016/j.nimb.2009.10.078.

Wacker, L., Němec, M., Bourquin, J., 2010a. A revolutionary graphitisation system: Fully automated, compact and simple. Nucl. Instrum. Methods Phys. Res. B 268(7–8), 931–934. https://doi.org/10.1016/j.nimb.2009.10.067.

Wassiliew, A.S., 1925. Océan Glacial arctique. Spitzberg. Région des travaux de l'expédition de l'Académies de sciences de Russie pour la mesure d'un arc de méridien en 1899–1901. Carte dresie d'après les matériaux de l'expédition sous la rédactin de O.E. Stubendorff par A.S. Wassiliew. Échelle de 1:200 000.

Wawrzyniak, T., Osuch, M., 2020. A 40-year High Arctic climatological dataset of the Polish Polar Station Hornsund (SW Spitsbergen, Svalbard). Earth Syst. Sci. Data. 12, 805-815. https://doi.org/10.5194/essd-12-805-2020.

Werner, A., 1993. Holocene moraine chronology, Spitsbergen, Svalbard: lichenometric evidence for multiple Neoglacial advances in the Arctic. Holocene. 3(2), 128-137. https://doi.org/10.1177/095968369300300204.

Włodarska-Kowalczuk, M., 2007. Molluscs in Kongsfjorden (Spitsbergen, Svalbard): a species list and patterns of distribution and diversity. Polar Res. 26(1), 48-63, https://doi.org/10.1111/j.1751-8369.2007.00003.x.

Włodarska-Kowalczuk, M., Węsławski, J., Kotwicki, L., 1998. Spitsbergen glacial bays macrobenthos – a comparative study. Polar Biol. 20, 66-73. https://doi.org/10.1007/s003000050277.

Young, N.E., Lamp, J., Koffman, T., Briner, J.P., Schaefer, J., Gjermundsen, E.F., Linge, H., Zimmerman, S., Guilderson, T.P., Fabel, D., Hormes, A., 2018. Deglaciation of coastal south-western Spitsbergen dated with in situ cosmogenic 10Be and 14C measurements. J. Quat. Sci. 33, 763-776. https://doi.org/10.1002/jqs.3058.

Young, N.E., Schaefer, J.M., Briner, J.P., Goehring, B.M., 2013. A 10Be production-rate calibration for the Arctic. J. Quat. Sci. 28, 515-526. https://doi.org/10.1002/jqs.2642.

Zagórski, P., Frydrych, K., Jania, J., Błaszczyk, M., Sund, M., Moskalik, M., 2023. Surges in Three Svalbard Glaciers Derived from Historic Sources and Geomorphic Features. Ann. Assoc. Am. Geogr. 113(8), 1835-1855. https://doi.org/10.1080/24694452.2023.2200487.

Table 1 a, b. ^{10}Be exposure ages and parameters used to calculate them.

Sample ID	Latitude, dec deg	Longitude, dec deg	Altitude, m a.s.l	Strike, deg	Dip, deg	Thickness, cm	Density, g cm^{-3}	Topographic shielding
AOH3	77.00630300	15.68286	79.16	135	15	2.5	2.59	0.963
AOH4	77.00261400	15.68833	27.48	95	30	2.5	2.68	0.995
AOH5	77.00296300	15.6885	31.06	145	15	4	2.6	0.995
AOH6	77.00314593	15.68708	34.65	305	18	3	2.66	0.995
AOH7	77.00355256	15.68921	34.8	260	45	2	2.51	0.990
AOH9	77.01887600	15.70975	159	40	25	4	2.52	0.982
AOH10	77.01887600	15.70975	159	20	30	2.9	2.67	0.982
AOH13	77.01894100	15.70876	160.9	90	15	4.5	2.6	0.984
AOH14	77.00350400	15.68706	37.3	70	27	3	2.6	0.994
AOH15	77.00304736	15.68707	34.6	95	10	2.5	2.63	0.994
AOH16	77.00239875	15.68835	27.23	160	7	2.8	2.55	0.996

Sample ID	Quartz mass, g	^{9}Be spike, mg	$^{10}Be/^{9}Be$ ratio, 10^{-12}	Error, %	^{10}Be conc. 10^3, at/g	Error, %	Age, ka	Error, ka
AOH4	60.22	0.213	0.103	2.9	21.55*	4.5	4.68	0.27
AOH9	59.97	0.214	0.073	3.8	14.60*	5.8	2.77	0.19
AOH10	60.19	0.213	0.235	3.1	52.98*	4.0	10.07	0.56
AOH14	60.03	0.213	0.103	2.8	21.69*	4.3	4.65	0.27
AOH15	55.11	0.212	0.136	2.4	31.89*	3.8	6.75	0.36
AOH16	60.04	0.214	0.013	12.4	0.33*	161.2	0.07	0.11
Blank 1		0.214	0.012	13.0				
AOH3	61.10	0.283	0.0047	10.8	0.95**	17.9	0.20	0.04
AOH5	60.85	0.280	0.0181	4.4	5.06**	5.5	1.09	0.07
AOH6	60.64	0.281	0.0180	4.1	5.09**	5.3	1.08	0.07
AOH7	60.35	0.283	0.0096	5.9	2.49**	7.9	0.57	0.05
AOH13	58.37	0.280	0.0091	6.1	2.40**	8.3	0.45	0.04
Blank 2		0.283	0.0019	15.2				
Blank 3		0.283	0.0014	17.0				

* corrected to background of preparation blank 1
** corrected to average background of preparation blanks 2 and 3

1560 Table 2. Historical maps and photographs used in the study.

Year	Type of data	Source*
1613	Map	Narrative of a voyage to Spitzbergen in the year 1613 (Fotherby, 1613)
1625	Map	"Greneland" [Spitsbergen] map in "Purchas His Pilgrimes" (Purchas, 1625)
1634	Map	Kaart van Spitsbergen door M.H. Middelhoven (Middelhoven, 1634)
1663	Map	Paskaert van Spitsbergen, met alle zijn zeekusten zoo veel tot noch toe bekent is (Doncker, 1663)
1714	Map	Nieuwe afteekening van Het Eyland Spits-Bergen opgegeven door de Commandeurs Giles en Outger Rep, en in't Ligt gebrat en uytgegeven (van Keulen, 1714)
1758	Map	Carte du Spits-Berg (Bellin, 1758)
1820	Map	A chart of Spitzbergen or East Greenland, comprising an original survey of the west coast (Scoresby, 1820)
1861–1864	Map	Karta ofver Spetsbergen: hufvudsakligast enligt iakttagelser under de svneska expeditionera aren 1861 och 1864 af N. Duner och A.E. Nordenskiold (Dunér and Nordenskiöld, 1865)
1872	Map	Die Arktische Expedition des Grafen Hans Wiltschek nach Spitzbergen & Nowaja Semlja Juni - Sept. 1872, 1:200 000 (Peterman, 1874)
1872	Photographs	The Austro-Hungarian North Pole expedition (https://onb.digital/)
1897	Map	Sir Martin Conway's expeditions to Spitsbergen (Conway, 1898; https://data.npolar.no/map/archive/)
1899	Map	Plan öfver det svebsk-ryska gradmätningsnätet på Spetsbergen efter nyaste sammanställd Maj 1900, 1:1 000 000 (de Geer, 1923)
1899–1901	Map	Océan Glacial arctique. Spitzberg. Région des travaux de l'expédition de l'Académies de sciences de Russie pour la mesure d'un arc de méridien en 1899–1901, 1:200 000 (Wassiliew, 1925)
1899–1901	Photographs	The Swedish-Russian Arc-of-Meridian Expedition in 1899–1901 (https://www.ras.ru/)
1917–1918	Terrestrial photogrammetric photos	Norwegian expeditions to Svalbard (https://bildearkiv.npolar.no/fotoweb/)
1918	Map	Nautical chart from 1917–1921, Hornsund to Dunderbay, 1:100 000 (Norwegian Polar Institute, 1921)
1918	Map	Nautical chart 504 from 1909–1935, Frå Sørkapp til Bellsund, 1:200 000 (Hoel, 1938)
1936	Oblique aerial photographs and derived ortophotomap	Norwegian expedition in 1936; Geyman et al., 2022 (available at https://toposvalbard.npolar.no/)
1960	Map	Nautical chart 504 from 1984, Frå Sørkapp til Bellsund, 1:200 000 (Norwegian Polar Institute, 1984)

1561 * Scale of the map is indicated when explicitly stated in the source material.

Fig. 1. Study area. **(a)** Division of Svalbard into S, NW and NE parts after van Pelt and Frank (2025); a map after © Norwegian Polar Institute (2014a). **(b)** Glacier hypsometry (area-elevation distribution) in the S (red), NW (dark blue) and NE (light blue) regions. The plot in the top right presents the cumulative glacier area-elevation distribution. **(c)** Field research areas of geomorphological mapping and sampling for ^{14}C and ^{10}Be dating (white rectangles). Glaciers (black letters): A – Angellkroken, Ch – Chomjakovbreen, D – Deileggbreen, F – Fuglebreen, G – Gåsbreen, Ha – Hambergbreen, Ho – Hornbreen, Is – Isingbreen, Kb – Körberbreen, Kv – Kvalfangarbreen, L – Lifjellfonna, Me – Mendeleevbreen, Mu – Mühlbacherbreen, N – Nannbreen, P – Petersbreen, Sa – Samarinbreen, Sk – Skilryggbreen, Sl – Slyngfjellbreen, St – Staszelisen, Sv – Svalisbreen, T – Tuvbreen, W – Wibebreen, Wrn – Werenskioldbreen. Bays (blue letters): AB – Austre Burgerbukta, VB – Vestre Burgerbukta, H – Hansbukta, S – Selbukta. Peninsulas (orange letters): B – Baranowski Peninsula (Baranowskiodden), O – Oseanograftnagen, T – Treskelen. Mountain peaks and saddles (yellow letters): Fa – Fannytoppen, Fg – Fugleberget, Fl – Flatpasset. The star marks the Polish Polar Station Hornsund; background: satellite scene Sentinel-2A from 08.08.2024 (https://browser.dataspace.copernicus.eu/).

Fig. 2. Glacier surge features within the marginal zones of selected glaciers in S Spitsbergen. **(a)** Crevasse-squeeze ridges (CSRs) in the inner forefield of Hansbreen (white arrows). **(b)** Black arrow marks the location of the lateral terminal moraine at Flatpasset. **(c, d)** Subfossil soil below glacial diamict on Oseanograftangen. **(e)** A cobble of quartzite on the trimline of Hansbreen on Fannytoppen, collected for ^{10}Be dating. **(f)** CSRs on Treskelen after the glacier surge of Hornbreen. **(g)** Little Ice Age terminal moraine of Hornbreen climbing up to the Treskelen peninsula crest (arrow). Note a person in a circle on the moraine crest as a scale. Photo by A. Osika (a–d, f, g) and M. Ciepły (e).

Fig. 3. Glacier surge geomorphological evidence on Vestre Torellbreen and Werenskioldbreen, SW Spitsbergen. **(a, b)** Overridden moraines and drumlins in the forefield of Vestre Torellbreen. **(c)** Terminal moraine of a surge advance of Vestre Torellbreen in the 1960s. **(d)** Fluted moraine and **(e)** a low CSR (arrow) in the forefield of Werenskioldbreen. A glove for a scale. **(f)** A low ridge of proglacial push moraine (arrow) in front of an ice-cored terminal moraine of Werenskioldbreen. Photo by A. Osika (a, b, d–f) and M. Ciepły (c).

Fig. 4. New (bold font) and previously reported radiocarbon ages (median values, cal BP) of mollusc shells, a whalebone and subfossil soils in the forefields of **(a)** Hansbreen and **(b)** Hornbreen. “x” marks three shell samples younger than 1950 CE. Dashed circle marks the samples with unknown exact locations. Background: Sentinel-2A from 08.08.2024 (https://browser.dataspace.copernicus.eu/).

Fig. 5. New (bold font) and previously reported radiocarbon ages (median values, cal BP) of mollusc shells, driftwood and subfossil vegetation in the forefields of **(a)** Vestre Torellbreen and **(b)** Werenskioldbreen. “x” marks a shell with the 1 and 2 sigma confidence intervals exceeding 1950 CE. Dashed circle marks the samples from literature with unknown exact locations. Background: Sentinel-2A from 08.08.2024 (https://browser.dataspace.copernicus.eu/).

Fig. 6. New and previously reported ^{10}Be ages in Hornsund. **(a, b)** New ^{10}Be ages (ka) from cobbles from the trimline and lateral terminal moraine of Hansbreen. **(c)** ^{10}Be ages (ka) from the Late Holocene moraine of Hornbreen on Treskelen published by Philipps et al. (2017). Imagery from TopoSvalbard, © Norwegian Polar Institute (https://toposvalbard.npolar.no/).

Fig. 7. Glacier surge evidence in historical photographs and maps. **(a)** Tidewater glaciers of inner Hornsund in the photograph from the Austro-Hungarian North Pole Expedition in 1872. Source: Austrian National Library, Vienna, Signature: Pk 650, 19 (modified). **(b)** Hornsund glaciers on a 1:200,000 map from 1900 (Wassiliew, 1925; https://data.npolar.no/map/archive). Glaciers: G – Gåsbreen, H – Hansbreen, K – Körberbreen, M – Mühlbacherbreen, P – Paierlbreen, S – Samarinbreen. **(c)** Frontal zone of Hornbreen in the photograph from the Norwegian expedition in 1918. Note the recession of Hornbreen and Samarinbreen compared to 1872, which had separated the latter from the Hornbreen-Hambergbreen system. Source: © Adolf Hoel, Norsk Polarinstitutt (Image ID: NBR9201_05204, cropped and modified).

Fig. 8. Comparison of proxy records spanning the Deglaciation-Holocene. From top to bottom: ice-rafted debris flux (IRD) in core OCE2019-HR7-GC (Devendra et al., 2023); December-February temperature from the Lomonosovfonna ice core (Divine et al., 2011); July air temperature reconstructed from Chironomidae assemblages from Svartvatnet lake in southern Spitsbergen (Luoto et al., 2017); bottom water temperature (BWT) in core OCE2019-HR7-GC (Devendra et al., 2023); sea surface temperature (SST) in core JM09-20-GC (Łącka et al., 2019); sea surface temperature in core JM09-KA11-GC (Berben et al., 2014); sea surface temperature in core OCE2019-HR7-GC (Devendra et al., 2023); and $\delta^{18}O$ from the GISP2 ice core (Grootes et al., 1993). Blue-red bar at the top and the bottom schematically represents reconstructed glacier fluctuations in southern Spitsbergen in the Holocene: glacier retreat in the warmer phases (red boxes), gradual ice mass build-up and glacier re-growth in the Neoglacial (light blue boxes) and known periods of glacier advances (including glacier surges) in the Late Holocene (dark blue boxes).

Figure 1 Click here to access/download;Figure;Fig1.jpg

Figure 1

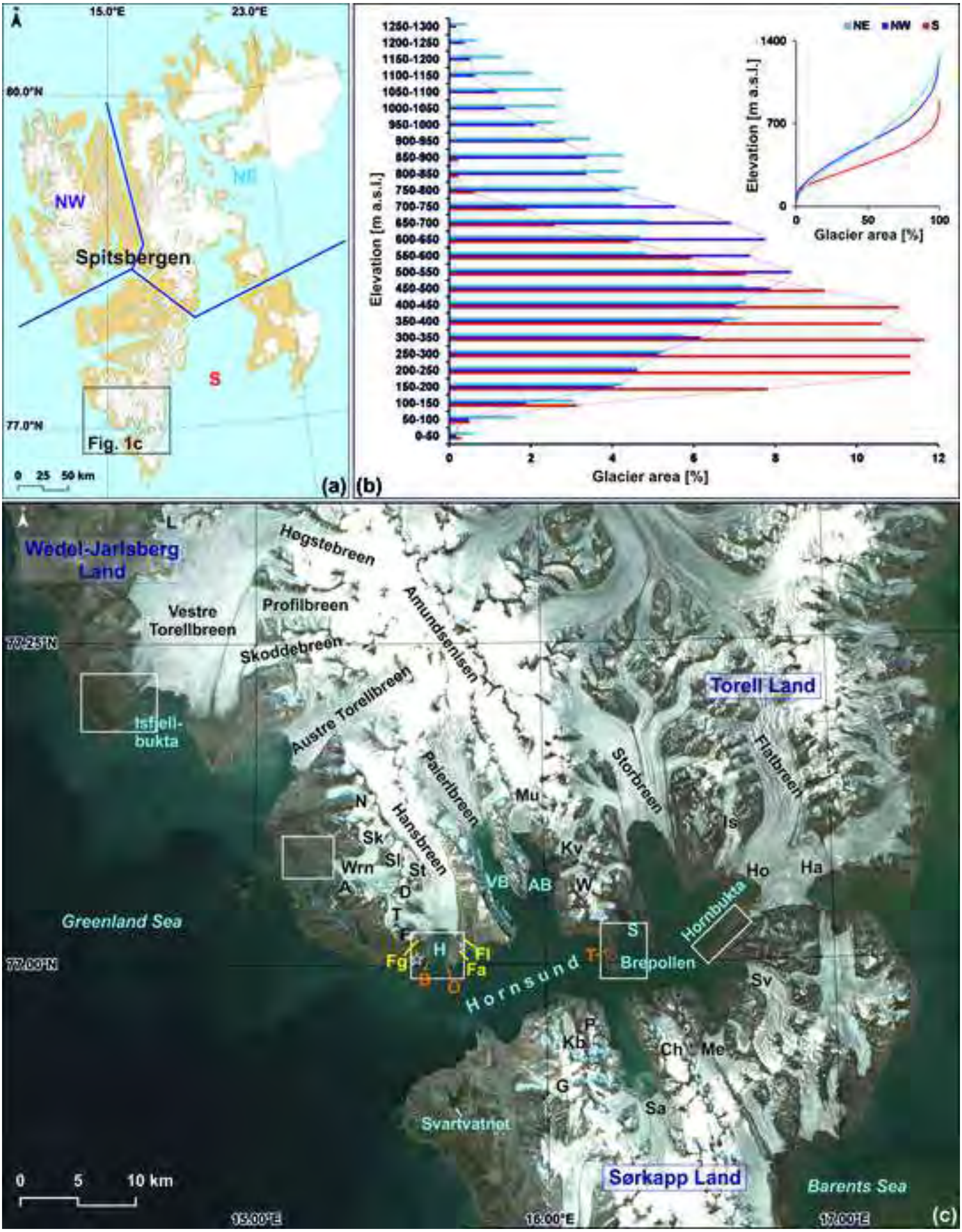

Figure 2

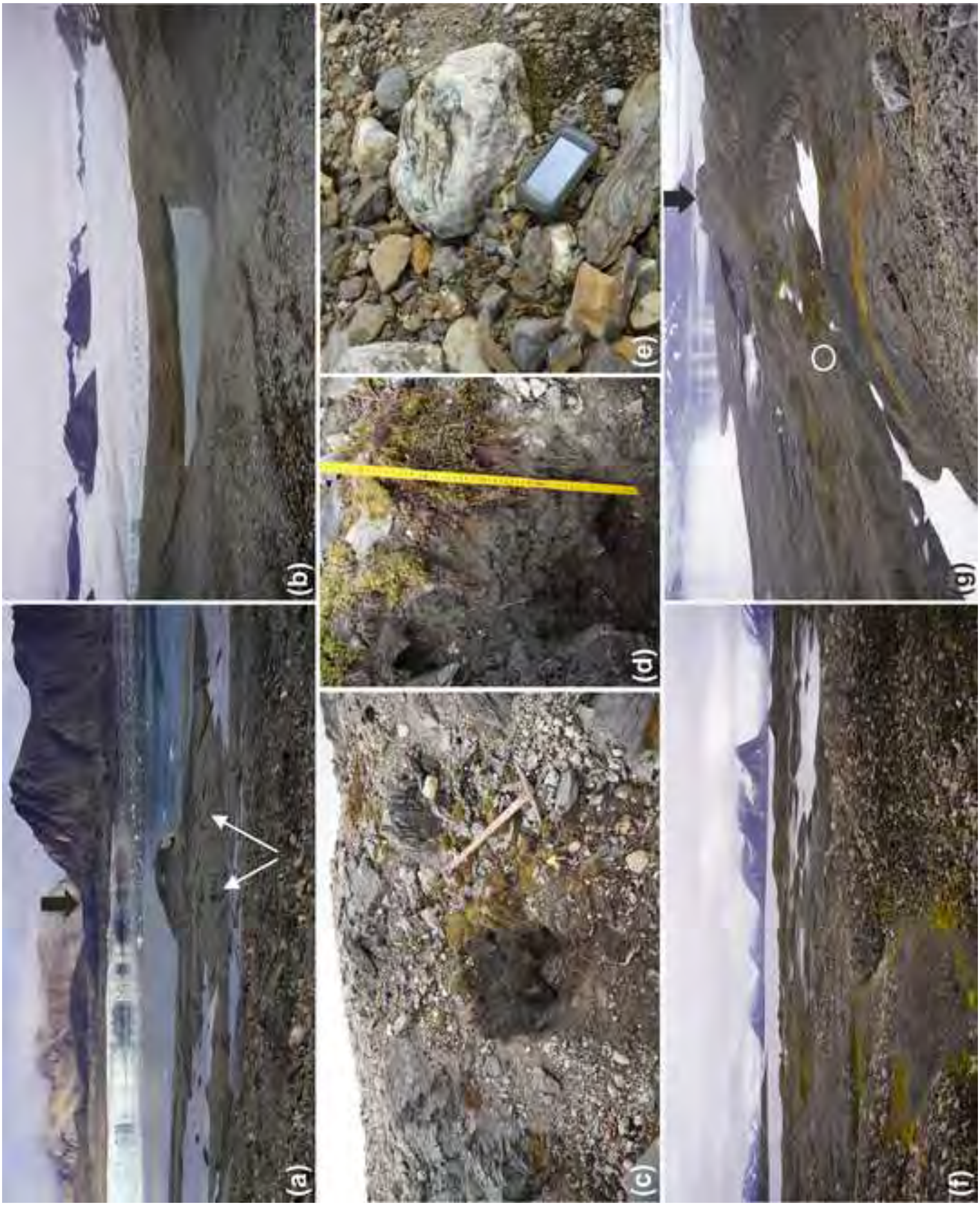

Figure 3

Figure 3

Figure 4

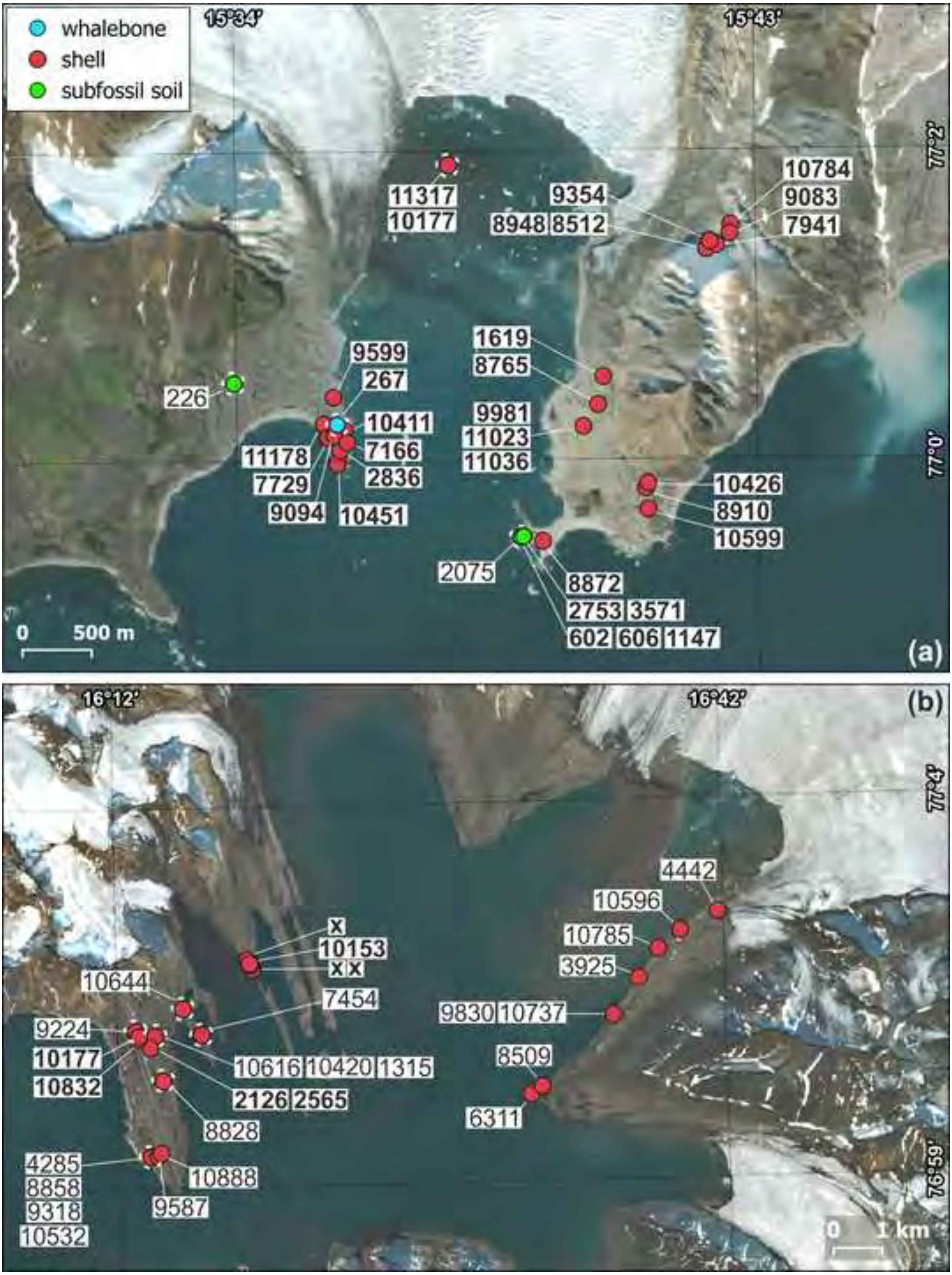

whalebone
shell
subfossil soil
15°34'
15°43'
77°2'
77°0'
11317
10177
9354
8948 8512
10784
9083
7941
1619
8765
9981
11023
11036
9599
267
226
10411
7166
2836
10451
11178
7729
9094
10426
8910
10599
2075
8872
2753 3571
602 606 1147
0 500 m
(a)
16°12'
16°42'
77°4'
76°59'
(b)
4442
10596
10785
3925
9830 10737
8509
6311
X
10153
X X
10644
7454
9224
10177
10832
10616 10420 1315
2126 2565
8828
4285
8858
9318
10532
10888
9587
0 1 km

Figure 5

Click here to access/download;Figure;Fig5.jpg

Figure 5

Figure 6

Figure 6

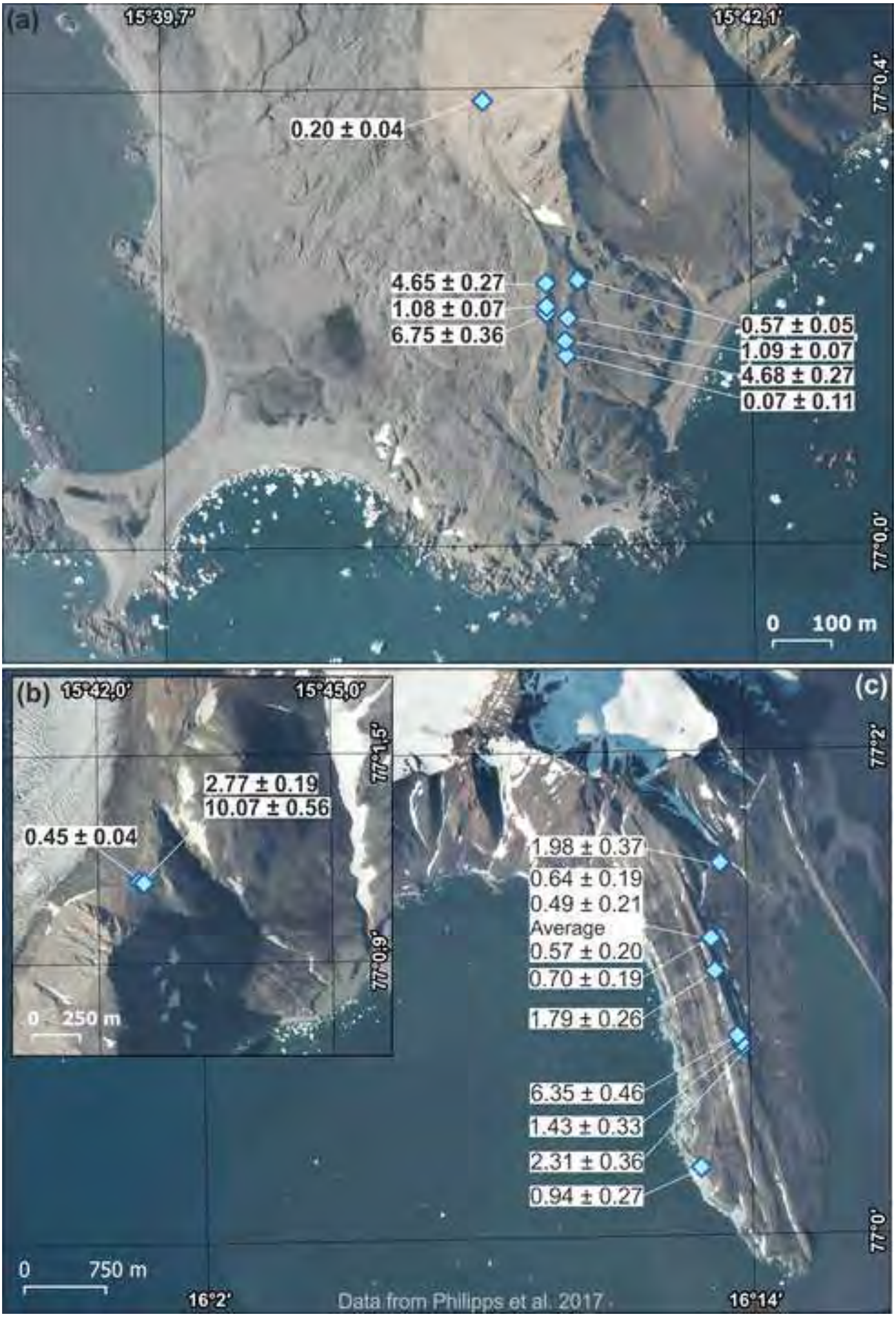

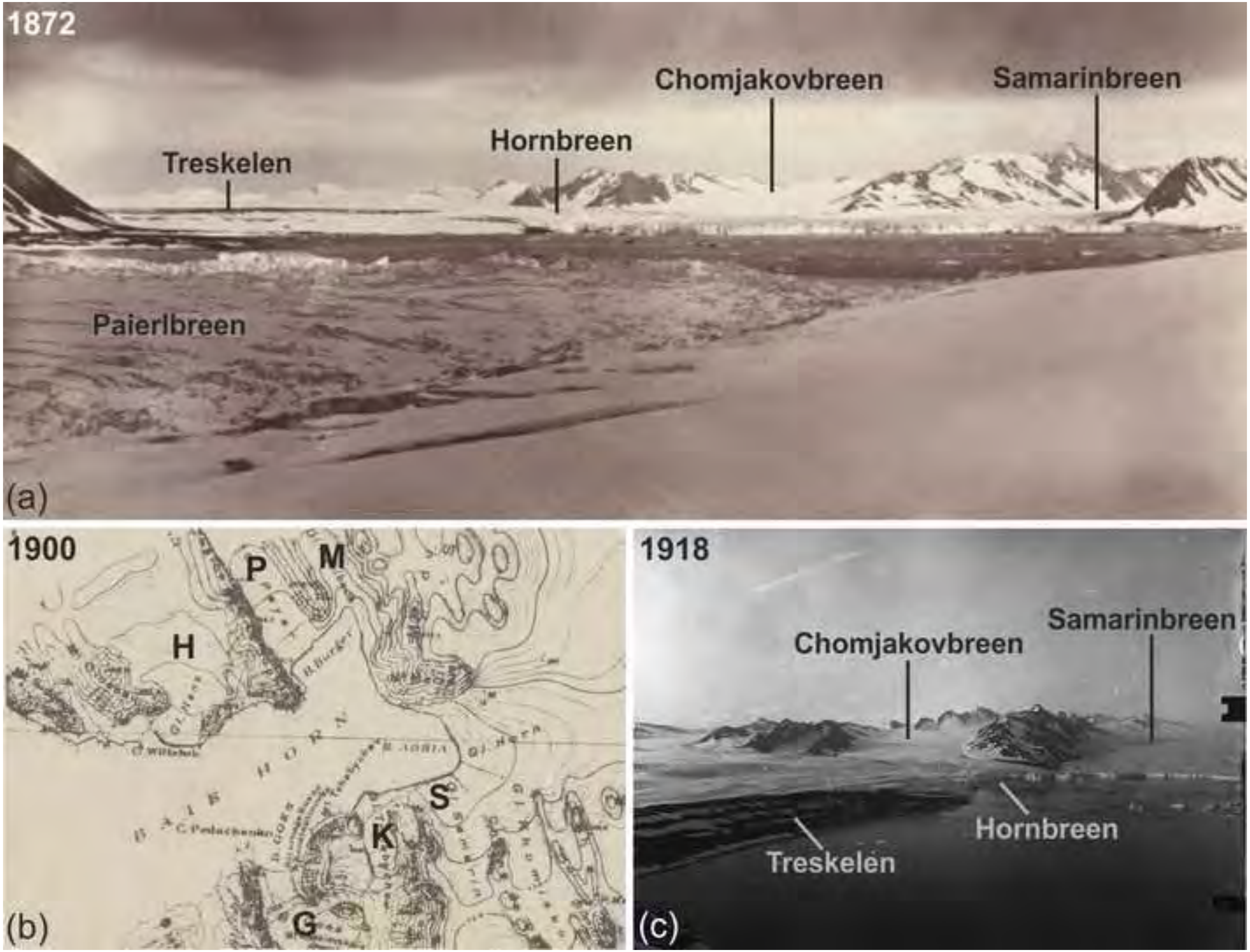
1872
Chomjakovbreen
Samarinbreen
Hornbreen
Treskelen
Paierlbreen
(a)
1900
P
M
H
S
K
G
(b)
1918
Samarinbreen
Chomjakovbreen
Hornbreen
Treskelen
(c)

Figure 7

Figure 8

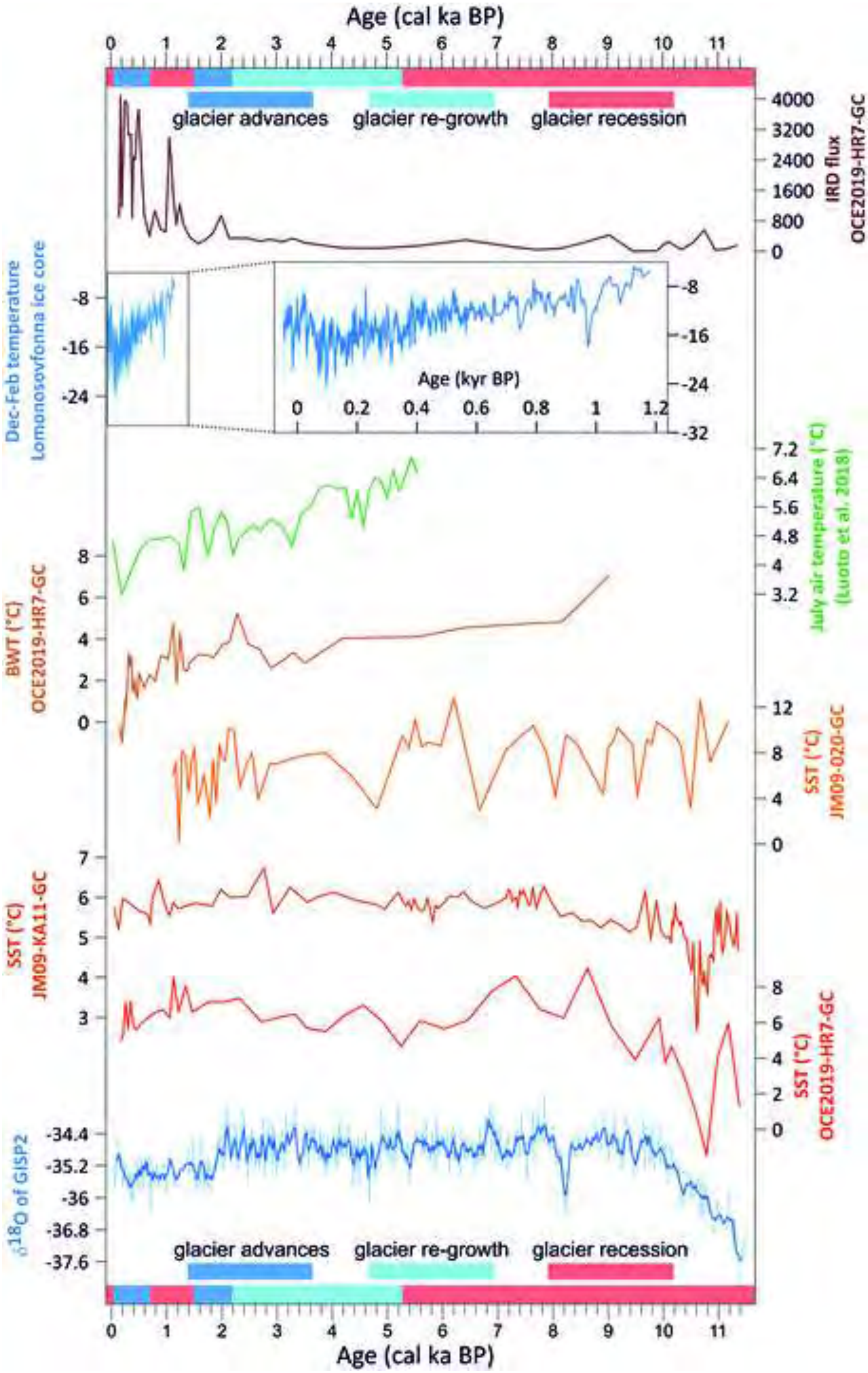

Age (cal ka BP)
0 1 2 3 4 5 6 7 8 9 10 11
glacier advances
glacier re-growth
glacier recession
4000
3200
2400
1600
800
0
IRD flux
OCE2019-HR7-GC
Dec-Feb temperature
Lomonosovfonna ice core
-8
-16
-24
Age (kyr BP)
0 0.2 0.4 0.6 0.8 1 1.2
-32
7.2
6.4
5.6
4.8
4
3.2
July air temperature (°C)
(Luoto et al. 2018)
BWT (°C)
OCE2019-HR7-GC
8
6
4
2
0
12
SST (°C)
JM09-020-GC
SST (°C)
JM09-KA11-GC
7
6
5
4
3
SST (°C)
OCE2019-HR7-GC
δ18O of GISP2
-34.4
-35.2
-36
-36.8
-37.6

Declaration of Interest Statement

Declaration of interests

☒The authors declare that they have no known competing financial interests or personal relationships that could have appeared to influence the work reported in this paper.

☐The authors declare the following financial interests/personal relationships which may be considered as potential competing interests:

Appendix. Figures A.1 - A.5

Research Data

Click here to download Research Data

https://doi.org/10.5281/zenodo.15831641

Supplementary maps and photographs for the paper “Holocene glacial history of southern Spitsbergen” (Aleksandra Osika[a]*, Jacek Jania[a], Natalia Piotrowska[b], Dmitry Tikhomirov[c], Joanna Ewa Szafraniec[a], Dhanushka Devendra[d], Marcus Christl[e], Markus Egli[c], Andreas Vieli[c])

[a] Institute of Earth Sciences, Faculty of Natural Sciences, University of Silesia in Katowice, Bedzinska 60, 41-200 Sosnowiec, Poland

[b] Institute of Physics, Silesian University of Technology, Stanislawa Konarskiego 22B/217, 44-100 Gliwice, Poland

[c] Department of Geography, University of Zurich, Zurich, Switzerland

[d] Department of Palaeoceanography, Institute of Oceanology, Polish Academy of Sciences, 81-712 Sopot, Poland

[e] Laboratory of Ion Beam Physics, ETH, Zurich, Switzerland

*Corresponding author: 1aleksandra.osika@gmail.com

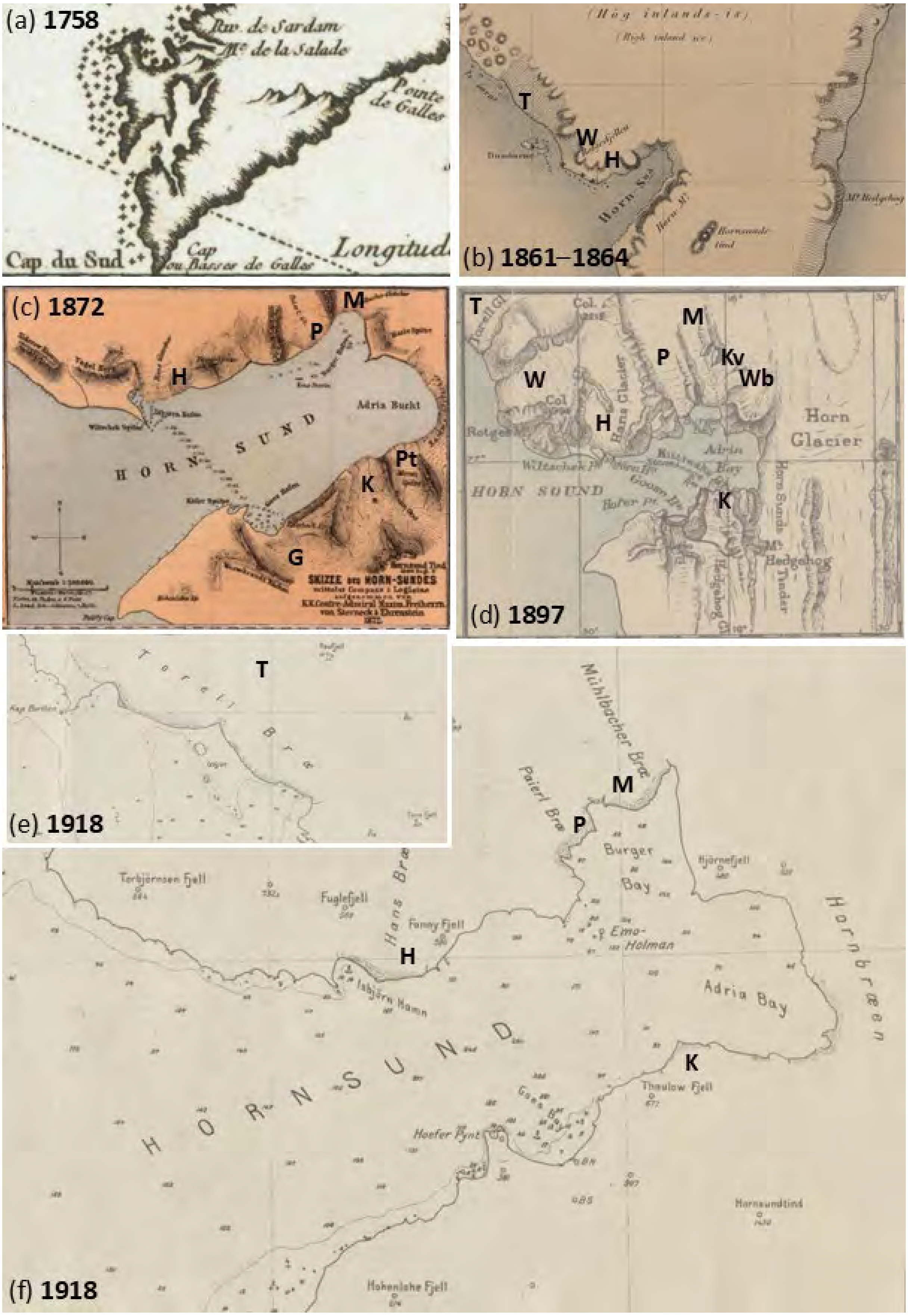

Fig. A.1. Hornsund on historical maps: **(a)** 1758, **(b)** 1861–1864, **(c)** 1872, **(d)** 1897, and **(e, f)** 1918. Glaciers: G – Gåsbreen, H – Hansbreen, K – Körberbreen, Kv – Kvalfangarbreen, M –

Mühlbacherbreen, P – Paierlbreen, Pt – Petersbreen, T – Torellbreen, W – Werenskioldbreen, Wb – Wibebreen.

Sources of maps:

(a) Bellin, J.N., 1758. Carte Du Spits-Berg: Suivant les Hollandois pour Servir a l'Histoire Generale des Voyages. Publisher J.N. Bellin, Paris.
Source: Universitätsbibliothek Bern, MUE Ryh 8403 : 1 B, https://doi.org/10.3931/e-rara-130665

(b) Dunér, N., Nordenskiöld, A.E., 1865. Karta öfver Spetsbergen, hufvudsakligast enligt iakttagelser under de svenska expeditionerna åren 1861 och 1864. Abrah. Lundquist & Cie., Stockholm.
Source: Lund University Library, alvin-record:465671

(c) Petermann, A., Peip, C., Domann, B., Perthes, J., Wiltschek, H., Daublebsky von Sterneck, M.V., 1874. Die Arktische Expedition des Grafen Hans Wiltschek nach Spitzbergen & Nowaja Semlja Juni-Sept. 1872: nach Aufzeichnungen des Contre-Admirals v. Sterneck & Ehrenstein.
Source: https://zs.thulb.uni-jena.de/receive/jportal_jparticle_00531743

(d) Conway, W.M., 1898. With ski & sledge over Arctic glaciers. J.M. Dent & Co., London. Map: *Central Spitsbergen, From sketch surveys made in 1896 & 1897, by Sir Martin Conway*.
Source: Digital map archive of the Norwegian Polar Institute, https://data.npolar.no/map/archive/

(e, f) Norwegian Polar Institute, 1921. (Kart over) Farvannet mellom Hornsund og Dunderbay 1917–1921.
Source: Digital map archive of the Norwegian Polar Institute, https://data.npolar.no/map/archive/

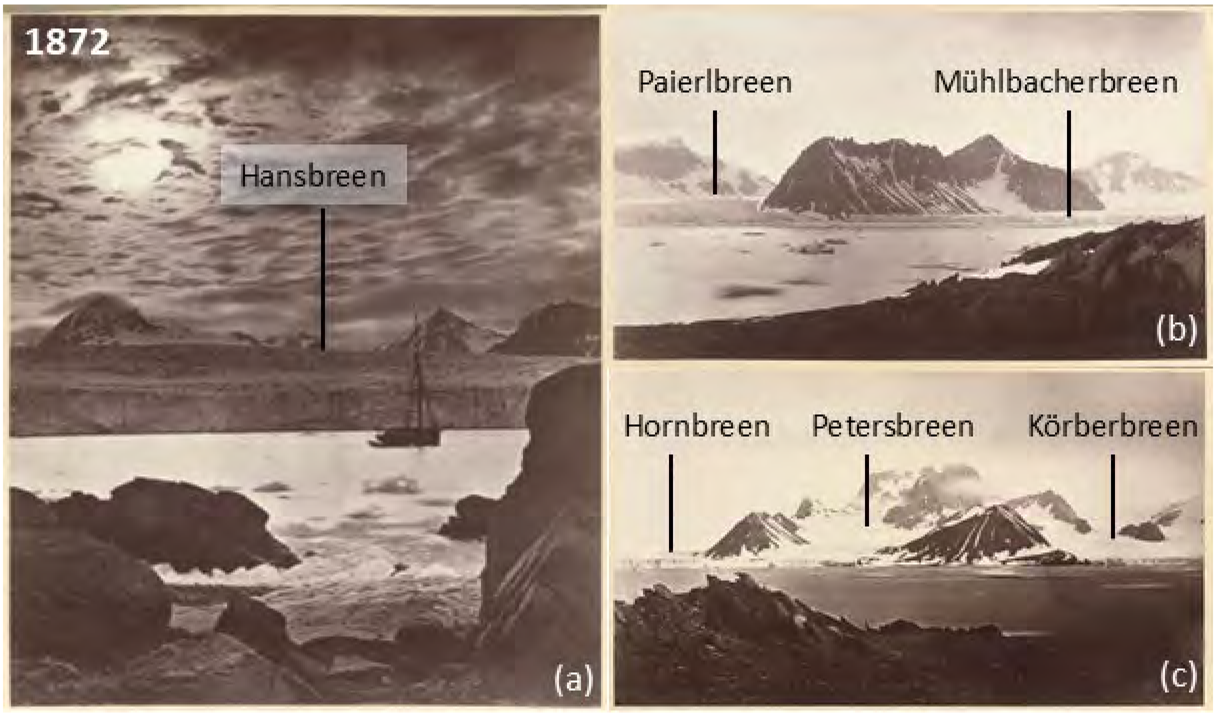

Fig. A.2. Photographs from the Austro-Hungarian North Pole Expedition in 1872: **(a)** Hansbreen, **(b)** Paierlbreen and Mühlbacherbreen, **(c)** Hornbreen, Petersbreen and Körberbreen.

Austrian National Library, Vienna, Signatures: Pk 650, 10; Pk 650, 21 and Pk 650, 20 (modified).

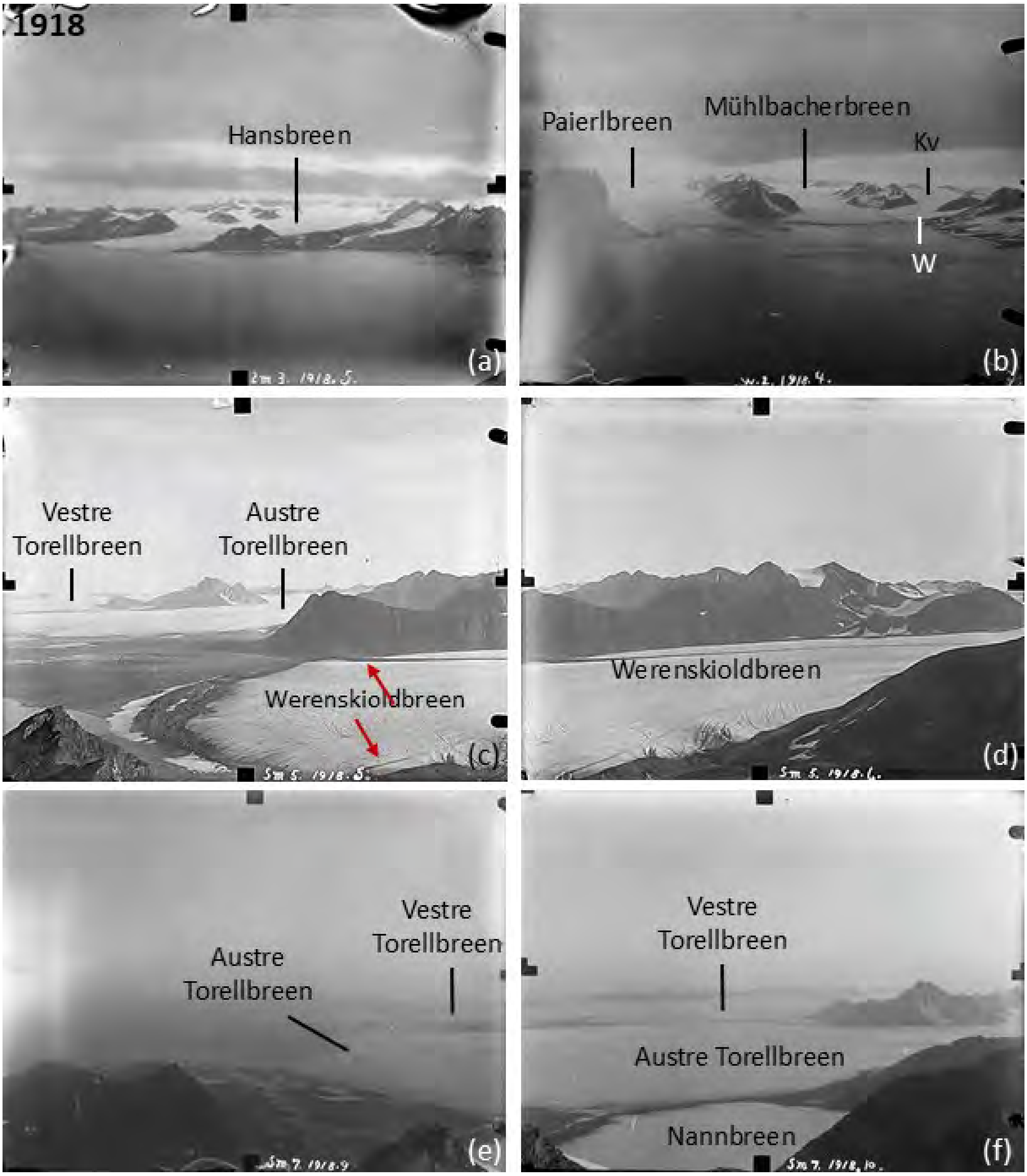

Fig. A.3. Terrestrial photogrammetric data from the Norwegian Spitsbergen expedition in 1918. Kv – Kvalfangarbreen, W – Wibebreen. Arrows in **(c)** mark looped moraines on the surface of Werenskioldbreen.

(a, c–e) © Olaf Holtedahl, Norsk Polarinstitutt (Image ID: NBR9201_05392; NBR9201_05415; NBR9201_05416 and NBR9201_05437, modified), (b) © Werenskiold, Norsk Polarinstitutt (Image ID: NBR9201_05547, modified), (f) © Wilhelm Solheim, Norsk Polarinstitutt (Image ID: NBR9201_05438, modified).

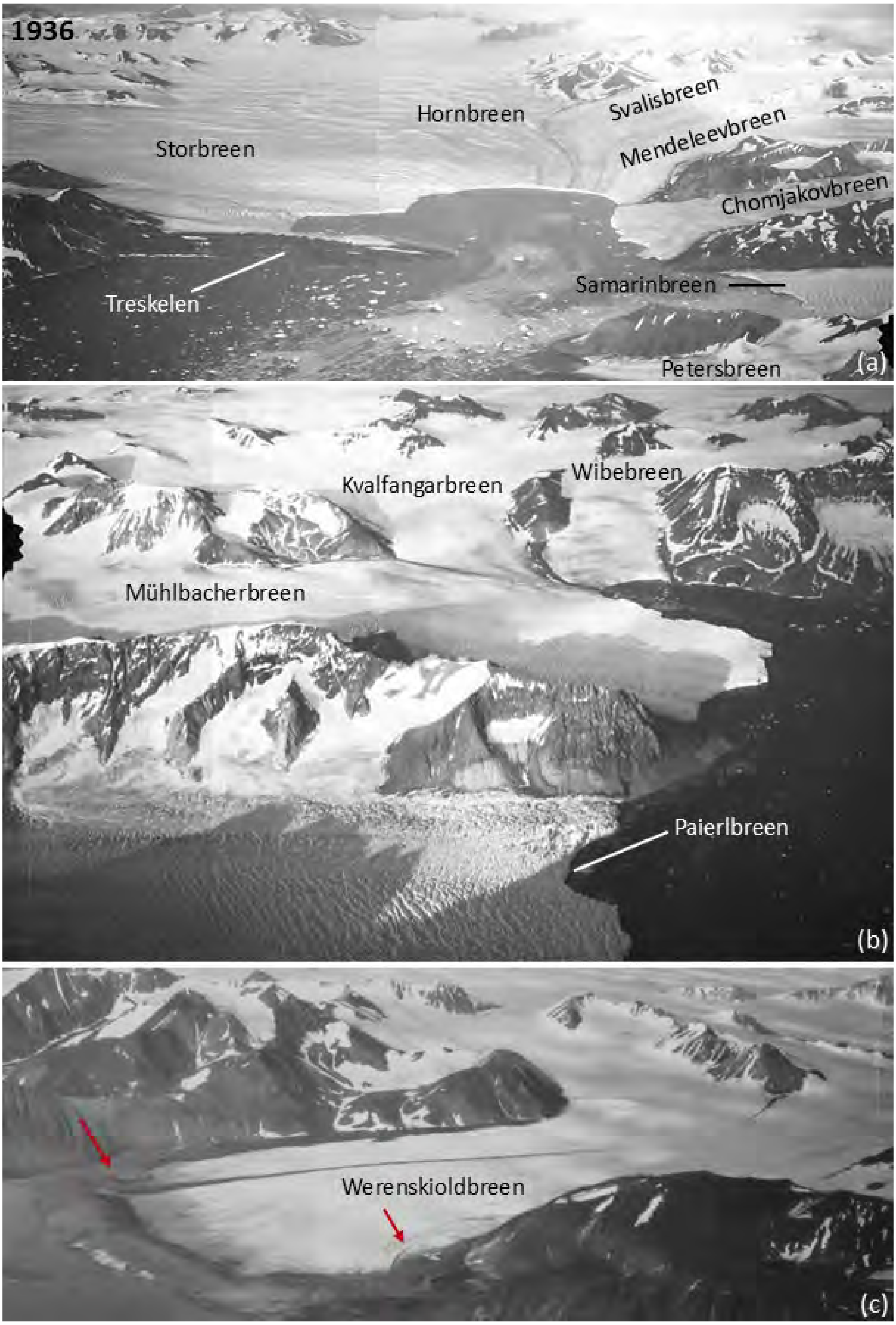

Fig. A.4. Oblique aerial photographs from 1936 of tidewater glaciers: **(a, b)** in inner Hornsund and **(c)** Werenskioldbreen. Arrows mark looped moraines on the Werenskioldbreen surface.

TopoSvalbard (https://toposvalbard.npolar.no/), © Norwegian Polar Institute (Photo ID: S36_2697; S36_2704 and S36_2643, modified).

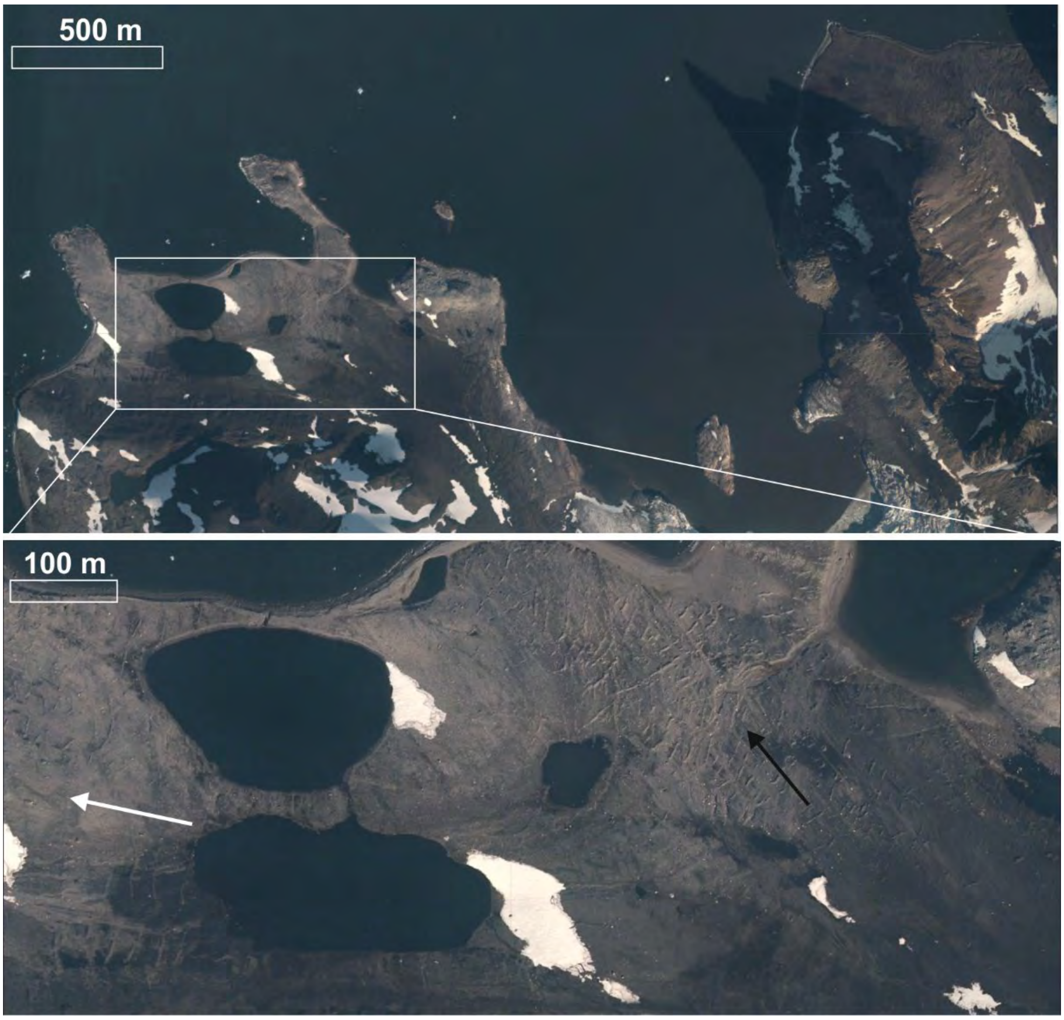

Fig. A.5. Fluted moraine with crevasse-squeeze ridges at Chomjakovbreen. Note the contrast between eroded flutes oriented W-E (white arrow) and distinct flutes oriented NW-SE (black arrow).

Załącznik 9

Załącznik nr 9
do pisma okólnego nr 2
Prorektora ds. nauki i finansów
z dnia 19 lutego 2024 r.

Sosnowiec, 22.09.2025 r.

Aleksandra Osika

OŚWIADCZENIE OSOBY UBIEGAJĄCEJ SIĘ O WŁASNYM WKŁADZIE W POWSTAWANIE PRACY

Oświadczam, że w pracy:

Osika A., Jania J., Szafraniec J.E., 2022: Holocene ice-free strait followed by dynamic Neoglacial fluctuations: Hornsund, Svalbard. The Holocene, 32(7), 664–679, doi:10.1177/09596836221088232

mój udział polegał na przeprowadzeniu badań terenowych i pobraniu materiału do datowania radiowęglowego, analizie wyników datowania i kalibracji dat radiowęglowych, przygotowaniu tekstu manuskryptu (z wyjątkiem opisu wskaźników morfometrycznych CfD i CfE), opracowaniu rycin (z wyjątkiem ryciny 6), modyfikacji tekstu zgodnie z uwagami recenzentów, odpowiedzi na komentarze recenzentów i kontakcie z redakcją jako autor korespondencyjny.

W pracy:

Osika A., Jania J., 2024: Geomorphological and historical records of the surge-type behaviour of Hansbreen (Svalbard). Annals of Glaciology, 65, e31, doi:10.1017/aog.2024.32

mój udział polegał na kierowaniu projektem NCN Preludium (*Rekonstrukcja zasięgu lodowców i środowiska południowego Svalbardu podczas Optimum Klimatycznego Holocenu jako wzorca konsekwencji współczesnego ocieplenia klimatu*; 2021/41/N/ST10/02070) obejmującym badania opisane w tej pracy, przeprowadzeniu badań terenowych, kartowaniu geomorfologicznym lądowego i morskiego przedpola Lodowca Hansa, pozyskaniu i analizie archiwalnych map i fotografii, przygotowaniu tekstu manuskryptu, przygotowaniu rycin, zestawieniu i udostępnieniu danych powiązanych z artykułem w repozytorium Zenodo (*Osika A., Jania J., 2024, Dataset from Osika and Jania (2024): Geomorphological and historical records of the surge-type behaviour of Hansbreen (Svalbard), Zenodo, https://doi.org/10.5281/zenodo.13646525*), modyfikacji tekstu zgodnie z uwagami recenzentów, odpowiedzi na komentarze redaktora i recenzenta oraz kontakcie z redakcją jako autor korespondencyjny.

Aleksandra Osika

W pracy:

Osika A., Jania J., Piotrowska N., Tikhomirov D., Szafraniec J.E., Devendra D., Christl M., Egli M., Vieli A., 2025: Holocene glacial history of southern Spitsbergen [złożona do Quaternary Science Reviews]

mój udział polegał na kierowaniu projektami NCN Preludium (*Rekonstrukcja zasięgu lodowców i środowiska południowego Svalbardu podczas Optimum Klimatycznego Holocenu jako wzorca konsekwencji współczesnego ocieplenia klimatu*; 2021/41/N/ST10/02070) i Arctic Field Grant no. 310661, które obejmowały badania opisane w tej pracy, przeprowadzeniu badań terenowych i pobraniu materiału do datowania ^{14}C i ^{10}Be, analizie wyników i kalibracji dat radiowęglowych, preparatyce próbek skał do datowania ^{10}Be podczas stażu na Uniwersytecie w Zurychu w ramach stypendium Bekker NAWA, analizie wyników ^{10}Be, pozyskaniu i analizie archiwalnych map i fotografii, przygotowaniu tekstu manuskryptu (z wyjątkiem opisu metod ^{14}C i ^{10}Be), przygotowaniu rycin (z wyjątkiem ryciny 1 i zestawienia danych paleoklimatycznych), zestawieniu i udostępnieniu danych powiązanych z artykułem w repozytorium Zenodo (*Osika A., Piotrowska N., Jania J., 2025, Radiocarbon dates of marine shells, subfossil vegetation, driftwood and a whalebone from glacial sediments in Hornsund (Spitsbergen, Svalbard), Zenodo, https://doi.org/10.5281/zenodo.15831642*), złożeniu artykułu jako autor korespondencyjny.

Aleksandra Osika
……………………………………………

Załącznik 10

Załącznik nr 10
do pisma okólnego nr 2
Prorektora ds. nauki i finansów
z dnia 19 lutego 2024 r.

OŚWIADCZENIE

WSPÓŁAUTORA OSOBY UBIEGAJĄEJ SIĘ O WŁASNYM WKŁADZIE W POWSTAWANIE PRACY

Miejsce Sosnowiec, dnia 25.08.2025

Jacek Jania
Imię i nazwisko współautora publikacji

Instytut Nauk o Ziemi, Uniwersytet Śląski w Katowicach
Afiliacja

OŚWIADCZENIE

Oświadczam, że w pracy:

Aleksandra Osika, Jacek Jania and Joanna Ewa Szafraniec, 2022: *Holocene ice-free strait followed by dynamic Neoglacial fluctuations: Hornsund, Svalbard*. The Holocene, 32, 7; 1–16: https://doi.org/10.1177/09596836221088232

(autorzy, rok wydania, tytuł, czasopismo lub wydawca, tom, strony)

Mój udział polegał na pomocy w planowaniu koncepcji badań, współudziale w pracach terenowych i poboru próbek do datowania radiowęglowego, także na współudziale w interpretacji wyników i współredagowaniu tekstu przygotowanego przez Aleksandrę Osikę.

opisać szczegółowo swój własny – (a nie osoby ubiegającej się) – udział w powstaniu pracy, (np. mój udział w powstanie tej publikacji polegał na wykonaniu doświadczeń techniką ....., analizie statystycznej wyników eksperymentów zilustrowanych na ryc. ...., przygotowaniu tekstu manuskryptu zamieszczonego w rozdziale......, kierowaniu projektem naukowym obejmującym badania opisane w tej pracy, itp.).*

Jacek Jania
....
Podpis współautora publikacji

Załącznik 11

Załącznik nr 10
do pisma okólnego nr 2
Prorektora ds. nauki i finansów
z dnia 19 lutego 2024 r.

OŚWIADCZENIE

WSPÓŁAUTORA OSOBY UBIEGAJĄEJ SIĘ O WŁASNYM WKŁADZIE W POWSTAWANIE PRACY

Miejsce Sosnowiec, dnia 25.08.2025

Jacek Jania
Imię i nazwisko współautora publikacji

Instytut Nauk o Ziemi, Uniwersytet Śląski w Katowicach
Afiliacja

OŚWIADCZENIE

Oświadczam, że w pracy:

Aleksandra Osika, Jacek Jania, 2024: *Geomorphological and historical records of the surge-type behaviour of Hansbreen (Svalbard).* Annals of Glaciology, 65, e31; DOI: https://doi.org/10.1017/aog.2024.32

(autorzy, rok wydania, tytuł, czasopismo lub wydawca, tom, strony)

Mój udział polegał na pomocy w planowaniu koncepcji badań, współudziale w pracach terenowych, a także na opiece merytorycznej poprzez współudział w analizie i interpretacji danych oraz współredagowaniu tekstu przygotowanego przez Aleksandrę Osikę.

opisać szczegółowo swój własny – (a nie osoby ubiegającej się) – udział w powstaniu pracy, (np. mój udział w powstanie tej publikacji polegał na wykonaniu doświadczeń techniką ....., analizie statystycznej wyników eksperymentów zilustrowanych na ryc. ...., przygotowaniu tekstu manuskryptu zamieszczonego w rozdziale......, kierowaniu projektem naukowym obejmującym badania opisane w tej pracy, itp.).*

Jacek Jania
....
Podpis współautora publikacji

Załącznik 12

Załącznik nr 10
do pisma okólnego nr 2
Prorektora ds. nauki i finansów
z dnia 19 lutego 2024 r.

OŚWIADCZENIE

WSPÓŁAUTORA OSOBY UBIEGAJĄEJ SIĘ O WŁASNYM WKŁADZIE W POWSTAWANIE PRACY

Miejsce Sosnowiec, dnia 25.08.2025

Jacek Jania
Imię i nazwisko współautora publikacji

Instytut Nauk o Ziemi, Uniwersytet Śląski w Katowicach
Afiliacja

OŚWIADCZENIE

Oświadczam, że w pracy:

Osika A., Jania J.,Piotrowska N., Tikhomirov D.,Szafraniec J.,Devendra D., Christi M., Egli M., Vieli A.,2025: Holocene glacial history of southern Spitsbergen [manuskrypt przygotowany do złożenia do publikacji]

(autorzy, rok wydania, tytuł, czasopismo lub wydawca, tom, strony)

Mój udział polegał na doradztwie przy opracowaniu koncepcji badań, zaangażowaniu w część badań terenowych, konsultacjach dotyczących zastosowanej metodologii i doboru źródeł danych, wsparcie w pozyskiwaniu finansowania, nadzór i doradztwo w opracowaniu wyników, udział w pisaniu fragmentów tekstu oraz krytyczną lekturę całości maszynopisu.

opisać szczegółowo swój własny – (a nie osoby ubiegającej się) – udział w powstaniu pracy, (np. mój udział w powstanie tej publikacji polegał na wykonaniu doświadczeń techniką ....., analizie statystycznej wyników eksperymentów zilustrowanych na ryc. ...., przygotowaniu tekstu manuskryptu zamieszczonego w rozdziale......, kierowaniu projektem naukowym obejmującym badania opisane w tej pracy, itp.).*

....
Podpis współautora publikacji

Załącznik 13

OŚWIADCZENIE

WSPÓŁAUTORA OSOBY UBIEGAJĄEJ SIĘ O WŁASNYM WKŁADZIE W POWSTAWANIE PRACY

Sosnowiec, dnia 27.08.2025.

Joanna E. Szafraniec
Uniwersytet Śląski w Katowicach, Wydział Nauk Przyrodniczych, Instytut Nauk o Ziemi

OŚWIADCZENIE

Oświadczam, że w pracy:

Osika A., Jania J., Piotrowska N., Tikhomirov D., Szafraniec J.E., Devendra D., Christl M., Egli M., Vieli A., 2025: **Holocene glacial history of southern Spitsbergen** [w przygotowaniu]

Mój udział polegał na współopracowaniu koncepcji artykułu, nadzorze promotorskim, recenzji, redakcji, przygotowaniu ryciny dot. obszaru badań.

Oświadczam, że w pracy:
Osika A., Jania J.A., Szafraniec J.E. 2022. **Holocene ice-free strait followed by dynamic Neoglacial fluctuations: Hornsund, Svalbard**. Holocene 32(7): 664-679. https://doi.org/10.1177/09596836221088232.

Mój udział polegał na obliczeniu wskaźników morfometrycznych (CfE, CfD), zwektoryzowaniu zasięgu czół lodowców na podstawie danych satelitarnych (ryc. 3 i 4), przygotowaniu ryciny 6.

Joanna Szafraniec
Podpis współautora publikacji

Załącznik nr 10
do pisma okólnego nr 2
Prorektora ds. nauki i finansów
z dnia 19 lutego 2024 r.

OŚWIADCZENIE

WSPÓŁAUTORA OSOBY UBIEGAJĄEJ SIĘ O WŁASNYM WKŁADZIE W POWSTAWANIE PRACY

Gliwice, dnia 09 września 2025

Natalia Piotrowska
Imię i nazwisko współautora publikacji

Politechnika Śląska
Afiliacja

OŚWIADCZENIE

Oświadczam, że w pracy:

Osika A., Jania J., Piotrowska N., Tikhomirov D., Szafraniec J. E., Devendra D., Christl M., Egli M., Vieli A., 2025: Holocene glacial history of southern Spitsbergen [w przygotowaniu].

Mój udział polegał na wykonaniu datowania radiowęglowego próbek muszli, osadów organicznych, drewna i kości, napisaniu fragmentu tekstu dotyczącego metodyki analiz, wsparciu w opracowaniu kompilacji dat radiowęglowych i ich interpretacji.

....

Podpis współautora publikacji

Załącznik 15

A STATEMENT OF THE APPLICANT'S CO-AUTHOR OF THEIR CONTRIBUTION TO THE WORK

Location: Sopot, date: 22/08/2025

Dhanushka Devendra
First and last name of co-author of the publication

Department of Paleoceanography, Institute of Oceanology, Polish Academy of Sciences
Affiliation

STATEMENT

I declare that for the following work:

Title and authors: Osika A., Jania J., Piotrowska N., Tikhomirov D., Szafraniec J., Devendra D., Christl M., Egli M., Vieli A., 2025: Holocene glacial history of southern Spitsbergen [in preparation]

(authors, year of publication, title, journal or publisher, volume, pages)

My participation consisted of the visualization of the paleoclimate data and the review of the manuscript draft.

....

Signature of the co-author of the publication

* applies to co-authors